

# **Expanding the Scope of the Paternò-Büchi Reaction**

Methodology Development and Mechanistic Studies



Weronika Z. Michalska

This dissertation is submitted for the degree of Doctor of Philosophy

March 2023

Department of Chemistry

*Dedicated to my best friend Katie Rees-Williams.*

## **Declaration**

This thesis has not been submitted in support of an application for another degree at this or any other university. It is the result of my own work and includes nothing that is the outcome of work done in collaboration except where specifically indicated. Many of the ideas in this thesis were the product of discussion with my supervisor Dr Susannah Coote.

Weronika Z. Michalska

Lancaster University, UK

## Abstract

This thesis describes the development of the Paternò-Büchi reaction between aliphatic ketones and maleic acid derivatives.

**Chapter 1** discusses the current literature around oxetanes, and methods for their synthesis, particularly via the Paternò-Büchi reaction. The potential and importance of oxetane rings is highlighted, alongside current scope limitations of the Paternò-Büchi reaction.

**Chapter 2** investigates the Paternò-Büchi reaction between acetone and maleic anhydride to yield an oxetane product that requires further transformations to allow complete purification. A series of transformation reactions was developed to easily and diversely functionalize the formed oxetane products. A side product formed through dimerization of maleic anhydride was successfully removed after the reaction was complete.

**Chapter 3** expands on the scope of the Paternò-Büchi reaction by using cyclic ketones in the reaction with maleic anhydride to form a series of spirocyclic oxetanes. The initial reaction conditions were based on work presented in Chapter 2 and these conditions were optimized; the dimerization of maleic anhydride was successfully suppressed with *p*-xylene, further increasing the isolated yield of the oxetane product. Different cyclic ketones were used in the Paternò-Büchi reaction, creating a library of oxetane-containing spirocycles.

**Chapter 4** includes mechanistic studies performed alongside the formation of oxetanes, such as the use of molecular oxygen in order to quench potential triplet excited states in the reaction mixture. UV-vis spectra of starting materials and reagents were collected, and the different absorption range of maleimide compared to maleic anhydride allowed for distinguishing between different possible reaction pathways of the Paternò-Büchi reaction.

**Chapter 5** shows a series of different electron-poor alkenes tested in the Paternò-Büchi reaction, giving mixed results.

**Chapter 6** provides overall conclusions, highlighting the expansion of the scope of the Paternò-Büchi reaction, as well as highlighting difficulties in establishing a full mechanistic picture for photochemical reactions. Additionally, ideas for further work are discussed.

**Chapter 7** provides the full experimental details and characterization of the novel compounds that have been reported in this thesis (including X-ray crystal structures).



## Acknowledgements

Firstly, I would like to thank my supervisor Dr Susannah Coote for giving me this opportunity, as well as all the help, support, and guidance over the last 4 years. Special thanks to my industry supervisor Dr Alvaro Enriquez and my panel members Dr Vilius Franckevicius and Dr Verena Görtz for helpful discussions throughout my PhD. I would like to thank Lancaster University and Lilly for funding my PhD project. I would also like to thank the analytical staff at university Dr Geoff Akien, Dr Nathan Halcovitch and Dr David Rochester for help with analytical equipment. Thank you to the members of C21 lab, special thanks to Pip, Sean, Jack (K and L) and Stuart for making every day much more enjoyable.

Special thanks to Dr Mike Coogan and Dr Rebecca Spicer for all the chemistry discussions, support and help. Mike, thank you for teaching me so much about chemistry but much more importantly about gardening. Bec, I would have not finished writing this thesis without your help, coffee with you were often the main motivation to come in. I will miss seeing you both every day.

Thank you, Katie, Pauline and Dilara for your friendship, it means a lot to me. I have had so much fun with you all, I cannot wait to see you again soon.

Wielkie podziękowania dla moich rodziców za pomoc i wsparcie przez cały doktorat i też przez całe moje życie.

Most important thanks must go to my partner Callum. You are my favourite person; you made my last few years so much easier and more fun, I cannot wait for our future. Thank you for agreeing to get a cat with me and thank you for not letting me get a dog (yet). Thank you to Willma for helping me take my mind off my PhD and for actually sleeping on her cat bed (Cat 1).



Cat 1 - Willma

## Contents

Declaration .....	ii
Abstract .....	iii
Acknowledgements.....	iv
Contents .....	v
List of Abbreviations and Acronyms.....	viii
<b>Chapter 1 Literature review .....</b>	<b>1</b>
1.1 Oxetanes.....	1
1.1.1 Introduction .....	1
1.1.2 Structure and properties of oxetanes.....	1
1.1.3 Oxetane rings in natural products and pharmaceuticals .....	3
1.1.4 Synthesis of oxetane rings .....	7
1.1.5 Reactions of oxetane rings.....	10
1.2 Photochemistry .....	11
1.2.1 Introduction to organic photochemistry.....	11
1.2.2 Jablonski diagram .....	12
1.2.3 Triplet-triplet energy transfer (TTET) .....	14
1.2.4 Practical approach to photochemical reactions .....	19
1.3 Paternò-Büchi reaction.....	21
1.3.1 History of Paternò-Büchi reaction.....	21
1.3.2 Mechanism of the Paternò-Büchi reaction.....	22
1.3.3 Scope of the Paternò-Büchi reaction.....	23
1.4 Conclusions .....	31
1.5 Aims of the project .....	32
<b>Chapter 2 Paternò-Büchi reaction between maleic anhydride and acetone .....</b>	<b>34</b>
2.1 Introduction and Chapter Aims .....	34
2.2 Optimization of the Paternò-Büchi reaction .....	35
2.2.1 Set-up and general information .....	35
2.2.2 Batch reaction Paternò-Büchi reaction .....	36
2.2.3 Flow reaction Paternò-Büchi reaction.....	40
2.2.4 Reducing the amount of acetone under batch and flow conditions .....	43
2.2.5 Removal of the dimer 4 .....	45

2.3	Nucleophilic ring-opening of the anhydride.....	46
2.4	Conclusions .....	52
<b>Chapter 3 Paternò-Büchi reaction between cyclic ketones and maleic anhydride</b>		
.....		<b>55</b>
3.1	Introduction .....	55
3.2	Paternò-Büchi reaction between cyclohexanone and maleic anhydride .....	56
3.2.1	Testing the initial reaction conditions.....	56
3.2.2	Optimization of reaction conditions.....	58
3.2.3	Optimization of the Paternò-Büchi reaction with the use of additives.....	63
3.2.4	Using flow to improve reaction time of the Paternò-Büchi reaction .....	77
3.3	Expanding the scope of the Paternò-Büchi reaction .....	81
3.3.1	Functionalization of the anhydride ring .....	82
3.3.2	Different cyclic ketones .....	87
3.3.3	Additional reactions and transformations.....	95
3.4	Conclusions .....	99
<b>Chapter 4 Investigations into mechanistic pathways of Paternò-Büchi and dimerization reactions</b>		
.....		<b>102</b>
4.1	Introduction .....	102
4.2	Using molecular oxygen as triplet quencher .....	103
4.2.1	Molecular oxygen as a triplet quencher in the dimerization reaction .....	104
4.2.2	Using molecular oxygen as a triplet quencher in Paternò-Büchi reactions. .....	106
4.2.3	Conclusion of molecular oxygen experiments .....	109
4.3	Identifying the excited state partner in the Paternò-Büchi reaction .....	109
4.3.1	UV-vis spectra of starting materials and reagents .....	110
4.3.2	Photochemical reaction of cyclohexanone and <i>N</i> -Boc-maleimide at 300 or 350 nm .....	112
4.3.3	Photochemical reaction of cyclohexanone and <i>N</i> -H-maleimide in at 419 nm in the presence of thioxanthone .....	117
4.3.4	Issues with <i>N</i> -H-maleimide during irradiation reactions .....	120
4.3.5	Conclusion of the mechanistic investigation into mechanism of the Paternò-Büchi reaction between cyclohexanone and electron poor alkenes .....	122
4.4	The role of the <i>p</i> -xylene in the suppression of dimerization reaction.....	125

4.4.1	Background.....	125
4.4.2	UV-vis experiments.....	126
4.4.3	Conclusion of the investigation into the role and effect of the <i>p</i> -xylene on the reaction mixture.....	131
4.5	Conclusions .....	132
<b>Chapter 5 Expanding the scope of the Paternò-Büchi reaction by using different electron poor cyclic alkenes .....</b>		<b>134</b>
5.1	Introduction .....	134
5.2	Maleic anhydride derivatives .....	135
5.2.1	2(5H)-Furanone (66) .....	135
5.2.2	Bromofuran-2,5-dione (69) .....	136
5.2.3	Dimethyl maleic anhydride (73) .....	138
5.2.4	Methyl maleic anhydride (76) .....	139
5.2.5	3-(Bromomethyl)-2,5-furandione (83) .....	143
5.2.6	Coumarin (87) .....	145
5.2.7	Conclusion of the Paternò-Büchi reactions between cyclohexanone and maleic anhydride derivatives .....	145
5.3	Maleimide derivatives.....	146
5.4	Conclusions .....	151
<b>Chapter 6 Conclusions and further work.....</b>		<b>153</b>
<b>Chapter 7 Experimental .....</b>		<b>157</b>
7.1	General information.....	157
7.2	Optimization and reactions tracking tables .....	158
7.3	Flow reactions.....	160
7.4	Characterization data of novel compounds.....	161
7.4.1	Chapter 2: Reactions of maleic anhydride (1) and acetone (2).....	161
7.4.2	Chapter 3: Reactions of cyclic ketones and maleic anhydride .....	173
7.4.3	Chapter 4 and 5: Reactions of cyclohexanone (10) with different electron-poor alkenes .....	215
7.5	UV-vis spectra.....	222
<b>References .....</b>		<b>225</b>

## List of Abbreviations and Acronyms

A	Absorbance
Ac	Acetyl
Aq	Aqueous
Ar	Aryl group
Bn	Benzyl
Boc	<i>tert</i> -butyloxycabonyl
br	Broad
Bu	Butyl
COSY	Correlation spectroscopy
d	Doublet
DABCO	1,4-diazabicyclo[2.2.2]octane
DCC	<i>N,N'</i> -Dicyclohexylcarbodiimide
DCM	Dichloromethane
DIBAL-H	Diisobutylaluminium hydride
DIPEA	<i>N,N</i> -Diisopropylethylamine
DMAP	4-dimethylaminopyridine
DMF	Dimethylformamide
DMSO	Dimethyl sulfoxide
DMU	Dimethylurea
EDC	1-ethyl-3-(3-dimethylaminopropyl)-carbodiimide
ee	Enantiomeric excess
Eq	Equivalents
ESI	Electrospray ionization
Et	Ethyl
FTIR	Fourier transform infrared
<i>h</i>	Planck's constant ( $6.626 \times 10^{-34} \text{ m}^2\text{kg}\text{s}^{-1}$ )
HIV	Human immunodeficiency viruses
HMBC	Heteronuclear multiple-bond coherence
HMPA	Hexamethylphosphoramide
HOBt	Hydroxybenzotriazole
HOMO	Highest occupied molecular orbital
HRMS	High resolution mass spectrometry
h	Hour(s)
Hz	Hertz
<i>i</i>	Iso

IC	Internal conversion
IR	Infrared
ISC	Intersystem crossing
<i>J</i>	Coupling constant
K	Kelvin
LCMS	Liquid chromatography–mass spectrometry
LUMO	Lowest unoccupied molecular orbital
m	Multiplet
<i>m</i>	<i>meta</i>
M	Molar
<i>m</i> CPBA	<i>meta</i> -Chloroperoxybenzoic acid
Me	Methyl
min	Minute(s)
mmol	Millimole
Ms	Mesyl
MS	Mass spectrometry
m/z	Mass/charge (mass spectroscopy)
NBS	<i>N</i> -bromosuccinimide
nm	Nanometre
NMR	Nuclear magnetic resonance
NOESY	Nuclear Overhauser effect spectroscopy
<i>o</i>	<i>ortho</i>
<i>p</i>	<i>para</i>
PG	Protecting group
Ph	Phenyl
ppm	Part per million
PPTS	Pyridinium <i>p</i> -toluenesulfonate
ppy	2-Phenylpyridine
Pr	Propyl
q	Quartet
r.t.	Room temperature
s	Singlet
t	Triplet
<i>tert</i> <sup>(t)</sup>	Tertiary
TBAT	Tetrabutylammonium difluorotriphenylsilicate
<sup>t</sup> Bu	<i>tert</i> -butyl

TBS	<i>tert</i> -butyldimethylsilyl
Tf	Triflate
TFA	Trifluoroacetic acid
THF	Tetrahydrofuran
THX	Thioxanthone
TLC	Thin-layer chromatography
TMS	Tetramethylsilane
TOF	Time-of-flight (mass spectroscopy)
Ts	Toluenesulfonyl (tosyl)
TTET	Triplet-triplet energy transfer
UV-vis	Ultraviolet-visible
Å	Angstrom
$\epsilon$	Molar absorption coefficient
$\nu$	Frequency
$\delta$	Chemical shift

# Chapter 1 Literature review

## 1.1 Oxetanes

### 1.1.1 Introduction

Oxetanes are four-membered cyclic ethers. Due to their small size and polarity, they can often be used as replacement groups for ketones in drugs, which can be metabolically vulnerable, making them very popular in medicinal chemistry. Some examples of natural products and drugs containing oxetanes are shown in Figure 1-1. One of the best known is oxetanocin A, which was first isolated from soil bacteria *Bacillus megaterium* and inhibits the in vivo replication of human immunodeficiency virus (HIV).<sup>1</sup> Other oxetane-containing natural compounds include mitrephorone A<sup>2</sup> and maoecrystal I,<sup>3</sup> which have cytotoxic properties. Another widely known compound containing an oxetane ring is paclitaxel (Taxol),<sup>4</sup> which is used in cancer chemotherapy, and was first isolated in 1971 from stem bark of the western yew. Some studies suggest that the biological activity of paclitaxol is reliant on the oxetane ring.<sup>5,6</sup>

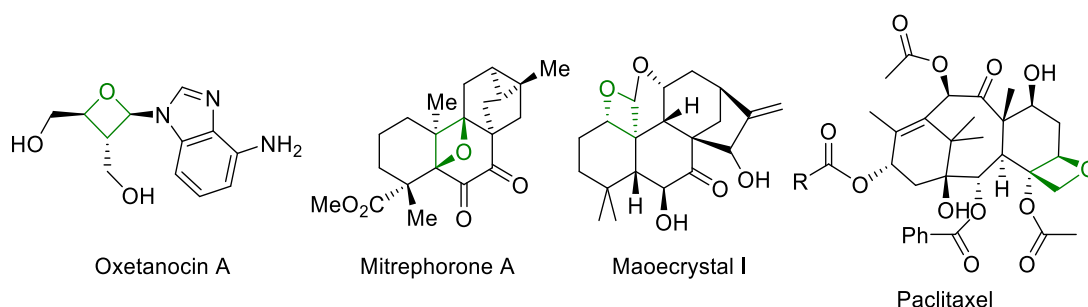


Figure 1-1 Examples of natural products and pharmaceuticals containing oxetane rings.

### 1.1.2 Structure and properties of oxetanes

The first crystal structure of the non-substituted oxetane ring was measured in 1984,<sup>7</sup> giving more insight to the structure and potential properties of these heterocycles (Figure 1-2). The bond lengths and angles (measured at 90 and 140 K) indicate an almost perfect square geometry. Due to statistical errors at 140 K, the results obtained at 90 K were used to discuss the properties of the oxetane.

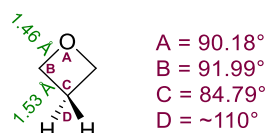
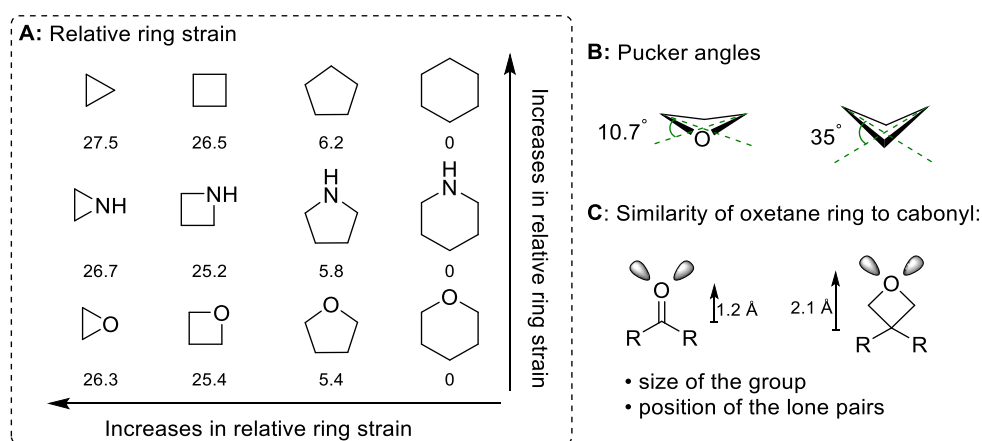


Figure 1-2 Bond lengths and angles based on the first crystal structure of an oxetane ring.

Oxetane has relatively high ring strain compared to other cyclic ethers due to the small size of the ring (Figure 1-3, A). Ring strain is mainly caused by the  $sp^3$  hybridised atoms preferring  $109.5^\circ$  bond angles, meaning the smaller the ring, the higher the strain, since



within small rings the bond angles are constrained to be smaller than the ideal 109.5°. Additionally, there is a small contribution to the ring strain if a heteroatom is present in the ring. The ring strain increases due to the angle of the molecular orbitals (decreasing from the ideal 109.5°) meaning there is a large difference between ring strain of 5- and 4-membered rings, as the angle changes drastically from ~108° to ~90° in 5- and 4-membered rings respectively.<sup>8</sup> Oxetanes are almost flat in contrast to cyclobutane; this is due to the oxygen atom that replaces the CH<sub>2</sub> group, with a much smaller pucker angle compared to cyclobutane (Figure 1-3, B). The puckering of rings takes place to avoid eclipsing strain (torsional strain) between atoms/groups. The general structure and orientation of the molecular orbitals on an oxetane ring makes it very similar in structure to a carbonyl group (Figure 1-3, C). The resemblance of the oxetane ring to a carbonyl group (with its lone pairs and similar size) has made the oxetane ring popular in recent years as a potential replacement group.<sup>9</sup> Additionally, oxetane has the highest hydrogen bonding ability compared to aliphatic aldehydes esters and ketones.<sup>10</sup>



**Figure 1-3 A: Comparison of the relative ring strains of different rings (kcal mol<sup>-1</sup>);<sup>11</sup> B: comparison of the pucker angle between an oxetane and cyclobutane ring; C: comparison of the structures of carbonyl group and oxetane ring.**

A recent review from 2022<sup>12</sup> compared the current rings used in clinical trials and drugs, showing that although the oxetane ring was not in the top 100 “Most Frequently Used Ring Systems from Small Molecule Drugs”, it was second in the top 100 new ring systems used in clinical trial compounds, highlighting its increased popularity. Overall, in recent years the popularity of small aliphatic rings increased,<sup>13,14</sup> in part due to the population of a new metric to assess pharmaceutical compounds, which describes the ratio between aromatic atoms and sp<sup>3</sup> atoms (Ar-sp<sup>3</sup>).<sup>15</sup> This has started the movement away from the “flatland”,<sup>16</sup> and with small aliphatic rings this ratio can be easily improved.

The pharmaceutical industry uses small rings, as in some cases they can improve properties for of a potential drug molecule. Small rings have a series of advantages due their properties: small size, rigidity and their 3-D structure, these properties lead to

favourable physiochemical properties. In general, the small size of the molecule can help with metabolism and solubility, while the rigid structure helps with specific 3-D requirements, this can improve interactions with biological sites e.g. enzymes active sites. As well as providing specific vectors allowing for effective H-bonding (and other interactions) to take place.<sup>13</sup> Overall, there is a real interest in synthesis of oxetane-containing compounds to be used as building blocks for potential drugs.<sup>17</sup>

### 1.1.3 Oxetane rings in natural products and pharmaceuticals

4-Membered heterocycles including oxetane, azetidine and thietane rings are important in many natural products and drugs. Examples of azetidine- and thietane-containing molecules are shown in Figure 1-4.<sup>18,19</sup> 4-Membered heterocycles have been identified to have many desirable properties and biological activities; compounds containing oxetanes, azetidines and thietanes have been used as therapeutic agents due to their unique 3-D structures.<sup>20</sup>

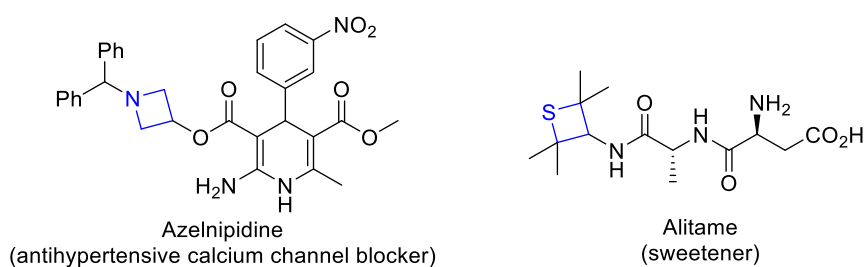


**Figure 1-4** Examples of azetidine and thietane rings.

Medicinal chemists use a series of properties to characterize potential drug molecules, with the five most common properties are summarized below:

- **Lipophilicity** (logP/logD) is a measurement of the interaction between the molecule and a lipid; measured by distribution of a molecule in oily vs aqueous phase (octanol and water is used most commonly).<sup>21</sup>
- **Metabolic stability** tests the stability of the molecule in different biological assays to show the behaviour of the molecule under biological conditions; low metabolic stability is usually undesirable.<sup>22</sup>
- **pK<sub>a</sub>** is acid-base dissociation constant often used in medicinal chemistry to indicate the ionization states of the molecule under different pH.
- **solubility** of the molecule in different mediums, often water ( $\mu\text{mol L}^{-1}$ ).
- **Ar-sp<sup>3</sup>** shows the ratio between aromatic and sp<sup>3</sup> atoms in the molecule.<sup>15</sup>

It is important to note that whilst medicinal/pharmaceutical chemists use these properties as guidance in order to find a good potential drug, there is not a “perfect value” for these properties as they will depend on the type of drug and often the properties must be

balanced. This section will focus on uses and examples of oxetane-containing compounds, highlighting the effect of the oxetane ring on the properties of the molecules.

One of the most popular compounds that contains an oxetane ring is Taxol. Taxol is an anti-cancer drug derived from the western yew tree.<sup>4</sup> Over the years, extensive studies of Taxol took place to understand its reactivity; in 2000 Snyder *et.al.*<sup>5</sup> published a study discussing the importance of the oxetane ring for the biological activity of Taxol. As shown in Figure 1-5, the investigation focused on the changes to the oxetane ring, as well as small changes to the side chain and the highlighted ester groups. The changes to the oxetane group were:

- 1) replacing oxygen with a different atom,
- 2) replacing the oxetane ring with an epoxide,
- 3) removal or cleavage of the ring.

The effects of these changes are summarized in Figure 1-5, by comparing the effectiveness of the derivative of Taxol to the original molecule. The oxetane ring in Taxol is involved in hydrogen bonding, which has an effect on solvation of the molecule, and the oxetane ring also adds to the rigidity of the core of the molecule. When the oxetane ring is present, these properties are well balanced, allowing for the effective drug. The oxetane ring suspected to be involved in H-bonding as well as adding to rigidity of the molecule core. Replacing oxygen with NH leads to over-effective solvation of the molecule, leading to ineffective migration of the drug into protein binding pockets (it cannot access cells guarded by the hydrophobic membrane bilayer). When the oxygen atom was replaced with sulfur or a CH<sub>2</sub> group the hydrogen bonding was affected, making the molecules 6-9 and 40 times less effective respectively than the oxetane analogue. Replacement of the oxetane ring with an epoxide did not have a large effect on the properties, as the hydrogen bonding was still possible, and the rigidity of the core molecule was not affected. However, cleaving the oxetane ring resulted in a large decrease in reactivity (by 20 times).<sup>23</sup> The analysis focused on the effect the oxetane ring has on the overall properties, concluding that the oxetane ring in Taxol provides: “a positive contribution to the bioactivity in terms of both hydrogen atom bonding and ring rigidification”.

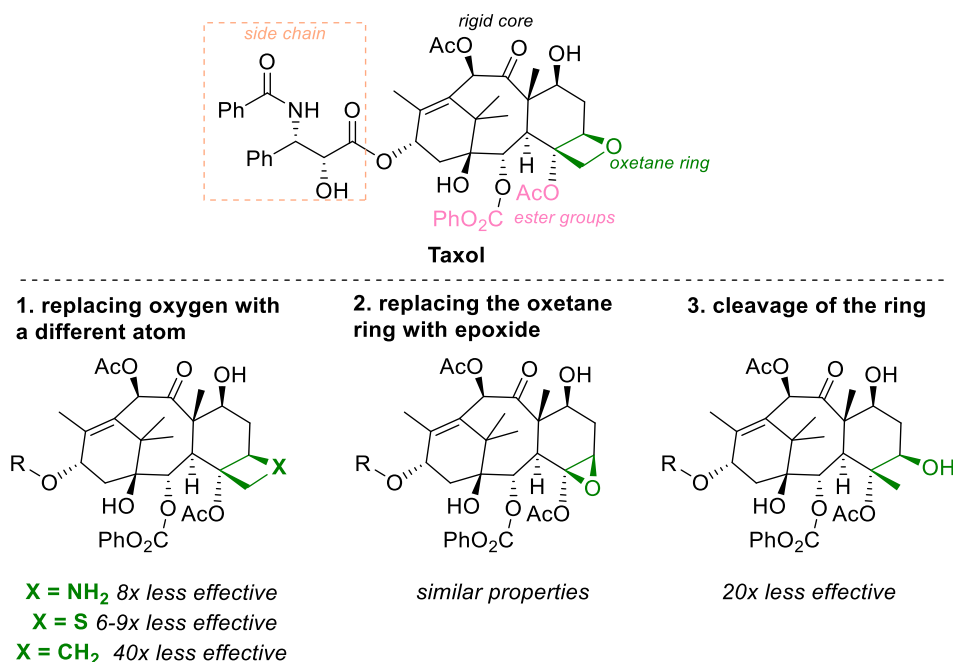


Figure 1-5 Structure of Taxol and the effects of changing the oxetane ring on the effectiveness of the drug.

In recent years, oxetane rings have been used as replacement groups for carbonyl groups or *gem*-dimethyl groups.<sup>9,24</sup> Carreira and co-workers have reported a series of different studies that used oxetanes as replacement groups and compared their properties.<sup>25-27</sup> In particular, Carreira showed the potential of *spirocyclic* oxetanes as replacements for heterocyclic derivatives, where a series of oxetane-containing spirocycles were synthesised and compared to the 4-piperidinone derivative (Figure 1-6).<sup>28</sup> The properties of the oxetane containing compounds were different to the 4-piperidinone derivative, as in general oxetanes decreased the solubility and increased the lipophilicity, while the metabolic stability was improved only in some cases. As mentioned above, these biological properties are all connected and a balance is required for an efficient drug; overall oxetane rings do have an effect on the properties, which in most cases can be considered positive (or neutral), however it has to be considered on case-to-case basis.

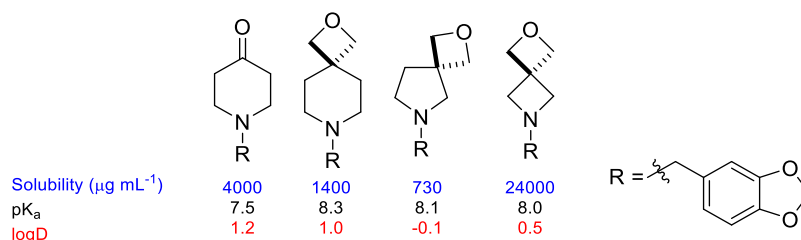
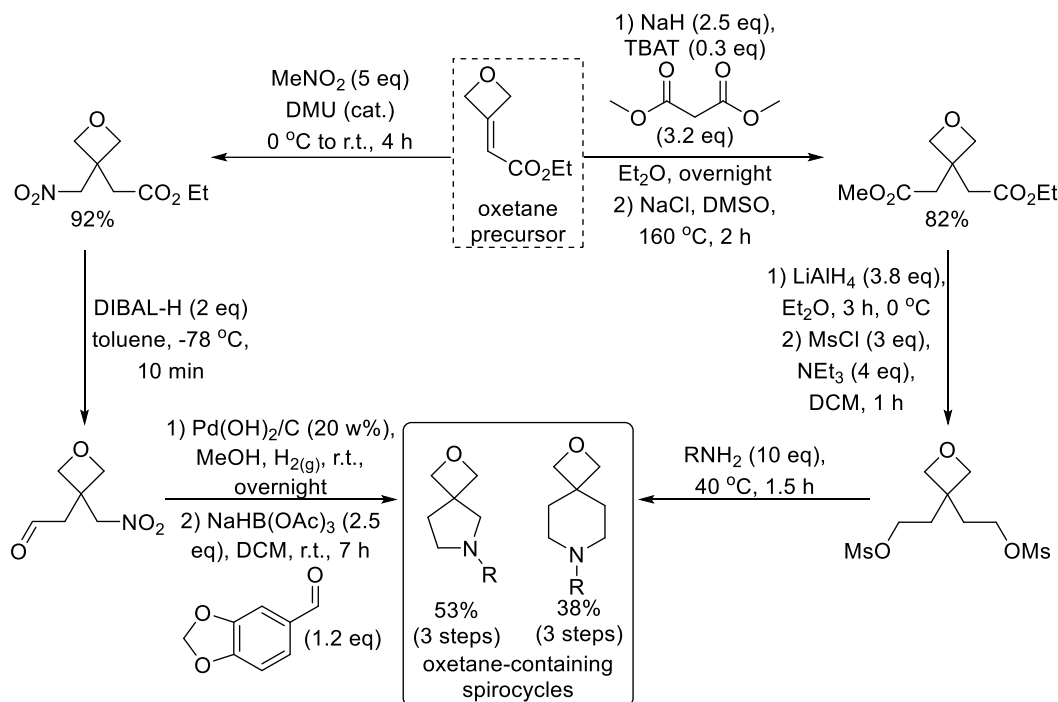


Figure 1-6 Biological properties showing the effects of oxetane ring as a replacement of a carbonyl group.

These oxetane-containing spirocycles were synthesised from oxetane precursors, which were reacted under different reaction conditions in order to form the final spirocyclic oxetanes. Scheme 1-1 shows the synthetic pathway for the 5- and 6-membered

spirocyclic oxetanes, generated from the same precursor via two routes. In the majority of cases the reaction yields were good, although each ring size necessitated a new synthetic pathway, thus the synthesis of libraries of spirocyclic oxetanes is rather labour-intensive. Therefore, there is a still need for new methodology capable of forming large libraries of oxetane-containing spirocycles from simple building blocks that can be easily derivatized.



**Scheme 1-1 Formation of spirocyclic oxetanes.**

A recent investigation into the effects of the oxetane ring compared to different biological motifs has been reported by Bull and Mousseau and their co-workers.<sup>24</sup> The study incorporated 3,3-diaryloxetanes into different drug-like molecules and compared the properties to analogous ketones and other alkyl groups (*gem*-dimethyl, cyclobutane). Similarly, to previous studies in the area, the presence of the oxetane ring on the drug-like molecule changed some of its properties, as summarized in Figure 1-7. Research so far has shown changes to the biological properties when oxetane is used as a replacement group, importantly these properties are still within the desired/accepted ranges.

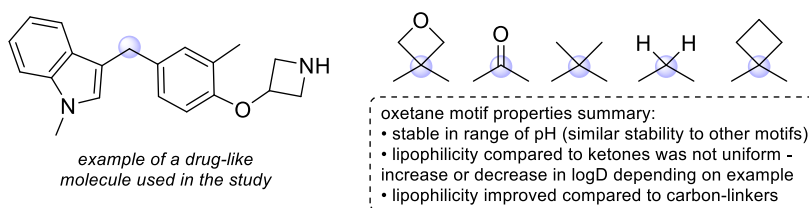
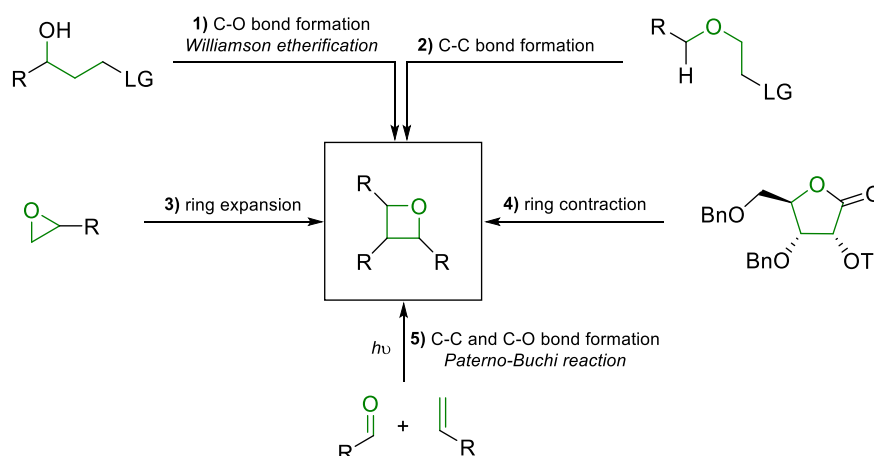


**Figure 1-7 Effect of using oxetane compared to ketone or other alkyl groups.**

To summarize, 4-membered heterocycles are important in various areas of chemistry, from natural products and drugs to sweeteners. Oxetane rings specifically are important as part of pharmaceutical molecules such as Taxol, where the oxetane ring contributes to the biological activity of the drug. Additionally, in recent years oxetane rings have been used as replacement groups in drug molecules. The effects of the oxetane ring on the drug-like molecules have so far been satisfactory, although often new synthetic approaches are required for each new oxetane target, meaning that there is still a need for new synthetic approaches that can synthesize large libraries of oxetanes, ideally through diversification of common intermediates.

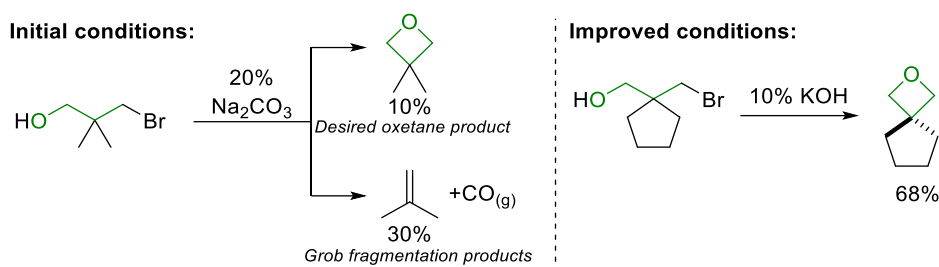
#### 1.1.4 Synthesis of oxetane rings

Synthesis of oxetane rings (Scheme 1-2) summarizes the possible ways to form oxetane rings. The first two reactions form oxetanes under basic conditions by forming either a C-O or a C-C bond (reactions 1 and 2). Alternatively, the 4-membered ring can be formed by either expanding an epoxide ring (reaction 3) or contracting a 5-membered ring (reaction 4). Finally, photochemical access to the oxetane ring is given by the Paternò-Büchi reaction between a ketone/aldehyde and an alkene (reaction 5). Each of these reactions have their advantages and disadvantages, and the ground state reactions (reaction 1-4) will be briefly discussed next, while the main focus will be given to the Paternò-Büchi reaction, which is examined in detail in section 1.3.



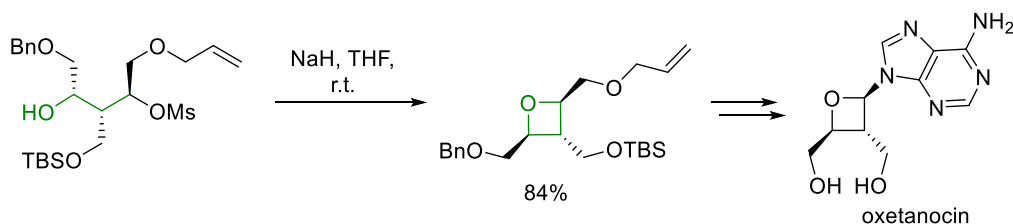
Scheme 1-2 Possible ways for formation of oxetane ring.

The Williamson etherification is a common way to form a C-O bond to produce ethers, and the use of this methodology to yield an oxetane ring was reported in 1959 (Scheme 1-3).<sup>29</sup> While the reaction gave the desired oxetane, a major downside to the reaction was the side reaction, a Grob fragmentation, which is a 1,2-elimination reaction of starting material, producing an alkene and carbon monoxide. Optimization of the reaction conditions, including testing different bases, solvents, as well as changing the starting material by adding a cyclopentane ring, meant a new oxetane was formed in 68% yield.



**Scheme 1-3 Williamson etherification reaction.**

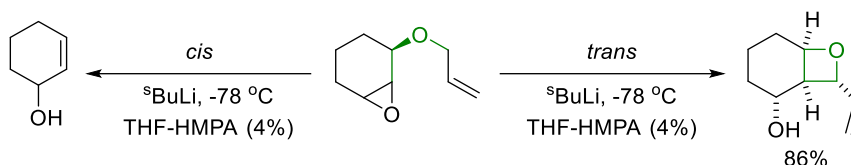
Over the years, the reaction has been expanded on and allowed the formation of many oxetanes under similar, basic conditions. The Williamson etherification is one of the most common ways of making oxetane rings, as the reaction conditions are straightforward. However, the reaction is substrate-dependent. The starting material requires the alcohol and leaving group to be in a 1,3-relationship with respect to each other. Additionally, the side decomposition reaction shown in Scheme 1-3 (Grob fragmentation) often lowers the percentage yield of the reaction, and for more highly substituted substrates, cyclisation becomes difficult. Nonetheless, the Williamson etherification is often used in the synthesis of complex oxetane-containing structures.<sup>30,31</sup> For example, the oxetane forming step in the synthesis of oxetanocin gave the desired oxetane-containing product in 84% yield (Scheme 1-4),<sup>32</sup> highlighting the success of optimising the Williamson etherification over the years, especially as the oxetane ring closing step is only the eighth step of the synthesis out of 21 steps. Overall, Williamson etherification is very common way of forming oxetanes, it is broadly applied in synthesis, however it is substrate dependent, often requiring synthesis of a precursor. Formation of oxetane rings from readily available materials is rare, which decreases the possible scope.



**Scheme 1-4 Williamson etherification as key step in the synthesis of oxetanocin.**

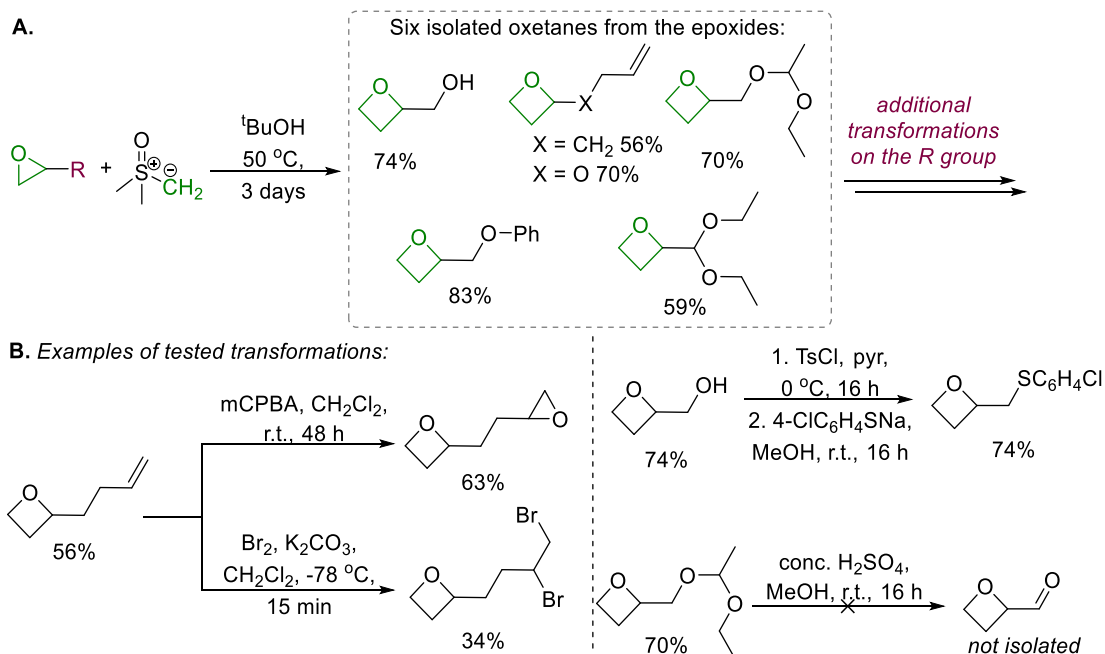
In contrast, forming of the oxetane ring by formation of the C-C bond is much less common than the Williamson etherification. An example of C-C bond formation of an oxetane ring is shown in Scheme 1-5, which involves ring opening of an epoxide after lithiation of the starting material at the allylic position. Upon optimization, the reaction yielded 86% of the desired oxetane, however, the starting material must be the *trans* isomer, as the *cis* isomer yielded 2-cyclohexanol instead, through elimination of the side chain. The C-C bond forming method is much less common, and similarly to the Williamson etherification, is often substrate specific. As both approaches involve

cyclisation processes, usually through S<sub>N</sub>2 reaction, these approaches can fail when applied to highly substituted substrates, especially when substitution at the 2- and 4-positions is required.



**Scheme 1-5** Formation of oxetane ring via C-C bond formation.

Ring expansion and contraction methods of oxetane formation involve breaking a C-O bond followed by either insertion or removal of a C-R group respectively. For example, Fitton and co-workers<sup>33</sup> described a reaction between monosubstituted epoxides and trimethylsulfoxonium ylide, which produced six different oxetanes (Scheme 1-6, A) in good yields. Next, the oxetanes underwent a series of further functionalisation in order to further expand the scope (Scheme 1-6, B). Epoxidation and bromination of a terminal alkene worked well, however not all modifications were successful. For example, oxetane-2-carbaldehyde was not isolated from the attempted deprotection of the acetal-protected oxetane, which could be due to the use of concentrated sulfuric acid in the reaction. Overall, these reactions show oxetanes can tolerate a variety of different transformations as long as acidic conditions are kept to minimum or ideally avoided.

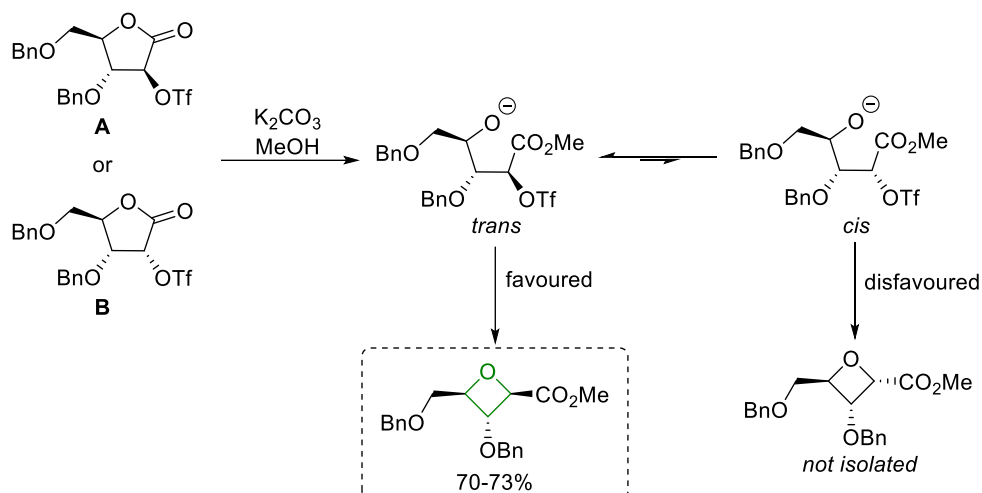


**Scheme 1-6** Formation of oxetane ring by expanding an epoxide ring.

Contraction of 5-membered rings is possible, by using sugar derivatives as starting materials. For example, Fleet and co-workers<sup>34</sup> used  $\alpha$ -triflates of  $\gamma$ -lactones to form a series of oxetanes by contracting the ring with potassium carbonate (Scheme 1-7). In



the case of isomers A and B, the reaction yields the same oxetane in 70-73% yield. Investigations into the stereochemical outcome of the ring contraction revealed that the  $S_N2$  ring closure of the *trans* isomer is much quicker than  $S_N2$  formation of the oxetane with the *cis* isomer, as there are two bulky groups too close together (at C(2) and C(3)). However, it was shown that changing the group on C(3) to Me or  $\text{CH}_2\text{OBn}$  allowed for the *cis* configuration (of the two groups) on the oxetane ring.<sup>35</sup>

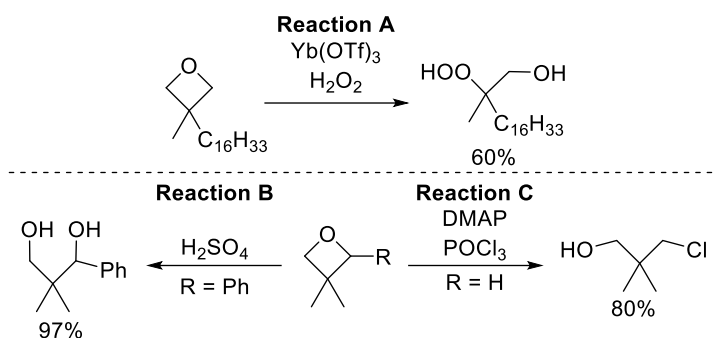


**Scheme 1-7** Formation of oxetane ring by contracting a 5-member ring (*cis/trans* refers to the relationship between OBn and OTf groups).

Formation of the oxetane via expanding or contracting the ring can often give a good yield, however a specific precursor is needed, lowering the possible reaction scope of the reaction. Both reactions discussed above only had a handful of oxetanes formed via each method.

### 1.1.5 Reactions of oxetane rings

Oxetanes can undergo ring opening reactions in the presence of either Lewis or Brønsted acid,<sup>36</sup> and this can make further transformations of oxetane containing compounds difficult. Scheme 1-8 summarizes the ring opening of the oxetane rings under different conditions, including Lewis acid (Reaction A),<sup>37</sup> Brønsted acid (Reaction B)<sup>38</sup> and also non-acidic conditions (Reactions C),<sup>39</sup> showing potential lack of stability of some oxetane rings to various environments. These reactions can give interesting products, however if the aim is to form and maintain the oxetane ring in the molecule, acidic conditions should be in general avoided.



**Scheme 1-8** Examples of ring-opening reactions of oxetane ring.

To summarize, there are a variety of ground state methods that form a wide range of oxetanes. However, as seen above, many reactions are substrate dependent and often require a lengthy synthesis of the starting material, which can lead to smaller libraries of oxetanes and/or inefficient syntheses. Many of these reactions, especially the Williamson etherification, are well established and are used reliably in the synthesis of natural products and pharmaceuticals. However, as discussed, side reactions can take place, reducing the yield of the desired oxetane. Moreover, further functionalization of oxetanes can prove difficult due to the vulnerability of the oxetane ring to acidic conditions. An alternative to these ground state methods is the photochemical [2+2] cycloaddition of a ketone/aldehyde with an alkene – the Paternò-Büchi reaction - in which the oxetane ring is created by the formation of two bonds at the same time (C-C and C-O). In principle, this approach is very attractive, as rapid formation of an oxetane ring is possible from simple starting materials. Next, the use of photochemistry in organic chemistry will be discussed (section 1.2), followed by the Paternò-Büchi reaction (section 1.3).

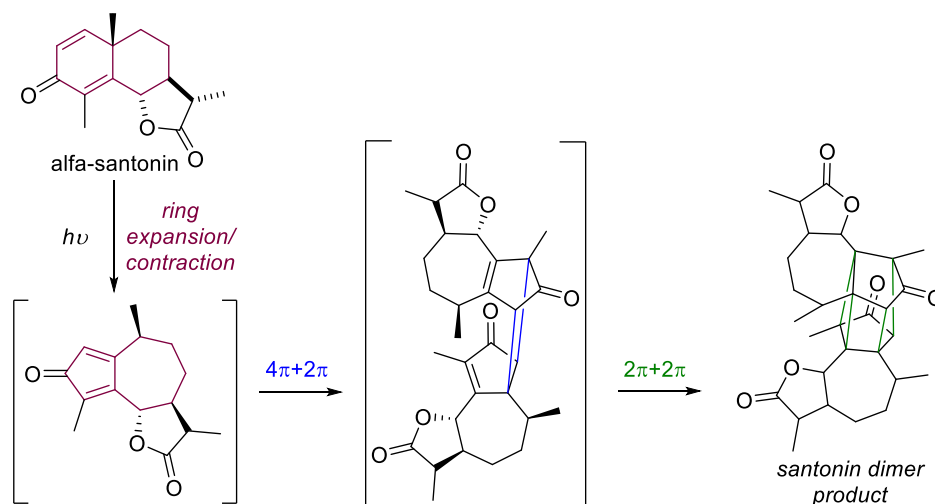
## 1.2 Photochemistry

### 1.2.1 Introduction to organic photochemistry

Photosynthesis is perhaps the most known chemical reaction, in which sunlight is used to form O<sub>2</sub> from CO<sub>2</sub>. Nature has evolved so that most reactions take place within the UV-vis (ultraviolet-visible) range (200-700 nm), meaning that the wavelength of light is specific to the reaction/reagents. Synthetic photochemistry began in the mid-19<sup>th</sup> century<sup>40</sup> when synthetic dyes were becoming popular, but there was a complete lack of understanding of these photochemical reactions due to their complexity.

Organic photochemistry started similarly, by using sunlight as the source of energy. The first synthetic photoreaction was reported by Trommsdorff in 1834,<sup>41</sup> where crystals of alfa-santonin “burst” and turned yellow when exposed to sunlight (Scheme 1-9). However, it took many more years to fully understand the reaction. In 2007, the accepted

reaction pathway via ring expansion/contraction was at last elucidated and the reaction was fully “solved”,<sup>42</sup> following two cyclization steps to give the final santonin dimer product. The changes in the crystal structures were followed while  $\alpha$ -santonin was exposed to UV irradiation for 24, 50 and 200 hours, resulting in the formation of the final product.



**Scheme 1-9** Reaction of the crystals of  $\alpha$ -santonin “bursting” and turning yellow.

Photochemical reactions use excited state molecules, allowing for new/different transformations compared to the ground-state chemistry. To fully understand photochemical reactions, it is important to understand the “movement” of the molecules between their excited states, which can be best summarized with a Jablonski diagram.

### 1.2.2 Jablonski diagram

A Jablonski diagram (Figure 1-8) is a state diagram, describing the energy levels and photophysical processes of a molecule. Molecular electronic states start with  $S_0$ , which is the singlet ground state. It is followed by excited states ( $S_{n>0}$ ) and in some cases molecules can also access their triplet states ( $T_{n>0}$ ) via intersystem crossing (ISC).<sup>43</sup> There are a series of different processes which allow the molecule to access different states. By absorbing light, the molecule can access singlet excited states ( $S_{n>0}$ ). Next, internal conversion (IC) is a fast radiationless transition that takes place between electronic states of the same multiplicity (e.g.  $S_2 \rightarrow S_1$ ). Intersystem crossing (ISC) is also a radiationless transition between states of different multiplicity (e.g.  $S_1 \rightarrow T_1$ ). Emission of radiation from the excited singlet state back to singlet ground state is called fluorescence ( $S_1 \rightarrow S_0$ ), while phosphorescence is the emission from (typically) the first triplet excited state to the singlet ground state ( $T_1 \rightarrow S_0$ ). In this case the multiplicity changes, which is why it is typically a slower process than fluorescence.

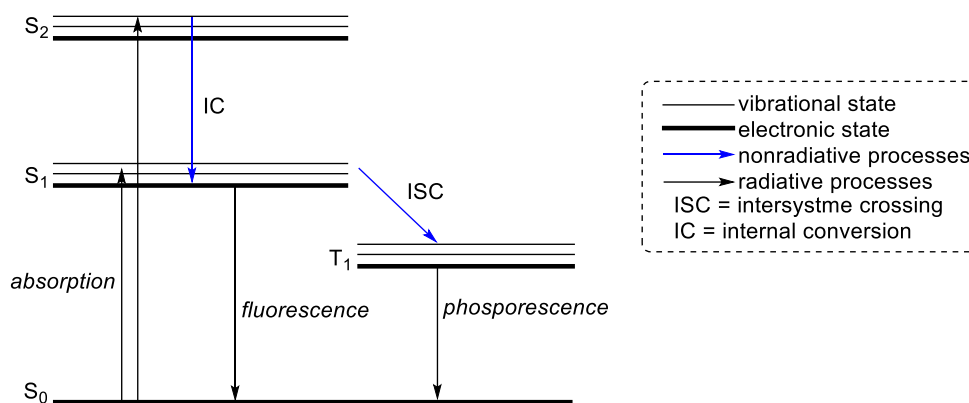


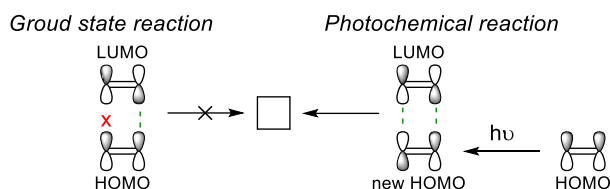
Figure 1-8 Jablonski diagram

Photophysical processes result in changes in bond lengths and angles between different electronic states because of changes to the occupancy of bonding and antibonding orbitals responsible for the molecule's structure. There are two types of photophysical processes: radiative and radiationless transitions. Radiative transitions absorb/emit a photon, while radiationless transitions are not related to absorption and/or emission. The general time scale of the different photophysical process is shown in Table 1-1. How fast a molecule can access and leave each state will influence the lifetime of that particular state.

Photophysical process	Time scale ( $\tau=1/k_{\text{process}}$ )s
Absorption	$10^{-15}$
Internal conversion	$10^{-12}$ - $10^{-6}$
Intersystem crossing ( $S \rightarrow T$ )	$10^{-12}$ - $10^{-6}$
Intersystem crossing ( $T \rightarrow S$ )	$10^{-9}$ - $10^1$
Vibrational relaxation	$10^{-13}$ - $10^{-12}$
Fluorescence	$10^{-9}$ - $10^{-7}$
Phosphorescence	$10^{-6}$ - $10^{-3}$

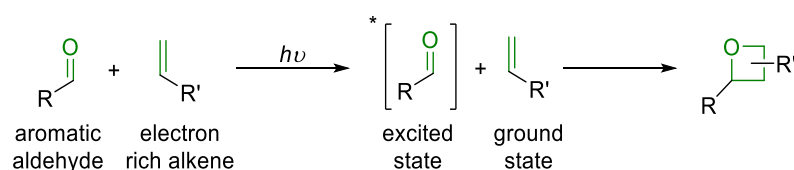
Table 1-1 Relative lifetimes of photophysical processes.<sup>43</sup>

Photochemistry enables access to excited states, allowing for different reactions to take place compared to ground state chemistry. The most common example of the difference in ground state versus excited state chemistry is the [2+2] cycloaddition reaction between two alkenes, which is allowed under photochemical conditions, but forbidden in the ground state. In the ground state, there is not good overlap of the HOMO (highest occupied molecular orbital) and the LUMO (lowest unoccupied molecular orbital) of the two alkenes. Scheme 1-10 illustrates how by absorbing light the alkene's HOMO changes and can overlap efficiently with a LUMO of another alkene, allowing formation of 4-membered ring.



**Scheme 1-10 Summary of the [2+2] cycloaddition reaction between two alkenes under ground state and excited state conditions.**

Of particular relevance to this work is the Paternò-Büchi reaction, which is a [2+2] photoaddition reaction between a carbonyl compound and an alkene to form an oxetane ring (Scheme 1-11).<sup>44</sup> The reaction usually uses the excited state of the aldehyde (or ketone) compound, which reacts with a ground state alkene, and this reaction will be discussed in more detail in the next sections.



**Scheme 1-11 Paternò-Büchi reaction.**

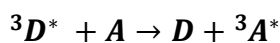
Excited states of molecules are easiest reached by direct irradiation of the molecule, however in some cases that might not be efficient or beneficial to the reaction. Photochemical reactions can take place via singlet or triplet excited state pathways, and often both pathways are possible, which could yield the same or different final product. The next section discusses triplet-triplet energy transfer (TTET), which is the transfer of energy between two molecules.

### 1.2.3 Triplet-triplet energy transfer (TTET)

In some reactions, selectively accessing either the singlet or the triplet excited state selectively is beneficial. For example, in some cases a triplet excited state pathway would yield the desired product but the ISC of the required reagent is slow, or the  $S_1$  energy is high, requiring high-energy irradiation, which can be dangerous. In those cases, the use of a triplet sensitizer can be very beneficial, as a triplet sensitizer can transfer its energy to the reagent, generating the triplet excited state of the reagent directly. Alternatively, an unwanted side reaction could take place via a triplet excited state; in this instance a triplet quencher can be used, which accepts the energy from the triplet excited state of the reagent (blocking the unwanted side reaction). Triplet sensitization and triplet quenching are examples of triplet-triplet energy transfers (TTET).

TTET is described by Equation 1-1 and the Dexter mechanism (Figure 1-9),<sup>45</sup> and is assumed to take place between the lowest triplet states ( $T_1$ ). Figure 1-9 shows that during an energy transfer the donor molecule, D, transfers energy to a neighbouring molecule/acceptor, A. The Dexter mechanism involves a simultaneous exchange of

electrons between the molecular orbitals of the donor and acceptor. For the exchange to take place the relative energy levels need to be similar, and the two molecules need to be physically close together ( $<10\text{\AA}$ ) if the transfer is intermolecular.



Equation 1-1

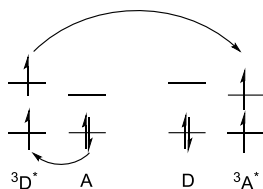


Figure 1-9 Dexter mechanism.

Triplet-triplet energy transfer can be very helpful in photochemistry, allowing access to triplet states of reagents that have a high-energy singlet excited state ( $S_1$ ) (and therefore would need high energy light to undergo excitation) or have a slow/non-existent ISC.<sup>46</sup> Triplet sensitization is irradiation of a donor molecule to access the triplet state of a reagent/acceptor directly without going via the singlet excited state, and it has been used in many different organic reactions.<sup>47</sup> Triplet sensitization and quenching can be easily compared using an energy level diagram (Figure 1-10). For an efficient triplet sensitization reaction there are a few things to consider, in particular, that the triplet energy of the triplet sensitizer (donor) needs to be higher than triplet energy of the reagent (acceptor), as well as the orbital overlap of the donor and acceptor must be good. The opposite process to triplet sensitization is triplet quenching. Triplet quenchers often have a range of triplet states with different energies allowing them to efficiently accept triplet energy from the reagent molecule. The most common examples of triplet sensitizer and triplet quencher are acetone<sup>48,49</sup> and molecular oxygen respectively.<sup>50,51</sup>

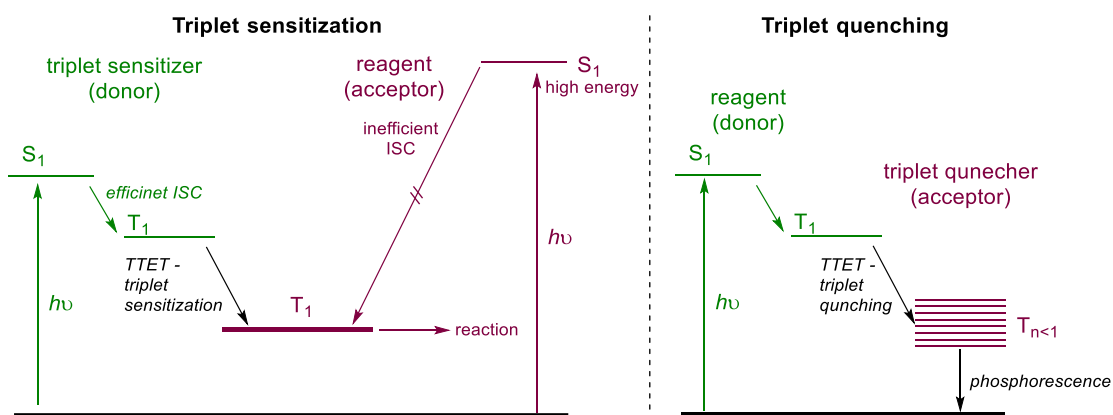


Figure 1-10 Energy diagram showing how triplet sensitization and triplet quenching operate.

### 1.2.3.1 Triplet sensitization

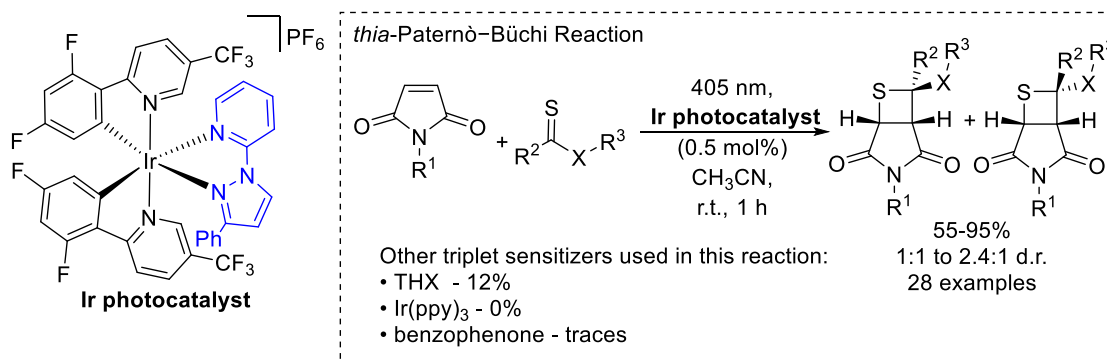
Triplet sensitization is common in organic photoreactions, and over the years various families of different triplet sensitizers have been developed, tested and used in different reactions. In order for the triplet sensitizer to be effective different properties should be considered:

- efficient ISC, which can be achieved by containing a heavy atom (eg. Ir, Pt, Ru, Os, I and Br etc.)<sup>52</sup>
- Strong absorption at the wavelength the triplet sensitizer is used
- The molecular orbitals of triplet sensitizer must overlap well with the molecular orbitals of the reagent.

The three general families of triplet sensitizers are:

- 1) Transition metal complexes
- 2) Iodo- and bromo- substituted organic chromophores
- 3) Heavy-atom free molecules (eg. Benzophenone, thioxanthone (THX))

A recent transition metal complex example from 2021 used iridium-based photosensitizers in a *thia*-Paternò-Büchi reaction (Scheme 1-12).<sup>53</sup> The reaction took place between a maleimide and thioester, and upon testing different types of photosensitisers the product formation was optimized to give 55-95% of the desired mixture of products, with varying diastereoselectivity. It is important to mention that a series of other common sensitizers were tested in the reaction, such as benzophenone and thioxanthone (THX), however in both cases the yield of the reaction was much lower (<12%). During optimization, ten similar Ir photosensitizers were tested, where the ligand in blue varied, all showing excellent yields (71-93%) and small variations of the d.r. (1.3 : 1 to 1.8 : 1). This reaction shows that using the right triplet sensitizer can have a greatly positive effect on the reaction outcome, however it often requires synthesis of a library of different sensitizers, as not all of these iridium complexes are readily available and small changes to only one of the ligands can have an effect on the final yield.



Scheme 1-12 *thia*-Paternò-Büchi reaction with the use of Ir photocatalysts as a triplet sensitizer.

The addition of a heavy atom can help with the efficiency of ISC. This effect is well illustrated by a series of triplet sensitizers derived from BODIPY reported by Zhao and co-workers.<sup>54</sup> The series of chromophores was designed and synthesised, and additional DFT calculations were performed to show the HOMO and LUMO orbitals of the potential triplet sensitizers, as well as to predict the triplet energy levels of the compounds. In theory, it can be very efficient to predict properties of compounds with the use of computational methods as it can allow for much faster and broader studies however, computational methods often must be designed for the specific system, rather than for a broad range of substrates. Four selected chromophores and their properties are shown in Table 1-2. “Unfunctionalized” BODIPY (Table 1-2, entry 1) shows a much lower quantum yield (of ISC) and lifetime of the triplet excited state compared to the other substrates (Table 1-2, entries 24), therefore indicating the clear effect of attaching a heavy atom (in this case iodine). Upon addition of one iodine atom (Table 1-2, entry 1 vs 2), both the lifetime of the triplet excited state (from 0.02 to 66) and the quantum yield of ISC (from 0.228 to 0.964) drastically increases. There is little to no difference between having one or two iodine atoms attached (Table 1-2, entry 2 and 3) as the two substrates show very similar values across all properties. Lastly, attachment of an additional conjugated group (Table 1-2, entry 4) lowered the lifetime of the triplet excited state and decreased its energy level, however the absorption was raised to over 600 nm. The family of BODIPY-based triplet sensitizers are all metal-free and exhibit long triplet excited state lifetimes. A small draw back to these sensitizers is the relatively low triplet excited energy, as this will limit the possible reagents that can be sensitized by these chromophores.



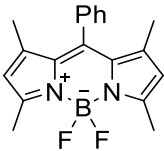
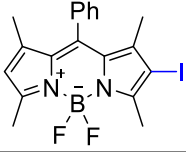
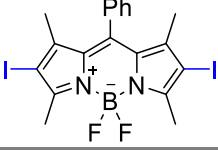
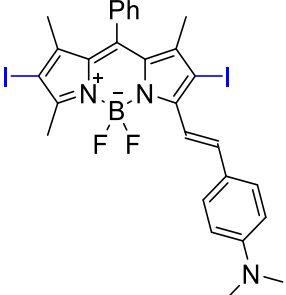
Entry	Structure	$\lambda_{\text{abs}}^{\text{a}}$ (nm)	$\lambda_{\text{em}}$ (nm)	$E(\text{T}_1)$ (kcal mol <sup>-1</sup> )	$\Phi_{\text{ISC}}$	$\tau_{\text{T}}$ ( $\mu\text{s}$ )
1		503	515	35.0 (37.1) <sup>a</sup>	0.228	0.02
2		510	532	34.9	0.964	66
3		529	552	34.6	0.973	57
4		629	706	26.6	0.905	4

Table 1-2 Comparison of properties of different chromophores. a = experimental value.  $\lambda_{\text{abs}}$  = absorption wavelength (in MeCN,  $1 \times 10^{-5}$  M).  $\lambda_{\text{em}}$  = emission wavelength;  $E(\text{T}_1)$  = triplet energy in kcal mol<sup>-1</sup> (predicted by DFT);  $\Phi_{\text{ISC}}$  = quantum yield of ISC (in MeCN);  $\tau_{\text{T}}$  ( $\mu\text{s}$ ) = lifetime of the triplet excited state (measured by transient absorption  $1.5 \times 10^{-5}$  M, MeCN)

The final example of triplet sensitizers that will be discussed are derived from THX (Figure 1-11).<sup>55</sup> Booker-Milburn and co-workers reported a series of THX-derived compounds that can absorb light from UV to visible ranges. In total, eleven substituted THX derivatives were reported, with absorption between 415 and 354 nm. The triplet energies of all were predicted computationally, followed by experimental measurements, showing pleasingly close values between the two methods. Subsequently, the triplet sensitizers were used in a series of different photochemical reactions, showing pleasing results as triplet sensitization took place allowing for a series of different [2+2] cycloadditions reactions. Reactions were completed in NMR tubes to rapidly screen different triplet sensitizers. In general, triplet sensitizers with a triplet energy above 62.3 kcal mol<sup>-1</sup> (THX<sub>a,b,c</sub> vs d) worked well in the [2+2] cycloaddition reaction (66-73% vs 4%). To summarize, Booker-Milburn showed the importance and potential of designing the possible triplet sensitizers computationally before undertaking unnecessary synthesis. Additionally, the family of the triplet sensitizers created had a higher triplet energy compared to previously discussed triplet sensitizers, allowing for sensitizations of molecules with higher triplet energies.

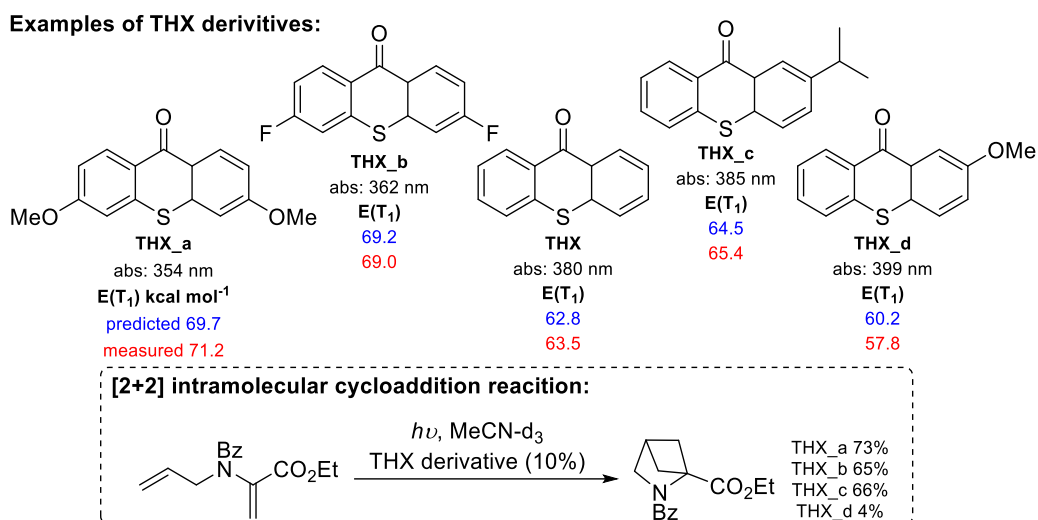


Figure 1-11 Summary of the THX triplet sensitizers and the [2+2] photocycloaddition in which they were used.

Triplet sensitizers can be a great tool in photochemistry, leading to faster and cleaner reactions. However, matching a reaction with a triplet sensitizer can be difficult, as the triplet energies and molecular orbitals of the reagent and triplet sensitizer must match correctly. In general, there is a wider choice if the triplet energy of the reagent is lower. It is important to remember though that some reactions do not take place via the triplet excited state, indeed there are many reactions that proceed via the singlet excited state.<sup>56</sup> However, it can be very difficult to establish a full mechanistic picture for photochemical reactions, as there are many different physical properties that need to be considered. Next, a series of different methods that are used to investigate photoreactions is discussed.

#### 1.2.4 Practical approach to photochemical reactions

Photochemistry gives access to new reactions and transformations, but it is important to remember that there are also new side reactions that can take place, reducing the yield of the desired reaction. This section focuses on practical approaches to photochemical reactions such as choosing reagents and potential mechanistic studies. Understanding photochemical reactions can involve photophysical studies, which can be aided by the study of by absorption and emission spectra.

Choosing photochemical reagents can be difficult, as a series of properties must be considered. When exciting molecules with light, it is pivotal to understand what energy of light is required as well as what energy can be emitted back by the molecule. Photophysical properties can be measured and are often used in mechanistic studies of photochemical reactions. Initially, the absorption spectrum of the reactant(s) must be measured, this can be done with the UV-vis measurement (Figure 1-12A). The collected UV-vis spectrum shows which wavelengths of light are absorbed by a molecule,

additionally the electronic transitions responsible for absorbing the energy can be assigned. The relative energies of the possible transitions are shown in Figure 1-12\_B. For example,  $\pi$ - $\pi^*$  is a common transition that has a higher energy (lower wavelength) than an  $n$ - $\pi^*$  transition, as the energy gap between the  $\pi$  and  $\pi^*$  orbitals is greater than that between the  $n$  and  $\pi^*$  orbitals.<sup>57,58</sup>

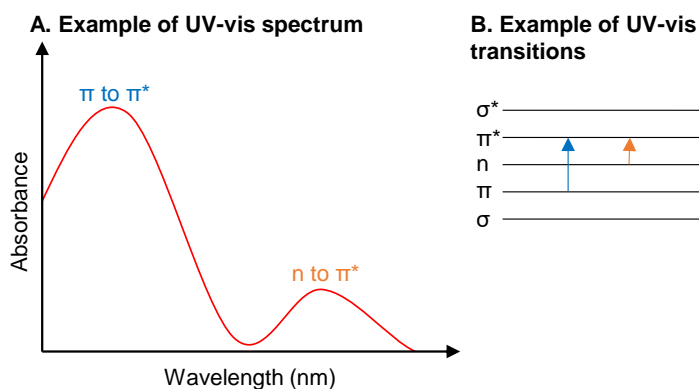


Figure 1-12 Example of a UV-vis and transitions.

One of the most common properties related to the UV-vis spectrum is molar absorptivity ( $\epsilon$ ), which can be described with Beer-Lambert law (Equation 1-2), which assumes that the absorbance ( $A$ ) and the concentration ( $c$ ) of the sample are proportional (with  $l$  = length of the light path).<sup>8,57</sup>

$$A = \epsilon lc$$

Equation 1-2 Beer-Lambert law.

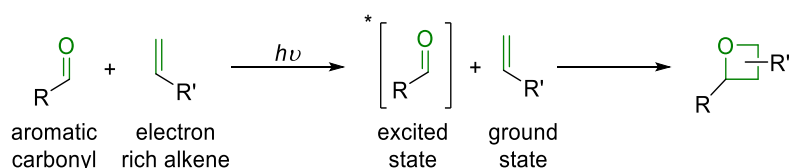
Next, emission spectra can be used to detect any emissions taking place from the excited molecule. During an emission experiment the molecule is excited by using the exact wavelength needed (often based on its absorption spectrum) followed by perpendicular detection of emission (fluorescence or phosphorescence), allowing for measuring the energies of the excited states. Triplet lifetimes is a common method of investigation into photochemical reactions as they indicate the stability of the triplet excited state. Additionally, the effect of different additives on reagent(s) can be measured by tracking the lifetimes of triplet excited states. For example, triplet-triplet energy transfer can be indicated by triplet lifetime experiments, as the value of the triplet lifetime will change.

Overall, photochemistry can be very useful tool in organic chemistry as extra transformations are allowed compared to those possible in the ground state. As it is of particular relevance to this work, next the Paternò-Büchi reaction will be discussed, highlighting the scope of the reaction and showing how different photochemical tools are used in order to understand and optimize reactions.

## 1.3 Paternò-Büchi reaction

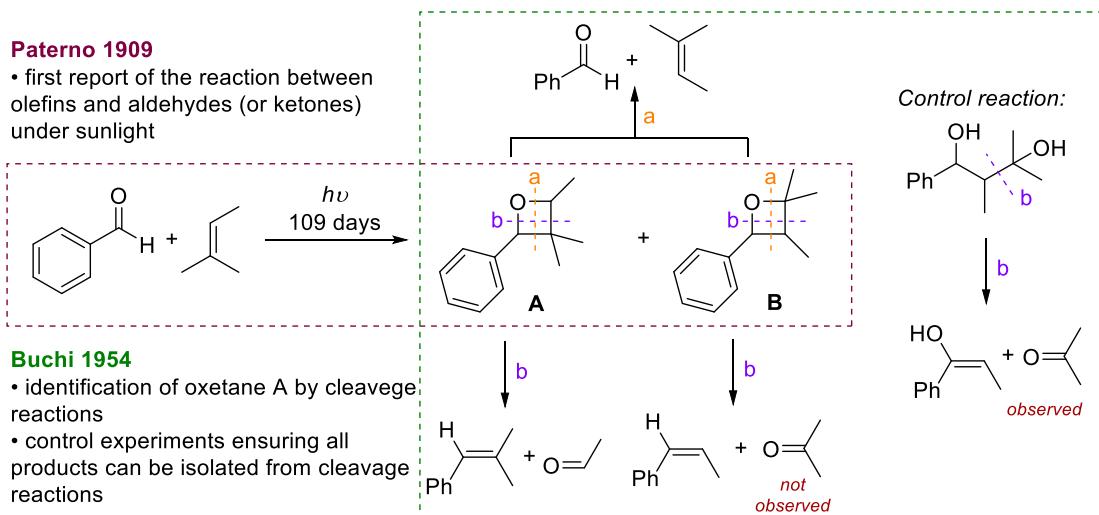
### 1.3.1 History of Paternò-Büchi reaction

The Paternò-Büchi reaction is a photochemical [2+2] cycloaddition reaction to generate oxetanes by formation of the C-O and C-C bond in the same reaction. The traditional Paternò-Büchi reaction requires the excited state of a carbonyl compound (usually an aldehyde or a ketone) reacting with the ground state of an alkene, which can limit the scope of the reaction as electron-rich alkenes and aromatic carbonyls are usually required (Scheme 1-13). However, recent studies showed the possibility of a “transposed” Paternò-Büchi reaction, which takes place between the ground state carbonyl compound and the excited state alkene.



Scheme 1-13 General reaction scheme for the traditional Paternò-Büchi reaction.

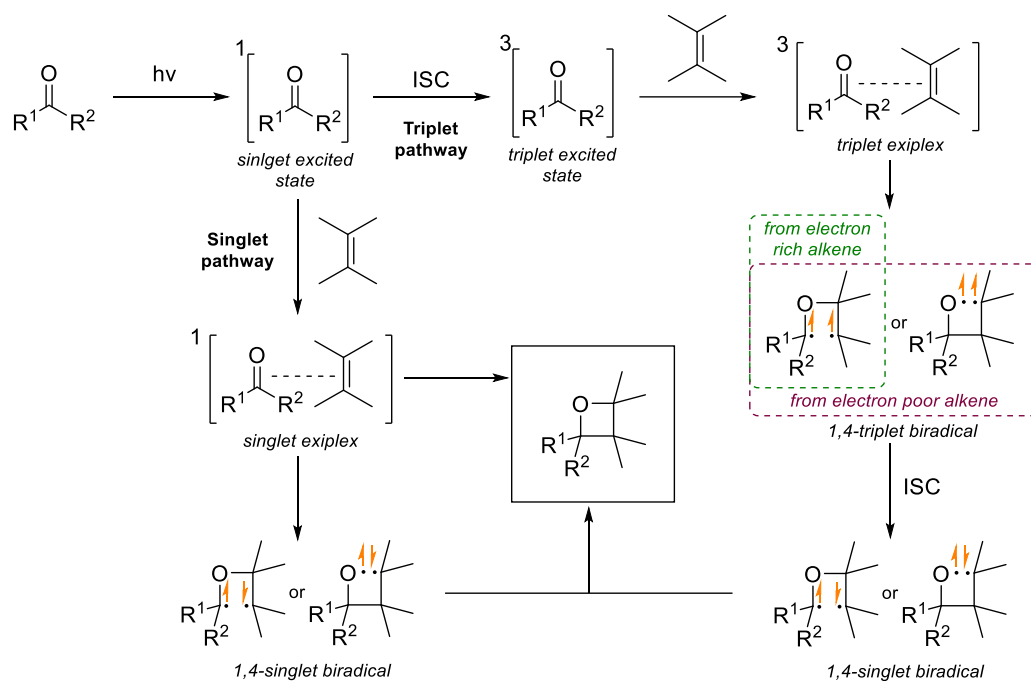
Paternò and Chieffi first reported what is now known as the Paternò-Büchi reaction in 1909,<sup>59</sup> while Büchi and co-workers later investigated the oxetanes formed.<sup>60</sup> The contributions of each team to the reaction is summarized by Scheme 1-14. The Paternò-Büchi reaction was discovered by exposing a solution containing a tri- or tetra-substituted olefin and an aldehyde (or ketone; benzaldehyde used in Scheme 1-14 to illustrate the reaction) to sunlight for 109 days, however the structures of the products were not confirmed at the time. In 1954, Büchi further investigated the reaction and attempted to identify the structures of the products by performing reactions on the formed oxetanes. Depending on the regioselectivity of the oxetane formation, a series of different small molecules can be generated (Scheme 1-14, green box). Cleaving along the *a* axis of oxetane A or B will give the same products, however if the ring was cleaved along the *b* axis, a different set of products was expected, implying oxetane A was formed during the Paternò-Büchi reaction. Control reactions were performed on similar molecules to ensure acetone is not lost during the process Scheme 1-14 (control reaction). Thus, the diol was placed under the same reaction conditions and resulted in the formation and isolation of acetone. Over the years, the Paternò-Büchi reaction was expanded, however in general, the vast majority of the examples focused on the use of aromatic ketones/aldehydes which limits the range of oxetanes that can be formed in the reaction.



Scheme 1-14 Summary of the beginnings of the Paternò-Büchi reaction.<sup>59,60</sup>

### 1.3.2 Mechanism of the Paternò-Büchi reaction

The general reaction mechanism for the Paternò-Büchi is summarized in Scheme 1-15. There are different pathways through which the oxetane can be reached, however in the majority of cases the reaction takes place between an excited state carbonyl compound and a ground state alkene. There are two main possible pathways taking place - singlet and triplet pathway - both pathways give the desired product, however the multiplicity can have an effect on the scope, regio- and stereoselectivity of the final product.<sup>61-63</sup> The singlet pathway takes place via formation of a *singlet exciplex*, which can either form the oxetane ring in one step or form a *1,4-singlet biradical* species, which subsequently reacts to give the final oxetane product. The triplet pathway requires that the carbonyl compound can undergo an efficient ISC process. Next, formation of a *triplet exciplex* intermediate occurs, which can react with the alkene to give one of two *1,4-triplet biradical* species. In general, electron-rich alkenes will prefer to react with the oxygen first, as the oxygen is very electron-deficient, while electron-poor alkenes can attack either the carbon or the oxygen atom. Nonetheless, the final photoproduct of all of these pathways is the same if the alkene is symmetrical. The *1,4-triplet biradical* cannot form the oxetane ring directly as the electron spin forbids bond formation, therefore another ISC process must take place forming the *1,4-singlet biradical*, which can form the final oxetane. The effect of the starting materials on the mechanism and the outcome of the reaction will be discussed next, as part of the discussion on the reaction scope (section 1.3.3).



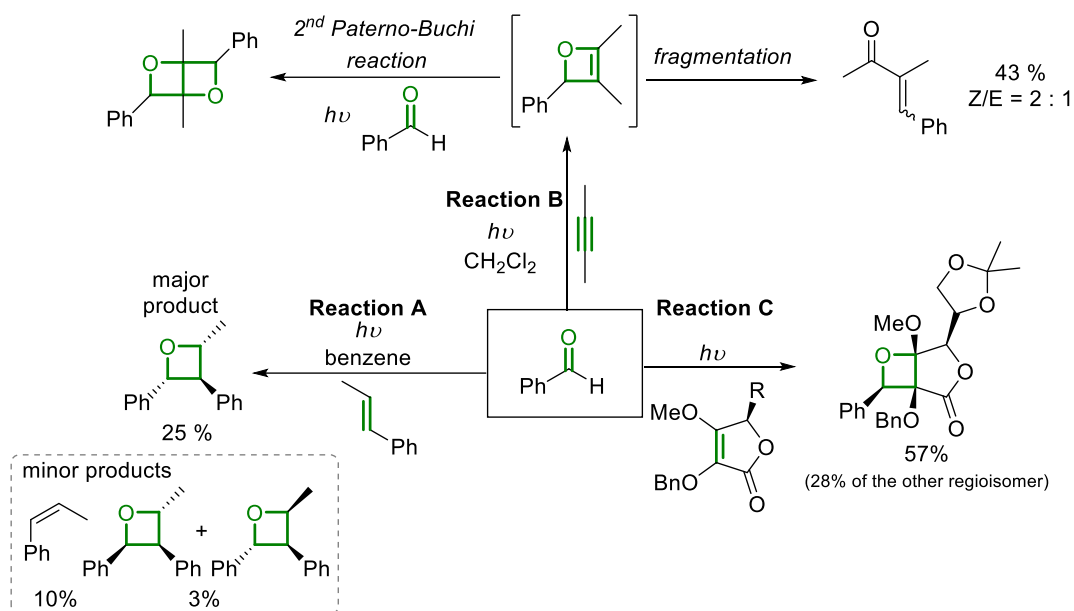
### 1.3.3 Scope of the Paternò-Büchi reaction

The vast majority of the Paternò-Büchi reactions in the literature use an aromatic carbonyl compound and an electron rich alkene to form oxetanes. Scheme 1-16 and Scheme 1-17 show a series of different Paternò-Büchi reaction (reactions A-E) that use benzaldehyde as the carbonyl compound, which can react with different alkenes (and alkynes) to yield oxetanes.

Reaction A,<sup>64</sup> was attempted in order to investigate stereoselectivity of the Paternò-Büchi reaction. The major oxetane product was isolated in 25% yield. The alkene (E-1-phenylpropene) was irradiated in the presence of benzaldehyde (1:1) to give a mixture of products (Scheme 1-16, Reaction A). The alkene used in the reaction underwent double bond isomerization to yield the Z alkene in 10% yield, which can further undergo Paternò-Büchi reaction, adding to the mixture of isomers. Other oxetane products gave a combined yield of 3%, showing good selectivity for the major product. Reaction B<sup>65</sup> uses an alkyne to form an oxetene, which rapidly undergoes a fragmentation to give an enone product (Scheme 1-16, Reaction B). Unfortunately, the formed oxetene can only be trapped at very low temperatures and is generally unstable, however it can undergo an additional Paternò-Büchi reaction to generate a fused bis-oxetane product (yield not reported).

Reactions C, D and E use cyclic alkenes, meaning that the double bond cannot undergo isomerization (as was observed as an energy-wasting process in Reaction A, which also contributes to the loss of stereoselectivity). Reaction C<sup>66</sup> shows poor regioselectivity as it yields a mixture of two products, each in significant amounts. The alkene is based on

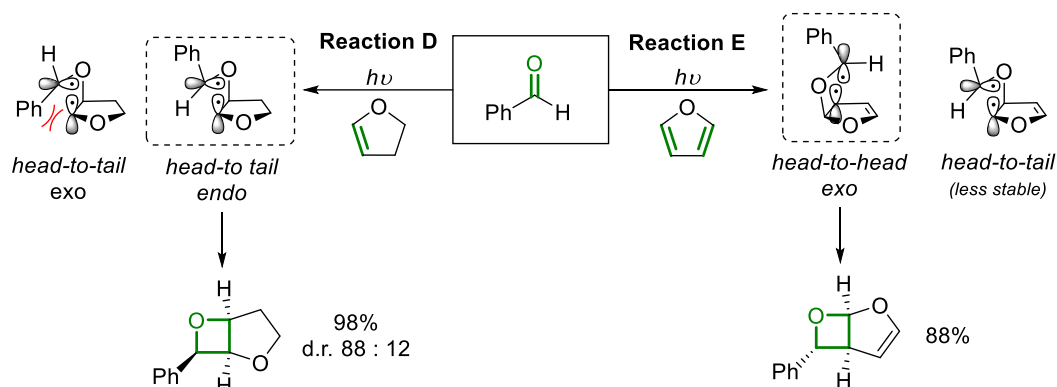
an L-ascorbic acid derivative, containing a chiral centre, which undergoes a Paternò-Büchi reaction with benzaldehyde (and other aromatic carbonyl compounds) to give the desired oxetane in good yield (57% of the major regioisomer was collected). In total, only five examples of these novel oxetanes were isolated, and whilst additional transformations involving cleavage of the oxetane ring worked well, attempted removal of the benzyl group only yielded starting material.



**Scheme 1-16** Examples of Paternò-Büchi reaction between benzaldehyde and varied alkenes (and alkyne).

Reactions D and E (Scheme 1-17) can show opposite result based on the alkene used, in the case of reaction D, high *endo* selectivity<sup>67,68</sup> is observed as well as *head-to-tail* arrangement of the two fused rings, while reaction E shows a *head-to-head* arrangement of the fused rings and high *exo* selectivity.<sup>69</sup> Reaction D takes place *head-to-tail* due to stabilizing effect of the oxygen on the intermediate biradical, while the *endo* selectivity is due to the sterics, as shown the radical resulting in an *exo* product has unfavourable steric interactions. The most stable and most likely radical intermediate is shown in Scheme 1-17.

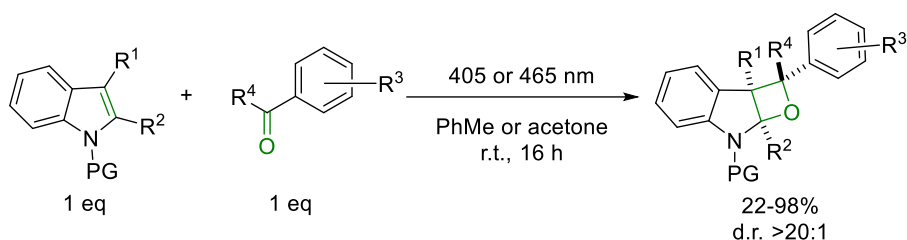
Reaction E takes place between furan and benzaldehyde. Furans (and their derivatives) are commonly used in the Paternò-Büchi reactions, yielding oxetane-containing bicyclic molecules. The stability of the biradical intermediate formed is responsible for the regioselectivity observed the *head-to-tail* radical intermediate is less stable by 16.5 kcal mol<sup>-1</sup><sup>70</sup> than the *head-to-head* radical intermediate, which benefits from allylic stabilization. To summarize, whilst the scope of the Paternò-Büchi reaction is relatively broad when benzaldehyde (or a similar aromatic carbonyl compound) is used in the reaction, this requirement for an aromatic carbonyl compound does restrict the diversity of oxetane products that can be generated using this approach.



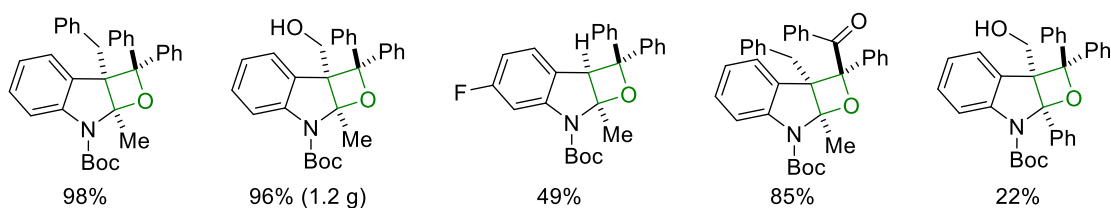
Scheme 1-17 Examples of Paternò-Büchi reaction between benzaldehyde and varied alkenes.

### 1.3.3.1 Visible light Paternò-Büchi reaction

More recently in 2020, a visible light Paternò-Büchi reaction was reported by Dell'Amico and co-workers.<sup>71</sup> Upon optimization the reaction took place at 405 or 465 nm, using indoles reacting with aromatic ketones; 35 examples of novel oxetanes were isolated in 22 to 98% yield (Scheme 1-18). The mechanism was theorized to go via the singlet excited state of the ketone, which next underwent efficient ISC in order to reach its triplet excited state. The reaction mechanism was confirmed by performing a reaction with (1,4-diazabicyclo[2,2,2]octane (DABCO), which efficiency quenches the triplet excited states of the ketones used in the reaction.



Selected examples:



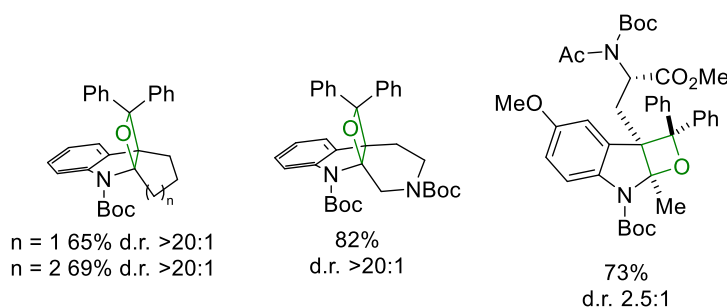
Scheme 1-18 Visible light Paternò-Büchi between indole and aromatic ketone.

Importantly, the reactions involve dearomatization of the indole ring, in order to access oxetanes with a higher proportion of  $sp^3$  atoms, as that is of interest in the pharmaceutical industry. The same reaction conditions were used, and eight oxetanes were isolated (selected examples in Scheme 1-19\_A); in some cases, the d.r. decreased but percentage isolated yields were comparable with the reaction shown in Scheme 1-18. Although the reaction worked with the selected indoles, in some cases these required synthesis. Additionally, expanding the reaction to benzofuran or benzothiophene did not

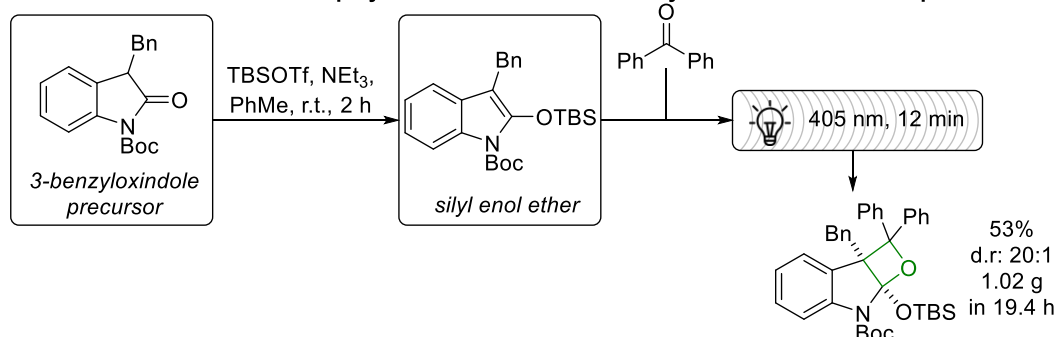


work well, showing 0 and 13% NMR yield respectively. Lastly, the reaction was even further expanded by using 3-benzyloxindole precursor (Scheme 1-19\_B) to form silyl enol ethers which underwent Paternò-Büchi reaction with benzophenone.<sup>72</sup> A microfluidic system was designed in order to form the silyl enol from the precursor, followed by reacting it in the Paternò-Büchi reaction with benzophenone. Microfluidics use micro-channels allowing for efficient light penetration required for the reaction, although not all reactions can use this method as any precipitate formation could block the channels. Nevertheless, the reaction of oxindole enol ethers with benzophenone gave satisfying results. The reaction gave the isolated oxetane in good yield, and over a gram of desired product could be isolated by running the microfluidic system for over 19 hours.

**A: Selected examples of oxetanes formed from dearomatized indoles and benzophenone.**



**B: Microfluidic method for two-step synthesis of oxetane from silyl enol ether and benzophenone**



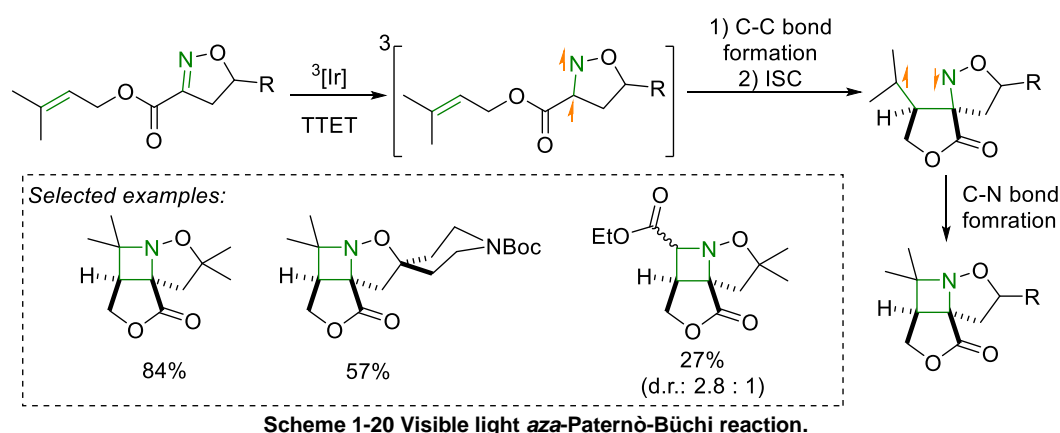
**Scheme 1-19 A:** Selected examples of oxetanes formed from dearomatized indoles and benzophenone. **B:** Microfluidic method for two-step synthesis of oxetane from silyl enol ether and benzophenone.

Overall, these reactions showed how limiting Paternò-Büchi reaction can be as changing either of the reagents often results in failure of the reaction. Additionally, although the indoles used were partially dearomatized, the ketone used in the reaction was not. This exposes a gap in the possible scope of the Paternò-Büchi reaction - use of non-aromatic ketones/aldehydes are very rare.

### 1.3.3.2 aza-Paternò-Büchi reactions

There are also versions of Paternò-Büchi reactions that make other 4-membered heterocyclic rings. For example, a *thia*-Paternò-Büchi reaction has already been shown in Scheme 1-12. The Paternò-Büchi reaction was also expanded to making azetidines

from an alkene and imine.<sup>73</sup> Schindler and co-workers have reported a series of different visible light [2+2] cycloadditions which form azetidines or azetines rings.<sup>74,75</sup> In 2022, Schindler and co-workers reported an intramolecular visible light *aza*-Paternò-Büchi reaction (Scheme 1-20);<sup>76</sup> similarly to the other reported reactions, the 4-membered ring was formed with the used of visible light and an iridium photocatalyst, and the reaction was tested with 20 different photocatalysts with triplet energy ranges between 55-61 kcal mol<sup>-1</sup>. The proposed reaction mechanism took place by using the iridium catalyst to transfer energy to the imine from triplet state of the catalyst, which then undergoes C-C bond formation to form a 1,4-biradical species which finally undergoes ISC to allow the final C-N bond formation to yield the desired product. Overall, the reaction worked well, giving highly functionalized azetidines, however the reaction relied on the triplet-triplet energy transfer, which was most efficient with the use of a specific iridium catalyst; a control reaction with no photocatalyst showed lack of reaction.

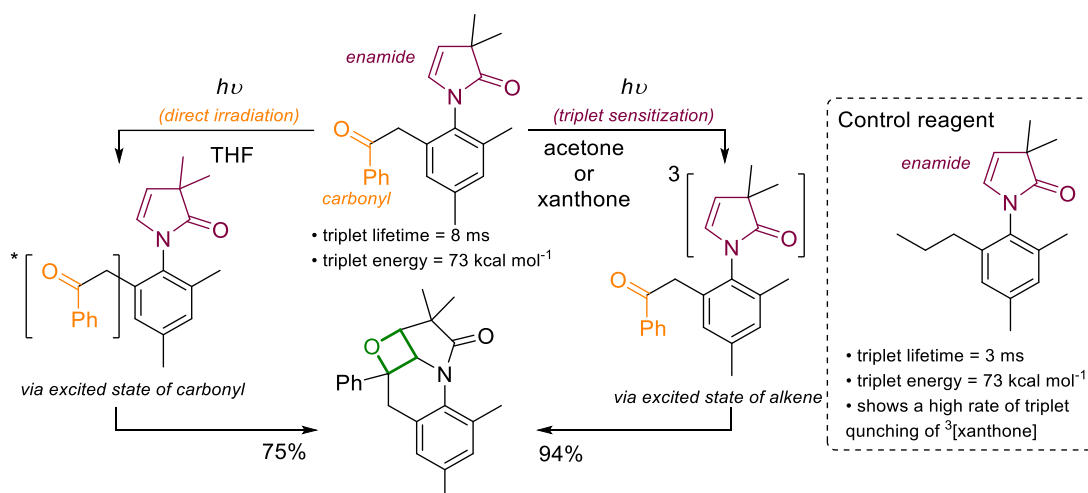


Use of visible light in photochemistry can be useful, however it can limit which reagents can be used, as they need to absorb visible light in order to reach their excited state, this often leads to very aromatic systems. Alternatively, rare metal catalysts or other photocatalyst are used in order to transfer the triplet energy, this can be difficult as the reagent and triplet sensitizer must match well in terms of triplet energies and molecular orbital overall, which can often limit scope of the reactions.

### 1.3.3.3 “Transposed” Paternò-Büchi reaction

Mechanistically, Paternò-Büchi reactions generally take place via the excited state of a ketone/aldehyde reacting with a ground state alkene. In 2017, a “transposed” Paternò-Büchi reaction was reported,<sup>77</sup> which took place via the excited state of the alkene in the intramolecular Paternò-Büchi reaction (Scheme 1-21). The starting enamides were formed in up to four steps, with the Paternò-Büchi reaction using acetone (or xanthone) to access the triplet excited state of the alkene. Under direct irradiation the reaction took place via the classic pathway, i.e. the excited state of the ketone reacting with the ground

state of the alkene. Alternatively, the enamide alkene triplet excited state was reached via triplet energy transfer, supported by photophysical and computational studies. A series of photophysical studies was performed on the reagents used in the photochemical reactions as well as on a series of control compounds. For example, the carbonyl group was removed and replaced with an alkyl chain; this allowed for accurate measurement of the triplet energy and triplet lifetime of the enamide unit (Scheme 1-21, control reagent). It was established that the triplet excited state of the xanthone can be quenched by the starting material as well as by the control reagent, meaning the enamide unit can accept the energy from xanthone and access its triplet excited state. This implied that a triplet excited alkene pathway can also be responsible for formation of the product. However, it is important to remember the same product is reached via direct irradiation of the carbonyl group on the starting material. This is an important example, as it both expands on the possibilities of the Paternò-Büchi reaction by implementing an alkene excited state pathway, and also shows that photochemical reactions can yield the same products via very different reaction pathways.



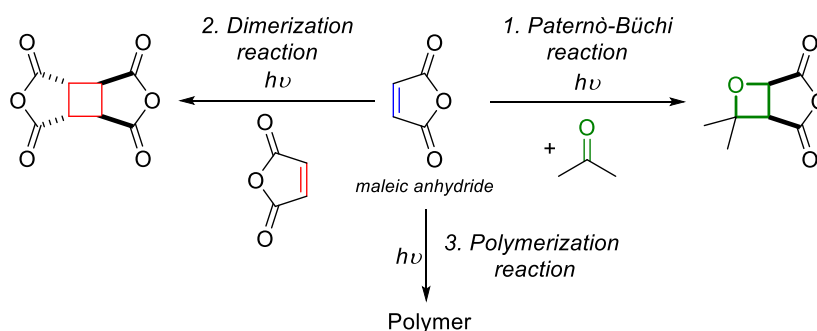
Scheme 1-21 Summary of the Paternò-Büchi reaction pathway via excited state of carbonyl or alkene ("transposed" Paternò-Büchi reaction).

#### 1.3.3.4 Paternò-Büchi reaction of aliphatic ketones and electron-poor alkenes

In 1967,<sup>78</sup> Turro and Wriede reported a Paternò-Büchi reaction between alkyl ketones and electron-poor alkenes, which was followed in 1969,<sup>79</sup> with a Paternò-Büchi reaction between acetone and maleic anhydride. The paper focused mainly on the reactions of 1,2-dicyanoethylene with aliphatic ketones, although the use of maleic anhydride as an alkene was also briefly mentioned. Although reaction with maleic anhydride yielded the desired oxetane, competing side reactions of maleic anhydride led to abandoning the reaction, as it was thought that the reaction did not hold much potential for the synthesis of oxetanes. There were a total of three reactions taking place during irradiation of maleic anhydride in acetone (Scheme 1-22):

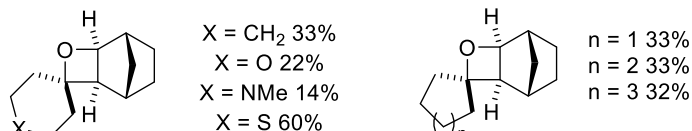
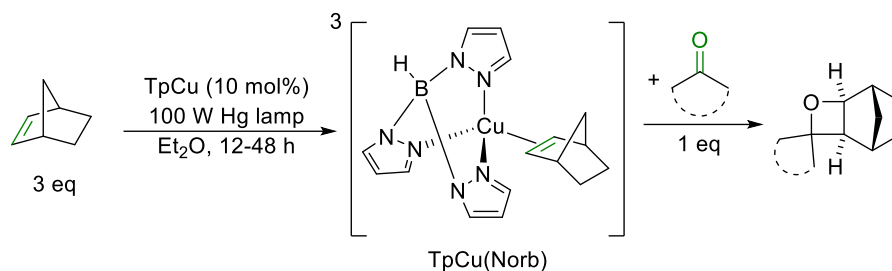
- 1) The desired Paternò-Büchi reaction
- 2) Dimerization of maleic anhydride
- 3) Polymerization of maleic anhydride

The Paternò-Büchi reaction takes place between an aliphatic ketone (acetone or cyclic ketones) and an electron poor alkene (maleic anhydride), which is a combination of reagents rarely seen in the Paternò-Büchi reaction due to a variety of potential side reactions of both the alkene and the ketone. As mentioned before, acetone is a known triplet sensitizer, therefore it is difficult to establish the reaction mechanism for this reaction, and although the reaction between 1,2-dicyanoethylene with alkyl ketones<sup>80</sup> was further mechanistically investigated, the corresponding reaction with maleic anhydride was not pursued further, despite the interesting nature of the bicyclic oxetane product formed.



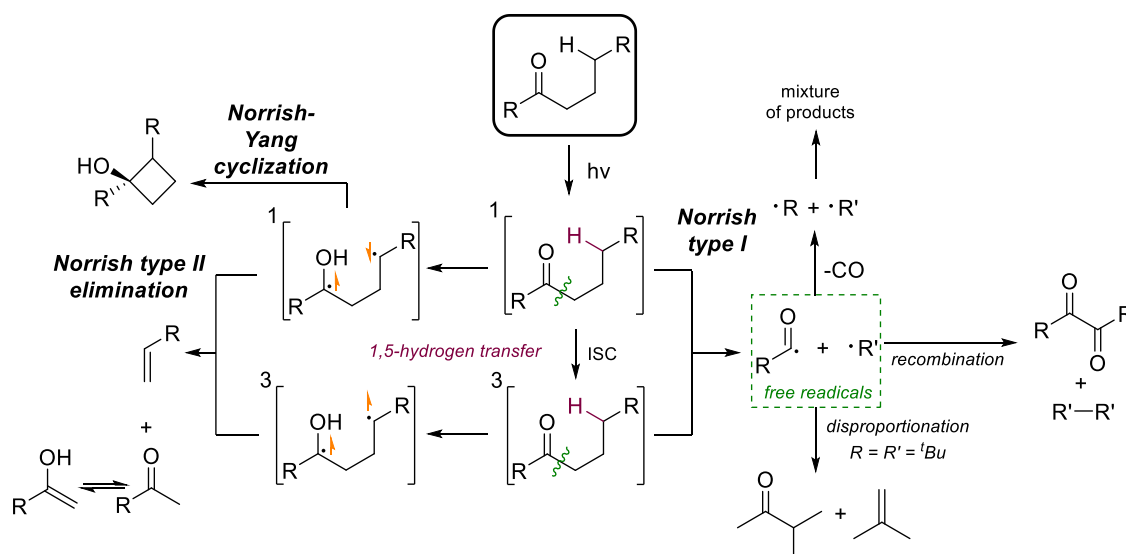
**Scheme 1-22** Photochemical reactions taking place during irradiation of maleic anhydride in acetone: dimerization of maleic anhydride polymerization and Paternò-Büchi reaction.

In 2019, Schmidt and co-workers<sup>81</sup> published a [2+2] carbonyl-olefin photocycloaddition between cyclic aliphatic ketones and norbornene in the presence of copper catalyst. Nine oxetane were reported in up to 76% isolated yield. Importantly, NMR yields were much higher for most of the examples than the isolated yields, and the loss of product was attributed to oxetane degradation on silica during purification. The reaction gave access to oxetane containing spirocycles, however it was limiting as the reaction only worked for norbornene reacting with a small library of ketones; 22 other alkenes and 28 other carbonyl compounds were tested in the reaction, showing traces or no oxetane forming. Importantly, a  $\text{TpCu}(\text{Norb})$  complex was reported to be formed, which was the basis of the mechanism for the reaction, the  $\text{TpCu}(\text{Norb})$  complex allowed for triplet energy transfer to norbornene which then reacted with the ketone forming the oxetane product. This reaction avoided direct irradiation of the carbonyl compound, which can lead to side reactions and often requires high energies. However, the scope of the reaction was very limiting, as only a handful of the tested reagents gave the desired oxetane.



**Scheme 1-23 [2+2] carbonyl-olefin photocycloaddition between cyclic aliphatic ketone and norbornene in the presence of copper catalyst.**

When a side reaction decreases the possible yield of the desired reaction, the side reaction can be avoided by using specific reagents, or suppressed. Aliphatic ketones are particularly prone to break down photochemically upon irradiation, which needs to be considered when they are chosen as a reagent for a photochemical reaction. Ketones can undergo Norrish type I, II and Norrish-Yang reactions (Scheme 1-24), and although those reactions are relatively simple, they are generally undesired as they lead to fragmentation, and can give rise to mixture of products, lowering the possible yield of the desired product. Norrish type I occurs when the C-C bond alpha to the carbonyl is cleaved. This forms two free radicals. Then, a series of elimination, recombination and disproportionation reactions take place to give a variety of products. Norrish type II and Norrish-Yang cyclization start with a 1,5-hydrogen atom transfer, followed by elimination or cyclization reaction respectively.<sup>82</sup>



**Scheme 1-24 Side reactions of carbonyls.**

The relevant side reactions of alkenes have been mentioned before, particularly the isomerization of the C=C bond, although this can be avoided by using cyclic alkenes. As

shown in the case of maleic anhydride, dimerization (and polymerization) of alkenes can take place upon irradiation, and often decreases the yield of the desired product if these processes are not desired.

To summarize, Paternò-Büchi reactions give 4-membered heterocycles – usually oxetanes in the strict sense, although variations that generate azetidines and thietanes are also known. Classical Paternò-Büchi reactions involve the formation of the oxetane ring from a carbonyl compound (in its excited state) and an alkene (in its ground state). The scope of the reaction is reasonably broad, with many different oxetanes being formed from the reaction of aromatic carbonyl compounds with electron rich alkenes. However, the use of aliphatic carbonyl compounds and electron poor alkenes is much less common. A handful of electron-poor alkenes have been used in the Paternò-Büchi reaction – in some cases showing a different mechanism (“transposed” Paternò-Büchi reaction via the excited state of the alkene). In particular, Turro and Wriede demonstrated that a Paternò-Büchi reaction is possible between acetone and maleic anhydride, but the reaction was abandoned due to the side reactions taking place, and the synthetic potential of the reaction and of the interesting oxetane products generated has therefore not been established.

#### **1.4 Conclusions**

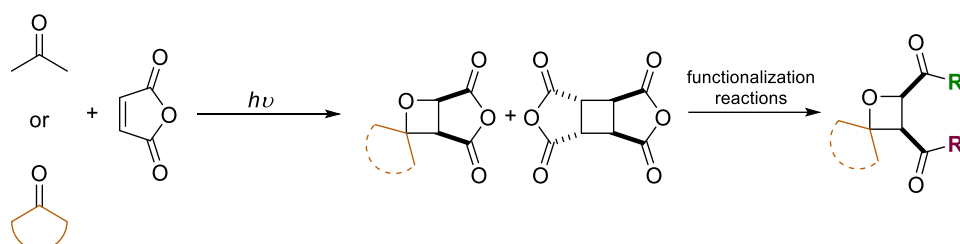
Oxetanes are important motifs in pharmaceutical and medicinal chemistry, as they show potential as replacement groups for metabolically vulnerable groups such as ketones. Additionally, oxetane-containing drugs and natural products are valuable compounds, and often their properties can be affected by the presence of the oxetane ring.

The formation of oxetane rings is possible via ground state chemistry, with four main methods of forming the 4-membered ring. Some of these reactions, like the Williamson etherification, are very well established and often used in synthetic pathways, but usually a specific starting material must be used in order to form the desired oxetane. Additionally, formation of spirocyclic oxetanes (which are particularly interesting from a medicinal chemistry perspective) using this approach often requires many steps. Conversely, the Paternò-Büchi reaction allows for rapid formation of oxetanes as two bonds are formed during the reaction (C-C and C-O). Paternò-Büchi reactions take place between a carbonyl compound and an alkene, and although the scope of the reaction is good, as many different aromatic carbonyl compounds and electron-rich alkenes can be used in the reaction, the main limitation of the Paternò-Büchi is that it is often limited to aromatic ketones/aldehydes, as their excited states are easier to reach, and they do not undergo photochemical fragmentation reactions. Using aliphatic ketones/aldehydes is

not very common in the Paternò-Büchi reaction, mainly because they also undergo photochemical fragmentation reactions upon irradiation, which can compete with a desired Paternò-Büchi reaction. However, the use of such aliphatic ketones/aldehydes would open up access to novel libraries of oxetanes. Rare “transposed” Paternò-Büchi reactions show that the Paternò-Büchi reaction might not always need the excited state of the carbonyl compound to form the oxetane ring. Turro and Wriede’s reaction between acetone and maleic anhydride shows a very “non-standard” Paternò-Büchi reaction that employs an aliphatic ketone and an electron-deficient alkene, however due to the competing side reactions the investigation into the reaction was incomplete. Nevertheless, the successful expansion of the Paternò-Büchi reaction between aliphatic carbonyl compounds and electron poor alkenes would give access to new oxetanes.

### 1.5 Aims of the project

The overarching aim of the project is expanding the scope of the Paternò-Büchi reaction by using aliphatic ketones and electron poor alkenes to give a series of novel oxetanes. Specifically, the project will focus on the reaction of maleic anhydride with aliphatic ketones, to produce bicyclic products that could then be derivatised through nucleophilic ring-opening of the anhydride ring.



Scheme 1-25 Summary of project aims.

This reagent pairing is uncommon in Paternò-Büchi reactions, as discussed above, but would allow access to functionalised oxetanes that cannot be accessed using existing methods.

Firstly, the Paternò-Büchi reaction between acetone and maleic anhydride will be optimized in both batch and flow. The optimization studies will aim to increase the selectivity for oxetane products, to allow isolation of pure oxetane products, and where possible, to suppress the competing side reactions of the maleic anhydride.

Next, the reaction between cyclic aliphatic ketones and maleic anhydride will be investigated, aiming to generate a library of currently inaccessible spirocyclic oxetane products. These reactions are expected to be more complex than those employing acetone, as the aliphatic ketone can no longer be used as both reagent and solvent, so

further optimization of the reaction is expected. The optimized methodology will then be applied to other electron-deficient alkenes to establish the scope of the reaction.

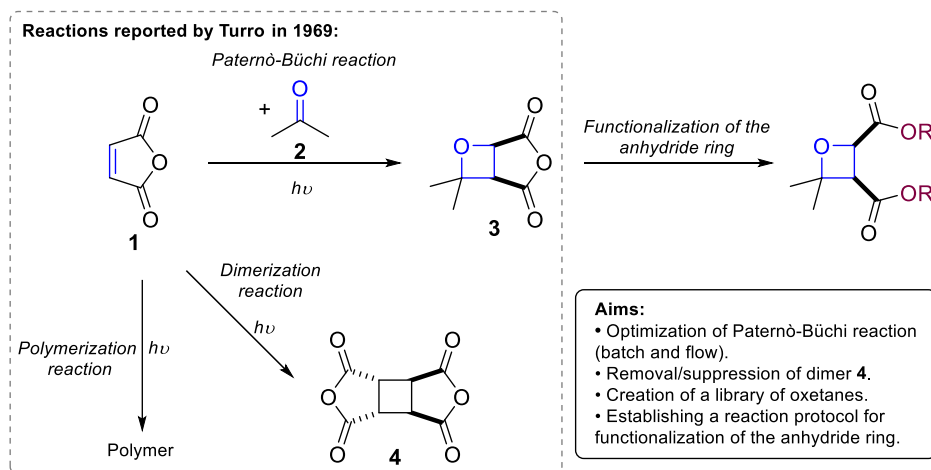
Throughout, relevant mechanistic studies will be carried out to aid in understanding the reactions, which will be crucial for the successful development of the methodology.



## Chapter 2 Paternò-Büchi reaction between maleic anhydride and acetone

### 2.1 Introduction and Chapter Aims

This chapter describes the investigations into the Paternò-Büchi reaction between maleic anhydride (**1**) and acetone (**2**), first reported by Turro in 1969 (Scheme 2-1).<sup>79</sup> Turro tested reactions between different aliphatic ketones and maleic anhydride, but due to competing side reactions (dimerization and polymerization of maleic anhydride) the reactions were not fully investigated and were thought to be synthetically unpromising. If optimized, the reaction could give rapid access to novel oxetanes, formed from aliphatic ketones and electron deficient alkenes, a combination that is uncommon for Paternò-Büchi reactions.<sup>44,83,84</sup> The literature review (Chapter 1) discusses the photochemistry of aliphatic ketones and activated alkenes and summarizes the possible side reactions leading to the complex mixture of products. To recap, the simple starting materials used in the reaction can give rise to a very complex mixture of products via different photochemical pathways. Additionally, the focus on maleic anhydride will generate oxetane products **3** with an adjacent anhydride ring, which will allow for further functionalization reactions through nucleophilic ring-opening reactions, facilitating access to a wide range of oxetane products.



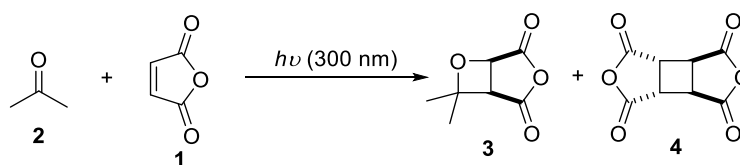
Scheme 2-1 Summary of previous work done by Turro in 1969 and aims of the work reported in this chapter.

Establishing all the reaction pathways taking place can be very complex and requires an in depth understanding of each individual reaction taking place. It is important to mention that acetone is a known triplet sensitizer and can influence photochemical reactions by triplet energy transfer, adding to the complexity of the possible reaction mechanism (Chapter 1). The main aim of this chapter was to establish a practical reaction protocol for the Paternò-Büchi reaction between an aliphatic ketone and maleic anhydride, as

well as the subsequent functionalization reactions. The mechanism of the reaction was difficult to establish and a detailed investigation is discussed in Chapters 3 and 4.

## 2.2 Optimization of the Paternò-Büchi reaction

The optimisation of the Paternò-Büchi reaction focused on the concentration of the reaction mixture (with respect to maleic anhydride), the number of equivalents of the ketone reagent, and the reaction time. Photochemical reactions are often run very dilute, since it can be difficult for light to penetrate well into more concentrated solutions, and this can make scaling up the reactions challenging. Detailed set-up of batch and flow photoreactions that is relevant to this reaction is described in section 2.2.1. - set up and general information. Due to the likely issues with scale up of the reaction, the performance of a flow photoreactor was compared to that of a batch photoreactor. The first reaction tested involved the Paternò-Büchi reaction between maleic anhydride and acetone to give oxetane **3** and dimer **4** (Scheme 2-2). Both of these products are a result of [2+2] cycloaddition reactions – the formation of **3** involves [2+2] photocycloaddition of maleic anhydride with acetone, whilst the generation of **4** involves the dimerization of maleic anhydride. It is important to add that the polymerization reaction of maleic anhydride also likely takes place during irradiation, however it was not observed during the reaction by <sup>1</sup>H NMR. Polymers are much heavier and the signals in their <sup>1</sup>H NMR spectra are often broad, and in this case it was not possible to observe polymer formation via <sup>1</sup>H NMR spectroscopy.



Scheme 2-2: Possible products of the Paternò-Büchi reaction between maleic anhydride (1) and acetone (2), and dimerization reaction of maleic anhydride (1).

### 2.2.1 Set-up and general information

All batch reaction were run in a Rayonet RPR-100 batch photoreactor, which are efficient and common reactors for organic photochemistry. The reactor allows for a number of parallel reactions to be performed at the same time, allowing for rapid reaction scoping. The reaction vessels were Pyrex/Duran glass tubes, which allowed for light to be transmitted through the glass (>285 nm). The lamps predominantly used in this project were 300 and 350 nm, although the lamps emit a range of light around the specified wavelength - emission spectra in Figure 2-1 show the wavelengths emitted by the 300 and 350 nm lamps. Rayonet batch photoreactors allow for relatively large-scale reactions, however, to further increase the reaction scale as well as decrease the

reaction time, optimization of photochemical reactions under flow conditions was performed. A Vapourtec UV-150 photochemical reactor was used for the flow reactions, equipped with a mercury lamp with filter to cut off wavelengths below 300 nm. Although a flow reactor can allow for a continuous photochemical reaction to take place, practically it is often challenging as the cooling system can easily fail, leading to overheating of the reactor and reaction mixture. Reactions were tested under both batch and flow conditions, with the following sections discussing the advantages and disadvantages of both set-ups.

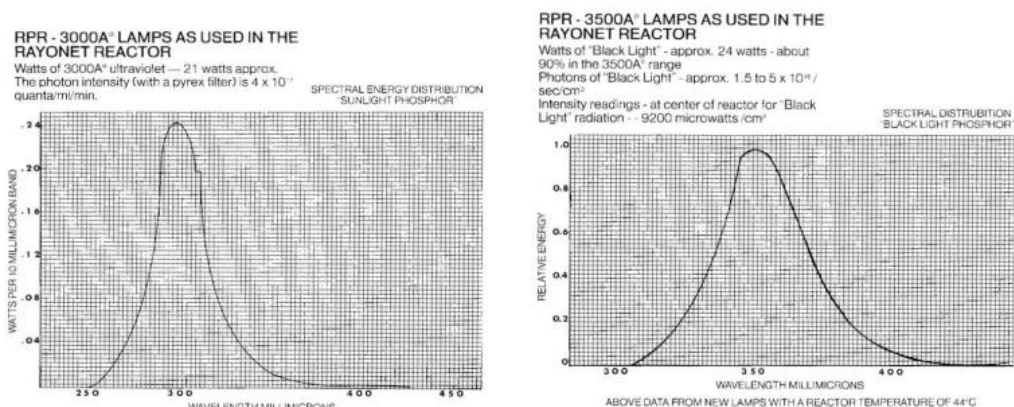


Figure 2-1 The emission spectra of the lamps used during the project, 300 nm lamps on the left, and 350 nm lamps on the right.

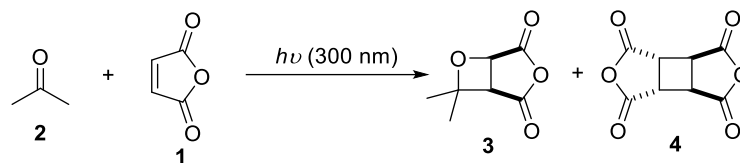
The reactions were tracked by <sup>1</sup>H NMR spectroscopy with solvent suppression, in which the largest signal (from the non-deuterated solvent employed) is suppressed, allowing straightforward analysis of the contents of the sample (the method can also be modified to use solvents that exhibit more than one <sup>1</sup>H NMR signal, by suppressing a defined number of signals). This sampling method is very effective, as it does not require deuterated solvents, and the reaction components can be directly observed without isolation from the solution, which is particularly useful for the observation of intermediates that are unstable out of solution. In this case, a 0.5 mL sample was taken out of the reaction flask and analysed by <sup>1</sup>H NMR spectroscopy.

### 2.2.2 Batch reaction Paternò–Büchi reaction

Firstly, the Paternò–Büchi reaction was performed between maleic anhydride and acetone, with acetone used in excess as the solvent, in a batch photoreactor, irradiating with 300 nm lamps. Two products were observed in the reaction: **3**, which is the desired product, and dimer **4**, which is an undesired side product. In addition, polymerization of maleic anhydride is likely to occur (as noted in the seminal work by Turro), but this polymer was not clearly visible by <sup>1</sup>H NMR spectroscopy, and no attempt was made to quantify any polymeric material formed. The reaction progress was followed by <sup>1</sup>H NMR spectroscopy with solvent suppression; and irradiation was continued until all of the

maleic anhydride was consumed. The resulting  $^1\text{H}$  NMR spectra were used to calculate the conversion of the maleic anhydride into **3** and **4** (Figure 2-2), the calculations only include the observed three reagents: **1**, **3** and **4**. Additionally, the anhydride ring was observed to be sensitive to water in the air, undergoing a nucleophilic ring opening to give the corresponding diacid, and this reaction was especially prominent during longer reaction times, traces of the diacid were not included in the calculations of the percentage of the reagents in the reaction mixture. By following the reaction by  $^1\text{H}$  NMR spectroscopy, the formed product remained in solution, thus minimising its exposure to air, which decreased the undesired and uncontrolled ring opening of anhydride by water.

The concentration of the maleic anhydride was varied to observe its effect on the rate of conversion into **3** and **4**. Different reaction concentrations were tracked at different reactions times by  $^1\text{H}$  NMR spectroscopy (solvent suppression, in acetone) to assess the content of the reaction mixture, and the results are shown in Table 2-1. Reactions run at lower concentrations (up to 0.10 M) were completed in under 6 hours (Figure 2-2, Entries 1-4). The more concentrated reactions took more time (as expected, due to less efficient light penetration) showing <8% of maleic anhydride still present after 24 hours of irradiation for concentrations in the range 0.12-0.20 M (Table 2-1, Entries 5-9). Substrate concentrations of 0.50 and 1.00 M were also tested (Table 2-1, Entries 10 and 11), but were stopped before full conversion, due to crystals of dimer **4** forming on the side of the reaction tube, which made effective irradiation impossible, drastically slowing reaction progress. In addition, the precipitated dimer **4** in these runs resulted in a less accurate estimation of the proportion of oxetane **3** and dimer **4**, as not all of the dimer **4** was in the solution, thus analysis by  $^1\text{H}$  NMR spectroscopy underestimates the amount of dimer formed. Interestingly, the overall trend linking the concentration of maleic anhydride and the formation of the two products was counter intuitive. It was expected that as the concentration of the maleic anhydride increases, the amount of the formed dimer **4** will also increase, as there is a higher likelihood of the two maleic anhydride molecules reacting together. However, this was not the case, as the general trend showed that as the concentration of the maleic anhydride increases, less of the unwanted dimer **4** is formed compared to the desired oxetane **3** product, as shown in Table 2-1 (best seen by comparing the reaction composition at 2 h reaction time). This trend is currently not fully understood and cannot simply be attributed to dimer **4** precipitating from solution, as this trend was still observed even at intermediate concentrations, when no precipitation occurred.



Entry	[1]	% of reagents in the reaction mixture at different reaction times																													
		1 h			2 h			3 h			4 h			5 h			6 h			24 h			48 h			72 h					
		3 (%)	4 (%)	1 (%)	3 (%)	4 (%)	1 (%)	3 (%)	4 (%)	1 (%)	3 (%)	4 (%)	1 (%)	3 (%)	4 (%)	1 (%)	3 (%)	4 (%)	1 (%)	3 (%)	4 (%)	1 (%)	3 (%)	4 (%)	1 (%)	3 (%)	4 (%)	1 (%)			
1	0.04	16	24	60	<b>36</b>	<b>64</b>	<b>0</b>																								
2	0.06	13	13	75	23	23	53	29	40	31				40	56	4	<b>38</b>	<b>62</b>	<b>0</b>												
3	0.08	11	8	81	20	16	65	26	24	50				43	48	9	<b>48</b>	<b>52</b>	<b>0</b>												
4	0.10	10	6	84	19	13	67	26	21	53				42	42	17	<b>48</b>	<b>52</b>	<b>0</b>												
5	0.12	10	5	85	19	11	70	26	16	58				42	33	25	53	42	5	<b>59</b>	<b>41</b>	<b>0</b>									
6	0.14				13	7	80				26	13	62				40	20	40	<b>77</b>	<b>23</b>	<b>0</b>									
7	0.16				10	5	85				20	8	73				29	12	59	71	21	7									
8	0.18				10	4	86				19	8	74				29	11	60	71	21	7									
9	0.20				10	4	86				19	6	75				30	9	61	77	15	8									
10 <sup>a</sup>	0.50				5	2	93				16	5	79				16	5	79	67	7	27	<b>89</b>	<b>11</b>	<b>0</b>						
11 <sup>a</sup>	1.00				4	1	95				10	3	87				10	3	87	29	3	68	60	5	36	<b>95</b>	<b>5</b>	<b>0</b>			

Table 2-1 Results of the effect of the concentration on the Paternò-Büchi and dimerization reaction. The table shows the percentage of the reagents in the reaction mixture based on <sup>1</sup>H NMR analysis (solvent suppression, acetone, 400 MHz), the integrations are showed in detail Figure 2-2. All of the reaction were run at 10 mL scale, with 0.5 mL of solution taken out of the reaction for testing. a = <sup>1</sup>H NMR analysis performed two weeks later due to NMR fault.

The conversions presented in Table 2-1 were calculated by integrating the relevant signals after analysis of aliquots of the reaction by  $^1\text{H}$  NMR spectroscopy with solvent suppression (an internal standard was not used – see section 3.2.3 for more detail). Maleic anhydride exhibits a singlet at 7.76 ppm ( $\text{H}^{\text{A}}$ ) in acetone, and as shown by the spectra (Figure 2-2), the amount of the maleic anhydride decreases as the amount of **3** and **4** increases. Protons  $\text{H}^{\text{B}}$  and  $\text{H}^{\text{C}}$  from oxetane **3** appear as two very characteristic doublets, whilst all of the C-H signals in dimer **4** are equivalent and therefore appear as a singlet ( $\text{H}^{\text{D}}$ ). The percentage of reagents in the reaction mixture was used to assess the progress of the reaction was calculated based on  $^1\text{H}$  NMR.

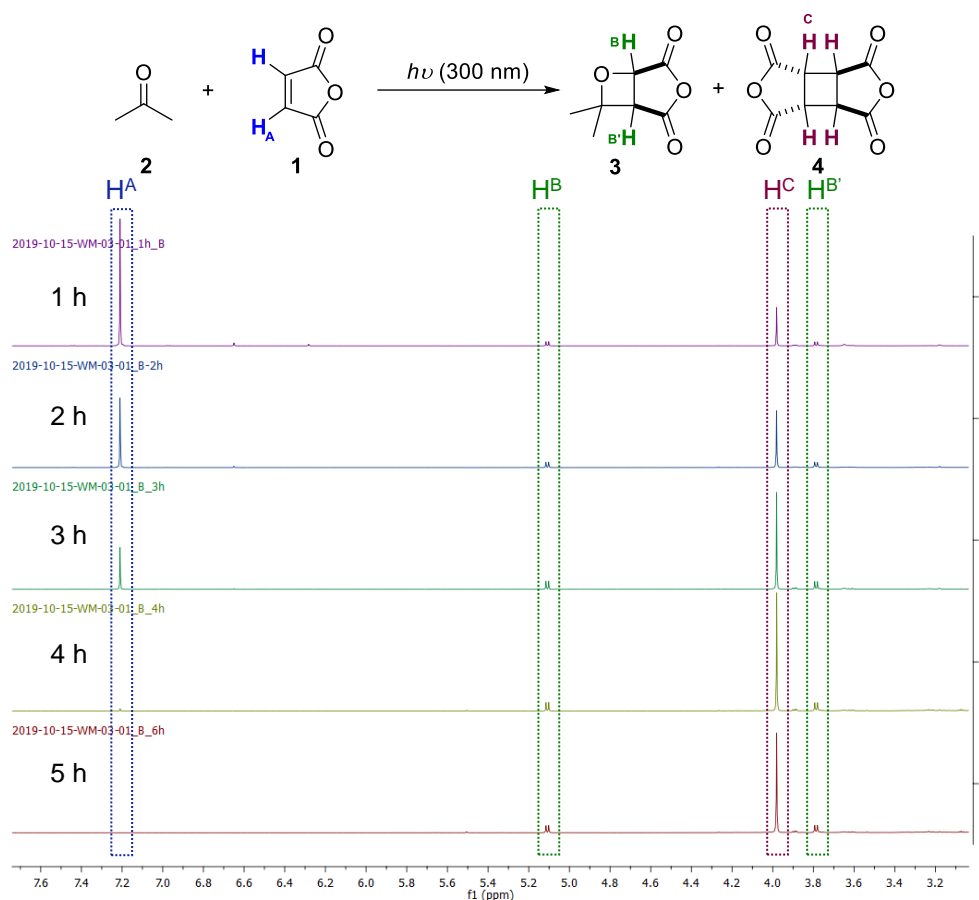


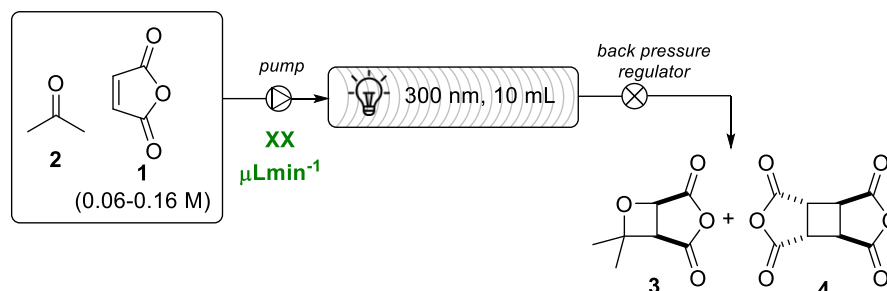
**Figure 2-2** Examples of  $^1\text{H}$  NMR spectra of aliquots taken from the Paternò-Büchi reaction of maleic anhydride (with acetone (spectra recorded at 400 MHz in acetone with solvent suppression; [maleic anhydride = 0.06 M])

These initial studies confirmed the results first published by Turro and Wriede, and allowed the development of an effective method for the observation of the progress of the reaction using  $^1\text{H}$  NMR spectroscopy. In addition, some potential issues were identified, which would need to be taken into account upon optimisation for effective scale-up. In particular, dimer **4** is an undesired side product, which is highly crystalline, and which precipitates readily from acetone even at relatively dilute concentrations. The presence of the dimer **4** complicates the analysis of the reaction, limits the yield of the desired oxetane **3** product and slows the reaction progress. It was hoped that running

the process in a flow reactor might allow for more straightforward Paternò–Büchi reaction, and these studies are discussed in the next section.

### 2.2.3 Flow reaction Paternò–Büchi reaction

Due to the very low concentrations generally involved in photochemical reactions, flow reactors are often used to facilitate scaling up a reaction. The main risk of using a flow reactor for this reaction is the possible formation and crystallization of dimer **4**, which could clog the tubes and block the reactor. To start with, three concentrations of maleic anhydride were chosen to find the optimal concentration and flow rate for the reaction (Scheme 2-3, Figure 2-3). Pleasingly, the time required for complete consumption of maleic anhydride was decreased upon changing from the batch reactor to the flow reactor, and this allowed the rapid formation of a large amount of **3** to be used in further reactions. Reactions of different concentrations showed the same general trend in decrease of the consumption of starting material with increased flow rate. Flow photoreaction of maleic anhydride at 0.16 M required at least 30 minutes irradiation time in the flow photoreactor for full consumption of maleic anhydride (which is equal to flow rate of 0.333 mL min<sup>-1</sup> in a 10 mL column). At faster flow rates the consumption of maleic anhydride decreased, to 66% at 0.500 mL min<sup>-1</sup> (20 min irradiation time). Ideal flow rates for each concentration and percentage of dimer **4** and oxetane **3** present during testing flow rates are described in Table 2-2, and in each case ~10 mL of solute was collected.



Scheme 2-3 Paternò-Büchi reaction between acetone and maleic anhydride (1) under flow conditions.

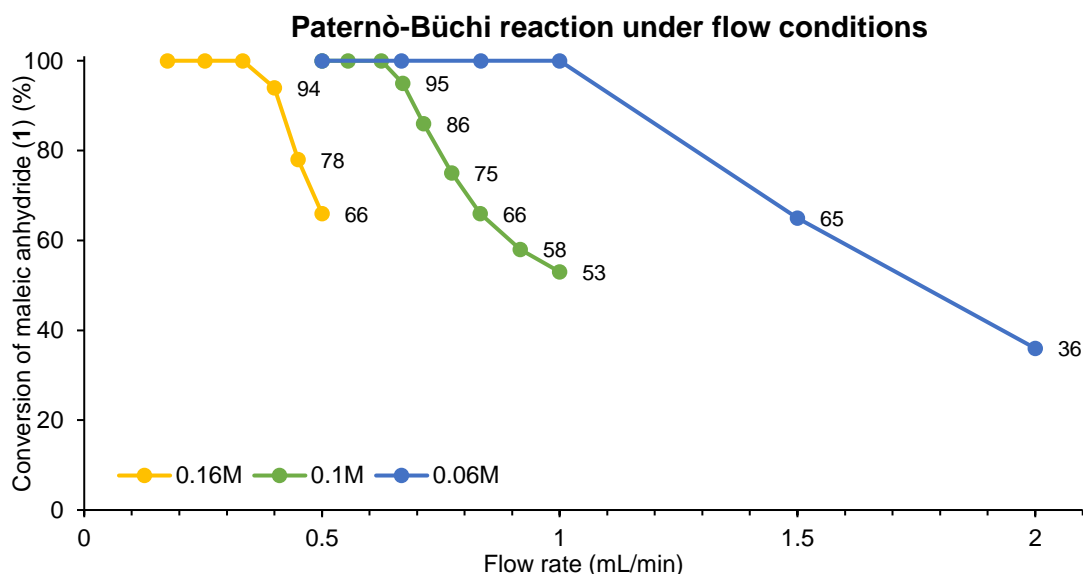


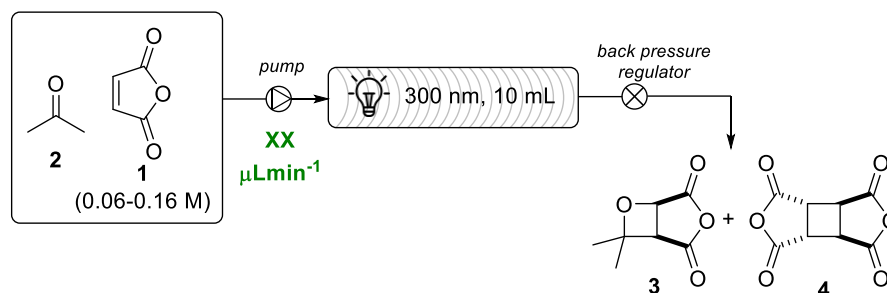
Figure 2-3 Consumption of maleic anhydride (1) in flow reactions at different flow rates and concentrations (0.16 M, 0.1M and 0.06 M with respect to maleic anhydride (1)). Flow column volume = 10 mL.

Entry	[1] in acetone	Flow rate (mL/min)	Exposure time (min)	3 (%)	4 (%)
1	0.16	0.333	30	68	32
2	0.10	0.625	16	52	48
3	0.06	1.000	10	47	53

Table 2-2 Optimized flow rates and exposure times for full consumption of maleic anhydride (1) at different concentrations of maleic anhydride (1), as well as percentage of oxetane 3 and dimer 4 in the reaction mixture based on  $^1\text{H}$  NMR (solvent suppression, acetone, 400 MHz).

Again, the composition of the reaction mixture was tracked at different stages, showing the consumption of maleic anhydride and formation desired oxetane **3** and dimer **4**. Reaction at 0.06 M (Table 2-3) requires only 10 minutes of the exposure time which is a great decrease from the 6 hours needed when reaction is performed under batch conditions (Table 2-1). Additionally, Table 2-3 entries 1-3 show that flow rate has no effect on the ratio of the formed oxetane and dimer. Table 2-4 and Table 2-5 show the results for the 0.1 and 0.16 M flow reactions respectively, and the other concentrations followed the same trend.





Entry	Flow rate ( $\mu\text{m min}^{-1}$ )	Exposure time (min)	3 (%)	4 (%)	1 (%)
1	500	20	45	55	0
2	667	15	48	52	0
3	1000	10	46	54	0
4	1500	7.5	31	33	36
5	2000	5	20	15	65

Table 2-3 Results of Paternò-Büchi reaction between acetone and maleic anhydride (1) under flow conditions at 0.06 M. Percentage of the reaction mixture based on  $^1\text{H}$  NMR (solvent suppression, acetone, 400 MHz).

Entry	Flow rate ( $\mu\text{m min}^{-1}$ )	Exposure time (min)	3 (%)	4 (%)	1 (%)
1	250	40	58	42	0
2	500	20	54	46	0
3	556	18	53	47	0
4	625	16	53	47	0
5	714	14	47	39	14
6	833	12	38	28	34
7	833	12	42	33	25
8	1000	10	34	19	47
9	2000	5	24	13	63

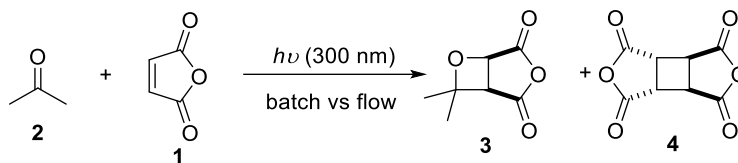
Table 2-4 Results of Paternò-Büchi reaction between acetone and maleic anhydride (1) under flow conditions at 0.10 M. Percentage of the reaction mixture based on  $^1\text{H}$  NMR (solvent suppression, acetone, 400 MHz).

Entry	Flow rate ( $\mu\text{m min}^{-1}$ )	Exposure time (min)	3 (%)	4 (%)	1 (%)
1	167	60	31	69	0
2	250	40	33	67	0
3	333	30	35	65	0
4	400	25	29	65	6
5	416	24	25	53	22
6	450	22	25	54	21
7	500	20	22	44	34

Table 2-5 Results of Paternò-Büchi reaction between acetone and maleic anhydride (1) under flow conditions at 0.16 M. Percentage of the reaction mixture based on  $^1\text{H}$  NMR (solvent suppression, acetone, 400 MHz).

In the case of this reaction, the flow photoreactor worked very well, greatly decreasing the time necessary for the reaction to reach completion. Table 2-6 compares the results of reactions with different concentrations of maleic anhydride in acetone, showing the rate of formation of oxetane **3** in mmol per hour (mmol/h). The flow reactions can easily produce over 1 mmol/h, compared to batch reaction, which even at 200 mL scale cannot

reach 1 mmol/h, with the best batch result given by a 0.1 M concentration of maleic anhydride, leading to 0.2 mmol/h output.



Entry	[1] in acetone (2)	Flow output (mmol/h)	Batch output - 200 mL reaction (mmol/h)
1	0.16	2.2	0.1
2	0.10	1.4	0.2
3	0.06	1.1	0.1

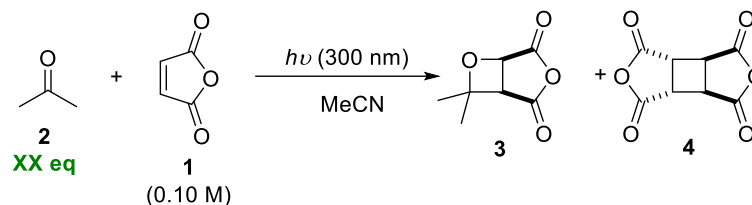
Table 2-6 Comparison of Paternò-Büchi reaction under batch and flow conditions. mmol/h calculated based on the full conversion reactions adjusting for the formation of the dimer 4.

Although the switch from batch to flow did allow a significant increase in the productivity of the reaction, it was still necessary to use relatively low concentrations of maleic anhydride, and even then, very slow flow rates were required for full consumption of maleic anhydride. These factors limit the amount of material that can be processed, and the flow reactor would need to be run for a considerable time to produce multigram quantities of oxetane products, whilst also requiring large volumes of acetone. In addition, so far acetone has been used as both the reagent and as the solvent, so is present in great excess compared to maleic anhydride. With the ultimate aim of a process suitable for multigram-scale, and compatible with other ketones (some of which will be solids and/or expensive), the use of the ketone reagent as the solvent would not be viable, and the next section describes attempts to reduce the equivalents of the ketone required for successful reaction, whilst also moving away from acetone as a solvent.

#### 2.2.4 Reducing the amount of acetone under batch and flow conditions

By changing the reaction solvent to acetonitrile, different numbers of equivalents of acetone could be tested, the goal of these reactions being to find the lowest loading of acetone needed for successful reaction. Starting in the batch reactor, five parallel reactions were followed by  $^1\text{H}$  NMR spectroscopy with solvent suppression (using acetonitrile as solvent), and stopped after 30 hours. Reactions with 10-20 equivalents of acetone went to completion in that time (Table 2-7, Entries 3-5). Fewer equivalents of acetone (1 and 5 equivalents) did not reach completion after 30 h (Table 2-7, entries 1 and 2). In the case of one equivalent of acetone, none of the desired product 3 was observed, while using five equivalents, 7% of the maleic anhydride was still left after 30 hours of irradiation. Comparing these results to reactions that use acetone as solvent

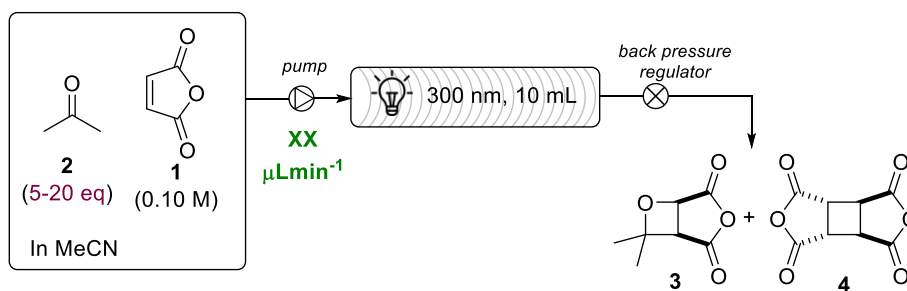
(Table 2-7, Entry 6) is very useful – it shows that only 10 equivalents of the carbonyl compound are needed for the reaction to be fully completed after 30 hours of irradiation.



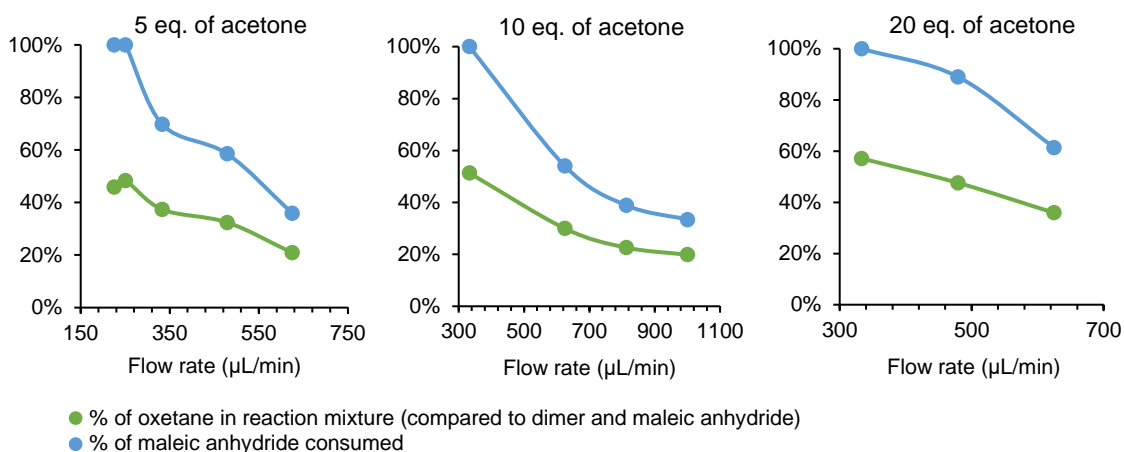
Entry	2 (eq)	3 (%)	4 (%)	1 (%)	Reaction time (h)
1	1	0	45	55	30
2	5	40	53	7	30
3	10	51	49	0	30
4	15	56	44	0	30
5	20	57	43	0	30
6 <sup>a</sup>	Excess	59	41	0	6

Table 2-7 Results of optimization of the Paternò-Büchi reaction between acetone (2) and maleic anhydride (1) in acetonitrile. a = reaction in acetone. Detailed results in Chapter 6.

Again, to reduce the time of the reaction, the flow reactor was used. 5 equivalents of acetone were necessary for the reaction to be completed after 40 minutes irradiation time, (Figure 2-4). The reaction with 10 and 20 equivalents of acetone were both completed after 30 minutes of exposure (equivalent to flow rate of 333  $\mu\text{L}/\text{min}$ ). The three graphs show the consumption of maleic anhydride (blue line) as well as percentage of the oxetane **3** present in the reaction mixture (compared to dimer **4** and maleic anhydride, green line).



Scheme 2-4 Results of optimization of the Paternò-Büchi reaction between acetone (2) and maleic anhydride (1) in acetonitrile under flow conditions.



**Figure 2-4 Percentage of consumption of maleic anhydride (1) in the flow reaction and percentage of oxetane 3 present in the reaction mixture.**

Overall, the initial optimization of the Paternò-Büchi reaction between acetone and maleic anhydride was successful. The reaction was translated from batch to flow conditions, which greatly improved the reaction time from 48 h to 30 minutes (concentration of maleic anhydride = 0.16 M). To summarize, the oxetane product **3** was isolated in 35-60 % yield (depending on batch/flow and reaction size), and the calculation of the ratio of **3** to **4** was based on  $^1\text{H}$  NMR spectroscopy. To obtain pure oxetane product, **3**, separation of the dimer **4** from the oxetane **3** was required, but chromatography of oxetane-anhydride **3** was unlikely to be successful. Thus, removal of the dimer **4** was attempted through (re)crystallization processes, which are described in the next section.

### 2.2.5 Removal of the dimer **4**

Dimer **4**, the undesired side product formed in the reaction, is highly crystalline, and can be partially removed from the crude product mixture by crystallization, increasing the purity of the oxetane **3** to over 85 %. After the reaction was completed and all maleic anhydride was consumed, the solvent was removed, and while the solvent was evaporating, crystals of the dimer **4** would crash out of the solution. This allowed for simple removal of the dimer **4** by filtering it out of the reaction mixture. The drawback to this reaction protocol was the ring opening of the anhydride ring, which took place when **3** is exposed to air for too long (Figure 2-5). Both compounds are very similar, however they can be easily distinguished using  $^1\text{H}$  NMR spectroscopy, by comparison of the coupling constants between protons A and B in each case – the coupling constant in **5** being much larger than that in **3**.

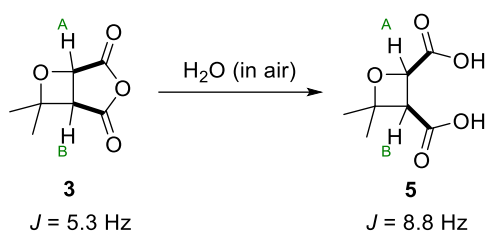


Figure 2-5 Reaction of **3** with water and comparison of  $J$  values of  $H^A$  and  $H^B$  of **3** and **5**.

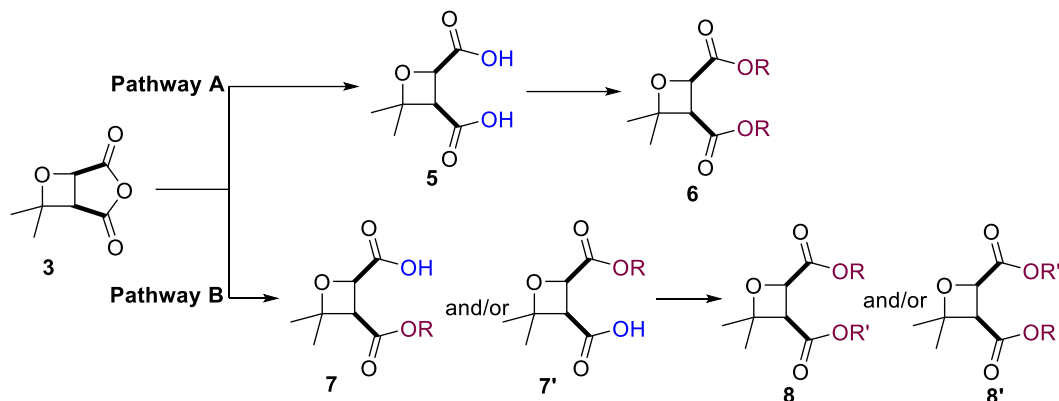
For example, a large scale flow reaction, with reaction time of 2 hours, for 40 mL of photolysate solution yielded 681 milligrams (65% yield) of oxetane **5** (contaminated with 5% of **4**) after the crystallization protocol. Tracking the reaction by  $^1\text{H}$  NMR spectroscopy shows that over 75% of the anhydride opened before the recrystallization, and the final 25 % of anhydride was opened during recrystallization. However, the partial purification of the oxetane **3** was still possible by crystallization of **4** – the reaction mixture was initially contaminated with 22% of the dimer **4** (meaning 44% of the available maleic anhydride was converted into this undesired side product).

The issue of ring opening of the anhydride was not observed during the optimization reactions, as these reactions were not exposed to air for extended periods. Overall, during the reaction and purification a compromise must be reached – more dimer **4** can be removed if more solvent is removed (thus crystallization and filtration is slower), but this leads to exposure to air (and water) resulting in the opening of the anhydride ring. As retaining the anhydride ring intact was a priority (so that two different functional groups could be formed from the anhydride ring through intentional ring-opening with a variety of nucleophiles), the competing ring-opening with water led to difficulties in obtaining pure oxetane products, and a loss of control of the ring-opening reaction. Quick and efficient recrystallization was key to the purification of oxetane **3**, as well as performing subsequent functionalization reactions immediately after purified oxetane **3** was collected. Ideally, the Paternò–Büchi and subsequent ring opening reaction should be run in the telescoped fashion, to reduce exposure of the cycloadduct **3** to air, and more easily isolate pure oxetane products.

### 2.3 Nucleophilic ring-opening of the anhydride

There are a variety of methods for the symmetric and asymmetric ring opening of anhydride rings. The first ring-opening reactions investigated in this project have a common goal of forming two ester groups from the anhydride ring (Scheme 2-5). Starting from **3**, there are three possible pathways to make two esters. Firstly, a dicarboxylic acid (**5**) can be formed through nucleophilic attack by water, and then alkylation or esterification of the resulting carboxylic acids (Scheme 2-5, Pathway A) to form the final product **6**. Secondly, **7** or **7'** could be formed from the anhydride ring through ring-

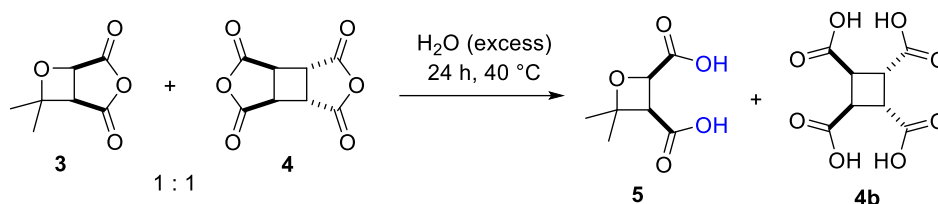
opening with an alcohol (Scheme 2-5, Pathway B), followed by esterification of the resulting carboxylic acid to give **8** and/or **8'**. Although the pathway B could lead to mixture of products, it could give rise to two different ester groups on the oxetane ring, greatly improving the further functionalization possibilities.



Scheme 2-5 Possible reaction pathways for opening of the anhydride ring on **3**.

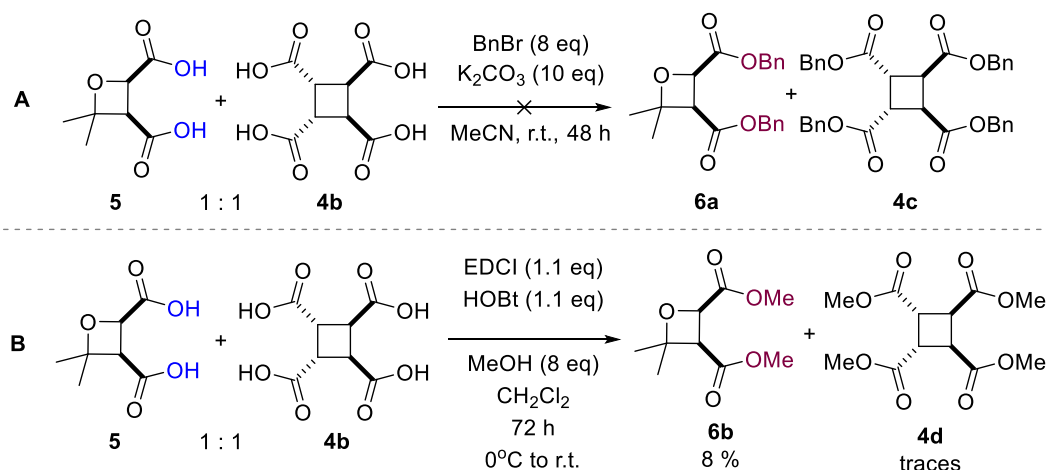
The advantage of the second approach is the possibility of forming two different ester groups by employing different alcohols in the two steps, whereas the first approach would result in two identical ester groups (**6**). Two different ester groups (**8/8'**) would be advantageous if they could subsequently be derivatized independently of each other, but the anhydride ring in **3** can potentially be opened at either of the carbonyl groups, which could lead to mixture of products **7** and **7'** (and therefore **8/8'**) if this ring-opening process is not selective. At the outset, it was not clear which of the carbonyl groups would be most reactive to nucleophilic attack, thus ring-opening was attempted with water and series of alcohols. All of the yields presented in this section are based on **3**, which as described above, usually contained a small amount of dimer **4**, as complete purification of **3** was not possible.

Initial reactions were performed on partially purified **3**, as the purification method was still in development at this stage, and the ratio of **3** and **4** in the starting material is stated for each reaction. Starting with pathway A, water was used to open the anhydride ring on **3** and form **5**, which contains two carboxylic acids. This reaction worked well, and after heating the reaction mixture at 40 °C for 24 hours, full conversion of the starting materials **3** and **4** was observed (Scheme 2-6). An excess of water was used to ensure full conversion of both starting materials (i.e. dimer **4** contains two anhydride rings and will also react under the chosen reaction conditions, consuming twice as much water per molecule as oxetane **3**). Dicarboxylic acid **5** could not be obtained in pure form, therefore esterification of the carboxylic acids was necessary to allow chromatographic purification.



Scheme 2-6 Ring opening of anhydride ring on oxetane **3** with water.

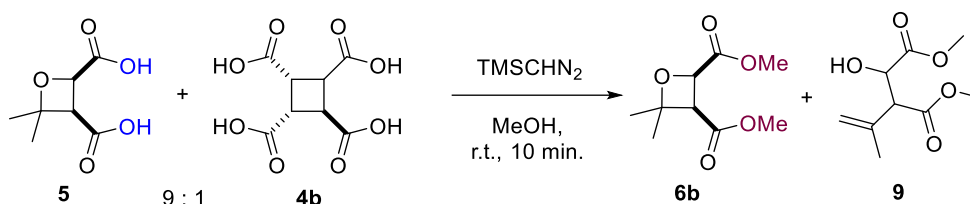
Several methods were considered to perform esterification on **5**. Due to concerns about the acid-sensitivity of **5**, basic conditions were first tested, using potassium carbonate with benzyl bromide as the alkylating agent (Scheme 2-7\_A). However, no reaction was observed after 48 hours, and analysis by  $^1\text{H}$  NMR spectroscopy only showed left over benzyl bromide. Next, 1-ethyl-3-(3-dimethylaminopropyl)carbodiimide (EDC) in conjunction with hydroxybenzotriazole (HOBt) was used with methanol in an attempt to form **6b** (Scheme 2-7\_B). The reaction took 72 h and gave only 8% yield of the oxetane **6b**, starting from a 1:1 mixture of **3** and **4**. The reaction required a higher number of equivalents of the EDC and HOBt as there were more than one carboxylic acid group present on the starting materials. Based on the  $^1\text{H}$  NMR spectrum of the crude product, very little diacid **5** remained at the end of the reaction, as the characteristic pair of doublets was very small compared to other signals. Additionally, more equivalents of the EDC and potentially of HOBt should have been used, due to the four carboxylic acids present on dimer **4b** compared to the two on oxetane **5**. Nevertheless, this approach allowed the isolation of pure oxetane **6b**, and full spectroscopic characterisation.



Scheme 2-7 Reaction conditions for esterification of **5**.

Finally, trimethylsilyldiazomethane ( $\text{TMSCHN}_2$ ) was used as the esterification agent.  $\text{TMSCHN}_2$  is a very strong methylating agent and the reaction is instantaneous (Table 2-8). These reactions were performed on partially purified **5** (**5** : **4b**, 1 : 0.18). The reaction gave a best yield of 40% (over the one step) with two equivalents of  $\text{TMSCHN}_2$  (Table 2-8, entry 3) used. The downside of these reaction conditions was the formation of **9**, which indicated breakdown of the oxetane ring. However, as **9** was not observed in the

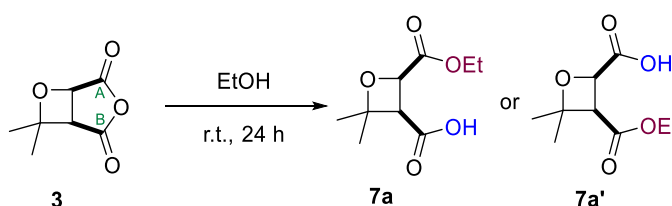
<sup>1</sup>H NMR spectrum of the crude product, it is speculated that the acidity of the silica gel used during column chromatography could have caused the breakdown of the oxetane **6b**. Dimer **4d** was only observed in traces in these reactions.



Entry	Eq. of TMSCHN <sub>2</sub>	Yield of <b>6b</b> (%)	Yield of <b>9</b> (%)	Purity of <b>6b</b> (%)
1	3	36	15	100
2	2.5	35	5	90
3	2	40	4	90

Table 2-8 Results of optimization reaction of esterification reaction of **5** with the TMSCHN<sub>2</sub>.

Next, the anhydride ring was opened with series of alcohols. Methanol was omitted as the goal was formation of two different ester groups. Different alcohols were used as both reagents and solvent. Thus, the solution of **3** (after the Paternò-Büchi step) was partially concentrated and 10 mL of alcohol was added. Ethanol was the first successful alcohol to open the anhydride ring and gave a single isomer of the product, either **7a** or **7a'** (Scheme 2-8), with the <sup>1</sup>H NMR spectrum of the crude product showing a very clean regioselective ring opening of the anhydride. It was proposed that the regioselectivity could be due to two reasons: 1) the two methyl groups blocking the approach of the nucleophile to carbonyl B of the anhydride and/or 2) the oxygen in the oxetane ring could make carbonyl A more reactive towards nucleophilic attack. In both of these cases, attack of the nucleophile at the carbonyl group adjacent to the oxetane oxygen would be favoured, which would give **7a**.



Scheme 2-8 Opening of the anhydride ring with ethanol.

To find out which regioisomer was formed in the reaction, the ring-opened product was first esterified using trimethylsilyldiazomethane, and the resulting diester **8a** was analysed by <sup>1</sup>H-<sup>1</sup>H correlation spectroscopy (COSY) NMR (Figure 2-6). A clear correlation was observed between proton A and protons B, as well as a lack of correlation between proton C and protons B, which suggested that the isomer formed is **8a**, resulting from initial ring-opening at the carbonyl group adjacent to the oxetane oxygen, as expected based on steric and electronic reasoning. Unfortunately, it was not possible to



obtain a suitable crystal of the product for X-ray analysis, so definitive proof for the regioselectivity of the ring-opening could not be obtained in this example.

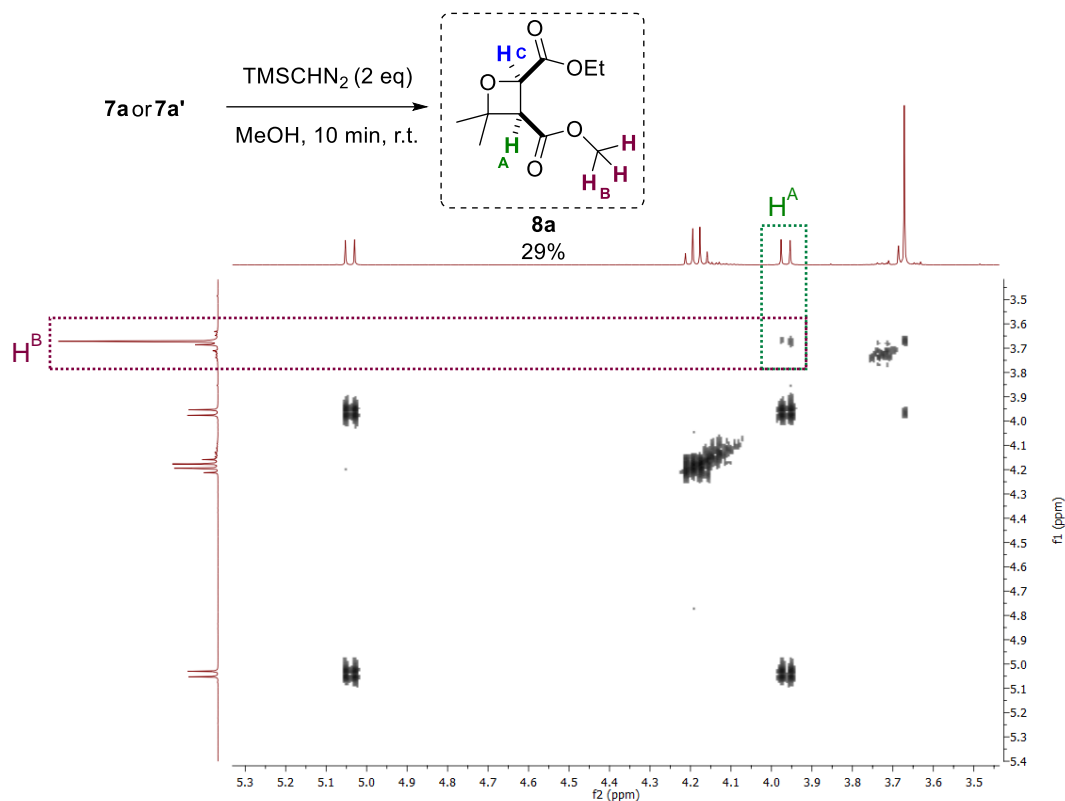
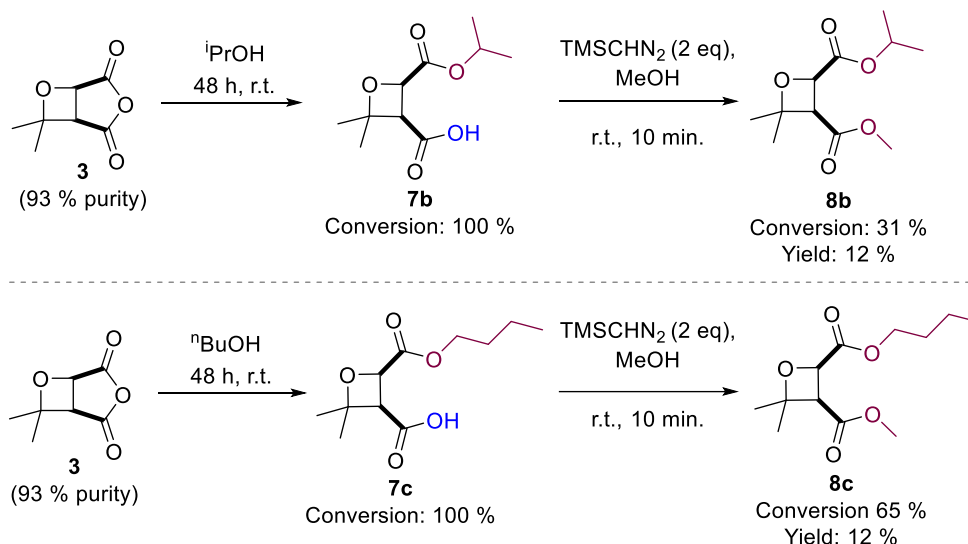


Figure 2-6 <sup>1</sup>H – <sup>1</sup>H COSY NMR spectra of oxetane **8a**.

Next, two more alcohols (isopropanol and *N*-butanol) were tested in the ring-opening, forming isopropyl and butyl ester groups respectively. After stirring for 48 hours at room temperature both reactions reached 100 % conversion of **3** (Scheme 2-9). Next, the carboxylic acid underwent methylation reaction with TMSCHN<sub>2</sub>, however in both cases the reaction did not reach completion. Nevertheless, the resulting two new oxetanes were purified to give **8b** in 12% yield, and **8c** in 12% yield. In both cases, the reaction did not convert **7b** and **7c** fully, as traces starting materials were also isolated at the end of the methylation reaction. Potentially, higher conversions/yields could be achieved by increasing the number of equivalents of TMSCHN<sub>2</sub>.



**Scheme 2-9** Opening of the anhydride ring with isopropanol and *N*-butanol, followed by methylation reaction to give two isolated oxetanes: **8b** and **8c**. Purity of **3** = 93 %

Fortunately, it was possible to grow a crystal of **7b** suitable for X-ray analysis (Figure 2-7), which clearly demonstrates that the ring-opening of the anhydride occurs at the carbonyl group adjacent to the oxetane oxygen, and that the ester and carboxylic acid groups remain positioned *cis* relative to each other after the ring-opening reaction. This was the only crystal structure that was collected in this series of oxetanes, but it is likely that the same regioselectivity operated when using the other alcohols.

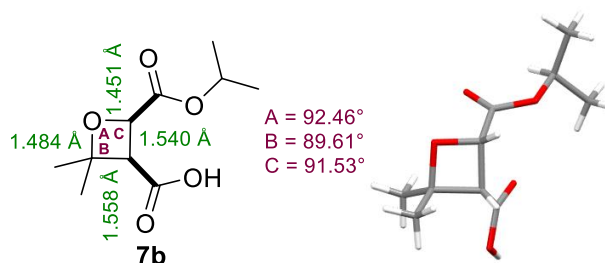
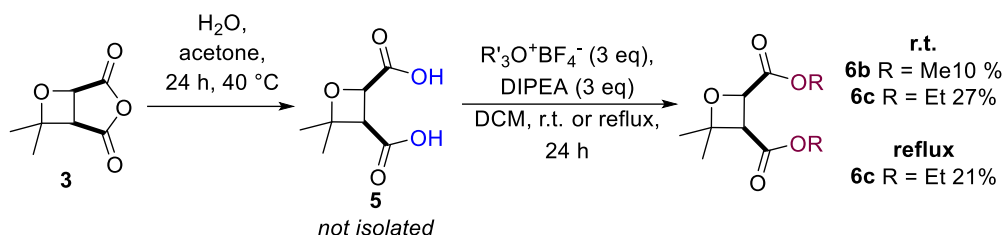


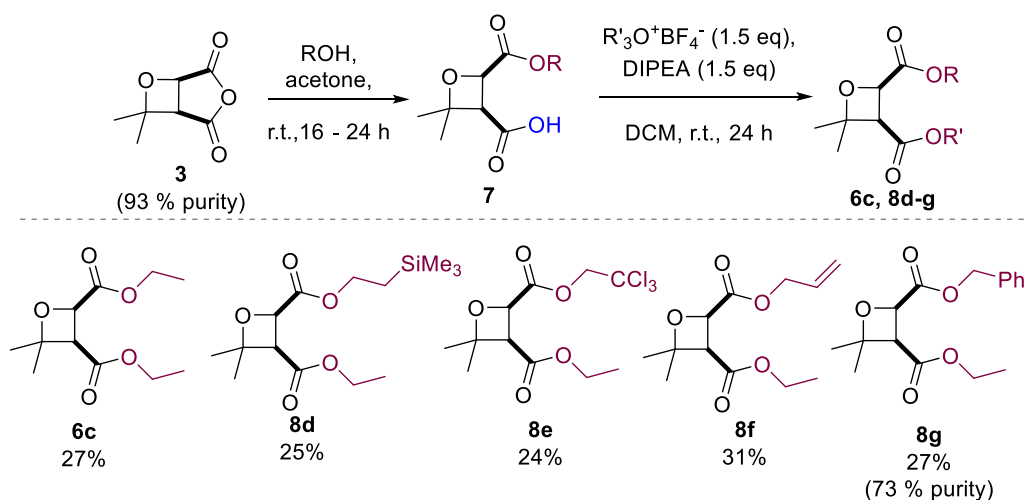
**Figure 2-7** Crystal structure of **7b**, showing the bond lengths and angles of the oxetane ring.

Due to the toxicity and expense of TMSCHN<sub>2</sub>, other esterification methods were explored. Because of the oxetane ring being relatively acid-sensitive (Chapter 1, section 1.1.5), acidic conditions must be avoided, which narrows down the possibilities. The use of Meerwein salts<sup>85</sup> was successful in the esterification of these oxetanes, and the standard work-up for the reaction was modified by reducing the volume of acid used during the aqueous wash, as the original work-up caused most of the oxetane to ring open. Two Meerwein salts were used (Me<sub>3</sub>O<sup>+</sup>BF<sub>4</sub><sup>-</sup> and Et<sub>3</sub>O<sup>+</sup>BF<sub>4</sub><sup>-</sup>) to perform esterification on the carboxylic acid **5**, giving 10 and 27% yields of the diesters **6b** and **6c** respectively (Scheme 2-10). In an attempt to increase the yield of the esterification

step, the reaction using  $\text{Et}_3\text{O}^+\text{BF}_4^-$  was also performed at reflux, but the product was isolated in 21% yield, which was lower than that of the room temperature reaction.



Next, further alcohols were used to ring open the anhydride ring, followed by the esterification of the carboxylic acid with the use of  $\text{Et}_3\text{O}^+\text{BF}_4^-$  (Scheme 2-11). An additional five oxetanes were isolated in good yields of 24-51%, with the alcohols for the initial ring-opening being chosen to potentially allow subsequent orthogonal deprotection of the ester groups. For example, the silylethyl ester in **8d** could be deprotected using a fluoride source, the trichloroethyl ester in **8e** could be deprotected using zinc, the allyl ester in **8f** could be deprotected using palladium catalysis, and the benzyl ester in **8g** could be deprotected through hydrogenation. The formation of **6c** was repeated by first ring-opening the anhydride with ethanol, and then using the Meerwein salt for esterification of the resulting carboxylic acid; the reaction gave a very similar yield to that obtained when the salt is used to form the two esters from the corresponding diacid. **8g** proved difficult to fully purify and a significant amount of benzyl alcohol was present in the final product, showing only 73% purity; multiple purification methods were run with no success.



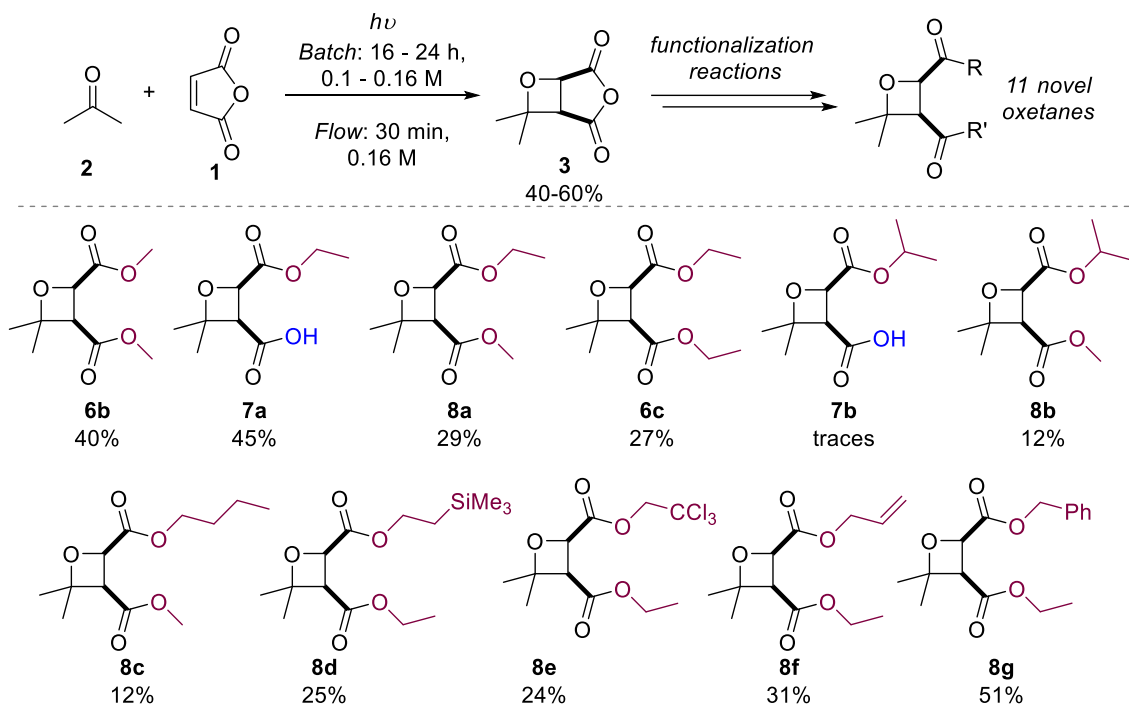
## 2.4 Conclusions

Overall, the Paternò-Büchi reaction between acetone and maleic anhydride has been optimized in both batch and flow. In each case, the undesired dimerization of maleic

anhydride took place alongside the desired Paternò-Büchi reaction, resulting in a highly crystalline double anhydride product **4**, which could not be completely separated from the oxetane products. Whilst running the reactions at higher concentrations of maleic anhydride appeared to reduce the proportion of the dimer **4** produced compared to oxetane **3**, the complete suppression of the dimer product was not possible. In addition, the precipitation of the dimer **4** from acetone at higher substrate concentrations meant that this approach was not suitable for scale-up. The Paternò-Büchi reaction was also run in acetonitrile, which allowed much lower amounts of the ketone to be used, and optimisation in flow allowed a decrease in the reaction time from 48 hours (in batch) to 30 minutes (in flow), allowing the production of larger batches of **3** (35-65% yield), which could be partially purified (purity 85-98%) and used in the subsequent diversification reactions.

A series of different ring-opening reactions of anhydride **3** was carried out, and subsequent esterification reactions were tested, which resulted in 11 novel oxetane products in reasonable yields (Scheme 2-12). Ring opening of the anhydride with alcohols took place regioselectively, which was confirmed by NMR spectroscopy (COSY), as well as a crystal structure, in the case of **7b**. In summary, it is quick and easy to ring open the anhydride with an alcohol to allow formation of two different ester groups in the final product, over two steps.

Overall, these reactions gave a good understanding of the practical formation and handling of the oxetanes formed, but the mechanisms for the Paternò-Büchi and dimerization reactions were still unclear. With the established conditions for ring opening of the anhydride and the isolation of final oxetanes, extension of the methodology to ketones other than acetone and mechanistic studies was envisaged, and this work is described in Chapters 3 and 4 respectively.

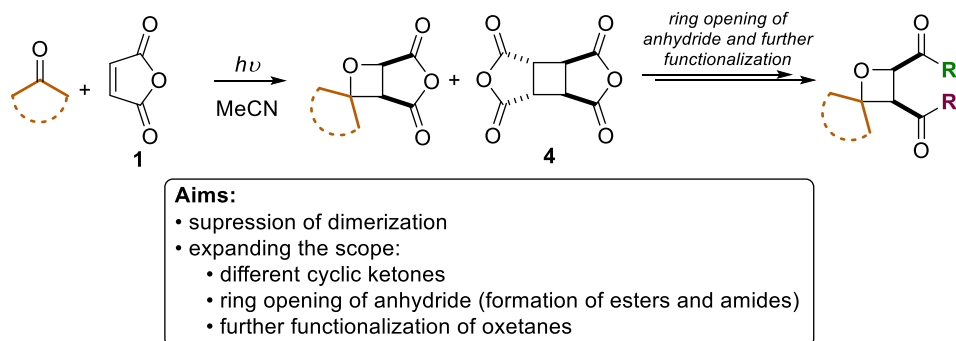


**Scheme 2-12** Summary of the isolated oxetanes formed from acetone and maleic anhydride; the yields is based on partially purified 3 (see text).

## Chapter 3 Paternò-Büchi reaction between cyclic ketones and maleic anhydride

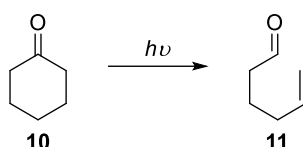
### 3.1 Introduction

Based on the results from Chapter 2, which discussed the Paternò-Büchi reaction between acetone (**2**) and maleic anhydride (**1**) initially reported by Turro, the Paternò-Büchi reaction was next expanded towards the formation spirocyclic oxetanes, by changing the ketone component from acetone to symmetrical cyclic ketones. This chapter focuses on the optimization of the Paternò-Büchi reaction between cyclic ketones and maleic anhydride, as well as further studies on the suppression of the dimerization reaction (Scheme 3-1). Starting with cyclohexanone (**10**) as the model cyclic ketone, the Paternò-Büchi reaction was optimized, and the starting reaction conditions were based on results from Chapter 2. Upon completion of the optimization of the Paternò-Büchi reaction, it was expanded to several different cyclic symmetric ketones to form a series of different spirocyclic scaffolds. Lastly, the functionalization of the anhydride ring was expanded on, as well as further functionalization of the final isolated oxetanes, which tested their stability towards a series of different reagents and conditions. Overall, this chapter focuses on a practical approach to this Paternò-Büchi reaction and the isolation of the desired oxetanes.



Scheme 3-1 Paternò-Büchi reaction between cyclic ketones and maleic anhydride (**1**) to give oxetane-containing spirocycles.

Both cyclohexanone and maleic anhydride give rise to new products when irradiated at 300 nm. Maleic anhydride undergoes dimerization, as discussed previously. Cyclohexanone breaks down via Norrish type 1 reaction to form a 5-hexenal (**11**) (Scheme 3-2). Breakdown of the ketone can be an issue, however in the case of cyclohexanone, after irradiation for over 70 h no more than 10% of the starting ketone had been broken down to the aldehyde. The ketone **10** and the aldehyde **11** were easily removed during the purification, therefore no major effort was put into trying to suppress this reaction.



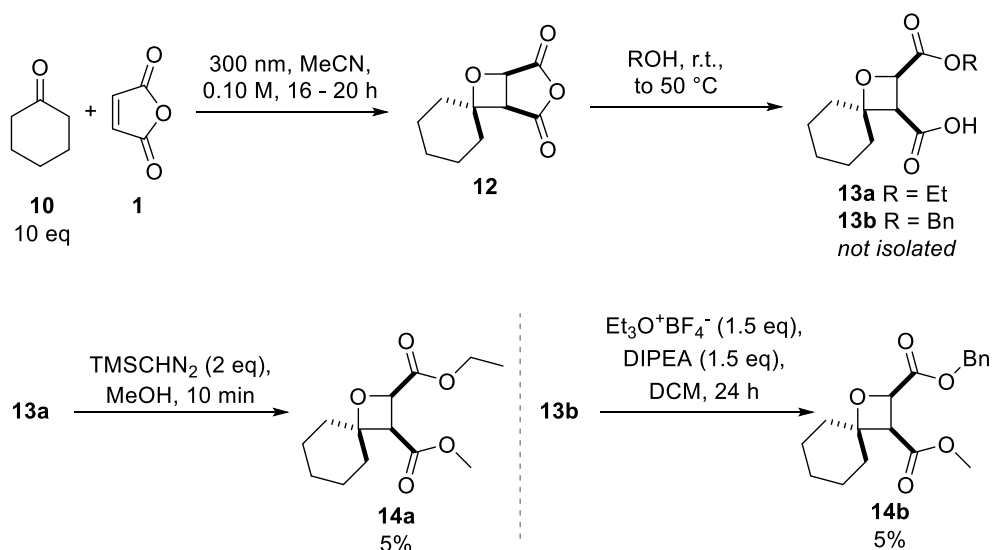
Scheme 3-2 Norrish type 1 reaction of cyclohexanone (**10**).

### 3.2 Paternò-Büchi reaction between cyclohexanone and maleic anhydride

Cyclohexanone was chosen as first cyclic ketone, as it showed the highest stability when irradiated at 300 nm, compared to cyclopentanone and cyclobutanone. The reaction conditions from Chapter 2 were used to further functionalize the formed oxetane and transform the anhydride ring into two ester groups. The three reaction steps included the Paternò-Büchi reaction, nucleophilic ring-opening of the anhydride, then esterification of the resulting carboxylic acid.

#### 3.2.1 Testing the initial reaction conditions

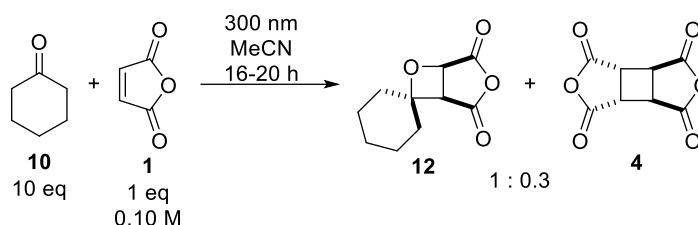
Firstly, reaction conditions based on the results from Chapter 2 were repeated to isolate the desired oxetane spirocycle **14** (Scheme 3-3). Although all the maleic anhydride was consumed during the Paternò-Büchi step and the ring opening of the anhydride was regioselective, the isolated yields of the final oxetanes were poor. After following the protocol established in Chapter 2, 5% of oxetane **14a** or **14b** was obtained, showing that the reaction can be expanded to for oxetane-containing spirocycles. Series of different issues with each reaction step were observed, the optimizations of each reaction step are discussed below.



Scheme 3-3 Initial Paternò-Büchi reaction between cyclohexanone (**10**) and maleic anhydride (**1**), followed by functionalization of the anhydride ring.

Starting with the photoreaction, maleic anhydride was consumed within 16-20 hours of irradiation, giving a mixture of two products: the desired oxetane **12** and the undesired dimer **4** (Scheme 3-4). Previously, the dimer **4** was removed by crystallization (See

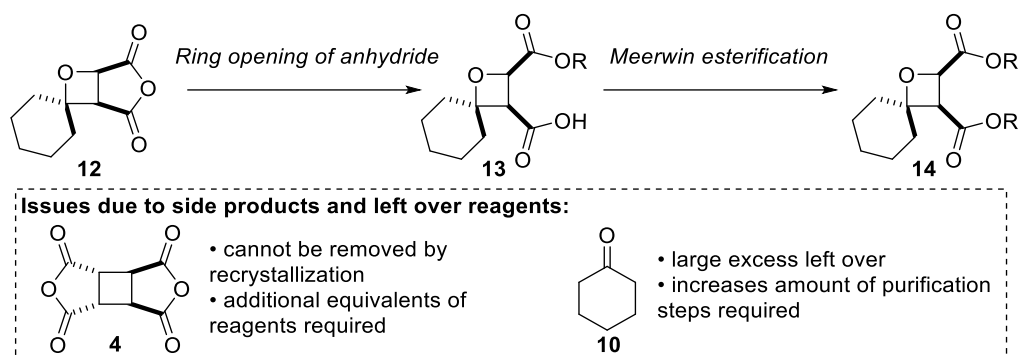
2.2.5), but this was not possible when cyclohexanone was used in the reaction, as the excess cyclohexanone impeded the crystallization of dimer **4**. Attempts to remove the cyclohexanone under reduced pressure and under high vacuum did not yield the desired effect, therefore dimer **4** had to be carried through to the other reaction steps. The presence of the dimer **4** in the subsequent reaction steps required an increased amount of reagents for each step. The percentage yield of the oxetane was calculated based on the maleic anhydride (three reaction steps), with only the final oxetane undergoing purification at the end of the three-step telescoped reaction pathway. The ratio of oxetane **12** to dimer **4** in the Paternò-Büchi reaction was comparable with the ratio of oxetane **3** and dimer **4** reported in Chapter 2. Thus, the ratio of the oxetane **12** to dimer **4** was 1 : 0.3, meaning ~40% of the starting maleic anhydride (**1**) was lost to the dimerization reaction.



**Scheme 3-4** Results of initial Paternò-Büchi reaction between cyclohexanone (**10**) and maleic anhydride (**1**) and dimerization of maleic anhydride (**1**).

The subsequent steps, ring opening of the anhydride and Meerwein esterification (Scheme 3-5) were difficult to track using  $^1\text{H}$  NMR spectroscopy (and TLC) due to the excess cyclohexanone present. When acetone was used as the ketone, solvent suppression in  $^1\text{H}$  NMR suppressed all the acetone present in the reaction, however, when cyclohexanone was used the reaction solvent (and therefore the suppressed solvent) was acetonitrile. Cyclohexanone was not suppressed due to two reasons: there would be partial overlap of the region of interest with the suppressed signals (which would result in less information gained), and secondly, tracking reactions with different ketones would be more complex, as each one would have different set of peaks. The excess cyclohexanone made it difficult to track each reaction step, which led to some uncertainty about reaction completion at each stage. In any case, the ring opening reaction was heated up to 50 °C, as the reaction was progressing very slowly at room temperature. Lastly, additional column chromatography passes were necessary to fully remove all the cyclohexanone left over from the Paternò-Büchi reaction, further decreasing the isolated oxetane yields.





**Scheme 3-5 Functionalization of the formed oxetane 13 and issues occurring due to initial reaction conditions.**

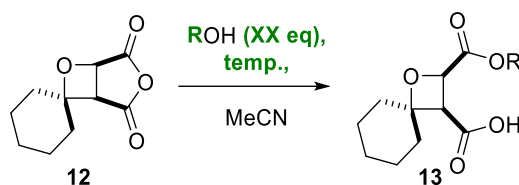
In summary, the reaction conditions that worked very well when acetone and maleic anhydride (with 10 eq of acetone used - 2.2.4) were used in the reaction were not ideal in the reaction between cyclohexanone and maleic anhydride, however, they were a very good starting point for optimization. The major issues with each reaction step were due to the excess of cyclohexanone, the formation of dimer and the final purification. The following section describes adjustments to the reaction conditions and the development of a reliable three-step telescoped pathway for the formation of novel spirocyclic oxetanes from simple starting materials.

### 3.2.2 Optimization of reaction conditions

A series of different reaction conditions was tested, showing that simple changes to the conditions led to improvements in the final oxetane yield.

#### 3.2.2.1 Optimization of the nucleophilic ring opening of anhydride

The nucleophilic ring opening of the anhydride was investigated to ensure full conversion of **12** to **13** (Table 3-1). A series of alcohols was used, as summarised in Table 3-1. The initial reaction conditions did not require higher reaction temperatures, however, while tracking the initial reaction it was quickly clear that an increase in temperature is necessary to increase the reaction rate. The reactions were tracked by solvent suppression  $^1\text{H}$  NMR spectroscopy, to assess the percentage conversion of **12** into **13** at various stages. The reactions showed a lack of (or very slow) ring opening of the anhydride ring at room temperature, however, increasing the reaction temperature resulted in the ring opening of the anhydride being completed in 20 – 96 hours. At reflux, primary alcohols successfully opened the anhydride ring (Table 3-1, entry 2, 5, 9 and 11). On the other hand, secondary alcohols such as isopropanol did not open the anhydride ring, even upon prolonged heating at reflux (Table 3-1, entry 7 and 8). The number of equivalents of alcohol used can be lowered to 1.2 equivalents (Table 3-1, entry 3, 6 and 10), which ensures that essentially all of the alcohol can be used and removed before the next reaction.



Entry	Alcohol (eq)	Temperature	Time (h)	Conversion of 12 (%)
1	EtOH (2 eq)	r.t.	24	0
2	EtOH (2 eq)	Reflux	40	100
3	EtOH (1.2 eq)	Reflux	110	99
4	<i>n</i> BuOH (2 eq)	r.t.	68	33
5	<i>n</i> BuOH (2 eq)	Reflux	20	100
6	<i>n</i> BuOH (1.2 eq)	Reflux	92	99
7	<i>i</i> PrOH (2 eq)	r.t.	68	0
8	<i>i</i> PrOH (2 eq)	Reflux	80	0
9	BnOH (2 eq)	Reflux	68	100
10	BnOH (1.2 eq)	Reflux	68	99
11	MeOH (2 eq)	Reflux	68	100
12	MeOH (1.2 eq)	Reflux	110	99

Table 3-1 Results of optimization of the 2<sup>nd</sup> reaction step: ring opening of the anhydride. Conversion based on <sup>1</sup>H NMR (solvent suppression, MeCN, 400 MHz).

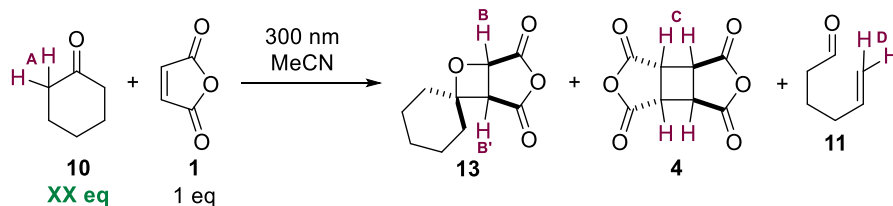
The ring opening of the anhydride was forced by increasing the temperature of reaction; this did indicate an improved stability of the anhydride ring towards nucleophilic attack (compared to the oxetane products derived from acetone), therefore water in the air was no longer an issue (as discussed in Chapter 2). The increase in stability made these systems easier to handle, as anhydrous conditions did not have to be followed as strictly once the oxetane was formed.

### 3.2.2.2 Optimization of the Paternò-Büchi reaction

Due to the issues arising from the excess of the cyclohexanone present in the crude product mixture, the photoreaction conditions were tested with lower amounts of cyclohexanone while increasing the overall concentration of the reaction from 0.10 to 0.16 M with respect to maleic anhydride. Table 3-2 summarizes the percentages of starting materials and products in the reaction mixture after 44 hours irradiation, when 10, 3, 2 and 1 equivalent(s) of cyclohexanone were used in the reaction. The percentages were calculated based on the integration of the following signals (Table 3-2, Figure 3-1): cyclohexanone (H<sup>A</sup>), oxetane (H<sup>B</sup>) and dimer (H<sup>C</sup>); additionally H<sup>D</sup> is marked which is due to the aldehyde product. The top spectrum shows that the oxetane is formed, however the neighbouring signals are stronger, and this was even more important in the functionalization reactions as additional reagents were added. During the ring opening of the anhydride ring, the peak for H<sup>B</sup> often overlapped with some of the peaks arising from 5-hexenal (H<sup>D</sup>), while H<sup>B'</sup> often overlapped with peaks arising from

the alcohols that were added to the reaction, making it difficult to track the reaction conversion. It is important to note that no internal standard was used in these reactions, so the percentages of the components of the reaction mixture are calculated based only on cyclohexanone, oxetane and dimer present in the reaction mixture, and isolated yields would be much lower, as other processes (including polymerisation) are likely occurring. The use of an internal standard in these reactions could be complicated, as it is difficult to choose a standard that is certain not to influence the course of the reaction (as will be discussed later in section 3.2.3, even very simple compounds such as toluene can alter the course of the reaction).

The first observation from Table 3-2 was that the amount of cyclohexanone present in the mixture was higher than expected. The apparent excess of the ketone can be due to some of the maleic anhydride reacting with itself (either dimerization or possible polymerization), as well as overlap of  $^1\text{H}$  NMR signals of the cyclohexanone ( $\text{H}^{\text{A}}$ ) and cyclohexyl ring signals due to the oxetane formed. Table 3-2, entry 1 shows the results from the previous reaction with 10 equivalents of cyclohexanone, showing that the reaction mixture contains 97% of cyclohexanone. As expected, lowering the number of equivalents of cyclohexanone increased the reaction time (Table 3-2, entry 2, 3 and 4), and also the amount dimer **4** increases. To ensure that a minimal amount of dimer **4** is formed in the reaction, 3 equivalents (Table 3-2, entry 2) of cyclohexanone was chosen as final reaction conditions. The improvement in the reaction can be seen by comparing the  $^1\text{H}$  NMR spectra of the two sets of conditions (Figure 3-1), with the oxetane signals being more prominent under the optimized conditions.



Entry	10 (eq)	[1] (M)	% in reaction mixture				Reaction time (h)
			1	13	4	10 + 11	
1	10	0.10	0	2	<1	97	16
2	3	0.16	0	9	3	87	44
3	2	0.16	<1	12	6	81	44
4	1	0.16	4	17	12	67	44

Table 3-2 Results of optimization of the Paternò-Büchi reaction based on the number of equivalents of cyclohexanone (10). Percentage of components in the reaction mixture based on  $^1\text{H}$  NMR (suppression, MeCN, 400 MHz).

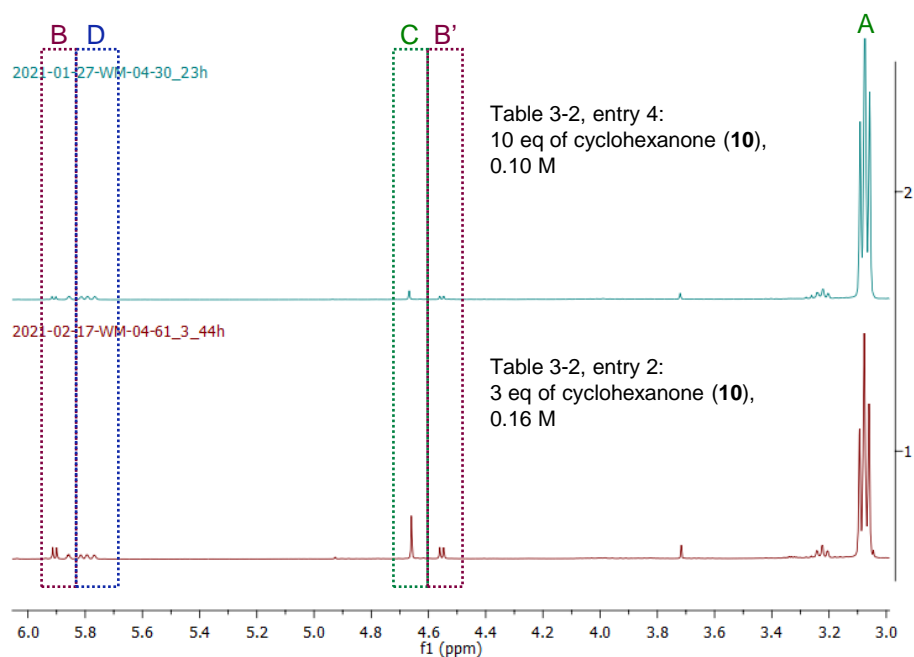
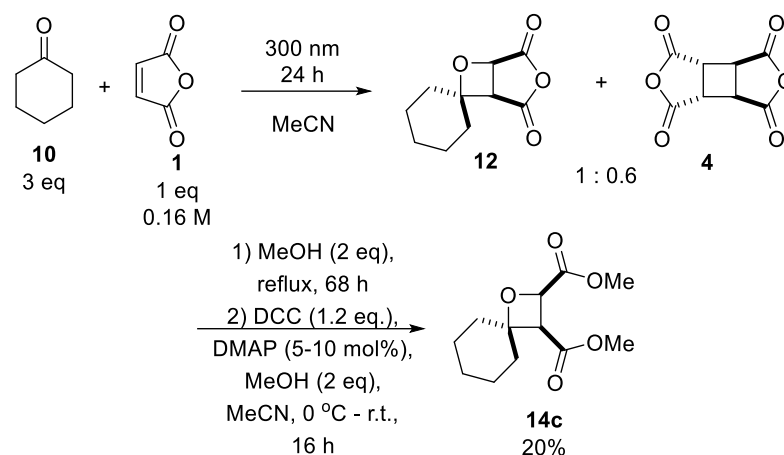


Figure 3-1  $^1\text{H}$  NMR spectral (suppression, MeCN, 400 MHz) comparison of two Paternò-Büchi reactions with different equivalents of cyclohexanone (**10**) and maleic anhydride (**1**) concentrations.

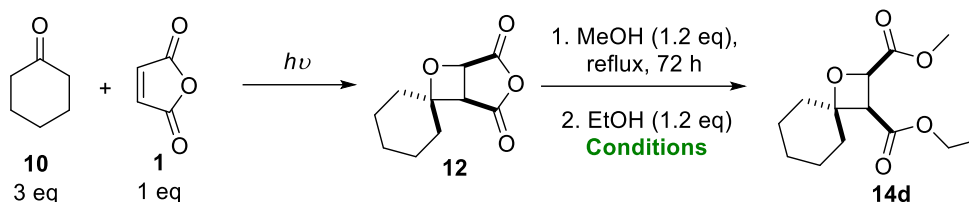
### 3.2.2.3 Optimization of the esterification reaction

Finally, the third reaction step (the esterification reaction), was studied. In the past (section 2.3), using Meerwein salts worked well, however, this method does limit the possible esters formed to only methyl and ethyl esters. Thus, a different method of esterification was tested using *N,N'*-dicyclohexylcarbodiimide (DCC) as a coupling reagent (Scheme 3-6). A first run of the three-step telescoped reaction implementing all the above improvements yielded 20% of the final oxetane **14c**. The esterification reaction procedure was based on the original method reported by Steglich *et.al.*,<sup>86</sup> changing only the solvent to acetonitrile due to the lack of solubility of the crude product in dichloromethane. The reaction was successful and resulted in the formation of a series of different esters from the carboxylic acid (Section 3.3).



**Scheme 3-6** Three-step telescoped sequence: Paternò-Büchi reaction between cyclohexanone (10) and maleic anhydride (1), followed by functionalization of the anhydride ring. Isolated percentage yield based on maleic anhydride.

A series of other standard carboxylic acid coupling conditions were also tested (Scheme 3-7, Table 3-3), although the first combination of reagents worked best (DCC (1.2 eq, DMAP (5-10 mol%), MeCN). Addition of hydroxybenzotriazole (HOBt) did not have a significant effect on the isolated yield, decreasing it slightly to 16% (Table 3-3, entry 2). Using 1-ethyl-3-(3-dimethylaminopropyl)carbodiimide (EDC) in the reaction led to fairly insoluble crude product mixtures, and therefore poor purifications, causing very low yields (Table 3-3, entry 3 and 4).



**Scheme 3-7** Optimization of the esterification by carboxylic acid coupling.

Entry	Reaction conditions	14d % yield
1	DCC (1.2 eq), DMAP (5 mol%), 0 °C to r.t., 16 h	20
2	DCC (1.2 eq), DMAP (5 mol%), HOBt (5 mol%), 0 °C to r.t., 16 h	16
3	EDC (1.2 eq), DMAP (5 mol%), DIPEA (5 eq), 0 °C to r.t., 16 h	5
4	EDC (1.2 eq), DMAP (5 mol%), DIPEA (5 eq), 0 °C to 80 °C, 16 h	0

**Table 3-3** Results of optimization of the esterification by carboxylic acid cross coupling. Isolated % yield based on maleic anhydride (1).

To summarize, the following changes were made to the original reaction conditions.

- 1) *The Paternò-Büchi reaction*: Decreasing the amount of ketone to 3 equivalents and increasing the maleic anhydride concentration to 0.16 M.

- 2) *Ring opening of the anhydride*: Increasing the reaction temperature to decrease the reaction time.
- 3) *Esterification*: DCC-mediated coupling of the carboxylic acid with alcohols, allowing for formation of a wide range of esters.

All of these small optimizations increased the overall oxetane yield to 20% from 5%, but the biggest issue was still the formation of dimer **4**. Dimer formation consumed ~40-50% of the maleic anhydride during the first step of the sequence, halving the possible yield of the final product. Therefore, further optimization of the Paternò-Büchi reaction was attempted, with a focus on suppression of the dimerization reaction, to ensure that more of the maleic anhydride goes towards the formation of the oxetane.

### 3.2.3 Optimization of the Paternò-Büchi reaction with the use of additives

One way to potentially block a photochemical reaction from taking place is to block the specific excited state required for the reaction to take place. To block the dimerization reaction, more information about the system was necessary.

#### 3.2.3.1 Background

Cyclohexanone and maleic anhydride absorb light at 300 nm. This is confirmed by the UV-vis spectra (Figure 3-2), and results in the formation of side products during irradiation at 300 nm (i.e. 5-hexenal (**11**) from cyclohexanone, and dimer **4** from maleic anhydride). The 300 nm absorption in both cases is due to  $n\text{-}\pi^*$  transitions.

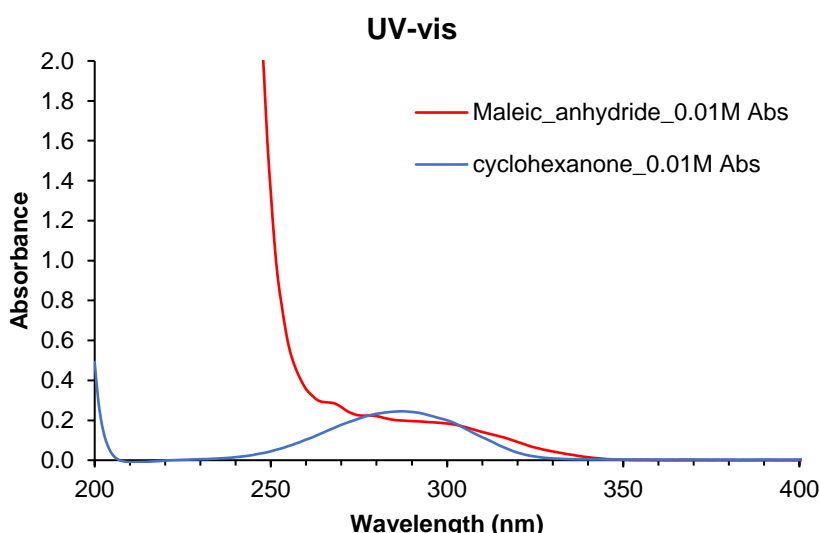


Figure 3-2 UV-vis of maleic anhydride (0.01 M in MeCN) and cyclohexanone (0.01 M in MeCN).

Reactions at longer wavelength were tested, but no reaction was observed at >350 nm (Table 3-4), which was expected based on the UV-vis spectra. Both maleic anhydride

and cyclohexanone did not absorb any light, and therefore could not access the excited state(s) necessary for photochemical reactions to take place.

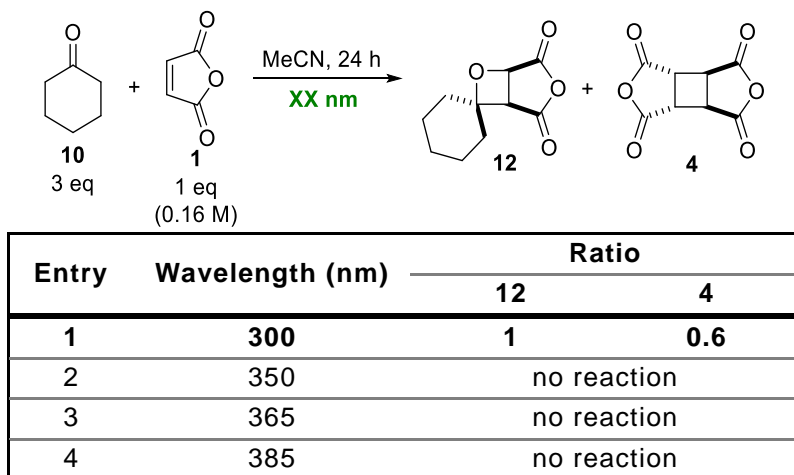
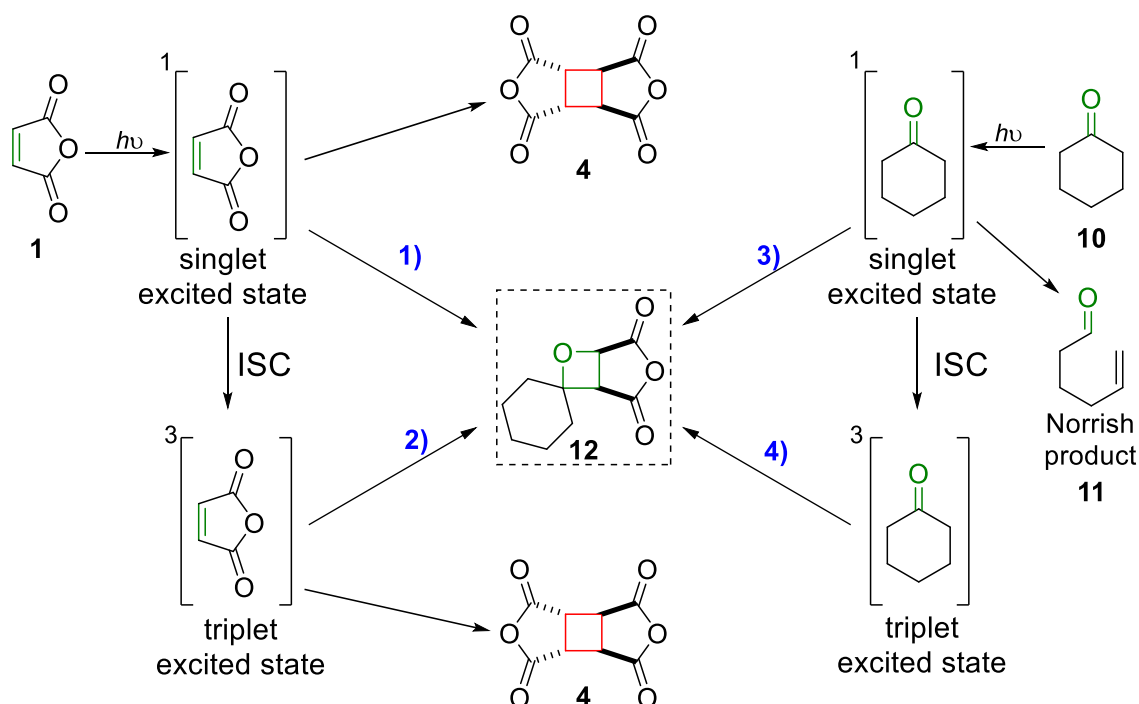


Table 3-4 Results of Paternò-Büchi reaction at different wavelengths.

The starting materials used in this reaction system are simple organic molecules, but there are different possible reaction pathways, resulting in this being a very complex system. Both of the starting materials absorb light in the same region and undergo their own reactions (dimerization and Norrish reaction) in addition to the desired Paternò-Büchi reaction. Possible reactions pathways are summarised in Scheme 3-8. Maleic anhydride undergoes dimerization through a [2+2] photocycloaddition, which requires an excited state, however, it is not clear if it requires a singlet or triplet excited state. Similarly, the Paternò-Büchi reaction can take place via either the singlet or triplet excited state, and to further complicate the matter, there is also a choice of which reagent is excited (ketone or alkene). The majority of Paternò-Büchi reactions take place via the excited state of the carbonyl compound, however there is a handful of Paternò-Büchi reactions taking place via the excited state of the alkene (section 1.3). This leads to four obvious pathways for the desired Paternò-Büchi reaction:

- 1) singlet excited state of maleic anhydride.
- 2) triplet excited state of maleic anhydride.
- 3) singlet excited state of cyclohexanone.
- 4) triplet excited state of cyclohexanone.



**Scheme 3-8 Summary of possible reaction pathways taking place when maleic anhydride (1) and cyclohexanone (10) are irradiated.**

Without knowing the exact mechanistic pathways for both dimerization and the Paternò-Büchi reaction, it is difficult to optimize the reaction conditions to promote the Paternò-Büchi reaction. However, manipulation of the excited state populations could help with the understanding of this reaction system. For example, triplet quenching could promote singlet excited state pathways while triplet sensitization could promote triplet excited state pathways.

As shown by the Jablonski diagram (Figure 3-3), the excited state of reagents can be reached by direct excitation (absorption,  $h\nu$ ). Upon absorption, the molecule reaches its singlet excited state ( $S_1$ ), next, it can either undergo fluorescence (returning to ground state,  $S_0$ ), inter-system crossing (ISC) (which results formation of the triplet excited state ( $T_1$ )), or internal conversion. Phosphorescence is the loss of energy from triplet excited state back to ground state ( $S_0$ ). Triplet excited state populations can also be manipulated by triplet-triplet energy transfer between different molecules, which includes sensitization and quenching of the triplet state.



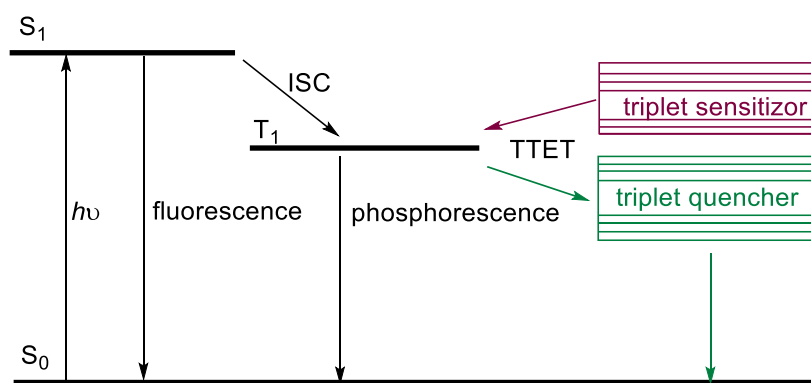


Figure 3-3 Jablonski diagram

The ground state, singlet excited state and triplet excited state correspond to different configurations of the electrons in molecule's orbitals (Figure 3-4). In the ground state ( $S_0$ ), the electrons are paired up in the lowest energy orbitals. When a molecule absorbs energy ( $h\nu$ ) and the singlet excited state ( $S_1$ ) is formed, an electron moves from the HOMO (highest occupied orbital) to the LUMO (lowest unoccupied orbital). Lastly, formation of the triplet excited state take place due to intersystem crossing, which changes the spin of the promoted electron.

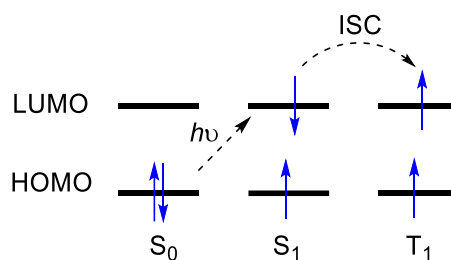


Figure 3-4

### 3.2.3.1.1 Triplet-triplet energy transfer (TTET)

There are two types of triplet-triplet energy transfer: triplet sensitization and triplet quenching (Figure 3-5). Triplet sensitizer compounds can absorb light at longer wavelengths (sometimes making the reaction safer, as lower energy light sources can be used) and easily undergo intersystem crossing (excited singlet state to triplet excited state transition). After reaching their triplet excited state, triplet sensitizers can donate that energy to the desired reagent, resulting in it reaching its triplet excited state without initially going through singlet excited state. This method is often used to avoid side reactions that can only take place via the singlet excited state, or to speed up reactions that require a triplet excited state, but for which the reagent either does not undergo efficient ISC, or it has a very high energy singlet excited state. Triplet sensitizers promote triplet excited state pathways, whilst triplet quenchers are used in the opposite way, by quenching triplet excited states; in this case singlet excited state pathways are promoted through depletion of the triplet excited state.

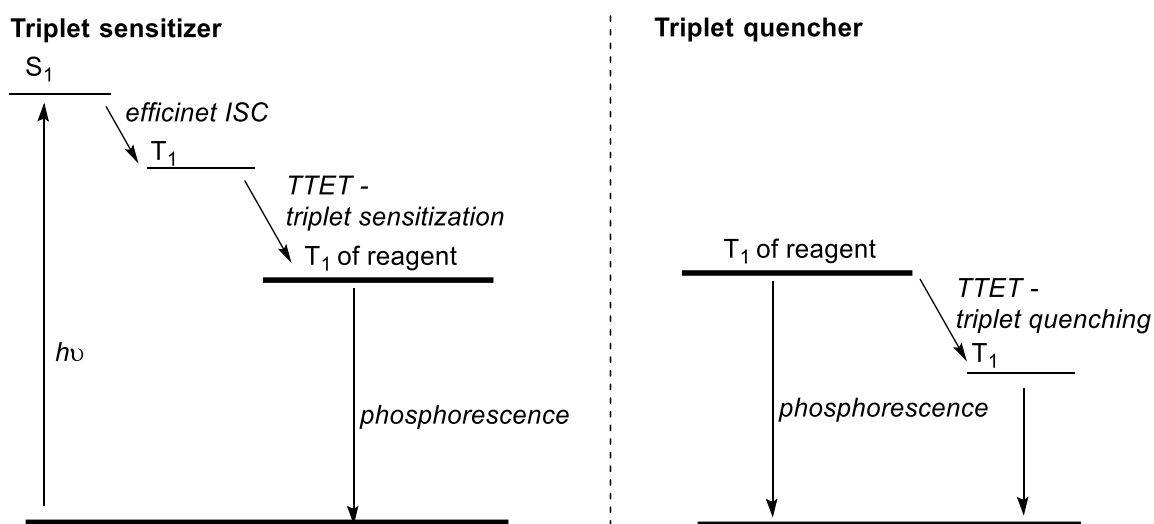
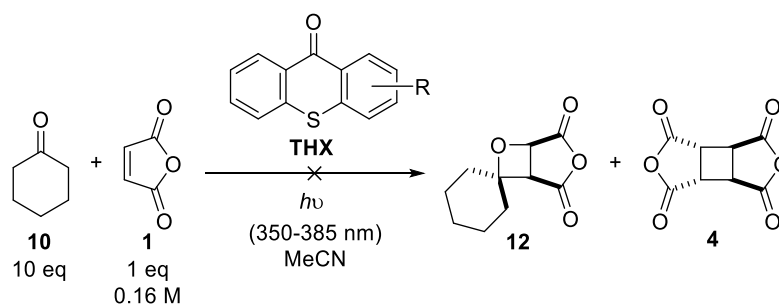


Figure 3-5

### 3.2.3.2 Using common Ir and THX photocatalysts

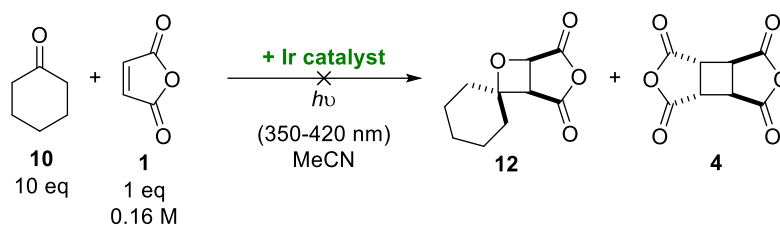
Two families of known, common triplet sensitizers available were tested: thioxanthone (THX)-based compounds and iridium-based catalysts (background provided in Chapter 1). The reactions employed catalytic amounts of the sensitizers, and were performed at  $>350$  nm to ensure only the potential triplet sensitizer is absorbing the light.

Eight different THX-based sensitizers were studied, and the reactions were tracked after 24 h of irradiation at 365/385 nm, followed for 3 h irradiation at 350 nm (Scheme 3-9). The reactions did not yield either of the products: oxetane or dimer (details provided in Chapter 7) only traces of 5-hexenal due to the Norrish reaction of cyclohexanone were observed.



Scheme 3-9 Lack of Paternò-Büchi reaction/dimerization in the presence of THX-based catalysts (structures shown in Chapter 7).

Next, nine iridium-based catalysts (details provided in Chapter 7) were tested. Again, a series of reactions were performed showing no formation of oxetane or dimer product. The reactions were irradiated at 450 nm (17 h), followed by irradiating at 350 nm (23 h).



**Scheme 3-10 Lack of Paternò-Büchi reaction/dimerization in the presence of iridium catalysts (catalysts structures shown in Chapter 7).**

These reactions gave very little information, as no reaction was observed; this could be due to lack of triplet-triplet energy transfer, or the need for a singlet excited state for the reaction to take place. Possibly, a higher amount of catalyst was required to see an effect. The triplet energies of maleic anhydride (1) and cyclohexanone (10) were measured. Figure 3-6 shows the emission of the cyclohexanone and maleic anhydride when excited between 280 to 320 nm. Each line shows emission observed when the solution of reagent in acetonitrile was excited at different wavelengths. For cyclohexanone, the strongest emission is observed between 284 and 300 nm, showing a clear peak at 415 nm, therefore the triplet energy was calculated to be  $E_T = 69 \text{ kcal mol}^{-1}$  (calculated based on Equation 3-1). In the case of maleic anhydride, a much weaker signal was reported at 407 nm ( $E_T = 70 \text{ kcal mol}^{-1}$ ). The emission of maleic anhydride closely matches the published triplet energies ( $72 \text{ kcal mol}^{-1}$ );<sup>87</sup> the small difference could be due to the solvent used, as the reported triplet energy was measured in benzene.

$$E = h\nu$$

Equation 3-1 Energy of the photon.  $E$  = energy,  $h$  = Planck's constant ( $6.626 \times 10^{-34} \text{ m}^2 \text{ kg s}^{-1}$ ) and  $\nu$  = frequency.

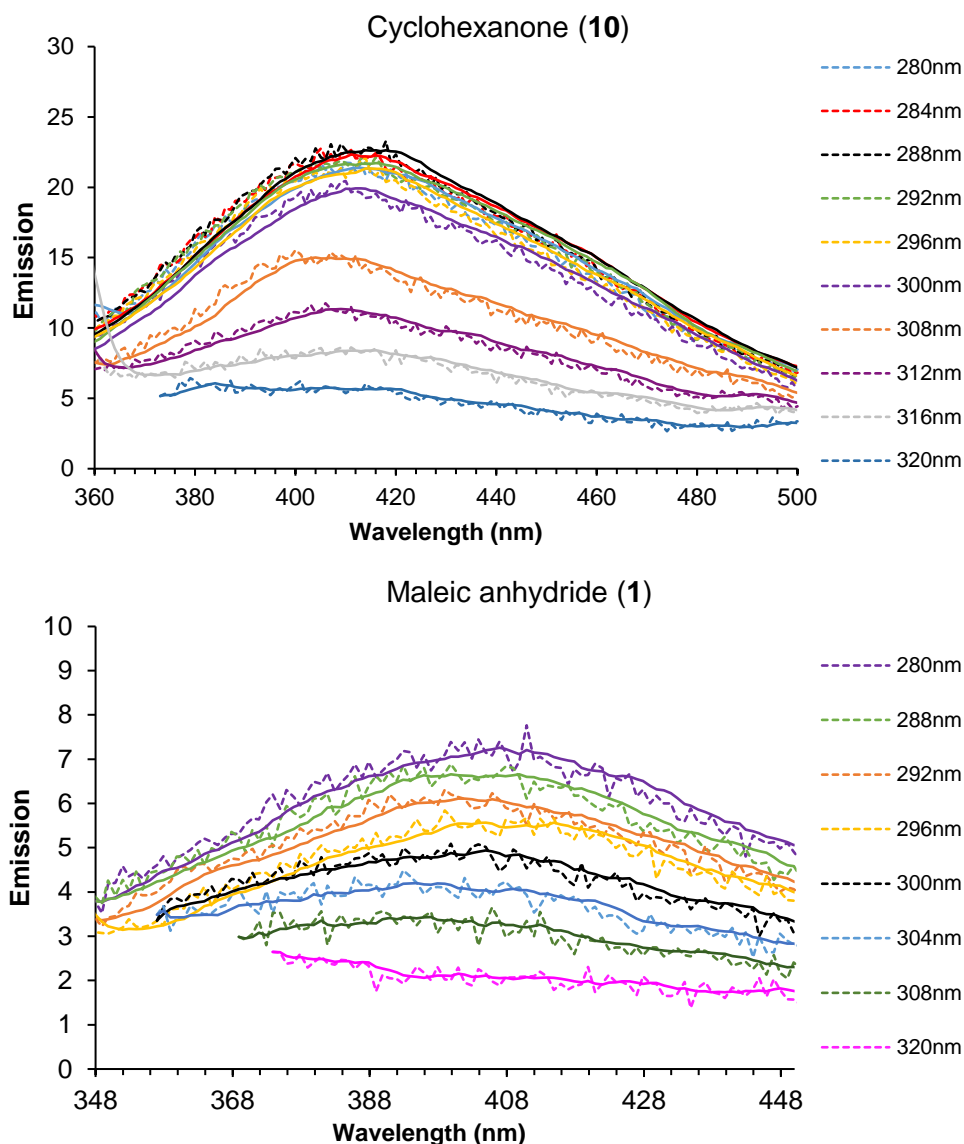


Figure 3-6 Emission spectra upon excitation at 280-320 nm.

Unfortunately, these emission spectra showed that the triplet energies of the starting materials were higher than the triplet energies of the THX and iridium catalysts used, meaning that THX and iridium catalysts could not be used to triplet sensitize either of the starting materials. Thus, a new collection of additives was devised, with compounds with higher triplet energies intended as potential triplet sensitizers, while compounds with lower triplet energies were intended as potential triplet quenchers.

### 3.2.3.3 Simple organic compounds as additives

A series of cheap and readily accessible materials with triplet energies between 65-80 kcal mol<sup>-1</sup> were chosen to be used in the reaction. The relative triplet energies are quoted from the Handbook of Photochemistry.<sup>88</sup> It is important to note that the triplet energies reported have been measured using different methods and conditions, meaning that there could be slight differences to the reported values under different conditions; for

example, the reported triplet energy<sup>87</sup> of maleic anhydride is 72 kcal mol<sup>-1</sup> but the experimental triplet energy measured in acetonitrile was 70 kcal mol<sup>-1</sup>. These small differences can be due to the solvent effects and methods of measuring. The additives used could change the populations of the singlet and triplet excited state of the maleic anhydride (and/or cyclohexanone) and therefore change the result of the reaction. Due to both reagents having very similar triplet energies, it is likely the additives chosen would interact with both reagents, but here the focus is on tracking the reactions of maleic anhydride, as the goal of these reactions was to suppress the dimerization reaction. Therefore, the additives were split into two general categories:

- (A) *Triplet quenchers*  $E_T < 70$  kcal mol<sup>-1</sup> (407 nm); potentially quenching the triplet excited state of maleic anhydride, therefore promoting singlet excited state pathways.
- (B) *Triplet sensitizers*  $E_T > 70$  kcal mol<sup>-1</sup> (407 nm); potentially quenching the triplet excited state of maleic anhydride, therefore promoting triplet excited state pathways.

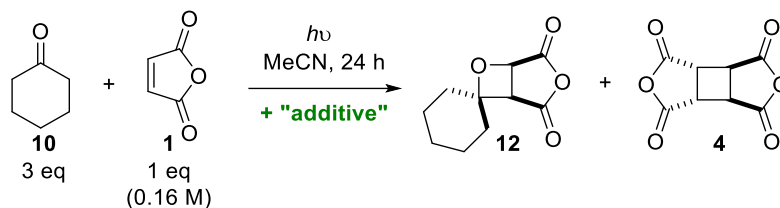
Firstly, the percentages of oxetane **12**, dimer **4** and maleic anhydride in the reaction mixture after 24 h of irradiation (300 nm) were measured. A reaction without cyclohexanone was also performed, to see if there is any effect on the amount of the dimer formed in the reaction (Table 3-5, entry 1 and 2). Both reactions had a similar amount of dimer present in the reaction after 24 h, with 21-25% of dimer **4** present, showing no effect of the presence of cyclohexanone on the rate of the dimerization reaction. It is important to remember that this is equivalent to 40% of the starting maleic anhydride being used to form the dimer, which greatly decreases the possible yield of the desired oxetane.

Table 3-5, entries 3-11 summarize the results from employing additives with triplet energies lower than maleic anhydride, which are intended to act as *triplet quenchers* (in practice, of course, they could have different effects). With the lower triplet energies, these additives could act as triplet quenchers by accepting the triplet energy from an excited triplet state of maleic anhydride. There were four additives in this group, of which 4,4-dichlorobenzophenone and *p*-dicyanobenzene slowed down the reaction but had little to no effect on the ratio of oxetane to dimer (Table 3-5, entry 3 and 11). *p*-Methoxybenzophenone (Table 3-5, entry 4) promoted the dimerization reaction, with no oxetane **12** formed during the reaction. Benzophenone, with a triplet energy of 69 kcal mol<sup>-1</sup> (413 nm), was also studied. When 1 equivalent was used, a small amount of the oxetane was observed (6%), while dimerization did not take place (Table 3-5, entry 5),

and reducing the amount of benzophenone resulted in the formation of both oxetane **12** and dimer **4**, with no improvement in ratio of two products. Additional reactions were performed at longer wavelengths to see whether benzophenone can act as triplet sensitizer.<sup>89,90</sup> As mentioned above, the triplet energies could differ slightly and with the triplet energy of benzophenone being very close to the triplet energy of maleic anhydride, and the known triplet sensitizing abilities of benzophenone, reactions at longer wavelength were performed. Reactions with irradiation at 365 and 385 nm were tested but no products were observed (Table 3-5, entry 7-10). Notably, benzophenone did not react directly with maleic anhydride to form an oxetane product; this shows that under these conditions, this Paternò-Büchi reaction of an electron poor alkene requires an aliphatic ketone.

Next, “*triplet sensitizers*” were tested to investigate whether maleic anhydride can be triplet sensitized. These additives suppressed the dimerization significantly, with less than 5% of dimer **4** observed in the reaction mixture after 24 h irradiation when the reaction was performed at 300 nm, in the majority of the examples (Table 3-5, entry 13-16, 21-23 and 27-31). The overall reaction rate was much slower, with conversions of maleic anhydride of 20-50% after 24 h irradiation. The exceptions from these trends were: xanthone, irradiating at 350 nm (Table 3-5, entry 12), which showed no reaction taking place after 24 h; and anisole (Table 3-5, entry 26), which promoted the dimerization reaction. Xanthone and 5-phenyl-1H-tetrazole absorb light at around 350 nm and could triplet sensitize maleic anhydride, however when reactions at longer wavelengths were performed, neither oxetane **12** nor dimer **4** were observed (Table 3-5, entry 12, 18-20). This could indicate a lack of TTET between the reagents or imply that the dimerization and Paternò-Büchi reactions require a singlet excited state, which cannot be reached under these conditions. Finally, the best results were observed when *p*-xylene, toluene, tolunitrile, fluoro- or chlorobenzene were used in the reaction (Table 3-5, entry 13-15, 23, 28-30), where the conversion of the maleic anhydride was 30-40% after 24 h, with only 1-2% of dimer **4** present in the reaction mixture. Due to availability and price, and the fact that its NMR signals are simplified compared to the other additives, *p*-xylene was chosen as the optimal additive, and with an extended reaction time to ensure full conversion of maleic anhydride, oxetane **12** was present as 97% of the reaction mixture after 72 h (Table 3-5, entry 31), with only traces of dimer **4** visible. Reactions at 365 and 385 nm with *p*-xylene present were also performed, showing no conversion of maleic anhydride. This was as expected, as none of the starting materials or reagents absorbs light of that wavelength. The changes in the reaction results when simple organic

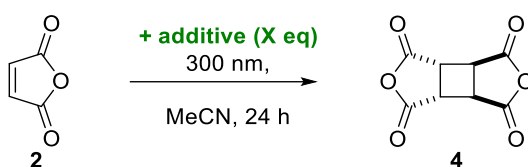
compounds were used shows that used of an NMR internal standard can be difficult as anything present in the reaction can have effect on the result.



Entry	Additive	Eq. of additive	hv (nm)	E(T) (nm) of additive	% in reaction mixture		
					1	12	4
1	-	-	300	-	0	75	25
2	no cyclohexanone	-	300	-	79	-	21
3	4,4-Dichlorobenzophenone	1	300	461	86	10	4
4	<i>p</i> -Methoxy-benzophenone	1	300	414	24	0	76
5		1	300		94	6	0
6		0.1	300		60	26	14
7	Benzophenone	1	365	413	100	0	0
8		0.5	365		100	0	0
9		1	385		100	0	0
10		0.5	385		100	0	0
11	<i>p</i> -Dicyanobenzene	1	300	406	60	31	9
12	Xanthone	1	350	386	100	0	0
13	<i>m</i> -Tolunitrile	1	300	381	45	50	5
14	<i>p</i> -Tolunitrile	1	300	379	59	40	1
15	<i>o</i> -Tolunitrile	1	300	379	56	31	1
16	1,4-Dibromobenzene	1	300	361	61	37	2
17		1	300		63	36	1
18	5-Phenyl-1H-tetrazole	1	350	360	100	0	0
19		1	365		100	0	0
20		1	385		100	0	0
21	1,4-Dichlorobenzene	1	300	357	73	25	2
22	Mesitylene	1	300	357	72	27	1
23		1	300		65	34	1
24	<i>p</i> -Xylene	1	365	355	100	0	0
25		1	385		100	0	0
26	Anisole	1	300	354	45	12	43
27	Cyclopropylbenzene	1	300	352	81	18	1
28	Chlorobenzene	1	300	348	66	33	1
29	Toluene	1	300	345	66	37	1
30	Fluorobenzene	1	300	341	64	35	1
31*	<i>p</i> -Xylene	1	300	355	0	97	3

Table 3-5 Results from optimization of Paternò-Büchi reaction with the use of additives. Percentages of compounds in the reaction mixture based on <sup>1</sup>H NMR (suppression, MeCN, 400 MHz). \* reaction time 72 h.

In parallel to the Paternò-Büchi reactions, control reactions were performed to check whether the additive is performing similarly when no cyclohexanone is present in the reaction mixture (Table 3-6). All the additives acted in the same manner when cyclohexanone was not present. Table 3-6, entry 16 shows the percentage of dimer **4** in the reaction mixture with no additive. Similarly, to the results from Table 3-5, the dimerization reaction was promoted by 4-methoxybenzophenone and anisole (Table 3-6, entries 4 and 9), while the majority of the additives suppressed the dimerization and all showed less than 7% of dimer **4** present in the reaction mixture.

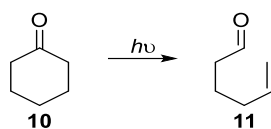


Entry	Additive	Eq. of additive	2 (%)	4 (%)
1	4,4-dichlorobenzophenone	1	93	7
2	4-fluorobenzophenone	1	98	2
3	Benzophenone	1	100	0
4	4-methoxybenzophenone	1	23	77
5	<i>p</i> -dicyanobenzene	1	86	14
6	<i>m</i> -tolunitrile	1	96	4
7	<i>p</i> -tolunitrile	1	98	2
8	<i>o</i> -tolunitrile	1	96	4
9	anisole	1	24	76
10	4-acetylpyridine	1	94	6
11	phenyl-tetrazole	1	97	3
12	1,4-dichlorobenzene	1	97	3
13	<i>p</i> -xylene	1	99	1
14	<i>p</i> -xylene	3	99	1
15	toluene	1	98	2
16	-	0	79	21

Table 3-6 Results of effect of additives on dimerization reaction. Percentages of reaction mixture based on <sup>1</sup>H NMR (suppression, MeCN, 400 MHz).

A final control reaction was performed to check the effect of additives on cyclohexanone. Table 3-7 shows the percentage of cyclohexanone and 5-hexenal (**11**) in the reaction mixture after 24 h irradiation. Overall, the additive has little effect on the Norrish reaction of cyclohexanone.

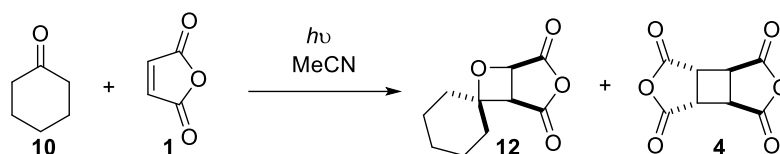




Entry	Additive	Eq. of additive	10 (%)	11 (%)
1	<i>m</i> -tolunitrile	1	1	99
2	<i>p</i> -tolunitrile	1	6	94
3	<i>p</i> -xylene	0.33	6	94
4	<i>p</i> -xylene	1	3	97
5	<i>p</i> -xylene	2	1	99
6	-	0	9	91

Table 3-7 Effects of additives on Norrish type 1 reaction of cyclohexanone. Percentage of components in the reaction mixture based on <sup>1</sup>H NMR (solvent suppression, MeCN, 400 MHz).

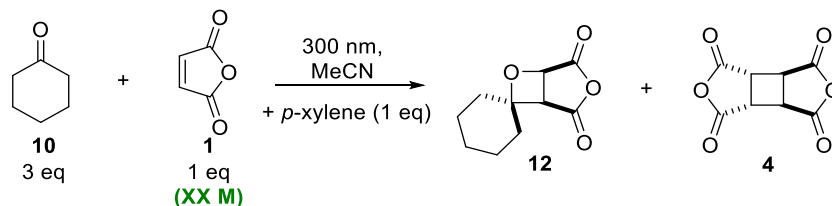
In summary, adding certain additives to the reaction mixture improved the reaction, by suppressing the dimerization reaction. For anisole and *p*-xylene, Table 3-8 summarizes the percentage of the compounds in the reaction mixture as well as how much maleic anhydride was converted into each product. Starting with the reaction with no additive before the initial optimizations, of the maleic anhydride that was converted to **12** and **4**, 38% of the maleic anhydride underwent dimerization, while 63% formed the desired oxetane **12** (Table 3-8, entry 1). Next, after the small optimizations, which included changes in the concentration of the solution and the number of equivalents of the cyclohexanone, 54% of the maleic anhydride was used to form the dimer **4** (Table 3-8, entry 2). When anisole was added, it promoted dimerization and after 24 h, 60% of the maleic anhydride underwent dimerization (Table 3-8, entry 3). Finally, when *p*-xylene is added, the vast majority of the maleic anhydride undergoes the Paternò-Büchi reaction (Table 3-8, entry 4 and 5) after 24 h, and only 1% of maleic anhydride undergoes dimerization; upon completion of the reaction (96 h), only 5% of maleic anhydride is lost to dimerization while 95% of maleic anhydride undergoes Paternò-Büchi reaction. It is important to reiterate here that the above assessment does not take into account alternative fates of maleic anhydride other than the formation of oxetane **12** and dimer **4**; it is very likely that competing polymerisation also consumes significant amounts of the starting maleic anhydride, but this could not be easily quantified. Instead, the main focus of the work was suppressing the dimerization reaction, and thus promoting the oxetane formation.



Entry	Additive and time	10 (eq) and [1] (M)	% in reaction mixture			Conversion % of 1 into	
			1	12	4	12	4
1	No additive - 24 h	10 and 0.1M	0	77	23	63	38
2	No additive - 44 h		0	63	38	45	54
3	Anisole - 24 h	3 and 0.16M	45	12	43	9	60
4	<i>p</i> -Xylene - 24 h		65	34	1	34	1
5	<b><i>p</i>-Xylene - 96 h</b>		<b>0</b>	<b>97</b>	<b>3</b>	<b>95</b>	<b>5</b>

Table 3-8 Summary of the key data points from Table 3-5 compared to previous reaction results.

The final optimization included studying the concentration of the reaction mixture with respect to maleic anhydride with *p*-xylene. Again, as the concentration of maleic anhydride decreased, the amount of dimer **4** increased. Reactions at both 0.12 M and 0.10 M substrate concentrations were finished after 86 h irradiation, and 0.10 M was chosen as final concentration to ensure full conversion of reactions on larger scales (a reaction at 0.14 M was 96% complete after 96 h, and it was irradiated for an additional 24 h to reach full completion).

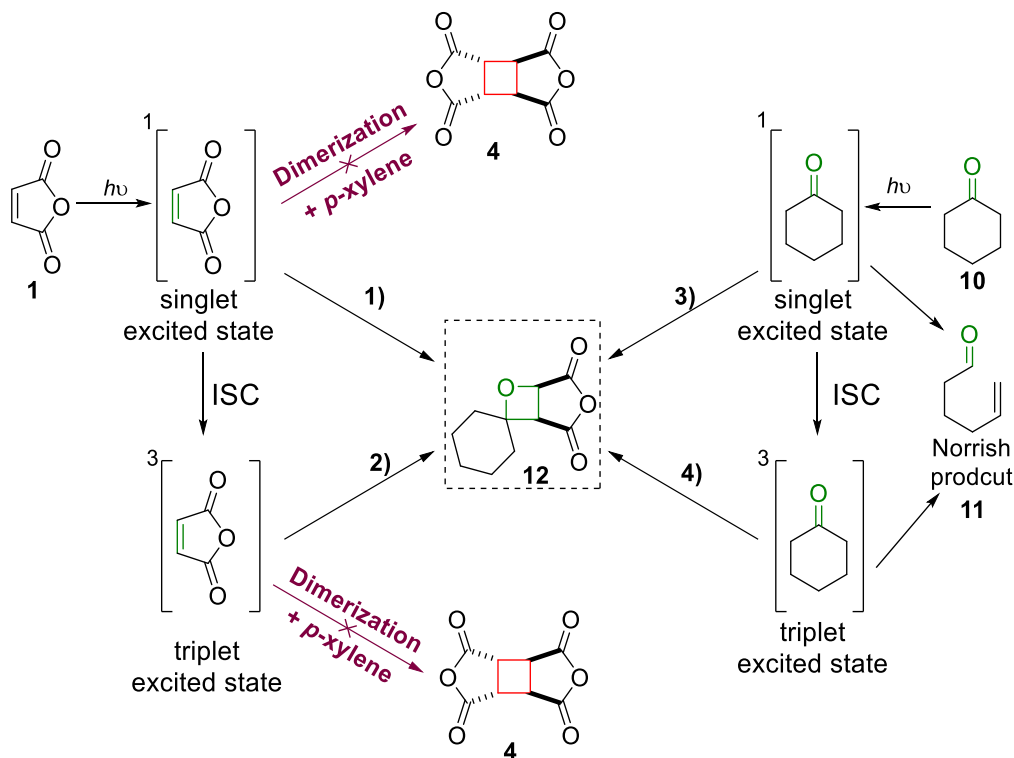


[1] (M)	Reaction time for full consumption of 1 (h)	4 (%)
0.16	96	2
0.14	120	2
0.12	86	2
0.10	86	3
0.08	72	2
0.06	72	3
0.04	60	4
0.02	48	7

Table 3-9 Results of optimization of the Paternò-Büchi reaction at different concentrations. Percentage of reaction mixture based on <sup>1</sup>H NMR (suppression, MeCN, 400 MHz).

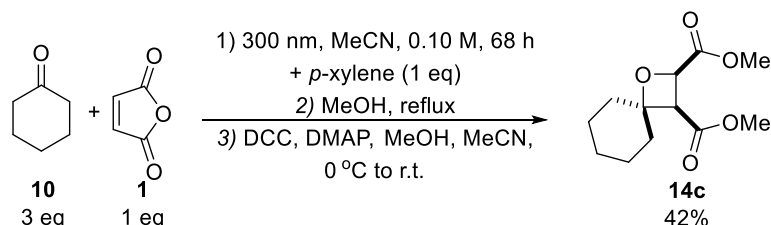
Although the original rationale for the addition of *p*-xylene (and other additives) was based on their triplet energies, it is not clear what kind of interaction exists between maleic anhydride and *p*-xylene. Scheme 3-11 adds the *p*-xylene into the reaction mechanism pathway, showing that when *p*-xylene is present, maleic anhydride undergoes Paternò-Büchi reaction and dimerization is suppressed, but these reactions

did not give any indication as to whether the dimerization reaction takes place via the singlet or the triplet excited state. Furthermore, it is still not clear which excited state is used to form the oxetane (ketone vs alkene, and singlet vs triplet). Further mechanistic studies are included in Chapter 4, but first, the practical application of the reaction was tested, to create a library of novel oxetanes.



Scheme 3-11 Summary of possible reaction pathways taking place when maleic anhydride (**1**) and cyclohexanone (**10**) are irradiated in the presence of *p*-xylene.

With the optimization completed, the three-step sequence was repeated to form and isolate the oxetane **14c** (Scheme 3-12). The addition of *p*-xylene increased the percentage yield to 42% (from 20% Scheme 3-6, and 5% Scheme 3-3). These batch photoreaction conditions worked well, and with the two additional steps a telescoped 3-step protocol was established and employed to create a library of oxetanes.



Scheme 3-12 Optimized Paternò-Büchi reaction between cyclohexanone (**10**) and maleic anhydride (**1**), followed by functionalization of the anhydride ring.

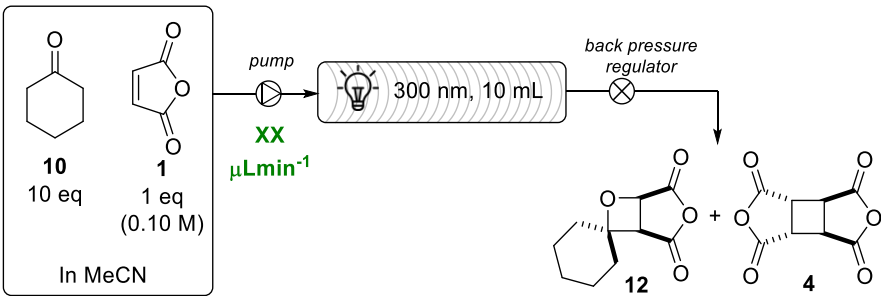
In summary, basic UV-vis and emission spectra were collected, showing the absorptions of the starting materials as well as estimating the triplet energy of maleic anhydride and cyclohexanone. Classical photochemical catalysts/triplet sensitizers were tested (THX

and Ir catalysts) but no significant reaction was reported; following these attempts, simple organic compounds were used as additives. Although the additives were chosen based on their triplet energies, it was not clear how they interacted with the maleic anhydride. A series of control experiments showed that the additives interact with maleic anhydride much more than cyclohexanone, however the nature of the interaction needs further investigation. The suppression of the dimerization reaction with simple organic compounds worked well, showing a substantial decrease in formation of the dimer, from 40% of maleic anhydride being converted into dimer to only 5% when 1 equivalent of *p*-xylene was added. The addition of the *p*-xylene was a simple change, which increased the yield of isolated oxetane from ~20% to over 40%. In parallel to the batch reactions, flow reactions were performed and are summarized next, followed by a study of the scope of the new Paternò-Büchi methodology.

### 3.2.4 Using flow to improve reaction time of the Paternò-Büchi reaction

After the successful translation of the Paternò-Büchi reaction between acetone and maleic anhydride into a flow system (section 2.2.3), the cyclohexanone-maleic anhydride system was also studied in flow.

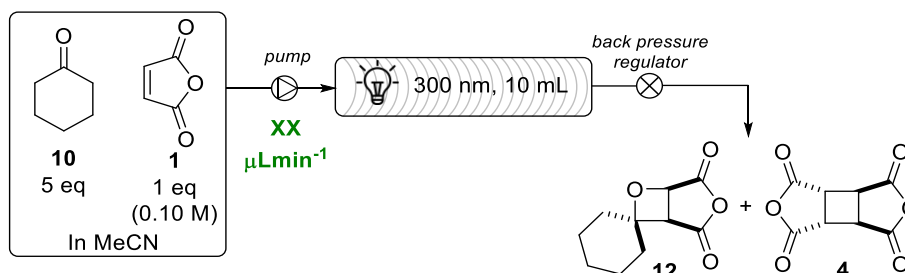
Starting with the reaction without an additive, a solution of maleic anhydride (0.10 M) and cyclohexanone (10 eq), was passed through the flow system fitted with a 300 nm lamp. The reaction mixture was exposed to light for 30 to 60 minutes (Table 3-10), showing full conversion of maleic anhydride into both oxetane and dimer. The ratio of the two products was comparable with the previous batch reaction (section 3.2.2.2).



Entry	Flow rate ( $\mu\text{Lmin}^{-1}$ )	Exposure time (min)	1 (%)	12 (%)	4 (%)
1	167	60	0	71	29
2	167/200	55	0	72	28
3	200	50	0	73	27
4	200/250	45	0	75	25
5	250	40	0	74	26
6	250/333	35	0	72	28
7	333	30	0	74	26

Table 3-10 Results of optimization of Paternò-Büchi reaction between cyclohexanone (10) and maleic anhydride (1) under flow conditions. Percentages of the components of the reaction mixture based on  $^1\text{H NMR}$  (suppression, MeCN, 400 MHz).

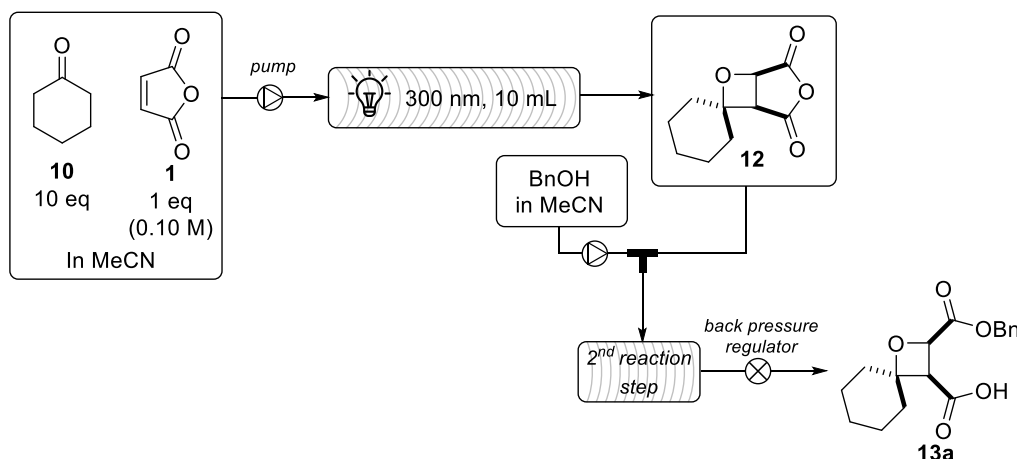
Similarly to the batch reactions, the number of equivalents of the cyclohexanone was reduced to 5 (Table 3-11). 60 minutes exposure time was necessary for full conversion of maleic anhydride (Table 3-11, entry 1). Slow flow rates showed a decrease in the conversion of maleic anhydride (Table 3-11, entry 2-5) to 66% at exposure time of 40 minutes.



Entry	Flow rate (μLmin <sup>-1</sup> )	Exposure time (min)	1 (%)	12 (%)	4 (%)
1	167	60	0	65	35
2	182	55	4	65	31
3	200	50	18	57	25
4	222	45	31	50	20
5	250	40	34	48	18

Table 3-11 Results of optimization of Paternò-Büchi reaction between cyclohexanone (10) and maleic anhydride (1) under flow conditions. Percentages of the components of the reaction mixture based on <sup>1</sup>H NMR (supression, MeCN, 400 MHz).

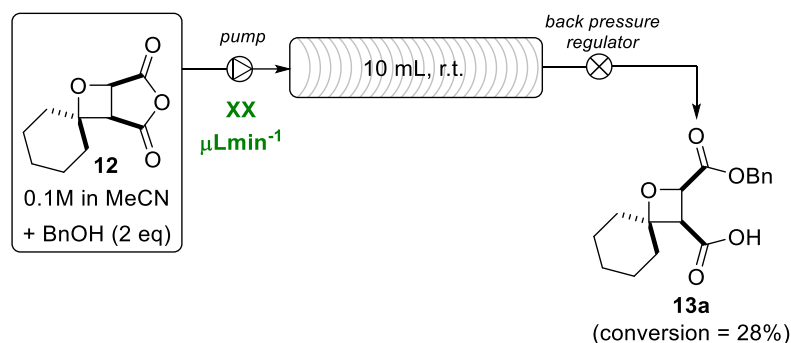
An advantage of the flow system can be performing two reactions steps one after the other, and a proposed reaction pathway is summarized in Scheme 3-13 formation of the oxetane via Paternò-Büchi reaction followed by ring opening of the anhydride with an alcohol to give oxetane **13a**.



Scheme 3-13 Proposed flow reaction for the formation of oxetane via Paternò-Büchi reaction followed by regioselective ring opening of the anhydride to give oxetane **13a**.

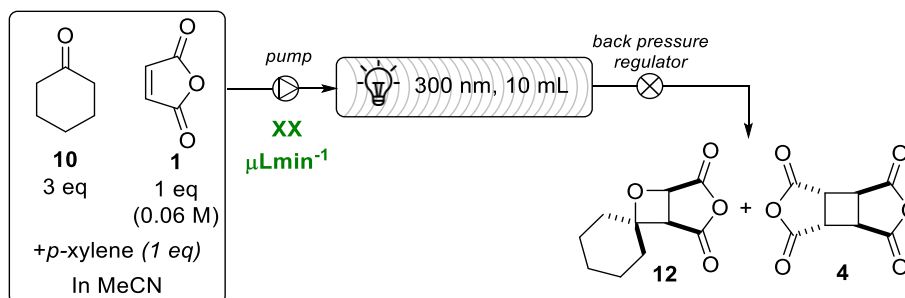
With that idea in mind, the 2<sup>nd</sup> reaction step, ring opening of the anhydride was also tested with flow. A solution of **12** (0.10 M) and benzyl alcohol (2 equivalents) in acetonitrile was passed through a 10 mL coil, mixing the solution for 30 or 40 min

(Scheme 3-14). However, the ring opening of the anhydride was low at only 28%, due to the lack of a heating column the reaction could not be performed at higher temperatures like the batch conditions (reflux). The reaction was not further investigated due to lack of heating column. The reaction likely would reach completion if the solution was run through the room temperature column multiple times, but the reaction was not further investigated under the flow conditions. However, if different equipment was accessible, the flow system for linking the two reactions would be expected to work.



**Scheme 3-14** Ring opening of anhydride under flow conditions. Conversion based on  $^1\text{H}$  NMR (suppression, MeCN, 400 MHz).

Finally, after the Paternò-Büchi reaction was fully optimized in the batch reactor by addition of the *p*-xylene (which suppressed the dimerization reaction), the flow Paternò-Büchi reaction was looked at again. Knowing that the addition of *p*-xylene extends the reaction time, the reaction mixture was run much more diluted at 0.06 M. A series of different flow rates was tested, giving exposure time between 10 and 33 minutes (Table 3-12). The results showed that the exposure time must be at least 25 minutes for the reaction to give a full conversion of maleic anhydride (Table 3-12, entry 5). As in the batch reaction, when *p*-xylene was added the formation of dimer was suppressed. Next, the reaction was performed on a larger scale, with 33-minute exposure time. First 100 mL of the reaction mixture was collected separately from the second 100 mL, A and B (Table 3-12, entries 7 and 8), showing a drastic decrease in the conversion of maleic anhydride, with 26% and 67% of maleic anhydride converted in the first and second 100 mL collected.



Entry	Flow rate ( $\mu\text{Lmin}^{-1}$ )	Exposure time (min)	1 (%)	12 (%)	4 (%)
1	1000	10	55	44	2
2	834	12	49	49	2
3	667	15	40	58	3
4	500	20	32	65	3
5	400	25	0	94	6
6	300	33	0	95	5
7 <sup>A</sup>	300	33	26	70	4
8 <sup>B</sup>	300	33	67	32	1

**Table 3-12 Results of optimization of Paternò-Büchi reaction between cyclohexanone (10) and maleic anhydride (1) in the presence of *p*-xylene under flow conditions. A and B: 100 mL of photosolute collected. % of reaction mixture based on <sup>1</sup>H NMR (suppression, MeCN, 400 MHz).**

This observation led to testing the conversion of the maleic anhydride at different stages of the flow reaction. Portions of the reaction mixture were collected, and the composition of the reaction mixture was determined by <sup>1</sup>H NMR spectroscopy. A brand-new lamp and reactor coil (of the flow photoreactor) were used, to ensure the best light intensity and clean reactor tubing. The percentage conversion of each portion of the reaction mixture can be easily shown by the Figure 3-7, which shows the conversion of maleic anhydride at different times during the flow photoreaction. Three reactions are summarized on the graph. Firstly, when the new lamp was used (Figure 3-7, green line), the conversion of maleic anhydride started at 72% but slowly decreased to about 60% over the 4-hour reaction time. This decreases the conversion of the maleic anhydride by 4% per hour. Next, a reaction with the old lamp was performed (Figure 3-7, blue line) showing a similar trend but at lower overall conversion at each reaction time, from 56 to 36%. Finally, in attempt to raise the overall conversion of the maleic anhydride, the concentration of the solution was decreased to 0.04 M (Figure 3-7, orange line). This did not work as expected, as the overall conversion decreased even further and still decreased during the reaction time.

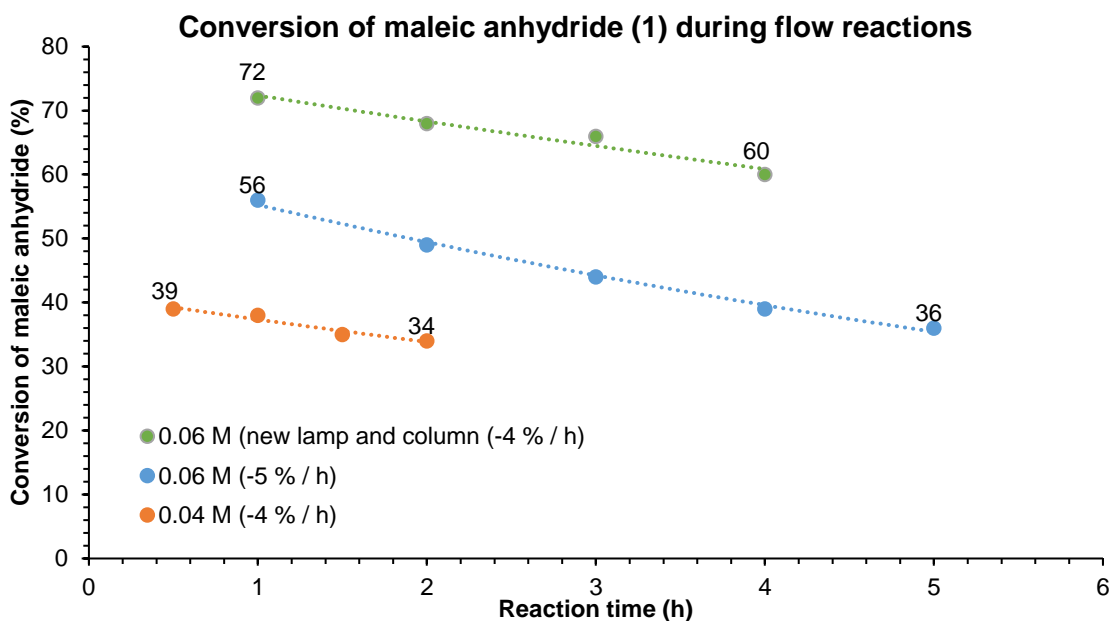
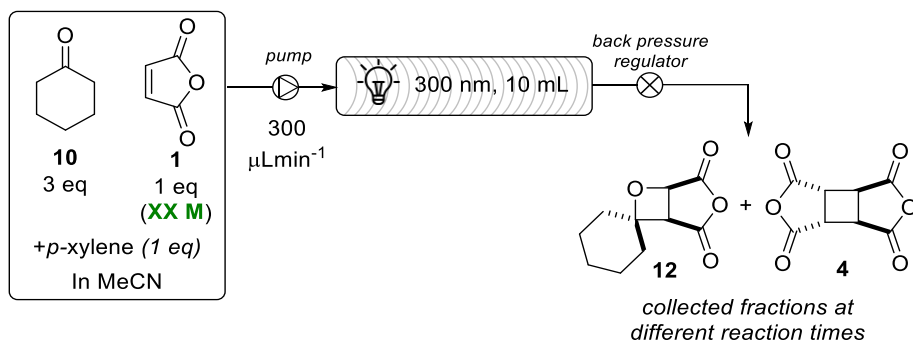


Figure 3-7 Graph showing the conversion of maleic anhydride (1) at different stage of the flow reaction.

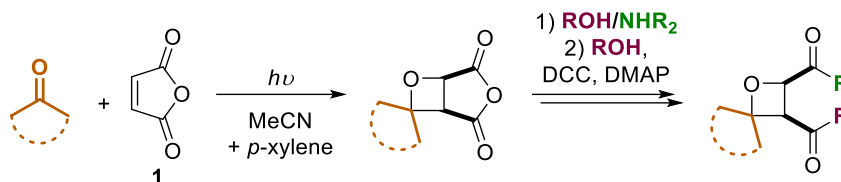
The flow reactions did not work as well when cyclohexanone was used as the ketone component in the Paternò-Büchi reaction as they did when acetone was employed. The overall decrease in the conversion was due to residue collecting on the tubes, which partially blocked the light, therefore slowing down the reaction rates. There is a possibility that a different flow system (one allowing for faster movement of the reaction mixture) might result in less residue being deposited on the tubes, resulting in higher conversion and for the conversion to remain constant throughout the reaction. No attempts were made to solve these issues with the flow system, as the batch reaction worked well and gave a good, practical way of forming the oxetanes. Although the reaction time was long, a series of reactions can be run in parallel, allowing for rapid formation of an oxetane library. The next section describes different functionalizations of the spirocyclic oxetanes formed, as well as expanding the scope of the Paternò-Büchi reaction by using different cyclic ketones.

### 3.3 Expanding the scope of the Paternò-Büchi reaction

The next section describes the formation of a library of oxetane-containing spirocycles (Scheme 3-15). As discussed before, the oxetane formed in the reaction contains an



anhydride ring, which is a good way of introducing new functional groups. Functionalization of the anhydride ring focused on the formation of ester and amide groups through nucleophilic opening of the anhydride ring. Additionally, a series of different cyclic ketones was used in the reaction, giving a range of different oxetane-containing spirocycles.



Scheme 3-15 Investigating the scope of the three-step sequence to give a library of oxetanes.

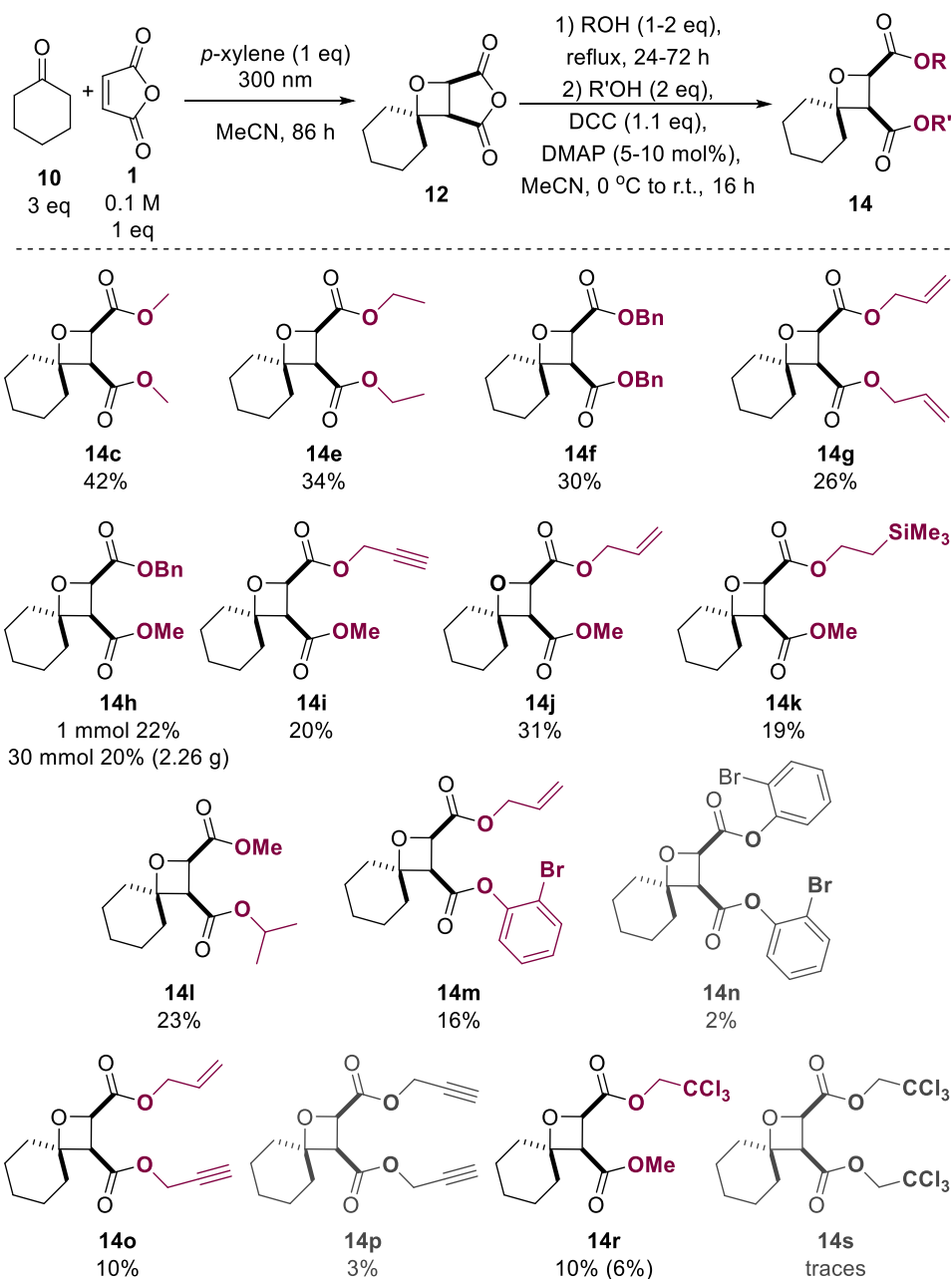
The following reactions were performed in a telescoped manner, with only one purification step to isolate the final oxetane. This allowed for the rapid formation of a range of oxetanes. The isolated yields reported are based on the maleic anhydride as the limiting reagent, over the three steps. Any changes or variations to the protocol are highlighted for the specific examples.

### 3.3.1 Functionalization of the anhydride ring

As discussed previously, primary alcohols are able to perform a regioselective ring opening of the anhydride ring adjacent to the oxetane, allowing for rapid diversification of oxetane **12**. Scheme 3-16 summarizes the oxetanes formed in the reaction, their isolated yields as well as any changes to the general reaction conditions. The reaction protocol was performed according to the optimized conditions, including the Paternò-Büchi reaction, regioselective ring-opening of the anhydride (with evaporation to dryness of the crude product) and esterification through DCC-mediated coupling with alcohols.

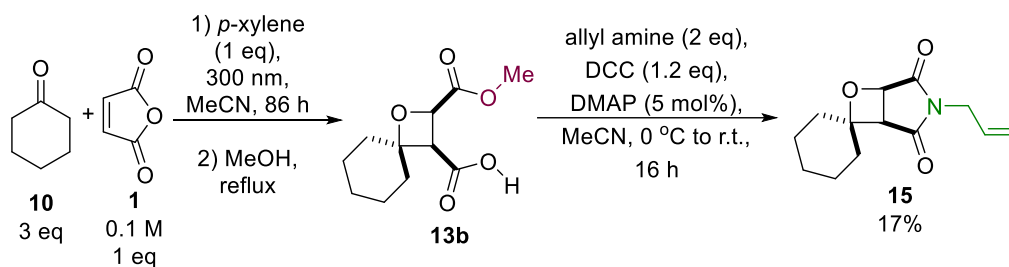
A series of primary alcohols was used to open the anhydride ring to give **12** followed by coupling of the carboxylic acid to give the final oxetane product **14c-s**. The first few examples used the same alcohol in both the ring-opening and esterification steps (**14c-f**), all giving satisfactory yields of 26-42% of the desired oxetanes. On the other hand, oxetanes **14g-s** were formed by using different alcohols in the ring-opening and esterification steps, allowing for the formation of two different ester groups. Importantly, the crude product formed in the ring-opening step had to be fully dried to allow the removal of the initial alcohol, to avoid it reacting in the coupling reaction. The majority of the examples gave suitable yields of 20-30% over three steps. The use of different alcohols potentially allows for orthogonal deprotection of the esters to the corresponding carboxylic acids, which could then be used in further synthetic transformations.

In contrast to these examples, a handful of examples (**14m**, **14o** and **14r**) gave a much lower yield, and in some cases an oxetane side product was isolated. In the case of **14n** and **14o**, it is possible that water was involved in ring opening of the anhydride, leading to formation of two carboxylic acids, which both underwent coupling in the final step. On the other hand, the formation of **14s** is likely due to the alcohol used in the ring-opening step not being fully removed before the coupling step. These two reactions were repeated and extended drying was performed, however the alcohol (HOCH<sub>2</sub>CCl<sub>3</sub>) could not be fully removed from the crude mixture, due to the high boiling point, causing the side product formation. Although secondary alcohols could not be used in the ring-opening step, **14i** shows that they can be successfully used in the coupling step, allowing for formation of an ester bearing a secondary chain. Finally, the scale of the reaction did not affect the isolated yield, with reactions performed at 1 or 5 mmol scale showing similar yields. Finally, 2.26g of **14h** was isolated, which resulted from a 30 mmol reaction scale, with a negligible change in percentage yield from 22 to 20% between the 1 and 30 mmol scale. This very wide scope of different esters formed allows for many different transformations, some of which are discussed in sections 2.3, while other possibilities will be summarized in the further work (Chapter 6).



**Scheme 3-16** Isolated oxetanes formed from the Paternò-Büchi reaction between cyclohexanone (**10**) and maleic anhydride (**1**) followed by functionalization of the anhydride ring to give a pair of esters.

The coupling of carboxylic acids with amines is well known, but using an amine in the coupling step proved challenging, and the desired product was not isolated. Instead, the ring underwent ring-closing again, and maleimide **15** was formed in 17% yield (Scheme 3-17).



**Scheme 3-17 Oxetane 15 - formed when allyl amine was used in the coupling step.**

Even though formation of an amide group from the carboxylic acid was not successful, an amide group can be formed if the anhydride ring is opened with an amine instead of an alcohol. Upon ring opening of the anhydride **12** with benzyl amine, solid was observed in the crude mixture of **16a**. Only traces of the crystals were isolated, but the resulting crystal structure is clear evidence of the regioselective ring opening of the anhydride ring, as well as of the relative *cis* configurations of the two carbonyl substituents (Figure 3-8). Pleasingly, these observations aligned with the crystal structure of **7b** reported in Chapter 2.

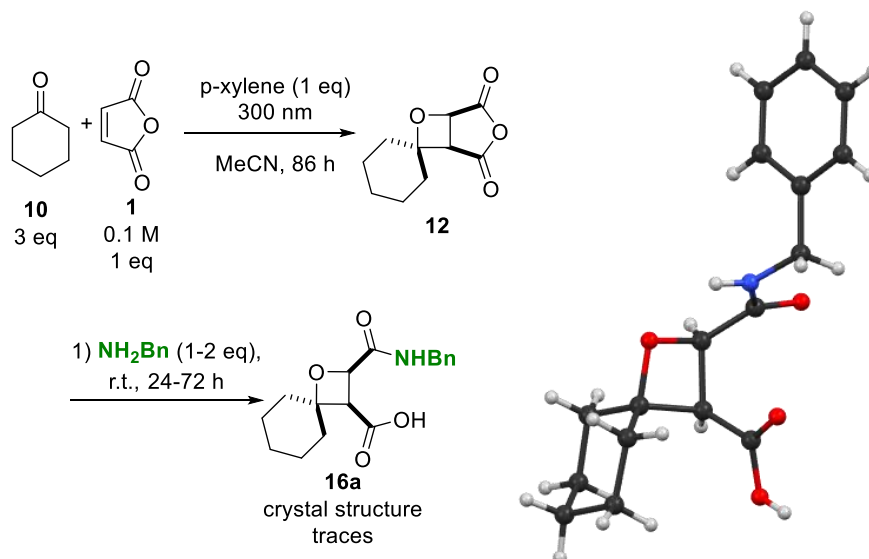
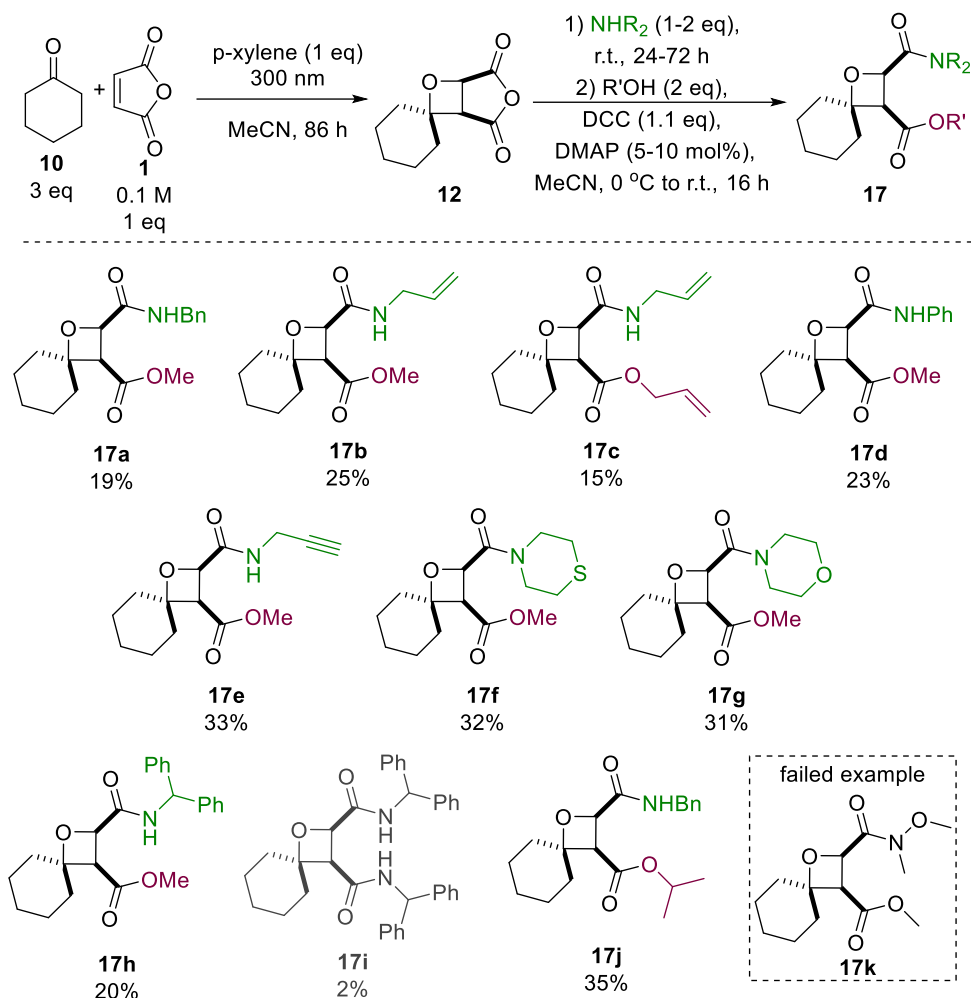


**Figure 3-8 Formation and XRD structure of 16a.**

Overall, five primary and two secondary amines were successful in the regioselective ring opening of the anhydride **12** (Scheme 3-18). The conditions of the ring opening were milder compared to when alcohols were used, showing reaction completion at room temperature, without no requirement for reflux. The isolated yields were satisfactory and comparable with previous isolated oxetanes in Scheme 3-16. Following the same protocol, the formation of a Weinreb amide (**17k**) was attempted, however the desired oxetane was not found, with only **14c** was isolated in trace amounts. It was suspected that during the ring-opening step decomposition occurred, as the key  $^1\text{H}$  NMR signals were no longer present. Similarly to the esters formed in Scheme 3-16, there is a large variety of amides formed (primary, secondary and bulky amines all performed well, as

did less nucleophilic amine such as aniline) allowing for series of different transformations, which are summarized in future work Chapter 6.



**Scheme 3-18 Isolated oxetanes formed from the Paternò-Büchi reaction sequence**

In summary, 29 novel oxetanes were formed from **12** as a result of the Paternò-Büchi sequence. The three-step telescoped reaction pathway was designed to allow for quick and efficient formation of the desired oxetanes that contain different functional handles, with only one purification step. The purification step worked well, however it is possible that the yield was affected by the purification process. The formed oxetane often did not stain strongly on a TLC plate (making it difficult to isolate all the product). The silica was washed out to ensure full removal of the desired oxetane, however it is possible that some of the oxetane product was lost on the column. Additionally, the excess ketone had to be removed first, often extending the column in order to obtain pure oxetane. Scaling up the reaction in batch showed no issues, and multigram quantities of desired oxetanes were isolated. The crystal structure reported confirmed the regioselective ring opening of the anhydride ring as well as showing the *cis* relationship between the two substituents. The variety of groups formed allows for further transformations (Section

3.3.3 and Chapter 6), making this a very desirable method for the formation of oxetane-containing spirocycles. Next, different cyclic ketones were tested in the reaction, allowing for the formation of other oxetane-containing spirocyclic scaffolds.

### 3.3.2 Different cyclic ketones

Further expanding of the scope of the possible oxetanes involved changing the ketone used in the Paternò-Büchi reaction. Varying one of the key starting materials allowed for a vast increase in the amount of possible oxetanes formed. The aim was to give access to four classes of oxetane-containing spirocyclic scaffolds, by using 4-7-membered ketones (Figure 3-9). For in-depth discussion of importance of oxetane containing spirocycles, see the literature review (Chapter 1).

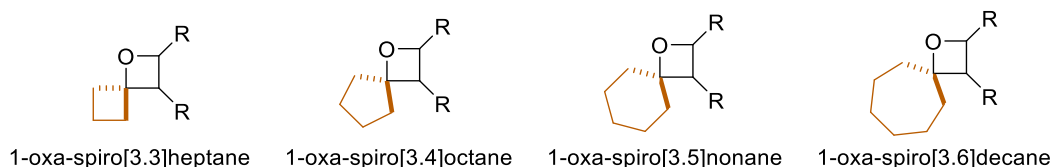


**Figure 3-9** Summary of the possible spirocycles formed when different size ketone is used in the Paternò-Büchi reaction.

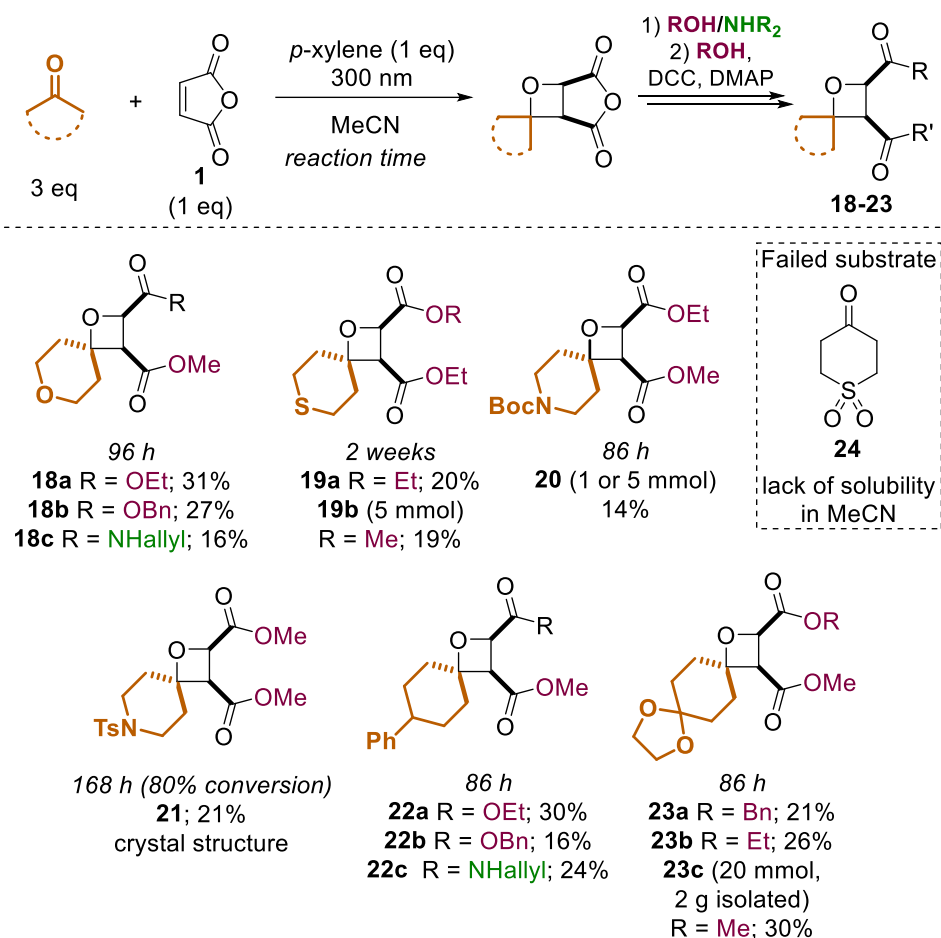
Pleasingly, a series of 5-7-membered cyclic ketones can be used in the Paternò-Büchi reaction without any major changes to the reaction protocol, with the only variable being the reaction time required for completion of the Paternò-Büchi reaction. In the case of 4-membered-ring ketones, the reaction did not work as expected and the expected oxetane was not isolated; these reactions are discussed in section 3.3.2.2.

#### 3.3.2.1 5-7-Membered cyclic ketones

A series of 6-membered symmetrical ketones were tested in the reaction (Scheme 3-19); the reaction time for each Paternò-Büchi reaction is specified for each ketone. The chosen ketones were symmetrical so that the Paternò-Büchi reaction results in only one product isomer, and without any groups that would be expected to react during the functionalization reactions.

The formed oxetanes underwent ring opening and functionalization reactions by following the same telescoped reaction protocol, all giving satisfactory yields of 14 – 31% (Scheme 3-18). The addition of a heteroatom into the cyclic ketone yielded a series of spirocyclic scaffolds (**18-23**). Similarly to the previous examples, the scale of the reaction did not have an effect on the yield, allowing for larger scale reactions to be performed. The change in the cyclic ketone did not have a major effect on the isolated yield, with the exception of **20**, which proved difficult to purify by column chromatography, yielding only 14% of the isolated oxetane (on both 1 mmol and 5 mmol scales). The Paternò-Büchi reaction of *N*-tosyl piperidone, to yield oxetane **21**, showed a very slow consumption of

maleic anhydride – only 80% conversion after 168 h. In contrast to the oxetane **20**, which contained Boc group, the Ts-protected example was much easier to isolate, and a crystal structure of the final oxetane **21** was obtained (Figure 3-10). Ketone **24** was expected to yield a sulfone-containing spirocycle, however the ketone was not soluble in MeCN. However, oxidation of **19** can be performed, allowing access to the same final product (Scheme 3-29). The new oxetane-containing spirocyclic scaffolds with different heteroatoms and groups on the spirocycles can also undergo a series of different reactions. The additional transformations are summarized in section 3.3.3 and further work section (Chapter 6).



Scheme 3-19 Isolated oxetanes from the telescoped Paternò-Büchi sequence. Isolated yields based on maleic anhydride (**1**).

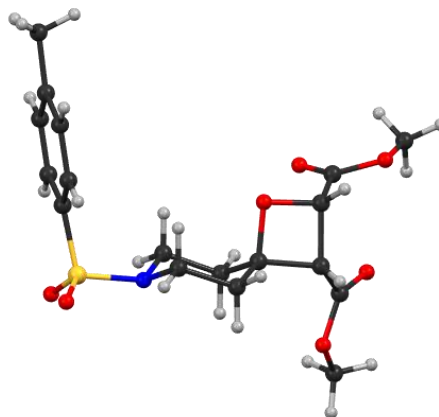
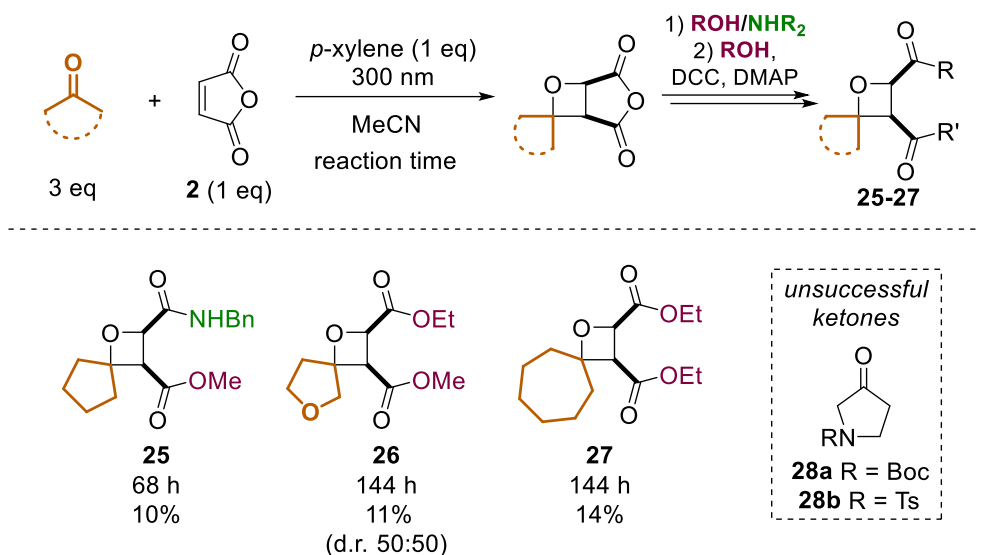


Figure 3-10 Crystal structure of **21**.

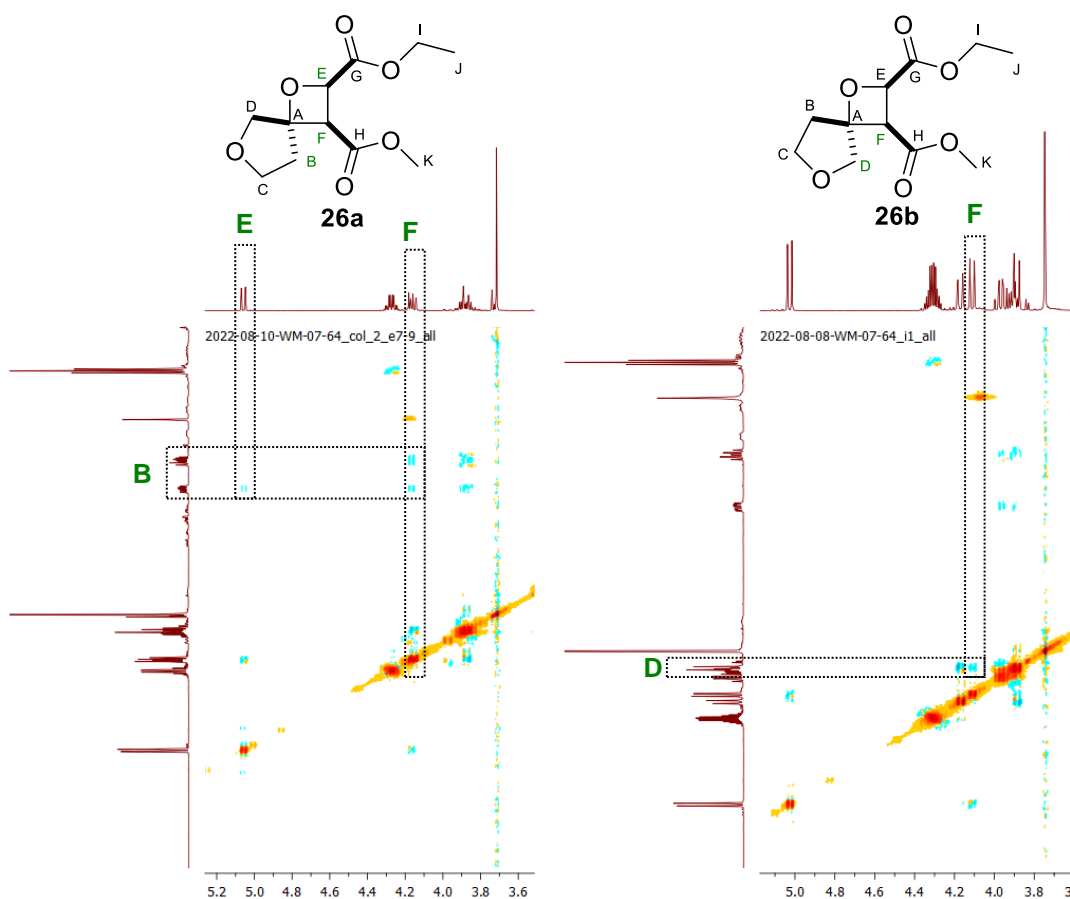
Following the success of 6-membered cyclic ketones and formation of a series of 1-oxa-spiro[3.5]nonane spirocycles, the method was expanded to 5- and 7-membered cyclic ketones to form 1-oxa-spiro[3.4]octane and 1-oxa-spiro[3.7]decane spirocycles respectively. Scheme 3-20 summarizes the novel oxetanes isolated; cyclopentanone and cycloheptanone both yielded the desired oxetane **25** in 10% and **27** in 14% yields respectively. The isolated yields were slightly lower than isolated yields of the 1-oxa-spiro[3.5]nonane examples, however it is not clear why the yields were lowered. Each reaction step was checked and full completion was ensured before moving on to the next step, and the formed oxetanes are expected to have similar stability to the 1-oxa-spiro[3.5]nonane examples, and there was no indication of breaking of the oxetane ring at any stage of the reaction. In the case of the 5-membered cyclic ketones, a reaction with a non-symmetrical ketone was also performed, in which the asymmetry was introduced by a hetero atom (O or NR). The reaction gave a mixture of two isomers (**26a** and **26b**) when tetrahydrofuran-3-one was used as a ketone. However, when *N*-protected 3-aminoketones (**28a/b**) were used, no final oxetanes were isolated; <sup>1</sup>H NMR signals of the starting material ketone were in the same region in which the oxetane peaks were expected, making it impossible to fully interpret the reaction.





**Scheme 3-20** Isolated oxetanes formed in Paternò-Büchi reaction between 5- and 7-membered cyclic ketones and maleic anhydride (1), followed by functionalization reactions. Isolated yields based on maleic anhydride (1).

A larger scale reaction with the use of tetrahydrofuran-3-one was performed in an attempt to separate the two diastereoisomers (**26a** and **26b**). The two isomers were separated by column chromatography to give 2% and 3% yields respectively, and the  $^1\text{H}$ - $^1\text{H}$  NOSY 2D NMR shows the difference between two isomers, allowing for full characterization of both isomers. The NOESY analysis was focused on the cross-peaks between  $\text{H}^{\text{F}}$  and protons on the 5-membered ring. The isomer **26a** (2%) shows interactions between  $\text{H}^{\text{F}}$  and  $\text{H}^{\text{B}}$  as well as a much weaker signal between  $\text{H}^{\text{E}}$  and  $\text{H}^{\text{B}}$ , while isomer **26b** (3%) shows a cross-peak between  $\text{H}^{\text{F}}$  and  $\text{H}^{\text{D}}$ .

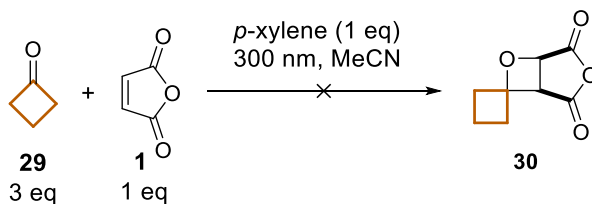


Scheme 3-21 NOSEY  $^1\text{H}$ - $^1\text{H}$  NMR showing the two isomers.

Overall, the 5-7-membered ketones can easily be used in the Paternò-Büchi reaction to give the desired oxetanes. As expected, non-symmetrical ketones give rise to two isomers, and it is possible that if a bulky enough group is used on one face of the ketone, then the selectivity towards one of the isomers would be improved. Changing of the ketone used in the reaction gave rise to 16 new oxetane-containing spirocycles. Next 4-membered symmetrical ketones were tested in the reaction.

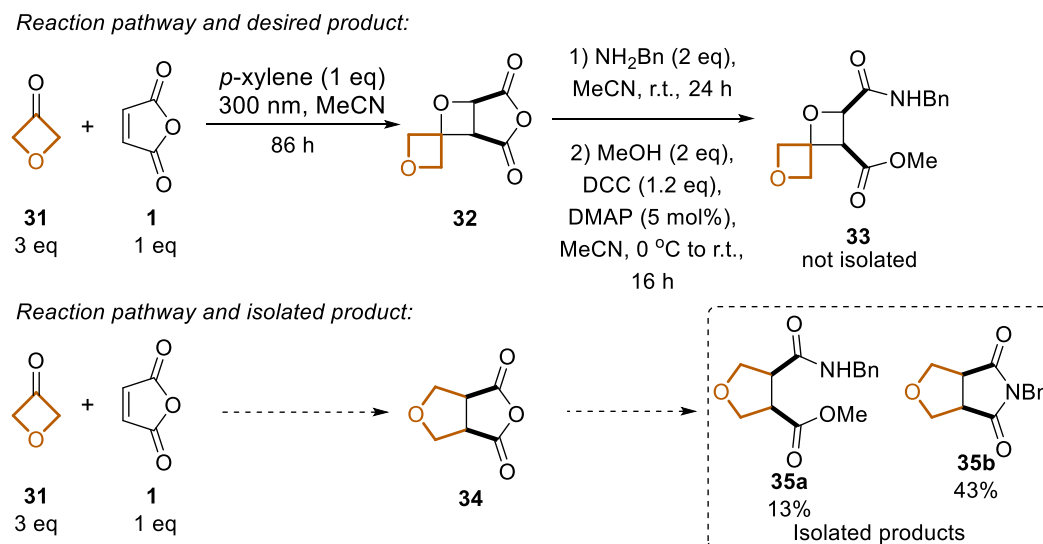
### 3.3.2.2 4-Membered rings

Three different 4-membered symmetrical cyclic ketones were tested, starting with cyclobutanone (**29**), which did not undergo the Paternò-Büchi reaction to form the desired oxetane **30** (Scheme 3-22). The reaction was tracked by solvent suppression  $^1\text{H}$  NMR spectroscopy, showing rapid decomposition of the cyclobutanone (**29**) and a lack of consumption of maleic anhydride.



Scheme 3-22 Reaction between cyclobutanone (**29**) and maleic anhydride (**1**).

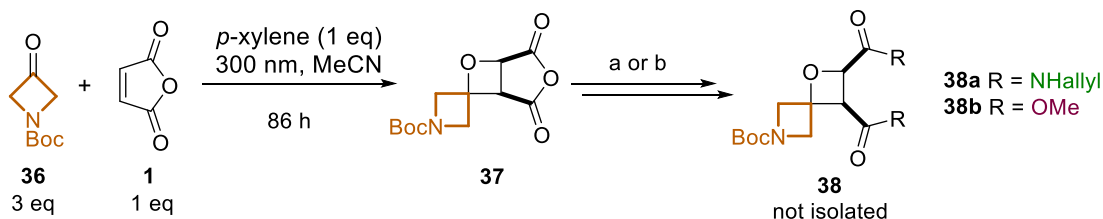
Changing the ketone to an oxetanone (**31**) gives a possibility of spirocycle made up of two oxetane rings **33**. Tracking the photochemical reaction indicated consumption of the maleic anhydride, but the final isolated product was not the desired oxetane **33**, instead **35a** and **35b** were isolated in 13% and 43% yield respectively (Scheme 3-23). The functionalization of the anhydride ring did not work as expected, as after formation of the benzylamide the 5-membered ring was re-formed, to give an imide product **35b**.



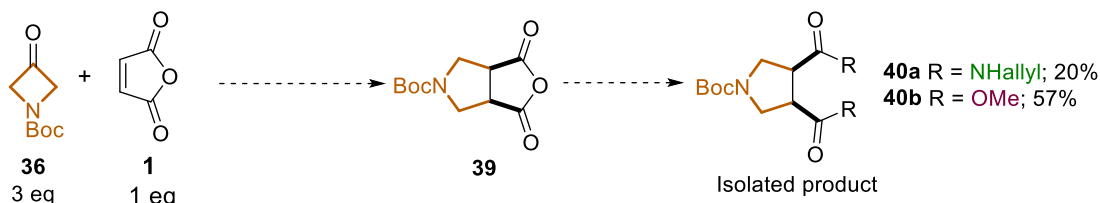
**Scheme 3-23** Reactions with 4-membered cyclic ketones.

Similarly, having a nitrogen in the 4-membered ring instead of oxygen gave the same results; the expected spirocycles **38a** and **38b** were not isolated but the 5-membered ring was formed, followed by the functionalization of the anhydride ring (Scheme 3-24) yielding **40a** and **40b** in 20% and 57% respectively. Two functionalization pathways were used, one to form two methyl esters, which worked very well giving the final product **40b** in 57% yield. This is the highest isolated yield attained from the three-step telescoped reaction pathway, and this could be due to the stability of this product on the silica compared to the previously formed oxetanes. Additionally, the left-over ketone was much more efficiently removed, allowing for the product **40b** to be the major product. The second functionalization pathway focused on the formation of an amide; in this case an imide was not formed (as in Scheme 3-23), instead two amide groups were formed and the final product **40a** was isolated in 20% yield.

Reaction pathway and desired product:



Reaction pathway and isolated product:



**Scheme 3-24** Reactions with 4-membered cyclic ketones. Conditions: a: 1) allyl amine (2eq), MeCN, r.t., 24 h 2) allyl amine (2 eq), DCC (1.2 eq), DMAP (5 mol%), MeCN, 0 °C to r.t., 16 h. b: MeOH (2eq), MeCN, r.t., 24 h 2) MeOH (2 eq), DCC (1.2 eq), DMAP (5 mol%), MeCN, 0 °C to r.t., 16 h

The structures of products **35** and **40**, (Scheme 3-23 and Scheme 3-24) were not easy to determine; due to their symmetrical nature the NMR data did not give a lot of information. **35b** and **40a** were recrystallized, and the final structures of the products was confirmed by X-ray diffraction (Figure 3-11).

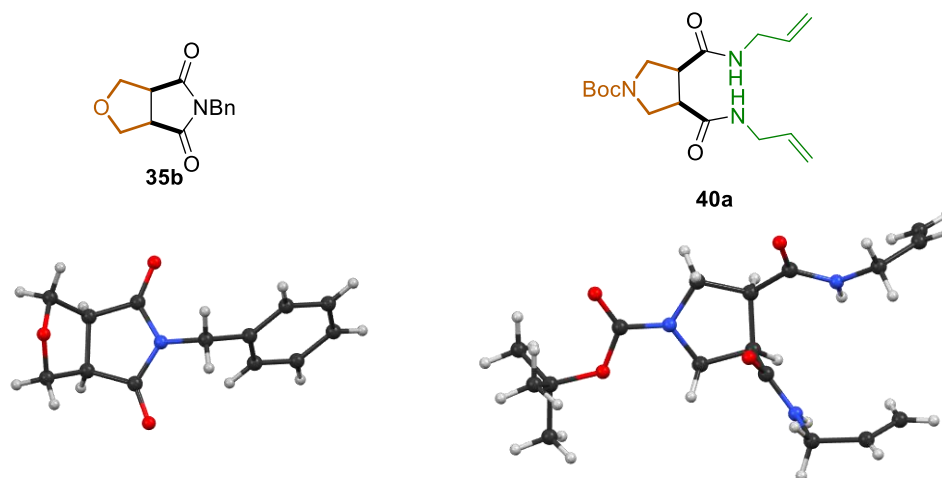
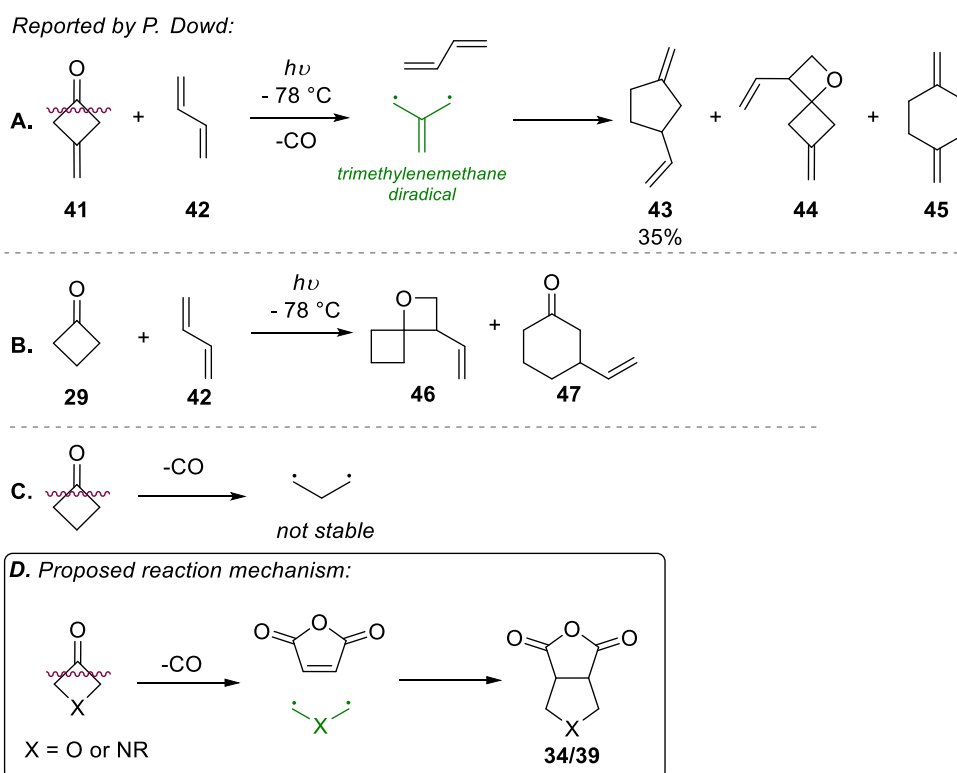


**Figure 3-11** Crystal structures of **35b** and **40a**.

The mechanism for the reaction between **31** or **36** and maleic anhydride vastly differs from the Paternò-Büchi reaction mechanism and has been theorized based on the chemistry of the diradical trimethylenemethane species (Scheme 3-25). In 1966, Dowd<sup>91</sup> reported the following two reactions: photolysis of 3-methylenecyclobutanone (**41**) and butadiene (**42**) (Scheme 3-25A), yielding a series of products (3-vinylmethylenecyclopentane (35 %, **43**), oxetane (**44**) and other minor products) as well as reaction between cyclobutanone (**29**) and butadiene (**42**) (Scheme 3-25B) which only yielded the oxetane products. 3-methylenecyclobutanone (**41**) is a precursor for the trimethylenemethane diradical species (Scheme 3-25A) allowing the formation of the 5-

membered ring. In the case of the cyclobutanone (**29**), the diradical that would be formed is not stable enough to be trapped, so it cannot react with the butadiene (**42**) (Scheme 3-25C). In the case of the reactions reported in Scheme 3-23 and Scheme 3-24, the diradical species formed from the ketone can be stabilized by the adjacent heteroatoms present, allowing for their reaction with the maleic anhydride (Scheme 3-25D) to give the final product **34/39**. This is consistent with cyclobutanone (**29**) not yielding a similar product, as the required diradical is not stable and may degrade rapidly through other reactions. An important detail is the formation of the oxetanes in these reactions, which was not possible in our system. This could be due to lowering the temperature of the reaction to  $-78\text{ }^{\circ}\text{C}$ , which would not be feasible using the photochemical equipment available in our laboratory.



Scheme 3-25 Background and proposed mechanism for formation of **34/39**.

In 2023, a photochemical decarboxylation of oxetanone (**31**) and azetidinone (**36**) has been reported by Boskovic and co-workers.<sup>92</sup> (This work has been published during the writing of this thesis.) The computational studies performed confirmed the likelihood of the formation of the diradical, via step-wise Norrish type I cleavage, which is stabilized by the presence of the heteroatom. The diradical form is stable enough to undergo [3+2] cycloaddition reactions with a range of alkenes.

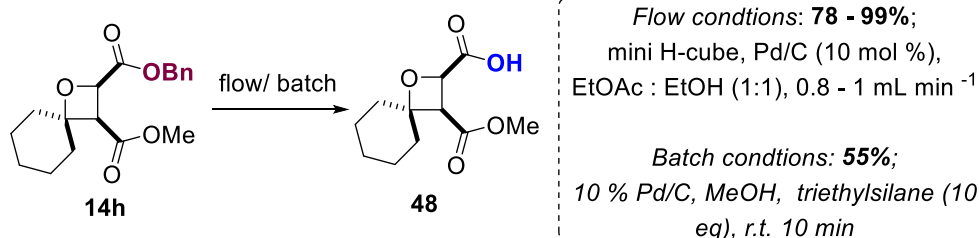
The majority of cyclic ketones were successful in the Paternò-Büchi reaction, yielding sixteen oxetanes in 10-30% yield. An example of a non-symmetrical ketone was also used in the reaction sequence, and as expected, two isomers were formed in a 1:1 ratio

(**26**), and successfully separated. A crystal structure of oxetane **21** was obtained, yet again confirming the regioselective ring opening of the anhydride ring as well as the *cis* relationship of the two carbonyl groups on the oxetane ring. Finally, the reactions between 4-membered ketones and maleic anhydride were partially successful, in that although the desired oxetane products were not formed, different products were formed. The new products were isolated in 20-52% yields, and a reaction mechanism has been proposed based on the diradical species that likely result upon decarboxylation of the starting 4-membered ketones.

### 3.3.3 Additional reactions and transformations

The next section shows how the oxetane products isolated in sections 3.3.1 and 3.3.2 can be used in further transformations, leading to a wider variety of products. Oxetane rings can be sensitive to acidic conditions, as discussed in the literature review, and this next section summarizes how the oxetanes formed via the three-step telescoped pathway behaved under different reaction conditions (including deprotection, oxidation and reduction conditions).

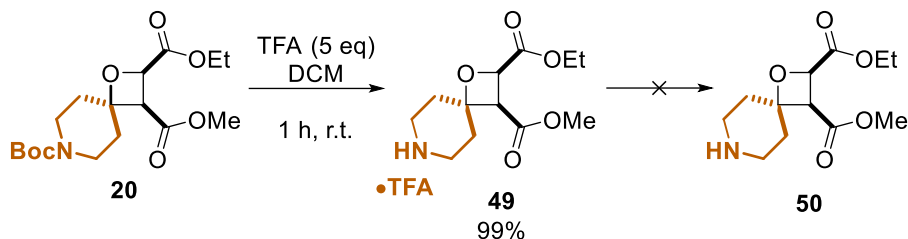
Deprotection reactions started with the removal of the benzyl ester to form a carboxylic acid **14h** (Scheme 3-26). The reaction was performed under flow and batch conditions and formed carboxylic acid **48** in good to very good yields. The flow conditions used a H-Cube Mini+ apparatus – a fast and efficient flow reactor commonly used for a variety of hydrogenation reactions. The flow reaction worked well and did not require purification making the yield much higher, however with time the conversion of the collected fractions decreased, likely due to the catalyst decomposing, leading to multiple reaction runs and lowering the yield of the final product **48**. The batch reaction took only 10 minutes, however the work up and purification were very time consuming. Additionally, it is very likely that the much lower percentage yield of the batch reaction compared to flow is due to the necessary column chromatography.



**Scheme 3-26** Removal of the benzyl ester and formation of **48** under flow and batch conditions.

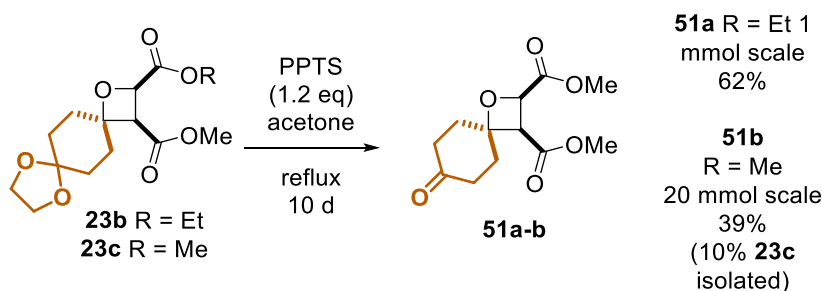
The second deprotection reaction studied was the removal of the Boc group (Scheme 3-27), showing good conversion under standard trifluoroacetic acid (TFA) conditions. Pleasingly, the oxetane ring stayed intact, and the oxetane **49** was isolated as TFA salt.

Attempts to isolate the free amine (**50**) led only to decomposition, generating a complex mixture of products.



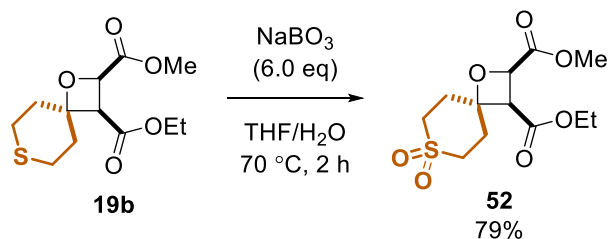
Scheme 3-27 Removal of the Boc group and formation of **49**.

Next, the acetal group was removed with pyridinium *p*-toluenesulfonate (PPTS) (Scheme 3-28), and whilst the reaction took a long time to reach completion, the corresponding ketone **51a** was obtained in a good yield of 62%. A larger-scale reaction was stopped before full completion, leading to a lower yield of **51b** and isolation of the starting material. Given the stability of the oxetane products upon exposure to TFA (for Boc deprotection), it is likely that more forcing conditions could be used to speed up the acetal deprotection.



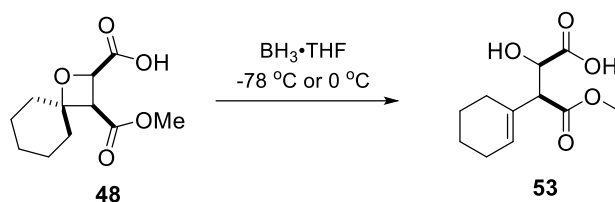
Scheme 3-28 Removal of acetal and formation of ketone **51**.

The oxidation of sulfane-containing oxetane **19b** was performed, pleasingly giving the desired sulfone-containing spirocycle **52** in 79% yield (Scheme 3-29).



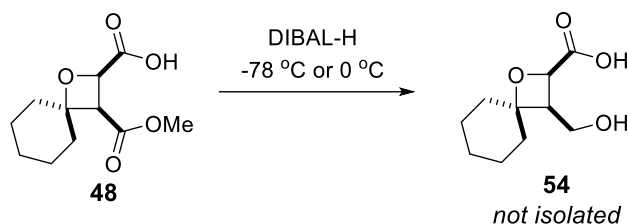
Scheme 3-29 Oxidation of sulfane (**19b**) to sulfone (**52**).

Next, reduction conditions were tested to reduce either the carboxylic acid or ester group.  $\text{BH}_3$ -THF is a commonly used reducing agent that can potentially reduce carboxylic acids in the presence of esters, which would allow for selective reduction. However, based on the isolated product **53** (Scheme 3-30) the  $\text{BH}_3$ -THF did not reduce either of the carbonyl groups, but instead coordinated to the oxygen atom in the oxetane ring, causing the ring to cleave.



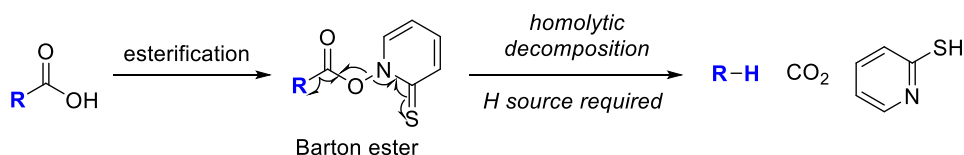
**Scheme 3-30** Reduction attempt with  $\text{BH}_3\text{-THF}$ .

The second reducing agent tested was diisobutylaluminium hydride (DIBAL-H). A reaction with 2 equivalents of DIBAL-H was performed on a small scale, with the aim that only one group will be reduced to give an alcohol group (Scheme 3-31). The crude  $^1\text{H}$  NMR spectrum showed a loss of methyl peak, suggesting that the ester was reduced, however the purification of the crude mixture was not successful, possibly due to the presence of carboxylic acid group. Only one oxetane (**48**) with a carboxylic acid group was isolated by column chromatography, with a major loss of the product during the purification. Therefore, it is likely that the oxetane **54** needs to be purified using a different method.



**Scheme 3-31** Reduction of **48** to **54** with the use of DIBAL-H.

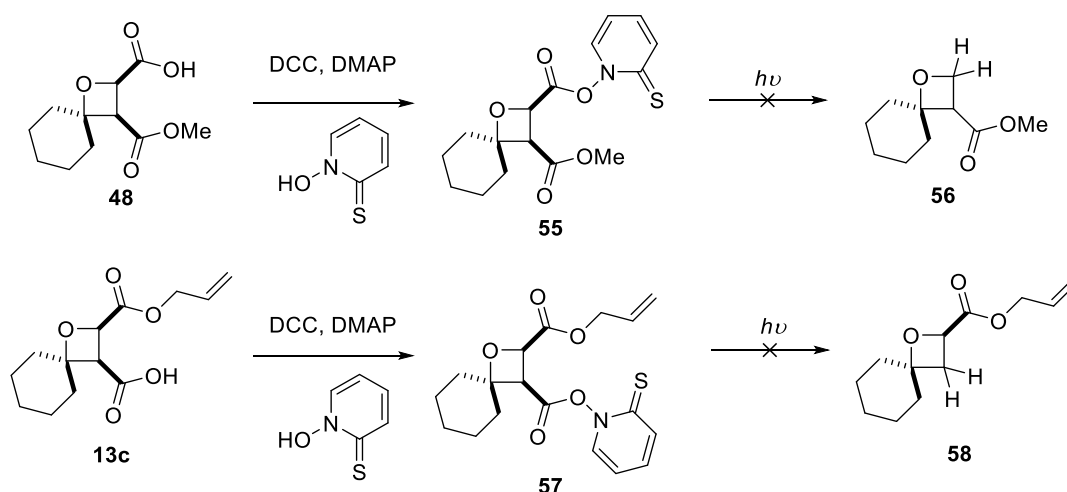
Next, a Barton decarboxylation<sup>93</sup> reaction was attempted, to remove the carboxylic acid group from the oxetane. The reaction has two major steps: formation of the Barton ester, which can be done via DCC cross coupling, followed by homolytic decomposition of the ester to give the desired product (Scheme 3-32).



**Scheme 3-32** General reaction pathway of the Barton decarboxylation reaction.

Traditional reaction conditions use tin to initiate the homolytic decomposition of the Barton ester, but recently a procedure for the Barton decarboxylation that uses chloroform (as H-donor) and light was reported, allowing for much less toxic reaction conditions.<sup>94</sup> Two different oxetanes were tested, to see whether the decarboxylation reaction works better at different positions on the oxetane.





Scheme 3-33 Barton decarboxylation reaction.

A series of different conditions were tested, and are summarized in Table 3-13. Starting with the reaction conditions reported by Williams and co-workers<sup>94</sup> (Table 3-13, entry 1-3) no desired product **56** was observed, and in all reactions small amounts of the Barton ester (**55**) and the starting material (**48**) were isolated. Therefore, it was theorized that the Barton ester is formed, but the homolytic decomposition step was the issue, either due to lack of a good H-donor or the wrong wavelength of light being applied. These two potential issues were addressed, firstly <sup>t</sup>BuSH was used as a potential H-donor,<sup>93</sup> as well as the reactions being irradiated at 300 nm followed by 350 nm. Two reactions were performed using the isolated Barton ester (**57**) from the previous reactions, and the reactions were performed in an NMR tube to allow for efficient tracking by <sup>1</sup>H NMR spectroscopy (Table 3-13, entry 4 and 5). However, observation of both reactions did not indicate formation of any major product. It is possible that the wavelength of the reaction should be lowered to 254 nm, however that is very high energy light and it could easily cause decomposition of the starting material, which was the main reason for avoiding the higher energy lights.

Entry	Starting material	Conditions changes	Solvent	Wavelength and reaction time
1	<b>48</b>	-	chloroform	300 nm (3 h)
2	<b>48</b>	-	chloroform	300 nm (3 h)
3	<b>13c</b>	-	chloroform	300 nm (overnight)
4	<b>57</b>	+ <sup>t</sup> -BuSH,	toluene	300 nm (overnight) → 350 nm (3 h)
5	<b>57</b>	+ <sup>t</sup> -BuSH	chloroform	300 nm (overnight) → 350 nm (3 h)

Table 3-13 Conditions tested for the Barton decarboxylation reaction.

Although some transformations were not successful, such as reduction reactions and Barton decarboxylation, other reactions worked well, giving the desired products. Deprotection reactions worked well, allowing for removal of the Boc, benzyl ester and acetal group without breaking the oxetane ring. Oxidation of the sulfane allowed access

to the sulfone, which could not be made by using the corresponding sulfone-containing ketone as the starting material in the Paternò-Büchi reaction. In summary, these reactions show that the formed oxetanes are stable under many different reaction conditions allowing for further functionalization, and these oxetane products are therefore ideal starting points for the preparation of arrays of oxetane-containing spirocycles – the focus of future work within the research group.

### 3.4 Conclusions

In summary, this chapter discussed the successful optimization of the Paternò-Büchi reaction between cyclic aliphatic ketones and maleic anhydride. The reaction conditions for the Paternò-Büchi reaction as well as the subsequent transformations were based on the initial reaction conditions described in Chapter 1, however, optimizations were necessary to improve the reaction yield (from 5% to 20%) starting with basic modifications (number of equivalents of reagents, reaction time and temperature). The final and most important reaction optimization was the suppression of the dimerization of maleic anhydride, which doubled the yield of the isolated oxetane (20% to 42%). The dimerization reaction was suppressed by the addition of *p*-xylene, which originally was chosen based on its triplet excited energy, and its potential ability to influence the triplet and singlet excited state populations of maleic anhydride. The triplet energy of *p*-xylene is higher than that of maleic anhydride, making triplet sensitization plausible, however, the interaction between maleic anhydride and *p*-xylene is not clear. Additionally, it is unlikely that *p*-xylene can absorb enough energy to triplet sensitize maleic anhydride at the wavelength employed for these reactions. A more in-depth investigation into the mechanism of the Paternò-Büchi reaction, the dimerization of maleic anhydride and the role of the *p*-xylene is discussed in Chapter 4.

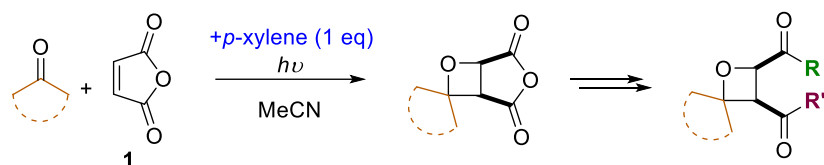
Optimization of the Paternò-Büchi reaction and additional transformations of the anhydride ring allowed for the development of a three-step telescoped reaction sequence, with only one purification step (Scheme 3-34), allowing for rapid formation of a library of oxetanes with different functional handles. The starting materials used were common, inexpensive reagents, which after the reaction protocol yielded complex oxetane-containing spirocyclic scaffolds. Each step of the three-step telescoped sequence can diversify the final products starting with using different ketones in the Paternò-Büchi reaction, then the regioselective ring opening of anhydride with an alcohol or amine (allowing for formation of a variety of different ester or amide groups), and finally coupling of the resulting carboxylic acid, which led to formation of a series of different ester groups. In total, 45 oxetanes were isolated using the newly developed protocol.

Additional synthetic transformations were also tested on the isolated oxetanes, with some yielding the desired oxetanes. For example, an acetal deprotection cleanly regenerated the ketone functional group, Boc deprotection liberated the corresponding amine salt, and oxidation of a sulfide to a sulfone proceeded well. In some cases, the oxetane ring cleaved, and different set of conditions should be screened for the desired transformation. However, there are still many other transformations that can be tested on the oxetane products (see Chapter 5).

The Paternò-Büchi reaction between acetone and maleic anhydride was easily translated into a flow system (Chapter 2 section 2.2.3), however when cyclohexanone was used in the reaction, the flow set-up worked less well. Potentially, the large excess of acetone present in the reactions discussed in Chapter 2 may allow side reactions to be prevented that occur when the loading of the ketone is greatly reduced. A series of different reaction conditions were tested in flow, but none were as successful or as practical as the batch reaction set-up; this was mainly due to the long reaction time at the slow flow rates required, and formation of side products, which formed a film on the inside of the tubing, partially blocking the light and decreasing the reaction conversion during the reaction run.

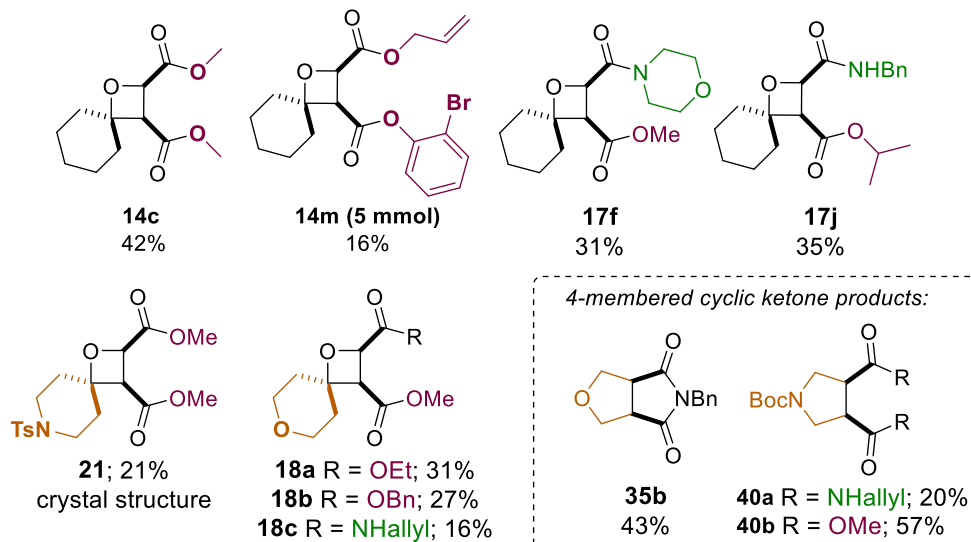
The Paternò-Büchi reaction was shown to be compatible with different cyclic ketones of different ring sizes, and the majority of the ketones tested in the reaction worked as expected, producing the desired spirocyclic oxetanes. In the case of 4-membered cyclic ketones, a new product was formed. This unexpected reaction needs further investigation, as it is potentially a promising method for the synthesis of disubstituted tetrahydrofuran and tetrahydropyrrole products. A mechanism for the formation of the product was proposed, involving initial decarbonylation of the four-membered ketone to give a diradical, which could then undergo addition to maleic anhydride.

Overall, cyclic aliphatic ketones work well in the Paternò-Büchi reaction with maleic anhydride. A successful and practical reaction protocol was designed for formation of highly functionalized spirocyclic oxetane scaffolds. This chapter focused mainly on the optimization of the reaction, as well as expanding the scope of the formed oxetanes at each of the three reaction steps. The mechanistic picture for this system is complex, due to different reactions that can take place: Paternò-Büchi, dimerization, polymerization and Norrish type 1 reaction. The next chapter focuses on an investigation into the mechanisms of the Paternò-Büchi and dimerization reactions, as well as shining a light on the role/interaction/effect of the *p*-xylene on the reaction.



- 45 oxetanes in 10 - 42 % yield
- suppression of dimerization with *p*-xylene
- three-step telescoped reaction pathway - one purification step
- modular design
  - variety of cyclic ketones (5-7 membered)
  - ester and amide formation

Selected examples of isolated spirocyclic oxetanes:



Scheme 3-34 Summary of the results from chapter 3.

## Chapter 4 Investigations into mechanistic pathways of Paternò-Büchi and dimerization reactions

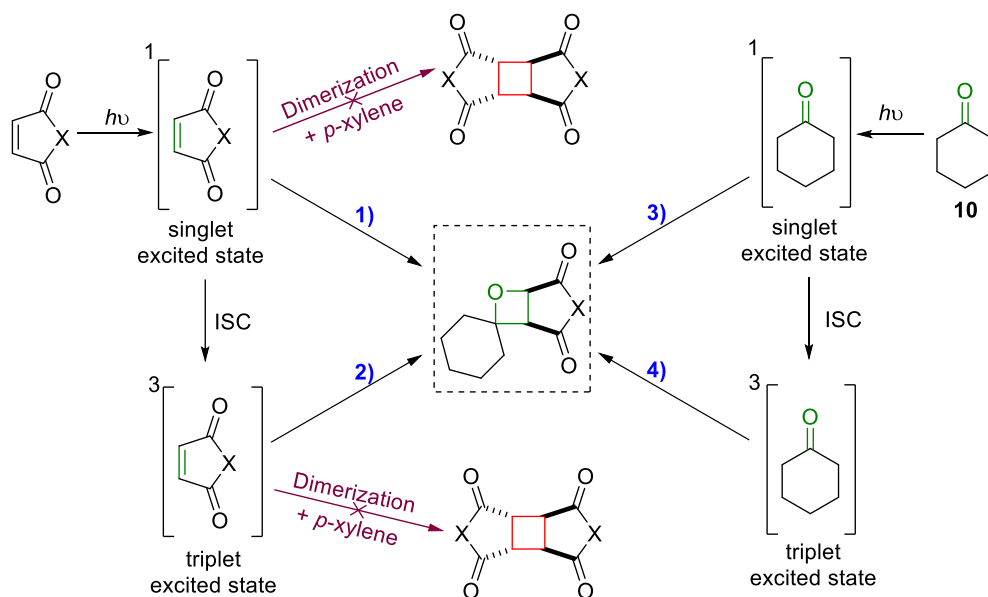
### 4.1 Introduction

Chapters 2 and 3 focused on the practical use of the Paternò-Büchi reaction between different aliphatic ketones and maleic anhydride and the isolation of novel oxetanes. Both chapters include a series of optimizations performed to increase the isolated percentage yield of the desired oxetanes. In Chapter 2 the dimer **4** was removed by crystallization from the reaction mixture. In Chapter 3, the dimerization reaction was successfully suppressed with *p*-xylene, however it was not clear how the *p*-xylene suppressed the dimerization.

This chapter focuses on studies into the reaction mechanism for the Paternò-Büchi reaction between aliphatic ketones and activated alkenes, as well as investigation into the dimerization reaction and how it is suppressed with *p*-xylene (Scheme 4-1). Photochemical reactions are complex and mechanistic studies often require different approaches than those used for traditional ground-state reactions; this is mostly due to the variety of excited states formed during the reaction. In general, photochemical reactions take place by an excited state species reacting with a ground state partner. Therefore, there are four obvious possible pathways to form the oxetane (Scheme 4-1):

- 1) Reaction via singlet excited state of the alkene.
- 2) Reaction via triplet excited state of the alkene.
- 3) Reaction via singlet excited state of the ketone.
- 4) Reaction via triplet excited state of the ketone.

The mechanistic investigations will focus on trying to narrow down the possible reaction pathways, by attempting to block different pathways and observing the effect on the reaction outcome. A series of different reactions was performed, starting with the use of molecular oxygen to quench potential triplet excited states (Section 4.2). Next, with the aid of UV-vis spectroscopy, studies were performed to gain an understanding of the absorption characteristics of the starting materials, and the study was extended to maleimide, which absorbs at longer wavelength than maleic anhydride (Section 4.3). After that, the investigation into the role of *p*-xylene in the reaction will be discussed (Section 4.4). Finally, new activated alkenes will be tested in the Paternò-Büchi reaction to form new oxetane scaffolds (Section Chapter 5).



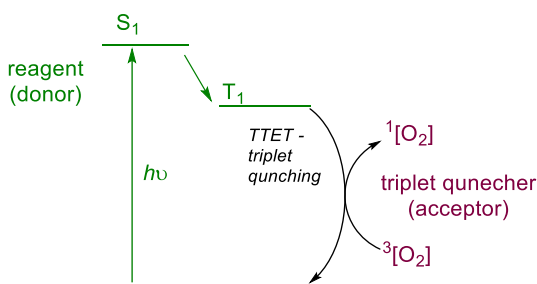
**Aims:**

- investigation into mechanism of Paternò-Büchi reaction and dimerization reaction:
  - molecular oxygen reaction (quenching triplet excited states)
  - effect on changing the alkene (different absorption range)
- investigating the role of the *p*-xylene in suppressing dimerization reaction
- expanding the reaction scope with new alkenes

**Scheme 4-1 Summary of possible reaction mechanism taking place when irradiating cyclohexanone and maleic anhydride and aims for Chapter 4.**

## 4.2 Using molecular oxygen as triplet quencher

Oxygen is a known triplet quencher;<sup>95,96</sup> by purging the reactions with air for 15 minutes, oxygen is dissolved in the reaction mixture and rapidly quenches triplet excited states. Consequently, oxygen is a common way of distinguishing between triplet and singlet excited state pathways.<sup>97</sup> Molecular oxygen has a triplet ground state which therefore is of relatively low energy, and allows for quenching of other triplet excited states present (Scheme 4-2) – following the quenching of a molecule by oxygen through triplet-triplet energy transfer, the reaction gives singlet oxygen and the ground state molecule. In practice, the rate of reaction under investigation is observed in the presence and absence of oxygen; if the reaction rate changes (decreases) when the oxygen is present it implies a triplet excited state is involved in the reaction mechanism, and when there is no change in the reaction rate a singlet excited state pathway is more likely.

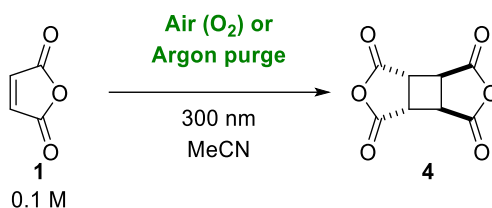


**Scheme 4-2 Using molecular oxygen as triplet quencher.**

In the case of the Paternò-Büchi system between maleic anhydride and cyclohexanone, the molecular oxygen would be expected to hinder the reaction pathways 2 and 4, which involve the formation of triplet excited states, while the pathways 1 and 3 are not affected as they take place via singlet excited states only (Scheme 4-1). Both the dimerization and the Paternò-Büchi reactions were investigated using this method.

#### 4.2.1 Molecular oxygen as a triplet quencher in the dimerization reaction

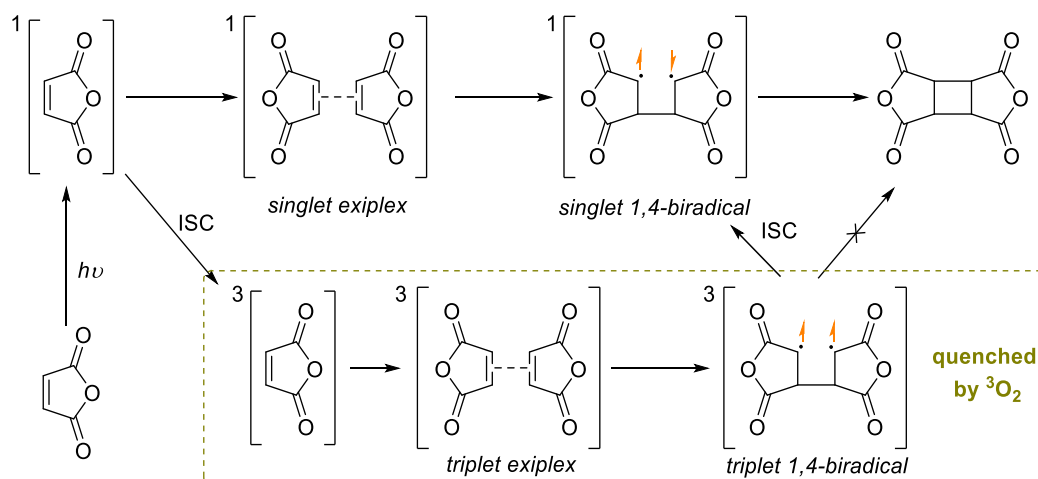
Starting with the dimerization of maleic anhydride (Table 4-1), the same reaction mixture was split into two, with one purged for 15 minutes with argon (as normal) and the other with air, allowing the oxygen to be introduced into the reaction mixture. The reactions were run simultaneously, and aliquots were removed periodically and analysed by <sup>1</sup>H NMR spectroscopy (solvent suppression, MeCN). The data obtained for both reactions are summarized in Table 4-1. The reaction rate of dimerization did not differ significantly between the two reactions, showing <3% difference in percentage of dimer **4** present at different reaction times. For example at 10 hours (Table 4-1, entry 5) 10% of dimer **4** was present in the reaction mixture when reaction was purged with argon, while the parallel reaction (which was purged with air) shows 8% of dimer **4**; only 2% difference is considered to be within experimental error, and implies that the triplet excited state of maleic anhydride is not involved in the reaction, as at least some of the triplet excited state formed would be quenched by oxygen present in the reaction, and a more significant difference between the reaction rates would be expected. Overall, these results suggest a lack of effect of oxygen on the dimerization reaction, which implies that the dimerization of maleic anhydride takes place via singlet excited state. Reactions with *p*-xylene present were also performed, but as expected the *p*-xylene blocked the reaction, and no conversion of maleic anhydride into dimer **4** was observed.



Entry	Time (h)	Argon purge		Air purge (O <sub>2</sub> )	
		1 (%)	4 (%)	1 (%)	4 (%)
1	2	97	3	98	2
2	4	94	6	97	3
3	6	93	7	95	5
4	8	91	9	93	7
5	10	90	10	92	8
6	12	88	12	90	10
7	24	81	19	82	18

Table 4-1 Results of the effect of molecular oxygen on the dimerization reaction of maleic anhydride (1). Percentages of components of the reaction mixture based on <sup>1</sup>H NMR (solvent suppression, MeCN, 400 MHz).

Scheme 4-3 summarizes the possible reaction mechanism for dimerization of maleic anhydride and highlights which pathway would be blocked by the molecular oxygen. The dimerization reaction is a [2+2] cycloaddition between two alkenes each conjugated to two carbonyl groups. Therefore, it might be expected to go via a triplet excited state pathway (which involves formation of a *triplet exciplex* followed by the *triplet 1,4-biradical* species) as intersystem crossing would be expected to be fast. However, that biradical species needs to undergo ISC in order to form the final C-C bond. Based on the molecular oxygen results the reaction rate of dimerization was not affected by the presence of oxygen, implying that the singlet excited pathway is the preferred way of forming the dimer. The singlet excited state pathway includes formation of a *singlet exciplex* followed by the *singlet 1,4-biradical* species which can undergo final cyclization. Still, additional investigations are required to understand the role of the *p*-xylene in blocking this reaction.



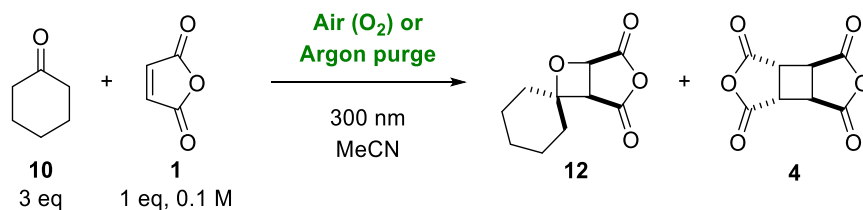
Scheme 4-3 Possible mechanisms for the dimerization reaction of maleic anhydride (1).



#### 4.2.2 Using molecular oxygen as a triplet quencher in Paternò-Büchi reactions

Following the results from the dimerization reaction, the Paternò-Büchi reaction between cyclohexanone and maleic anhydride was investigated in the same way. The reaction was investigated in the absence and presence of *p*-xylene to ensure that *p*-xylene does not affect the Paternò-Büchi reaction and only suppresses the dimerization reaction of maleic anhydride.

Starting with the reaction with no *p*-xylene (Table 4-2), two parallel reactions were performed to compare the rate of formation of the oxetane **12** in the presence and absence of oxygen. The percentage in the mixtures of starting materials and products did not differ between the two reactions, with <2% difference. Based on the results from Table 4-2 the presence of molecular oxygen does not change the rate of formation of the oxetane **12** (or dimer **4**). The percentage of oxetane in the reaction mixture is almost identical at each reaction stage, with ~21% of oxetane present in the reaction mixture after 24 h (and ~14% of dimer).

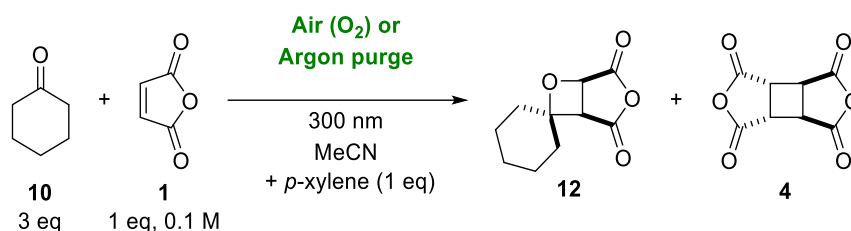


Entry	Time (h)	Argon purge			Air purge (O <sub>2</sub> )		
		1 (%)	12 (%)	4 (%)	1 (%)	12 (%)	4 (%)
1	2	94	4	2	96	2	2
2	4	90	5	4	91	5	4
3	6	87	7	6	88	7	5
4	8	83	10	7	86	9	6
5	10	81	11	8	83	10	7
6	12	78	13	9	79	13	8
7	24	63	22	15	67	20	13

Table 4-2 Results of the effect of molecular oxygen on the Paternò-Büchi reaction between cyclohexanone (**10**) and maleic anhydride (**1**), and the dimerization reaction of maleic anhydride (**1**). Percentage of components in the reaction mixture based on <sup>1</sup>H NMR spectroscopy (solvent suppression, MeCN, 400 MHz).

Next, *p*-xylene was added to the reaction mixture and the molecular oxygen test was performed again, with two parallel reactions taking place: one purged with argon and the other with air (O<sub>2</sub>) (Table 4-3). The results further confirmed the results from above, as Table 4-3 shows the formation of oxetane at the same rate in the presence or absence of O<sub>2</sub>, while the dimerization reaction is blocked by the addition of the *p*-xylene. The results from the two reactions are very similar showing a similar rate of formation of oxetane **12** in the absence and presence of oxygen. Comparing the two reactions, one can see that there is 29% of oxetane in the reaction mixture when the reaction was

purged with argon, compared to 22% of oxetane **12** in the reaction mixture when the reaction was purged with air (O<sub>2</sub>). This percentage difference is larger than the ones reported in Table 4-1 and Table 4-2, however it is unlikely to be significant. Although the percentage of oxetane in the reaction mixture is different, the general reaction rate is very similar, meaning oxygen has little to no effect on the reaction mechanism. Combining the results from the Paternò-Büchi reactions in the presence and absence of oxygen it can be suggested that the Paternò-Büchi reaction takes place via a singlet excited state as there was no significant effect on the reaction rate when oxygen was introduced to the reaction.



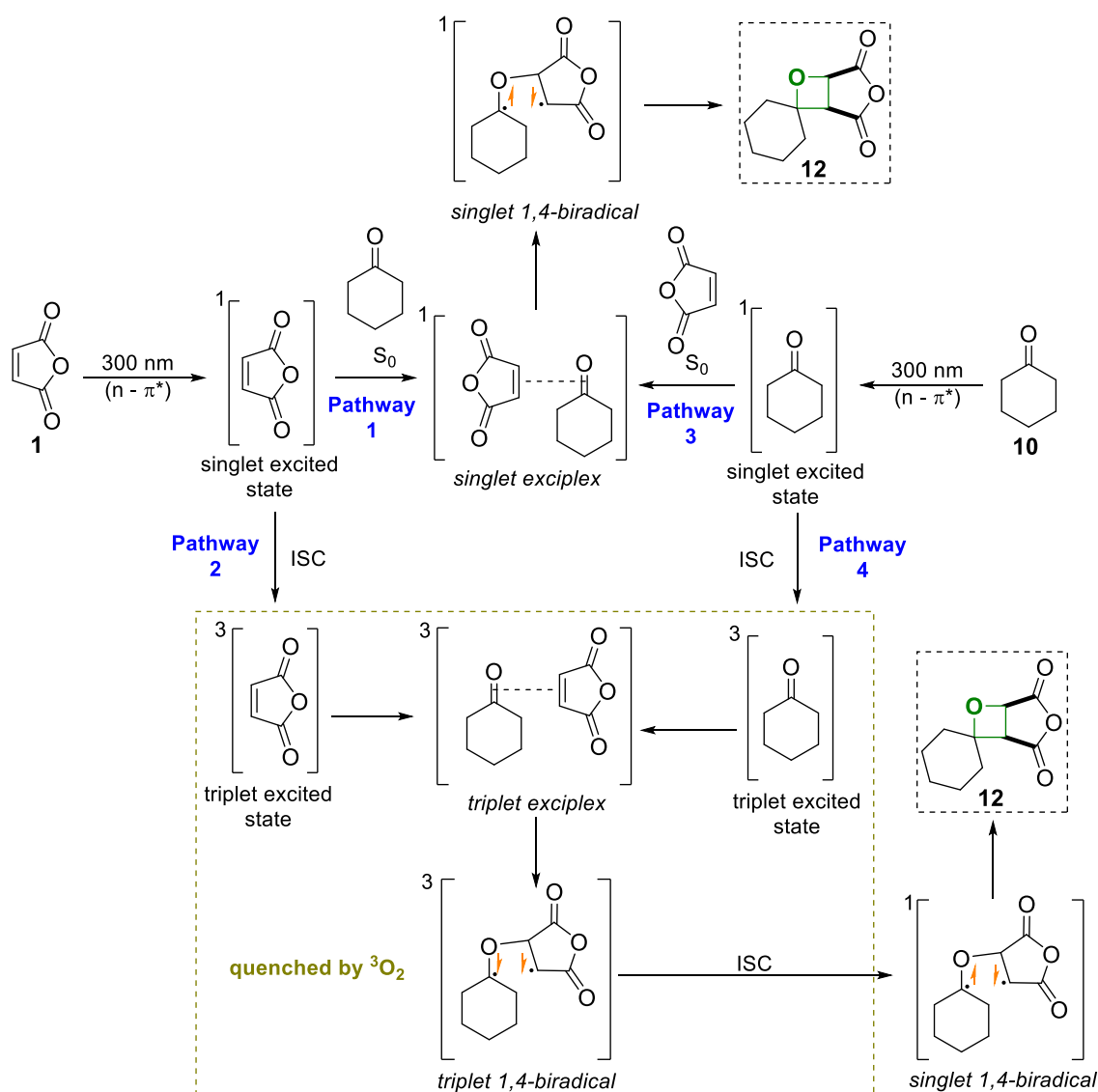
Entry	Time (h)	Argon purge			Air purge (O <sub>2</sub> )		
		1 (%)	12 (%)	4 (%)	1 (%)	12 (%)	4 (%)
1	2	96	4	0	98	2	0
2	4	94	6	0	94	6	0
3	6	90	9	0	92	7	0
4	8	87	12	0	90	9	0
5	10	84	15	0	89	11	0
6	12	83	17	0	87	12	0
7	24	70	29	1	78	22	0

Table 4-3. Results of the effect of molecular oxygen on the Paternò-Büchi reaction between cyclohexanone (**10**) and maleic anhydride (**1**) in the presence of *p*-xylene. Percentages of components in the reaction mixture based on <sup>1</sup>H NMR (solvent suppression, MeCN, 400 MHz).

These results suggest that mechanism for the Paternò-Büchi reaction is not affected by the triplet quenching effects of molecular oxygen, and therefore the reaction takes place via a singlet excited state, not a triplet excited state, narrowing down the possibilities for the final reaction mechanism for this system. There is a possibility that more than one pathway is being used in the Paternò-Büchi reaction, for example if 90% of the oxetane was formed via a singlet excited state, but 10% via the triplet excited state, the molecular oxygen reactions would not have a huge effect on the reaction. Nevertheless, the results discussed above imply that formation of oxetane takes place via singlet excited place the majority of the time.

Scheme 4-4 shows a detailed picture of the possible reaction pathways between the maleic anhydride and cyclohexanone during the Paternò-Büchi reaction. All four pathways give rise to the same oxetane product **12**. Similarly, to the dimerization reaction, the Paternò-Büchi reaction is a [2+2] cycloaddition which takes place via a

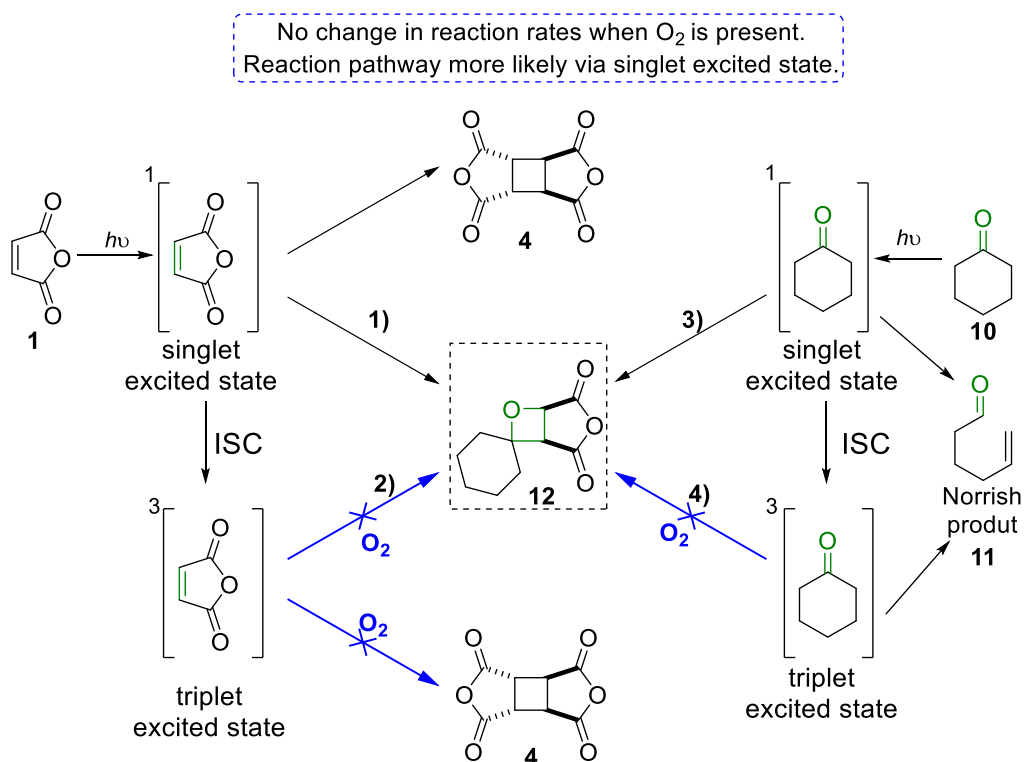
*singlet* or *triplet exciplex* in order to form a biradical species. The *singlet 1,4-biradical* can form the final C-C bond and result in the desired oxetane product **12**, while the *triplet 1,4-biradical* species must undergo intersystem crossing first as the electron spin does not allow *triplet 1,4-biradical* to form the final C-C bond. As discussed above, the oxygen quenching reactions hinder pathways 2 and 4; this is due the rapid quenching of the triplet excited states when oxygen is present in the reaction. The reaction rate of the Paternò-Büchi reaction was not significantly affected by the presence of the oxygen in the reaction, therefore it seems that the major reaction pathway for the Paternò-Büchi reaction takes place via singlet excited states (pathway 1 or 3). Pathways 1 and 3 differ by which of the starting materials is in the excited state and which in the ground state. An investigation into distinguishing between those two pathways is discussed in Section 4.3.



Scheme 4-4 Summary of the preferred reaction pathways for the Paternò-Büchi reaction.

### 4.2.3 Conclusion of molecular oxygen experiments

The use of molecular oxygen is a common way of investigating photochemical mechanisms. Based on the results discussed above there is a very small to negligible difference in the rate of formation of oxetane **12** (and dimer **4**) in the presence or absence of molecular oxygen. Even though oxygen is expected to quench any triplet excited states present in the reaction mixture, the rate of these reaction stays the same implying that triplet excited states are likely not implicated in for the Paternò-Büchi reaction between cyclohexanone and maleic anhydride to take place. Scheme 4-5 summarizes the possible reaction pathway for the Paternò-Büchi reaction between cyclohexanone and maleic anhydride, showing reactions pathways 2 and 4 would be expected to be affected by the oxygen quenching. The dimerization reaction of the maleic anhydride is likely taking place via the singlet excited state as well. Overall, the molecular oxygen experiments allowed additional insights about the reaction and narrowed down the possible reaction pathways to two: 1 and 3. Next, a series of tests was performed to distinguish whether the oxetane is formed via the excited state of the alkene (pathway 1) or of the ketone (pathway 3).



Scheme 4-5 Summary of the results of the molecular oxygen test, showing that the Paternò-Büchi reaction likely takes place likely via the singlet excited state.

### 4.3 Identifying the excited state partner in the Paternò-Büchi reaction

As discussed above, the possible mechanistic pathways have been narrowed down to pathway 1 or 3 (Scheme 4-5); the next section describes investigation into identification

of the excited state partner in the Paternò-Büchi reaction. In theory, distinguishing between the two excited states of the two starting materials could be achieved by irradiation of only one of the starting materials at a time. However, this can be difficult if both molecules absorb light at the required wavelength. Thus, UV-vis data of all starting materials was recorded and is summarized below.

#### 4.3.1 UV-vis spectra of starting materials and reagents

UV-vis spectra of all of the starting materials were measured in MeCN (0.01 M unless specified otherwise). Starting with the UV-vis spectrum of the maleic anhydride, there are two main transitions observed in the spectra. The major peak is due to the  $\pi\text{-}\pi^*$  transition at  $\lambda = 210\text{ nm}$  (Figure 4-1, green line) and can be easily seen at lower concentrations (0.002 M); the second and much weaker absorption is due to the  $n\text{-}\pi^*$  transition, it can be seen easily when the concentration of the solution is increased (Figure 4-1, red line, 0.01 M). The  $n\text{-}\pi^*$  absorption is at  $\sim 300\text{ nm}$ . The absorption starts at  $\sim 340\text{ nm}$ , above that wavelength no energy will be absorbed and therefore no reaction can take place.

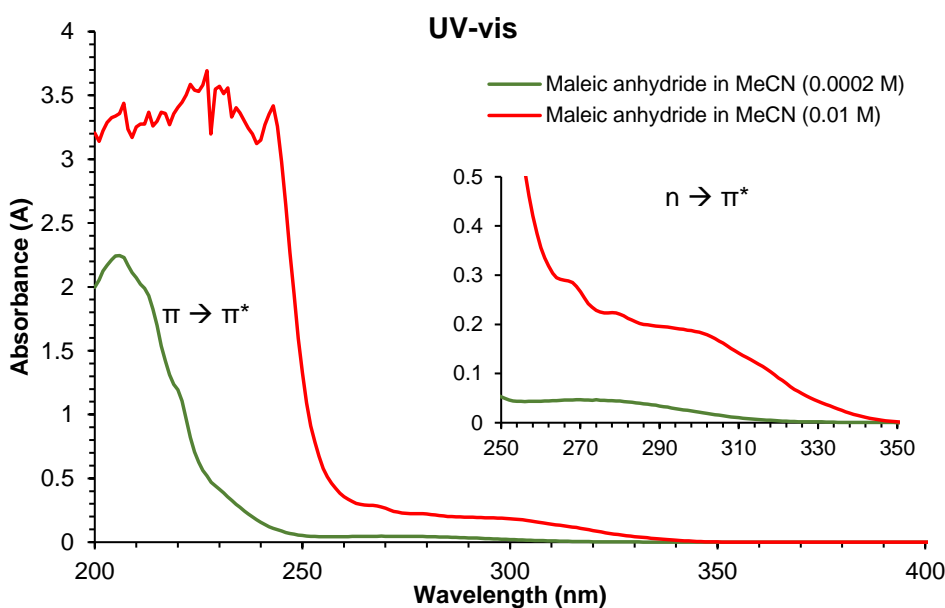


Figure 4-1 UV-vis spectrum of maleic anhydride (1) in MeCN.

The UV-vis spectra of the cyclic ketones used in the Paternò-Büchi reaction are shown in Figure 4-2. The absorption of the  $n\text{-}\pi^*$  transition is very similar for all ketones, showing a peak at  $\sim 290\text{ nm}$ . No major changes are observed when the size of the ring changes or there a different group (X) (Figure 4-2). Also, none of the ketones shows absorption above  $340\text{ nm}$ , therefore there will be no reaction taking place via the excited state of the ketone when  $350\text{ nm}$  (or longer wavelength) lamps are used.

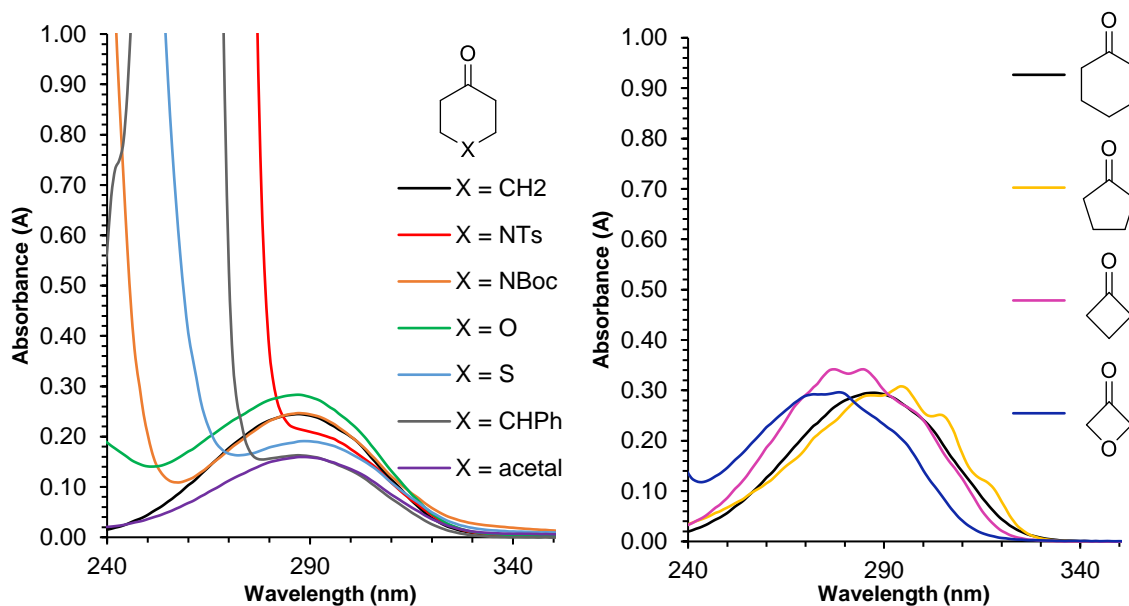


Figure 4-2 UV-vis spectra of ketones used in the Paternò-Büchi reaction (MeCN 0.01 M).

When comparing the two starting materials, maleic anhydride and cyclohexanone (and other ketones), the absorption of all the components overlap in the 300 nm region, making it difficult to excite only one of the reagents at a time. There were no lamps available that could irradiate one substrate and not the other, as the overlap is so close. On the other hand, maleimides, which have a similar structure to maleic anhydride, have significantly different absorption characteristics. Maleimides are also electron deficient alkenes, but with a nitrogen in the ring instead of an oxygen atom; this small change in structure gives a large change in the UV-vis spectrum. Figure 4-3 compares the UV-vis spectrum of maleic anhydride, *N*-Boc-maleimide and cyclohexanone. It shows that maleimide absorption starts at 380 nm, giving a range of wavelengths in which the alkene is excited while the ketone is not (340-370 nm). Therefore, a series of experiments with maleimides and cyclohexanone can be performed, to probe the reactivity of the starting materials at different wavelengths. Experiments at 300 nm will lead to absorption of light by both cyclohexanone and *N*-Boc-maleimide, while experiments at 350 nm will only result in exciting the maleimide while the cyclohexanone will stay in the ground state.

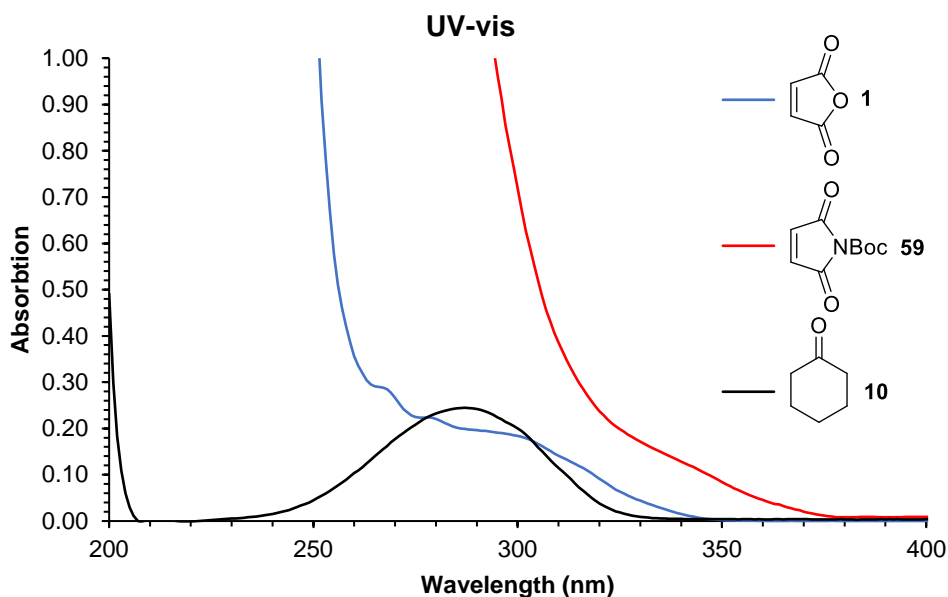


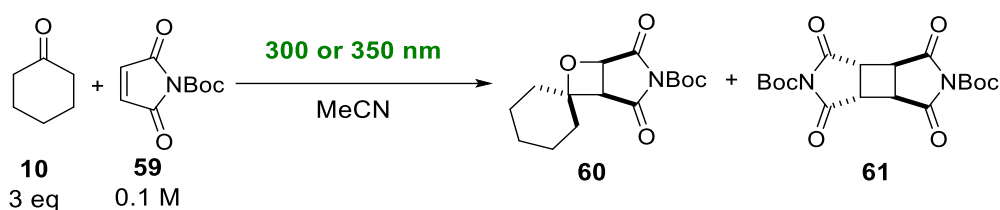
Figure 4-3 UV-vis spectra of maleic anhydride (**1**), *N*-Boc maleimide (**59**) and cyclohexanone (**10**) in MeCN (0.01 M).

To summarize, the reported UV-vis spectra of the reagents confirmed that the absorption of the maleic anhydride and cyclohexanone overlaps, making it difficult to irradiate only one of the reagents at a time. However, by changing the alkene to maleimide the absorption changes, allowing for selective irradiation of alkene in the presence of the carbonyl. Next, a series of reactions was performed with irradiation at 300 nm and at 350 nm with maleimide as an alkene.

#### 4.3.2 Photochemical reaction of cyclohexanone and *N*-Boc-maleimide at 300 or 350 nm

The theory behind these reactions was the selective absorption of light at 350 nm by *N*-Boc-maleimide (**59**), while the cyclohexanone does not absorb light in that range, allowing for excitation of the *N*-Boc-maleimide while cyclohexanone is in the ground state. Under the standard wavelength used in this work, 300 nm, the Paternò-Büchi reaction between cyclohexanone and *N*-Boc-maleimide yields the desired oxetane **60**, additionally there is still dimerization of the *N*-Boc-maleimide taking place, yielding dimer **61** (Scheme 4-5). Two parallel reactions were performed at 300 and 350 nm, and the results from both reactions are summarized in Table 4-4, which gives a breakdown of the reaction mixture at different reaction times. Reaction at 300 nm resulted in formation of both oxetane and dimer, with the reaction reaching completion after 10 h, with 78% of dimer **61** and 22% of oxetane **60** in the reaction mixture (Table 4-4, entry 1-4). The dimerization was very prominent, and again will have to be suppressed in order to fully optimize the formation of the oxetane **60**. In contrast at 350 nm, no oxetane **60** was observed while the dimerization reaction still took place with 83% of the dimer **61** present in the reaction mixture after 10 hours (Table 4-4, entry 5-8). The rate of dimerization

reaction was comparable at 300 and 350 nm. As discussed previously at 350 nm the cyclohexanone does not reach its excited state, therefore pathway 3 is blocked (Scheme 4-5), while pathway 4 is still allowed; the lack of oxetane product at 350 nm suggests that the excited state of the ketone is necessary for the Paternò-Büchi reaction to take place. In conjunction with the oxygen quenching reactions, which narrow down the possible reaction pathway to 1 or 3 (reaction pathways via the singlet excited state of the alkene or the ketone respectively), the results from this experiment add to the evidence showing that the excited state of cyclohexanone is necessary for the Paternò-Büchi reaction to take place. Therefore, the reaction is likely taking place via pathway 3 via the singlet excited state of the ketone.



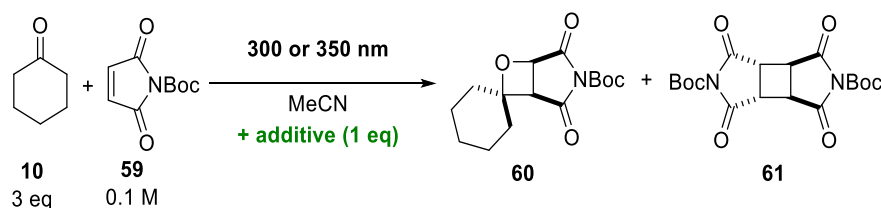
Entry	Time (h)	Wavelength (nm)	59 (%)	60 (%)	61 (%)
1	1	300	89	2	9
2	3		66	8	26
3	6		31	14	54
4	10		0	22	78
5	1	350	92	0	8
6	3		70	0	30
7	6		46	0	54
8	10		17	0	83

Table 4-4 Results of reaction between cyclohexanone (**10**) and *N*-Boc-maleimide (**59**) at 300 and 350 nm. Percentage of components in the reaction mixture based on <sup>1</sup>H NMR (solvent suppression, MeCN, 400 MHz).

As shown in the results above the dimerization reaction consumes a lot of the starting *N*-Boc-maleimide, therefore a series of additives were added to suppress the dimerization reaction and increase the yield of the desired oxetane. Table 4-5 summarizes the reaction results where different additives were present in the reaction mixture at 300 or 350 nm. Again at 300 nm, the formation of both products oxetane **60** and dimer **61** is observed. *p*-Xylene or toluene are two additives that worked very well in suppressing of the dimerization of maleic anhydride. The percentage of the oxetane present in the reaction after 10 hours when *p*-xylene or toluene is present increased to 30% and 42% (Table 4-5, entry 2 and 5) respectively from 22%. This is presumably due to the higher availability of the *N*-Boc-maleimide to undergo Paternò-Büchi reaction while dimerization reaction is blocked. *m*-Tolunitrile (Table 4-5, entry 3) was also used as an additive, showing slight suppression of the dimerization, but it was not as effective as the *p*-xylene or toluene. Anisole (Table 4-5, entry 4) had the least effect on the reaction,



showing slight suppression of both dimerization and Paternò-Büchi reaction. This is in contrast to when anisole was used in the Paternò-Büchi reaction between cyclohexanone and maleic anhydride (section 3.2.3, Table 3-8), where the dimerization reaction of maleic anhydride was greatly promoted; this implies that there could be a difference in the dimerization reaction pathway between the maleic anhydride and *N*-Boc-maleimide. At 350 nm (Table 4-5, entry 6-9) there is only dimerization reaction taking place. Both xanthone and benzophenone (Table 4-5, and 7 and 8) absorb light in that region so could triplet sensitize any compounds with lower triplet energy than theirs; in both cases dimerization was not significantly affected, showing that with only a slight difference in the percentage of the dimer **61** present in the reaction mixture in the presence and absence of the sensitizers, most likely there is a lack of interaction between the two molecules. In the case of *m*-tolunitrile (Table 4-5, entry 9), the dimerization is slightly suppressed, while no oxetane **60** is observed. Overall, *p*-xylene was again chosen as the additive, however a higher loading is likely required to fully suppress the dimerization reaction.



Entry	Additive	Wavelength (nm)	59 (%)	60 (%)	61 (%)
1	-		0	22	78
2	<i>p</i> -xylene		54	30	15
3	<i>m</i> -tolunitrile	300	34	31	34
4	anisole		23	16	61
5	toluene		41	43	17
6	-		17	0	83
7	xanthone	350	32	0	68
8	benzophenone		0	0	100
9	<i>m</i> -tolunitrile		66	0	34

Table 4-5 Results of reaction between cyclohexanone (**10**) and *N*-Boc-maleimide (**59**) at 300 and 350 nm with different additives. Percentages of components in the reaction mixture based on <sup>1</sup>H NMR (solvent suppression, MeCN, 400 MHz).

Four <sup>1</sup>H NMR spectra are shown in Figure 4-4, highlighting the results from the reactions above. Spectrum 1 shows the reaction between *N*-Boc-maleimide and cyclohexanone at 350 nm after 11.5 hours, showing the formed dimer **61** and lack of the desired oxetane **60**. Next, spectrum 2 shows the same reaction mixture irradiated at 300 nm, showing the formation of oxetane **60**, as the signal for H<sup>B</sup> is present at ~5.6 ppm (H<sup>B'</sup> overlaps with the singlet due to the dimer **61** protons, H<sup>C</sup>). Spectrum 3 adds *p*-xylene to the reaction

mixture, showing a decrease in the overall reaction rate, as at 11.5 hours there is still a significant amount of *N*-Boc-maleimide present in the reaction mixture. Additionally, the oxetane peak is much more prominent, showing the partial suppression of the dimerization reaction. The final spectrum is of the completed Paternò-Büchi reaction between *N*-Boc-maleimide and cyclohexanone, with an additional a 5 equivalents of *p*-xylene, showing full suppression of the dimerization reaction. The reaction took a total of 6 days for full conversion of the *N*-Boc-maleimide to take place.

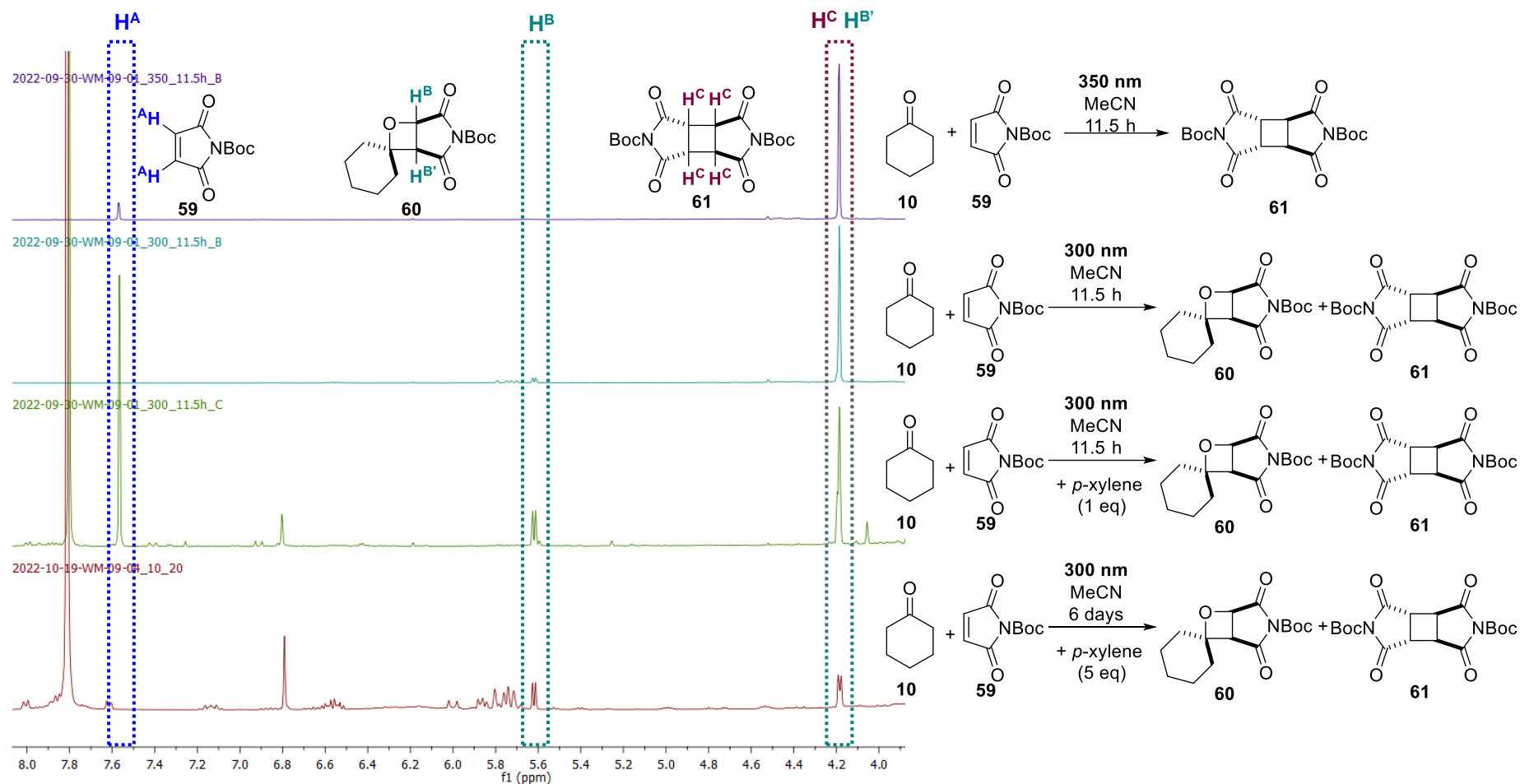
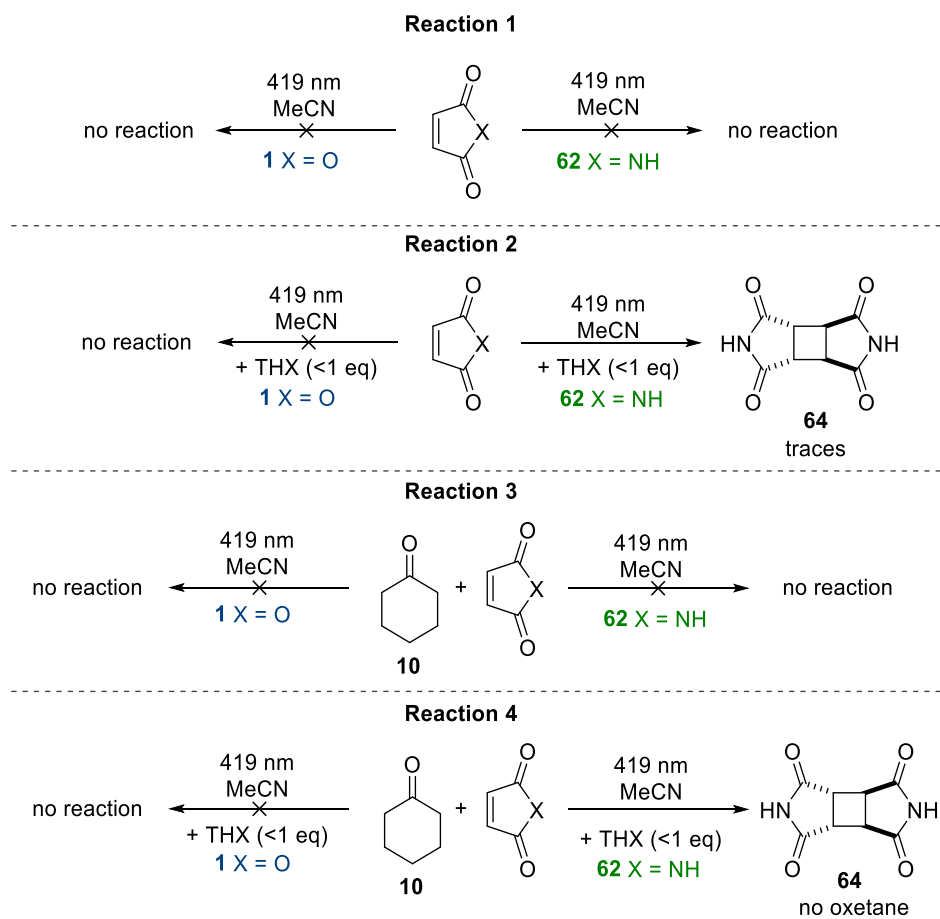


Figure 4-4 <sup>1</sup>H NMR spectra of photochemical reactions of *N*-Boc-maleimide under different conditions (solvent suppression, MeCN, 400 MHz).

### 4.3.3 Photochemical reaction of cyclohexanone and *N*-H-maleimide in at 419 nm in the presence of thioxanthone

Next, reactions with addition of thioxanthone (THX) were performed with irradiation at 419 nm (Scheme 4-6) to measure the effect of THX on the reaction, as THX is a common triplet sensitizer. The  $^1\text{H}$  NMR spectra of the reactions can be seen in Figure 4-5; spectrum 1 shows the Paternò-Büchi reaction at 300 nm between cyclohexanone and *N*-H-maleimide (**62**) to show where the oxetane **63** and dimer **64** signals would be expected to be observed in the  $^1\text{H}$  NMR spectrum (solvent suppression, MeCN). Control reactions of the two alkenes, maleic anhydride and *N*-H-maleimide, irradiated at 419 nm showed no reaction taking place (Scheme 4-6, reaction 1, Figure 4-5, spectrum 2). Reaction 2 shows the effect of the THX on both alkenes, in the case of maleic anhydride no reaction was observed, as expected due to the high triplet excited state energy which cannot be reached via triplet sensitization with THX. On the other hand, reaction with *N*-H-maleimide reaction showed consumption of the alkene and a very small signal at 4.1 ppm likely due to the dimer **64**, and spectra at 3.5 hours and 24 hours are shown in Figure 4-5 (spectra 3 and 4). The consumption of the alkene and observation of the small dimer signal might imply that the formation of the dimer **64** is possible by accessing the triplet excited state of the maleimide by triplet sensitization or via direct irradiation (it is important to note that light emitted by the lightbulbs gives a range of light not a specific wavelength). Although the amount of dimer **64** observed by  $^1\text{H}$  NMR was small, a precipitate was formed in the reaction (section 4.3.4 discusses the issues of solubility of the dimer **64**, indicating a possibility of a higher rate of dimer formation but limited observation of it by  $^1\text{H}$  NMR spectroscopy. Previously it has been discussed (section 4.2) that the dimerization reaction (of maleic anhydride) takes place via a singlet excited state under direct irradiation, however it is crucial to remember that does not eliminate the possibility of an additional triplet excited state pathway via triplet sensitization, which is plausible due to the lower triplet energy of the *N*-H-maleimide compared to maleic anhydride. Reaction 3, which was the Paternò-Büchi reaction without any additive, was as expected, as no reaction took place when either maleic anhydride or *N*-H-maleimide were used. Finally, reaction 4 was the Paternò-Büchi reaction irradiated at 419 nm with THX as an additive. Maleic anhydride showed no reaction, while the *N*-H-maleimide showed formation of the dimer **64** only, and the dimer was visible by  $^1\text{H}$  NMR in this reaction mixture (Figure 4-5, spectrum 6).



**Scheme 4-6** Photochemical reactions irradiated at 419 nm with and without THX.

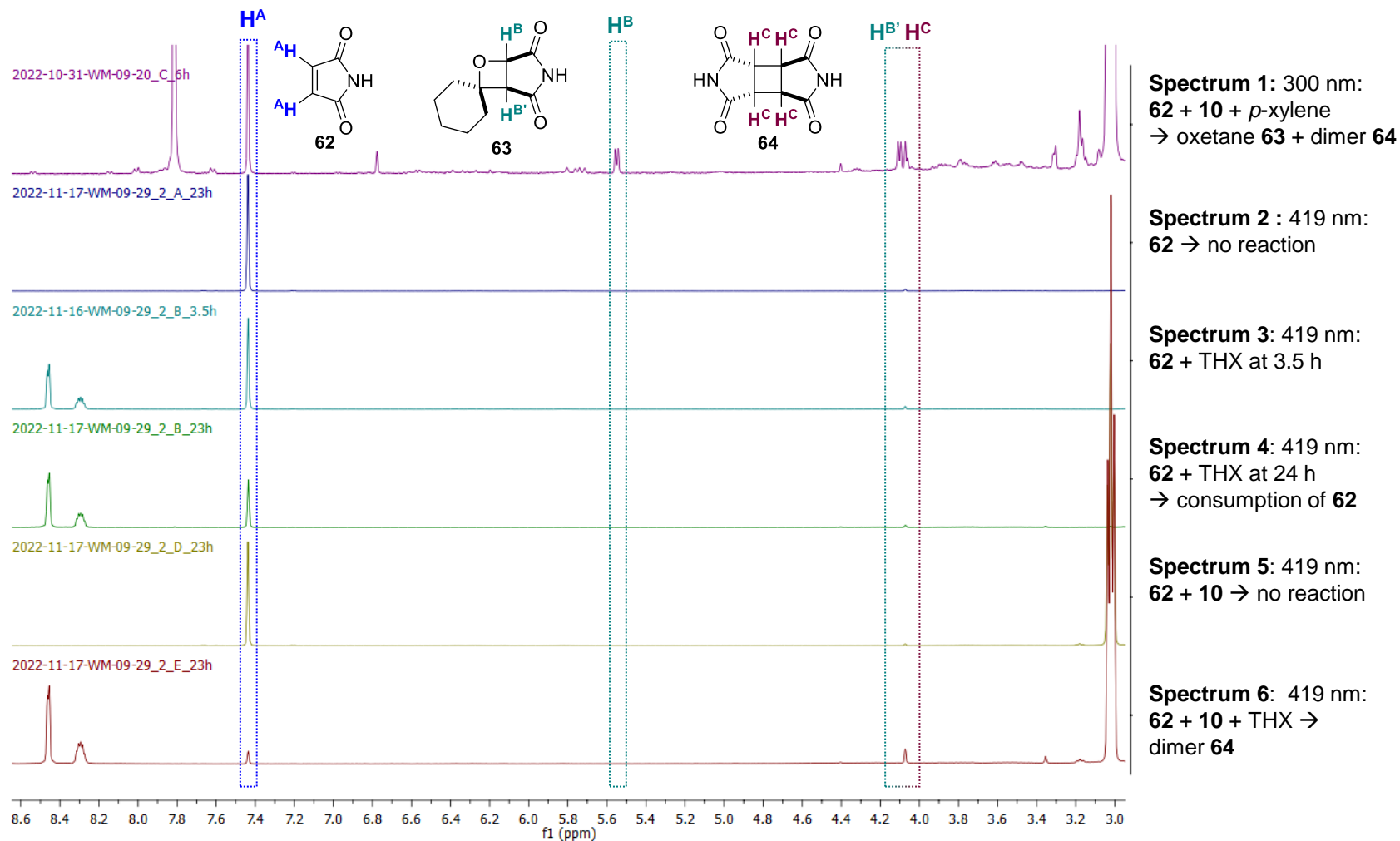
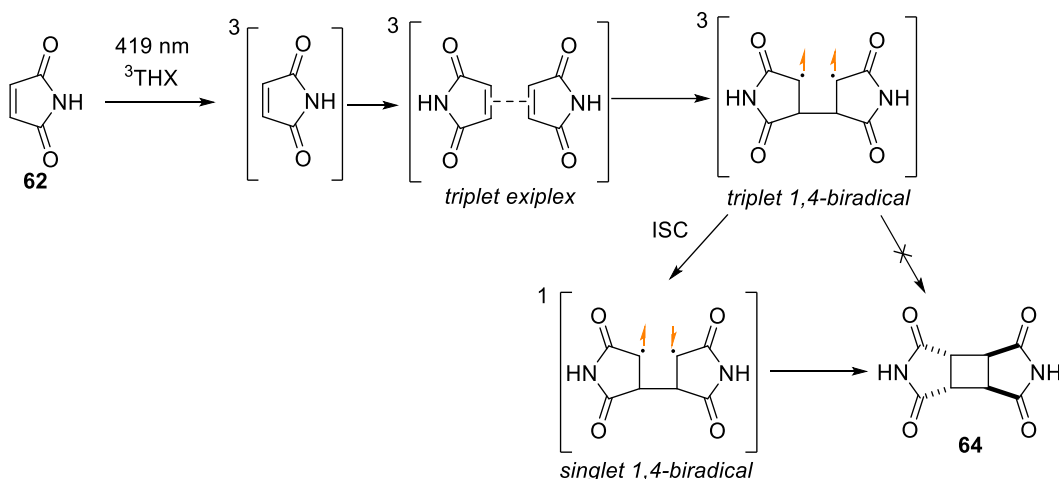


Figure 4-5 Selected  $^1\text{H}$  NMR (MeCN, solvent suppression, 400 MHz) of reactions showed in Scheme 4-6.

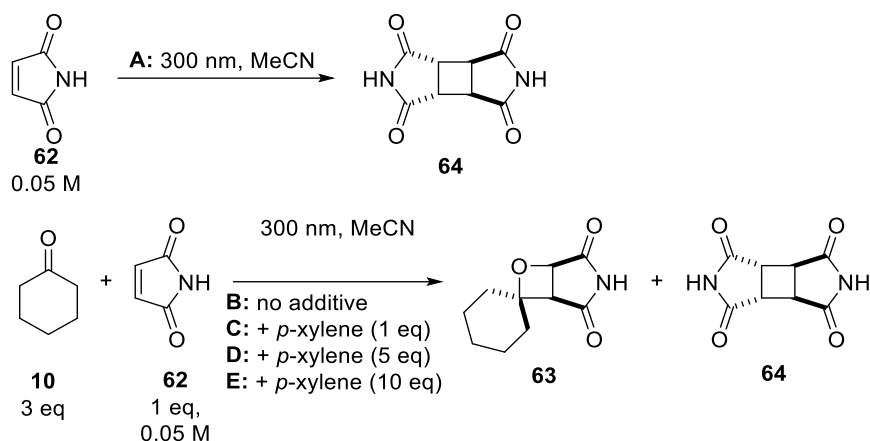
To summarize, maleimides ( $50\text{-}60\text{ kcal mol}^{-1}$ )<sup>98</sup> have a lower triplet energy than maleic anhydride ( $\sim 70\text{ kcal mol}^{-1}$ , section 3.2.3.2), potentially allowing for the triplet sensitization to take place between THX ( $\sim 63\text{ kcal mol}^{-1}$ )<sup>55</sup> and maleimide. In the case of dimerization during the direct irradiation the singlet pathway is preferred (for maleic anhydride at least), however, the triplet excited state pathway is still possible when the triplet-triplet energy transfer takes place. The possible reaction mechanism for the sensitization of the *N*-H-maleimide and subsequent dimerization is shown in Scheme 4-9. Importantly, none of the reactions discussed in this section showed formation of the oxetane product, leading to conclusion that the reaction does not take place via triplet excited state of the alkene. However, due to the triplet energy levels it is unlikely that the THX can triplet sensitize the cyclohexanone ( $68\text{ kcal mol}^{-1}$ ) meaning that the formation of oxetane via triplet excited state of cyclohexanone (accessed by sensitization) could be possible but would not take place during the above reactions.



Scheme 4-7 Summary of the reaction mechanism for the dimerization of *N*-H-maleimide (62) irradiated at 419 nm in the presence of THX.

#### 4.3.4 Issues with *N*-H-maleimide during irradiation reactions

In the *N*-H-maleimide reactions, a significant issue arose, which was the formation of precipitate during the reaction. This causes issues with light penetration as well as with assessing the true content of the reaction mixture. A series of reactions was performed, and photos of the reaction mixture were taken to show the extent of the formed precipitate at different reaction times. Five reactions were performed in parallel, which are shown in Scheme 4-8. In summary, one dimerization reaction (Reaction A) was performed and compared to four Paternò-Büchi reactions with 0, 1, 5 or 10 equivalents of *p*-xylene (Reactions B-E).



**Scheme 4-8** Dimerization of *NH*-maleimide (**62**) and Paternò-Büchi reactions between *N*-*H*-maleimide (**62**) and cyclohexanone (**10**) in the presence of 0-10 eq of *p*-xylene.

Figure 4-6 shows the reactions at different reaction times: 1, 3 and 6 hours. The photos show a high level of precipitate forming in all reactions. Reactions with a higher amount of *p*-xylene (5 and 10, D and E) show a slower formation of precipitate as the reaction is clear after 1 hour of irradiation, and in the case of reaction E (10 equivalents of *p*-xylene) the reaction was clear at the 3 hour mark as well. It has been theorized that the precipitate formed is the dimer **64** or polymer that forms from the reaction of *N*-*H*-maleimide with itself. To ensure an accurate understanding, the reactions were evaporated and  $^1\text{H}$  NMR spectra were recorded in  $d_6$ -DMSO, as DMSO was the only solvent that fully dissolved the precipitate.

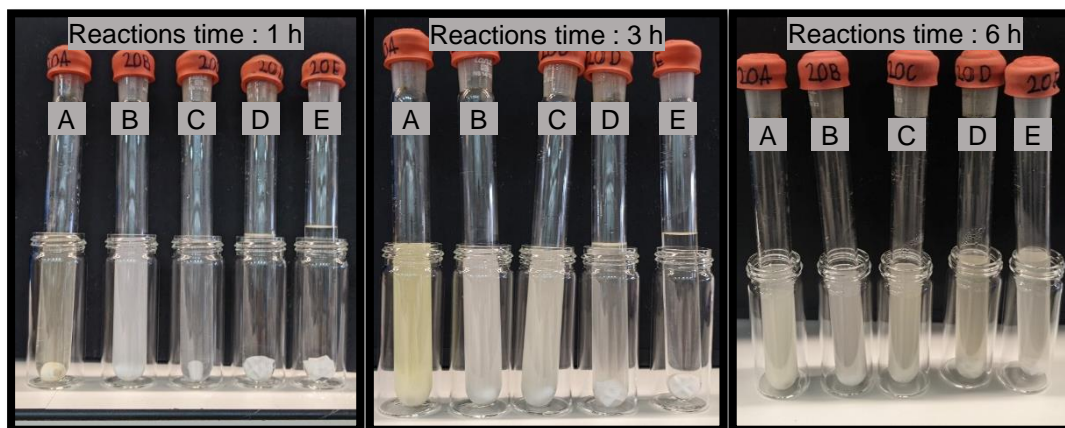


**Figure 4-6** Photos of reactions summarized in Scheme 4-8 at 1, 3 and 6 hours.

Table 4-6 shows the difference in the percentages of the components of the reaction mixture when the reaction was investigated by solvent suppression  $^1\text{H}$  NMR spectroscopy in MeCN, versus  $^1\text{H}$  NMR spectroscopy  $d_6$ -DMSO. In all cases, when the  $^1\text{H}$  NMR was repeated in  $d_6$ -DMSO, the amount of dimer **64** present in the reaction increases, and as shown by the photos of the reactions this is due to the fact the dimer **64** formed is not fully soluble in acetonitrile and thus an accurate assessment of the



percentage of the products in the reaction mixture cannot be performed under these conditions. The results still show the suppression of the dimerization reaction by the *p*-xylene as the trend of the percentage of dimer **64** decreases as the amount of *p*-xylene in the reacting mixture increases.

Entry	Reaction conditions	NMR type	64 (%)	63 (%)
1	B	<sup>1</sup> H NMR (solvent suppression, MeCN)	24	76
2		<sup>1</sup> H NMR <i>d</i> <sub>6</sub> -DMSO	70	30
3	C	<sup>1</sup> H NMR (solvent suppression, MeCN)	7	93
4		<sup>1</sup> H NMR <i>d</i> <sub>6</sub> -DMSO	74	24
5	C (repeat)	<sup>1</sup> H NMR (solvent suppression, MeCN)	10	90
6		<sup>1</sup> H NMR <i>d</i> <sub>6</sub> -DMSO	60	40
7	D	<sup>1</sup> H NMR (solvent suppression, MeCN)	9	91
8		<sup>1</sup> H NMR <i>d</i> <sub>6</sub> -DMSO	40	60
9	E	<sup>1</sup> H NMR (solvent suppression, MeCN)	4	96
10		<sup>1</sup> H NMR <i>d</i> <sub>6</sub> -DMSO	17	83

Table 4-6 Comparison of the percentages of the components in the reaction mixture based on solvent suppression <sup>1</sup>H NMR in MeCN vs <sup>1</sup>H NMR in *d*<sub>6</sub>-DMSO (400 MHz).

Overall, maleimides work well in the reactions, however in the case of the unprotected *N*-H-maleimide, the formed dimer **64** is not fully soluble in acetonitrile causing inaccurate assessment of the percentages of the components in the reaction mixture; this issue is easily fixable by running the <sup>1</sup>H NMR under different conditions (*d*<sub>6</sub>-DMSO). Overall, this is not a large issue as different groups can be easily used to protect the *N*-H-maleimide – as shown above, *N*-Boc-maleimide (section 4.3.2) works well in the reaction and no insoluble precipitate was observed when it was used in the reaction.

#### 4.3.5 Conclusion of the mechanistic investigation into mechanism of the Paternò-Büchi reaction between cyclohexanone and electron poor alkenes

Starting with the dimerization reaction, mechanistic evidence collected suggested that dimerization of maleic anhydride takes place via a singlet excited state based on the molecular oxygen reactions. However, that does not exclude the possibility of a triplet-sensitized pathway with maleimide, which can seemingly undergo dimerization when triplet sensitized by THX. Additional reactions are needed to fully understand the differences and similarities between the dimerization of maleic anhydride and maleimides. However, importantly, both dimerization reactions are blocked by the addition of *p*-xylene, which greatly improves the practicality of the reaction. Next, an examination into the role/interaction of the *p*-xylene in the system will be performed.

The main focus of the mechanistic investigation was the Paternò-Büchi reaction between the aliphatic ketone and activated alkene. The results when molecular oxygen was

present in the reaction indicated formation of the oxetane via a singlet excited state as the rate of the reaction was not altered. The UV-vis spectra showed that a possible change in the alkene can help to distinguish between the cyclohexanone excited state pathway vs alkene excited state pathway. The reactions of *N*-Boc-maleimide and cyclohexanone showed formation of oxetane only at 300 nm, while at 350 nm only dimer was observed. Based on evidence from those reactions it is suggested that the excited state of the cyclohexanone is required for the Paternò-Büchi reaction to take place (this is true for many Paternò-Büchi reactions – Chapter 1 – literature review). Therefore, by combining the different experiments, it can be suggested that the formation of oxetane likely takes place via singlet excited state of the cyclohexanone (Scheme 4-9). The mechanistic picture of the Paternò-Büchi reaction starts with exciting the ketone (via  $n-\pi^*$  absorption) to form a singlet excited state. The singlet excited state reacts with a ground state electron deficient alkene to form a *singlet exciplex* followed by the *singlet 1,4-biradical* species which can undergo a final cyclization step to form the oxetane ring. The triplet excited state of the ketone is unlikely to be involved in the reaction based on the molecular oxygen experimental results. Overall, the investigation into the mechanistic pathway of the Paternò-Büchi reaction was successful; by combining the different experimental results a plausible reaction mechanism was chosen out of a series of different possible pathways.



## 4.4 The role of the *p*-xylene in the suppression of dimerization reaction

### 4.4.1 Background

Although the reaction was optimized, it was not clear how *p*-xylene suppressed the dimerization reaction. Based on the UV-vis spectrum of *p*-xylene, it does not absorb at 300 nm (showing a very low absorption at 290 nm). However, the lamps used for the photoreactions have a range of output (see section 2.2.1), therefore *p*-xylene could absorb some energy using 300 nm lamps, but it is unlikely it would be enough to triplet sensitize an adequate amount of alkene molecules to block the dimerization reaction by blocking its singlet excited state (due to alkenes having a much higher absorption at the wavelengths used). Additionally, blocking of dimerization of the maleimide was observed, which also underwent triplet sensitized dimerization reaction with THX. This suggests a different type of interaction between the *p*-xylene and alkenes.

First, the expected solvent effects on UV-vis absorption of maleic anhydride were considered. Figure 4-7 gives a general representation of the peak movement expected when a red or a blue shift takes place:

- (A) *Red shift* is expected to be caused by polar solvents – a smaller energy gap is expected between the neutral ground state of the maleic anhydride and the polar excited state, with movement of the absorption peak towards longer wavelength.
- (B) *Blue shift* is expected to be caused by non-polar solvents (e.g. *p*-xylene) – a larger energy gap is expected between the neutral ground state of the maleic anhydride and the polar excited state, with movement of the absorption peak towards shorter wavelength.

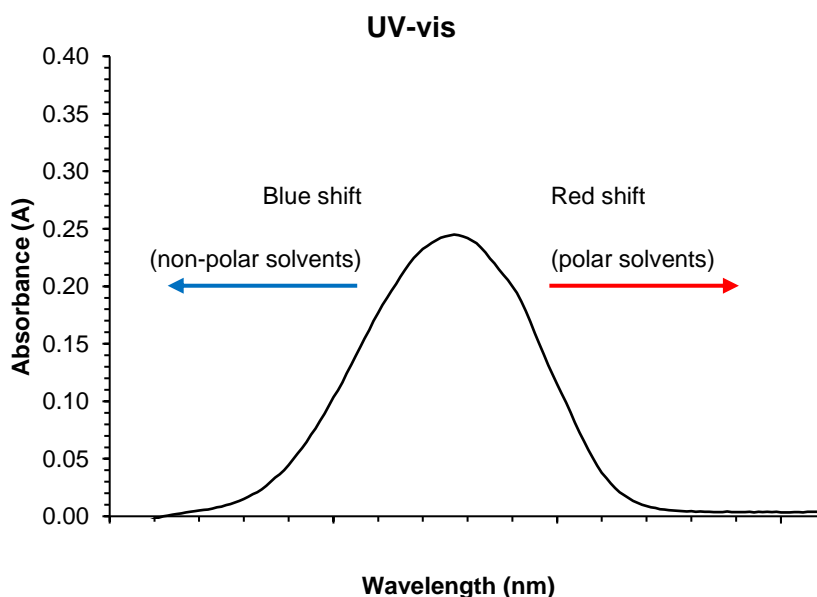


Figure 4-7 A summary of general expected solvent effects on a peak in a UV-vis spectra.

#### 4.4.2 UV-vis experiments

A UV-vis experiment was designed to see the variation in absorption of maleic anhydride as *p*-xylene is added. This series of UV-vis measurements was performed with MeCN as baseline (Figure 4-8). A series of solutions was made up with maleic anhydride and increasing equivalents of *p*-xylene (1 - 20 eq). The UV-vis spectra are shown in Figure 4-8, including the UV-vis spectra of *p*-xylene in MeCN (green line) and maleic anhydride (black line) followed by a mixture of both (blue lines). The general trend shown by the UV-vis measurements shows that as more *p*-xylene is present in the solution (light to dark blue lines) a red shift is observed. When comparing with the general expected solvent effect *p*-xylene should have on maleic anhydride, a blue shift in UV-vis measurement would be expected, due to *p*-xylene being a less polar solvent (compared to MeCN). *p*-Xylene would be expected to cause a larger energy gap between ground state and polar excited state, which would lead to blue shift.

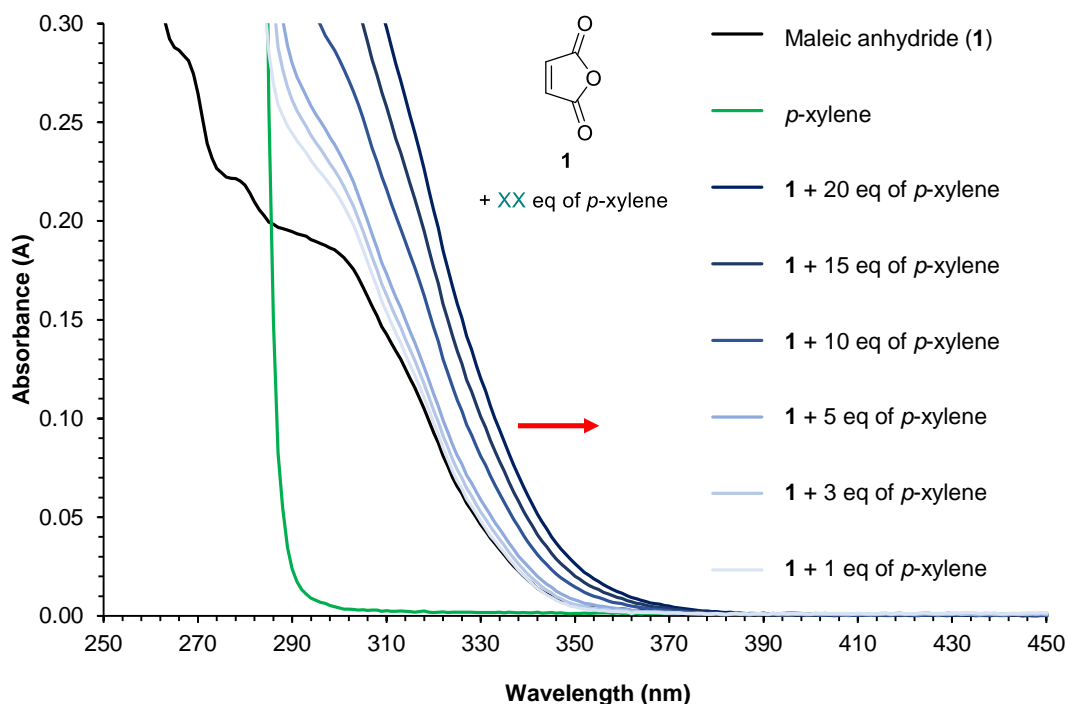


Figure 4-8 All absorbance run with MeCN as baseline (0.01M, MeCN).

Although there was a clear shift in the absorption of maleic anhydride, a more accurate experiment was designed to ensure the least amount of error. Thus, different amounts of *p*-xylene were included in the baseline; this should have ensured that any *p*-xylene peaks are hidden in the baseline. A check of the new baselines clearly shows that the amount of *p*-xylene does not affect the spectra above 310 nm (Chapter 6 – experimental 7.5).

A series of different alkenes (maleic anhydride, MH-maleimide and NBn-maleimide (**65**)), and cyclohexanone were tested, and detailed versions of the spectra are shown in Figure

4-9 (with full spectra shown in Chapter 6 – experimental). Again, the maleic anhydride UV-vis spectrum shows a clear red shift, confirming that there is an interaction between maleic anhydride and *p*-xylene that is not just solvent interaction, and which is possibly causing the suppression of the dimerization reaction. In the case of both maleimides (*NH* and *NBn*) a red shift is still observed, but it is not as strong as when maleic anhydride was used. Finally, cyclohexanone shows a blue shift, which is what would be expected based on the general expected solvent effects on UV-vis spectra (as summarized in Figure 4-7).

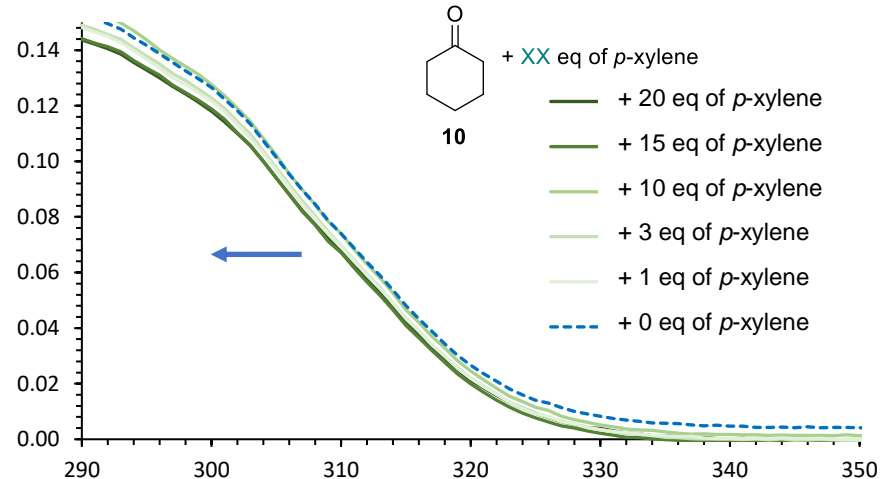
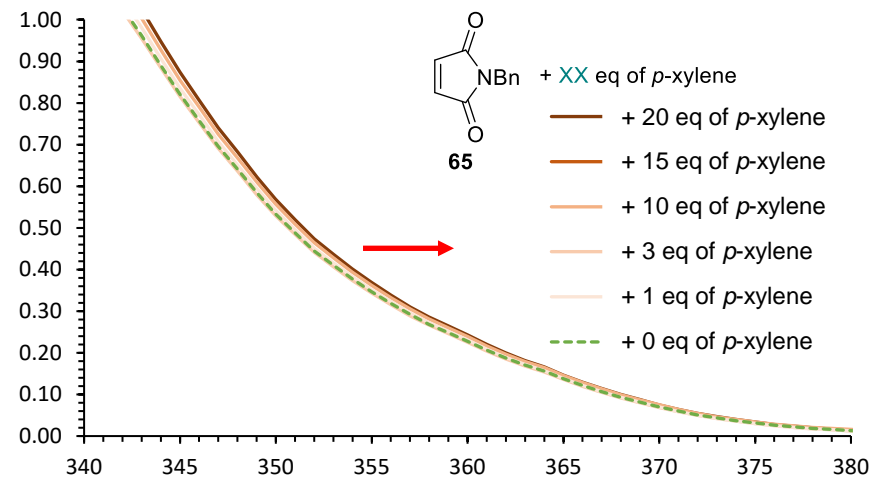
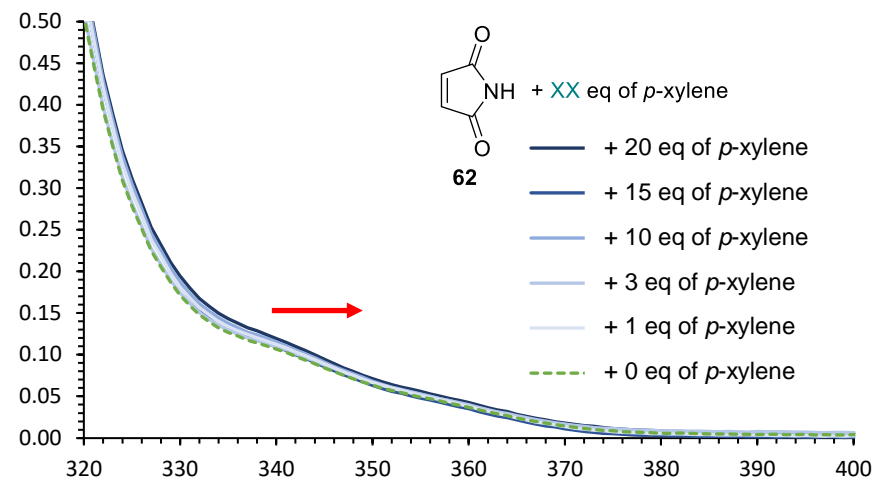
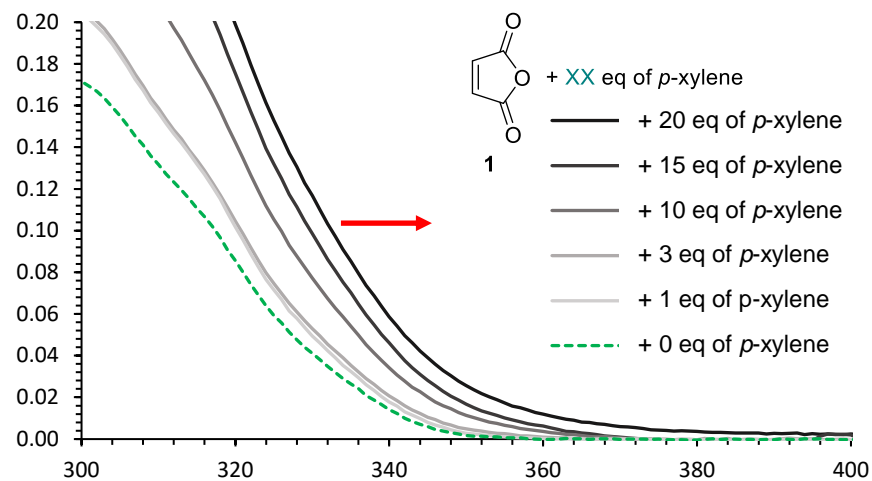


Figure 4-9 A series of UV-vis spectra collected to observe the effect of adding *p*-xylene on maleic anhydride (1, top left), NH-maleimide (62, top right), NBN-maleimide (65, bottom left) and cyclohexanone (10, bottom right). Concentration: 0.01M in MeCN. y-axis = absorbance (A); x-axis = wavelength (nm).

When comparing the effect of the *p*-xylene on the maleic anhydride versus maleimide, a red shift is reported in both cases. However, maleic anhydride has a much stronger red shift and therefore a much stronger interaction with the *p*-xylene. This observation correlates well with the experimental results; only 1 equivalent of *p*-xylene is required to suppress the dimerization of maleic anhydride, while 1 equivalent of *p*-xylene does not fully suppress the dimerization reaction of maleimides. A possible  $\pi$ - $\pi$  interaction between the alkene and *p*-xylene could take place, as they are both flat and could easily stack. In the case of both maleimides, the red shift is still present, but it is much weaker compared to maleic anhydride. Importantly, the difference in the red shift between the two maleimides is not very large; *N*-H-maleimide and *N*-Bn-maleimide were tested, both showing similar red shift magnitude, showing that a protecting group (or lack of) does not have a large effect on the red shift. Lastly, cyclohexanone shows a clear blue shift, which is in agreement with the general rules of expected solvent effects. Table 4-7 compares the molar absorptivity changes (at 320 nm for maleic anhydride and cyclohexanone; and at 360 nm for the *N*-H-maleimide and *N*-Bn-maleimide), calculated based on the Beer–Lambert law (Chapter 1, Equation 1-2). The table shows the strengths of the red shifts in the case of the alkene, and although the red shift of the maleimides (Table 4-7, entry 5-12) is much lower than that of maleic anhydride (Table 4-7, entry 1-4), it can be clearly seen that the molar absorption coefficient increases as the *p*-xylene is added. In contrast, the molar absorption coefficient of cyclohexanone decreases (Table 4-7, entry 13-16) upon addition of increasing amounts of *p*-xylene.

Entry	Compound	Wavelength (nm)	<i>p</i> -xylene (eq)	$\epsilon$ (M <sup>-1</sup> cm <sup>-1</sup> )	$\Delta \epsilon$ (20-0 eq of <i>p</i> -xylene)
1	Maleic anhydride (1)	320	0	8.01	+ 10.99
2			1	9.57	
3			10	13.48	
4			20	19.00	
5	<i>N</i> -H-maleimide (62)	360	0	3.66	+ 0.58
6			1	3.80	
7			10	3.94	
8			20	4.24	
9	<i>N</i> -Bn-maleimide (65)	360	0	22.76	+ 1.54
10			1	23.10	
11			10	23.93	
12			20	24.30	
13	Cyclohexanone (10)	320	0	2.36	-0.50
14			1	1.88	
15			10	2.15	
16			20	1.86	

Table 4-7 Difference in molar absorption coefficient in the presence of *p*-xylene. Concentration = 0.01 M, length of light path = 1 cm.



The clear change in absorption in the UV-vis measurements of the above alkenes correlates with the experimental results of the dimerization reaction; the addition of the *p*-xylene suppresses the dimerization reaction as well as clearly affecting the absorption of the maleic anhydride and maleimides.

A possible reason for this effect might be due to interactions between these flat aromatic molecules in the reaction mixture. A simple way of showing the possible interaction is by showing the possible way of  $\pi$ - $\pi$  stacking of the maleic anhydride as a flat aromatic molecule in solution, as maleic anhydride could stack, head-to-tail, with other maleic anhydride molecules. In the absence of *p*-xylene, there is a possibility of sandwich stacking interaction of the maleic anhydride molecules, in the case one of them reaches an excited state by irradiation it can quickly react with another molecule that could be close by, leading to formation of a dimer (Figure 4-10a). However, in the presence of *p*-xylene molecules, the original stacking interaction can be interrupted by insertion of the flat *p*-xylene molecule, leading to blocking the reaction site for dimerization reaction and affecting the absorption of the maleic anhydride observed by UV-vis. The UV-vis measurements collected imply a possible interaction between the pi-pi orbitals of the maleic anhydride and *p*-xylene.

In the terms of the HOMO and LUMO orbitals the UV-vis observations can be explained by interaction between the HOMO of *p*-xylene and the LUMO of the maleic anhydride (or maleimide) (Figure 4-10b). *p*-Xylene and maleic anhydride are flat, aromatic molecules, with *p*-xylene being electron-rich while maleic anhydride is electron-poor. Upon addition of *p*-xylene, a red shift was observed, which could be due to the charge transfer absorbance band (Figure 4-10c). A charge transfer absorbance band can be observed when the HOMO of *p*-xylene donates an electron to the LUMO of the alkene. The energy difference between the HOMO and the LUMO of these two different molecules is smaller than the energy difference between the HOMO and the LUMO of maleic anhydride (original absorbance). The charge transfer absorbance band implies that there is a mixing between the pi orbitals of the maleic anhydride and *p*-xylene, and that interaction could result in the blocking of the dimerization reaction. In the case of maleimide, a similar interaction takes place, but due to relative energy levels the interaction is less strong. Charge transfer transitions between pi stacking systems have been previously reported.<sup>99,100</sup>

The final piece of evidence for the interaction between the alkenes and the *p*-xylene is the increase in the intensity of the absorbance. The intensity of the absorbance is due to the change in the dipole moment caused by the transition from the ground state to the excited state – as the dipole moment increases, the absorbance is more intense.<sup>57,58</sup> In

the case of the maleic anhydride and *p*-xylene, there is a large increase in the absorbance, implying a large dipole moment (i.e. an electron moving from *p*-xylene to maleic anhydride) compared to the electron moving between molecular orbitals in the same molecule.

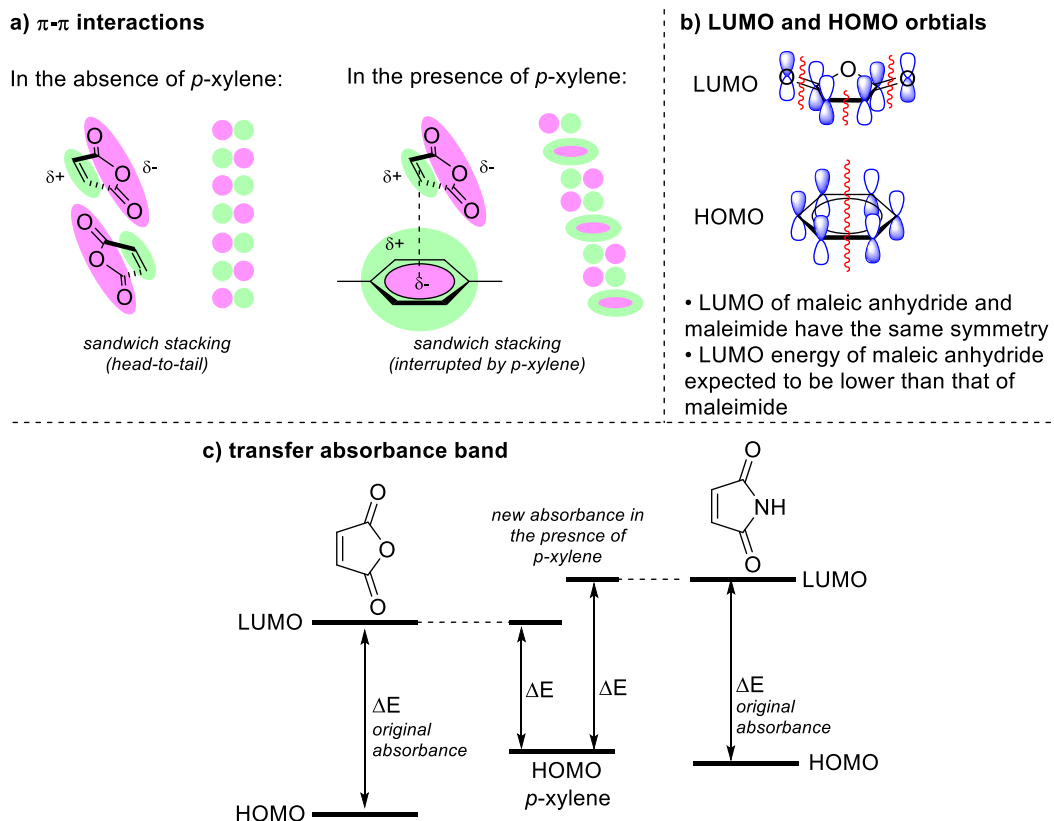


Figure 4-10 a) Summary of the possible  $\pi$ - $\pi$  interactions in the absence and presence of *p*-xylene; b) LUMO of maleic anhydride and HOMO of *p*-xylene; c) transfer absorbance band explanation.

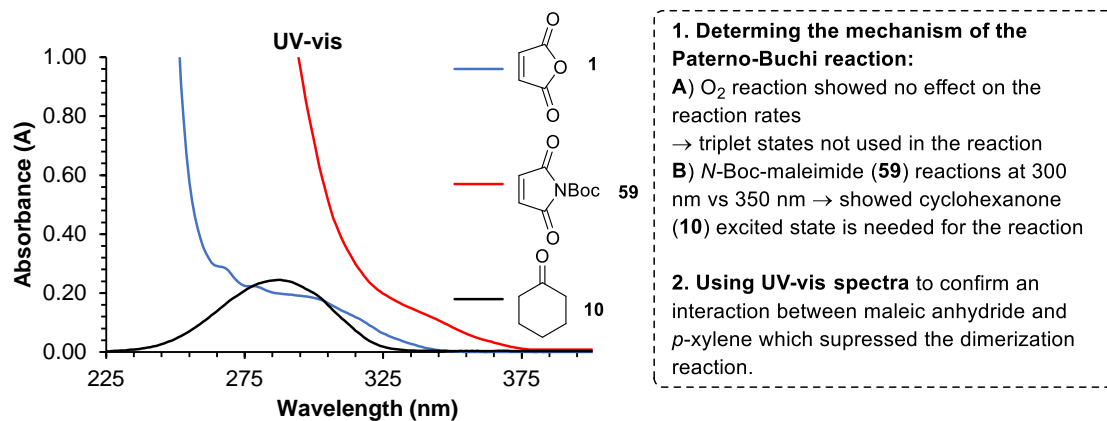
#### 4.4.3 Conclusion of the investigation into the role and effect of the *p*-xylene on the reaction mixture

In summary, a series of UV-vis measurements were collected of the starting materials (maleic anhydride, maleimides and cyclohexanone) in the presence of the *p*-xylene. *p*-Xylene caused the absorption ranges of the alkenes to red shift; this was unexpected based on initially predicted solvent effects that the *p*-xylene would have on the absorption. The red shift was most prominent with maleic anhydride, and also showed an increase in the intensity of absorption. Based on the results collected, it was theorized that there is an interaction between *p*-xylene and maleic anhydride that could involve mixing of their pi orbitals as likely a charge transfer absorbance could be the reason for the observed red shift. That possible interaction between the maleic and *p*-xylene could result in blocking of the dimerization side reaction. Although it was not possible to fully understand how the dimerization reaction is blocked, the collected UV-vis measurements imply  $\pi$ - $\pi$  interactions between the maleic anhydride and *p*-xylene. To fully understand

the interaction between the maleic anhydride and *p*-xylene, and how it blocks the dimerization reaction further investigations are necessary, but this preliminary investigation resulted in a number of interesting observations that will lead to future collaborative projects in the research group.

#### **4.5 Conclusions**

This chapter showed the mechanistic investigation into the Paternò-Büchi (Figure 4-11). Molecular oxygen which is known for quenching triplet excited states had no effect on the reaction rates of either the Paternò-Büchi or dimerization reaction, therefore suggesting that the mechanisms for the reactions does not involve triplet excited states. Next, the excited state partner of the Paternò-Büchi reaction was determined by changing the alkene to a maleimide which has a higher wavelength absorption range allowing for selective excitation of maleimide in the presence of cyclohexanone (Figure 5-5, UV-vis). These experiments showed formation of oxetane and dimer when the reaction mixture was irradiated at 300 nm, however at 350 nm only dimer was observed suggesting that the excited state of the ketone is necessary for the formation of the oxetane. Mechanistic investigations indicated that the likely mechanism that takes place between a cyclohexanone and electron-poor alkene takes place via a singlet excited state of the cyclohexanone during direct irradiation. Additional tests are needed in order to fully confirm the mechanism. Studies into the role of the *p*-xylene in the reaction took place, UV-vis showed a clear interaction between maleic anhydride and *p*-xylene which is likely responsible for suppressing the dimerization reaction.



Proposed mechanism for the Paterno-Buchi reaction under direct irradiation:

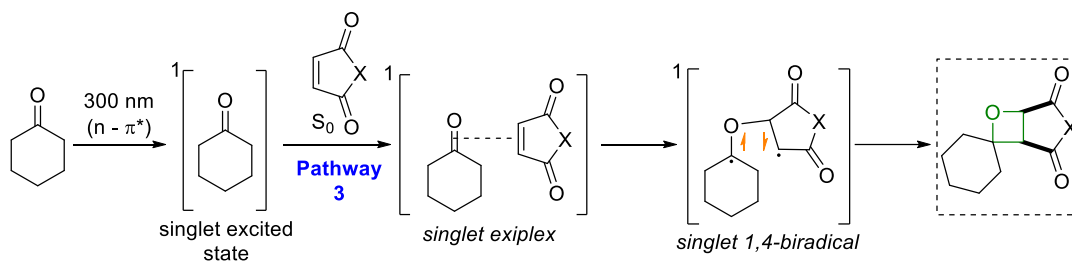
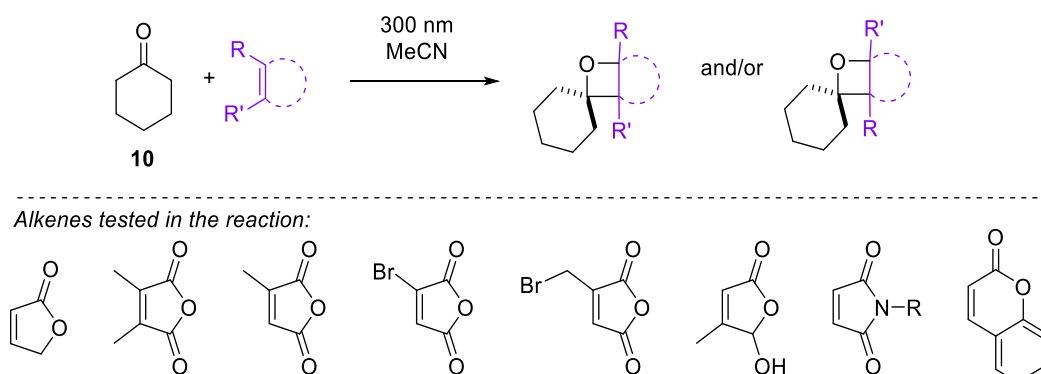


Figure 4-11 Summary of results from chapter 4.

# Chapter 5 Expanding the scope of the Paternò-Büchi reaction by using different electron poor cyclic alkenes

## 5.1 Introduction

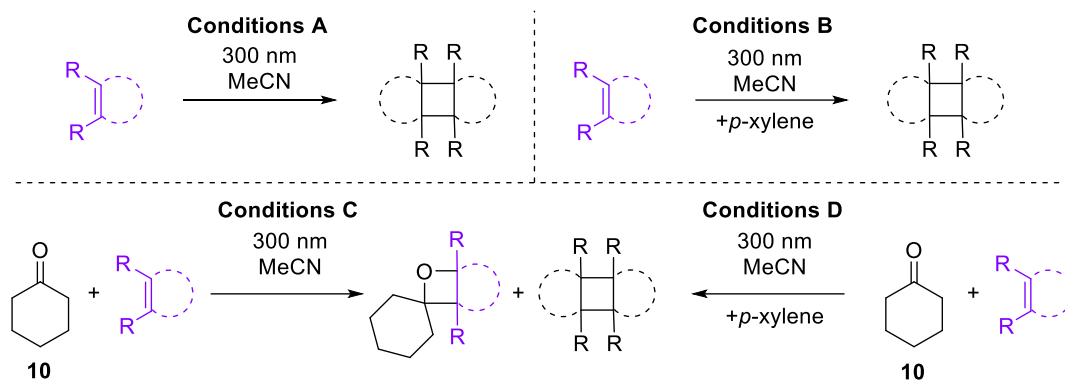
Previously in Chapter 3, the scope of the Paternò-Büchi reaction was broadened by variation of the cyclic aliphatic ketone used as well as with the use of different functionalization reactions performed on the anhydride ring. The following section describes Paternò-Büchi reactions between different activated alkenes and aliphatic cyclic ketones (Scheme 5-1). Derivatives of maleic anhydride, maleimides and coumarin were tested as potential partners for the Paternò-Büchi reaction with cyclohexanone. The changes in structure of the alkene would lead to new spirocyclic oxetanes and likely expand the number of transformations and possible products. However, most of the new alkenes are no longer symmetrical, and this could lead to mixtures of products, as observed when asymmetric ketones were used (Section 3.3.2.1).



**Scheme 5-1** Summary of new electron poor alkenes tested in the Paternò-Büchi reaction with cyclohexanone (10).

In order to efficiently test a large number of reactions with different alkenes, test reactions in NMR tubes were performed (NMR tubes made from Duran glass were employed, to ensure light penetration at 300 nm). Each new alkene was tested under at least four different environments, this allowed for testing the behaviour of the alkene under reaction conditions and gave an indication of any small optimizations needing to be performed based on the alkene used in the reaction before scaling up the reaction. Pleasingly, these experiments also gave an idea about the reaction time needed for a normal scale reaction (usually ~1 mmol). Four reactions allowed for rapid test of the potential reactions taking place when the new alkenes were irradiated on a very small scale (Scheme 5-2). The four basic reactions conditions involved: reaction A, which showed the rate of dimerization reaction (and any other side reactions); reaction B, which tested if there is any effect of the *p*-xylene on the dimerization reaction; then reactions C and D tested the

Paternò-Büchi reaction and compared the ratio of the formed oxetane and dimer in the absence and presence of the *p*-xylene. The following sections will refer to these general conditions.

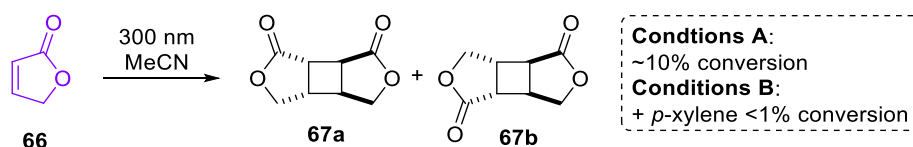


The alkenes tested can be split into two main categories: the maleic anhydride derivatives (5.2 Maleic anhydride derivatives, also including coumarin) and maleimides (5.3 Maleimide derivatives). Many of the reactions were performed before having the partial mechanistic picture of the Paternò-Büchi reaction, meaning that some reactions discussed in the following section were performed at different wavelengths in an attempt to manipulate the Paternò-Büchi reaction to form the desired oxetane. However, based on the results discussed in sections 4.2 and 4.3, the desired results could not have been achieved as excitation of cyclohexanone is only possible at 300 nm.

## 5.2 Maleic anhydride derivatives

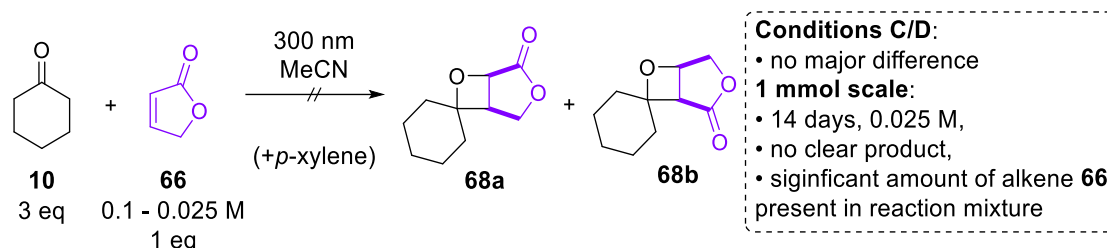
### 5.2.1 2(5H)-Furanone (66)

2(5H)-furanone (**66**) can give rise to two possible dimer products: **67a** and **67b** (Scheme 5-3), due to the partial loss of symmetry compared to maleic anhydride. The dimerization reaction (conditions A) was not very prominent, showing only 10% of the dimer formed after 24 hours of irradiation. *p*-Xylene successfully blocked the dimerization reaction (conditions B), which was observed by <sup>1</sup>H NMR spectroscopy (solvent suppression, MeCN) (Scheme 5-3).



During the Paternò-Büchi reaction of cyclohexanone and alkene **66**, the loss of symmetry would likely lead to formation of two oxetanes **68a** and **68b** (Scheme 5-4). Analysis by <sup>1</sup>H NMR spectroscopy did not give clear oxetane peaks (possibly due to overlap of peaks

due to mixtures of products as well as the overall complexity of the potential signals arising). The major problem with the reaction was the lack of conversion of the alkene during the reaction time. The test reactions were performed in Duran NMR tubes (conditions C and D), allowing for very small scale as well as excellent light penetration due to size. Therefore, it was expected for the majority of the alkene to be consumed during the reactions, but this was not the case with 2(5H)-furanone (**66**), which still showed a majority of the starting alkene after 24 hours irradiation. The NMR tube reactions showed that the dimerization most likely is not a major issue, and the two test Paternò-Büchi reaction showed no major difference between conditions C and D (C = no additive Paternò-Büchi reaction, D = + *p*-xylene). The reaction showed very slow conversion in the NMR tube as well as quite a complex mixture due to the different products that can be formed in the reaction. To push the reaction to completion, the concentration of the reaction mixture was decreased to 0.025 M (from 0.1 M) and the reaction was performed on 1 mmol scale, however even after 14 days of irradiation a large amount of alkene **66** was still present in the reaction mixture; this observation led to abandoning alkene **66** as a possible reagent for the Paternò-Büchi reaction.



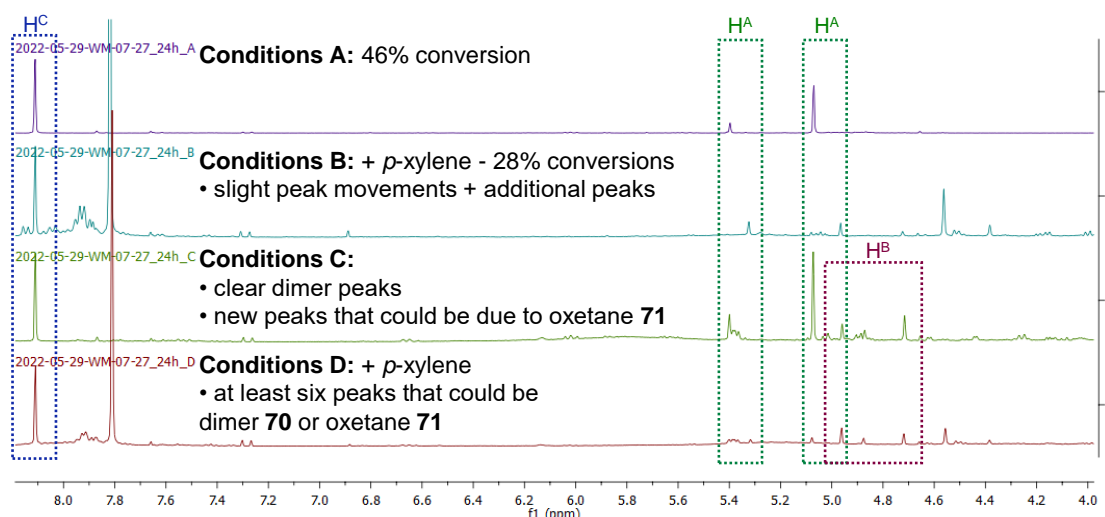
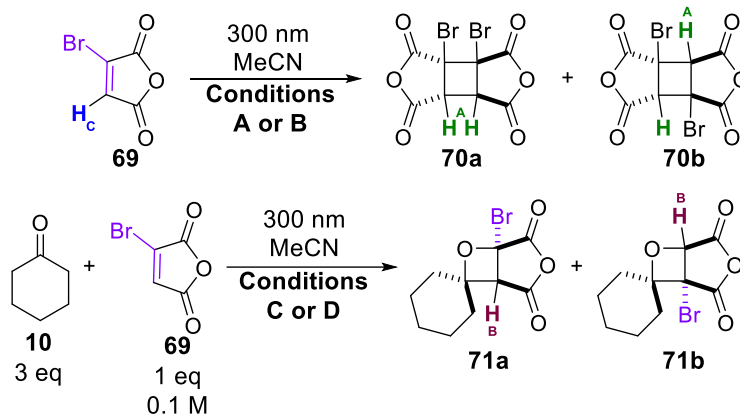
Scheme 5-4 Summary of the results of the Paternò-Büchi reaction of cyclohexanone and 2(5H)-furanone (**66**).

### 5.2.2 Bromofuran-2,5-dione (**69**)

Next, bromofuran-2,5-dione (**69**) was used in the Paternò-Büchi reaction (Scheme 5-5), with the bromine atom present on the ring adding a possible functional handle to the final oxetane product **71**. There was a loss of symmetry and therefore two isomers of the dimer (**70a** and **70b**) and oxetane (**71a** and **71b**) were expected leading to a potential complex mixture of products.

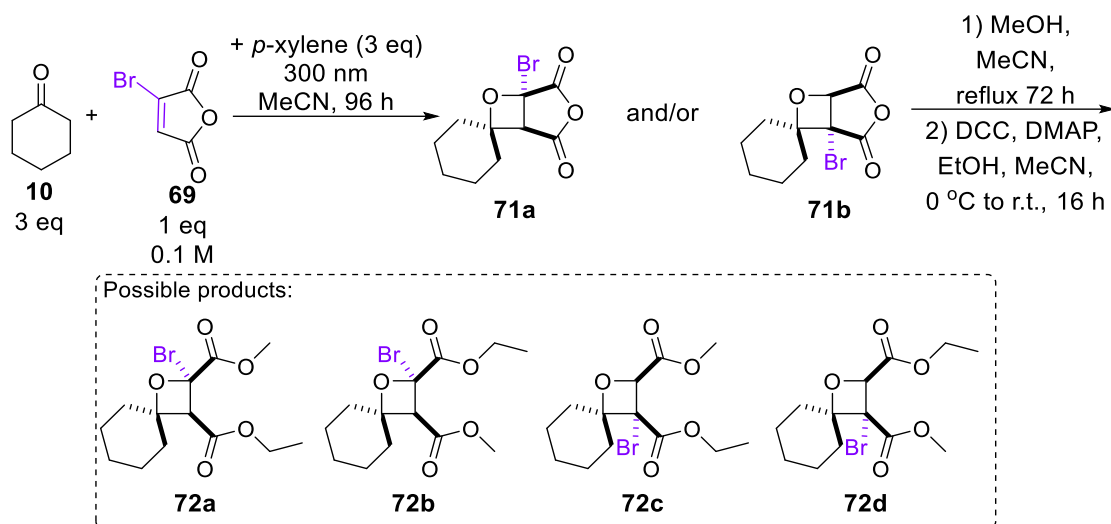
Indeed, the reaction was difficult to track as the  $^1\text{H}$  NMR spectra (solvent suppression, MeCN) showed more signals than expected; the four main sets of reaction conditions are summarized in Scheme 5-2 and the  $^1\text{H}$  NMR spectra of all reactions at 24 h is shown in Figure 5-1. Starting with just the dimerization reaction, under conditions A two peaks were observed and assigned as dimer **70a** and **70b**, next *p*-xylene was added (conditions B), and the conversion of alkene into the two dimers decreased from 46 to 28%, and a slight movement of the dimer peaks was observed. More importantly, additional singlets in the 4-5.5ppm were observed, suggesting formation of other side products. Next,

reaction conditions C are shown, showing the two dimers formed as well as two new signals that could be due to the oxetane **71**. Under conditions D, it was expected that the dimerization reaction was suppressed, however there were at least six signals that could be due to the oxetane ( $H^B$ ) or dimer ( $H^A$ ), due to the peak shift observed in the presence of *p*-xylene it was difficult to identify the desired oxetane products.



Although the initial reaction results were difficult to fully understand, the functionalization reaction of the anhydride was undertaken in order to form an oxetane **71** that can be purified chromatographically. A reaction on 1 mmol scale was performed and tracked, starting with the Paternò-Büchi reaction between the cyclohexanone and bromofuran-2,5-dione (**69**), which took 96 hours to consume all of the starting alkene. An important detail was a rise in the baseline of the  $^1\text{H}$  NMR spectrum, which could indicate the formation of a polymer. Nevertheless, the crude product of the Paternò-Büchi reaction underwent the standard functionalization reactions: ring opening of the anhydride followed by the carboxylic acid cross-coupling reaction. Disappointingly, none of the four possible oxetane products was isolated.



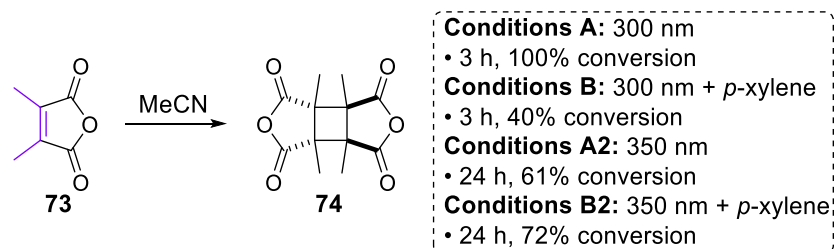


Scheme 5-6 Possible products formed during Paternò-Büchi reaction between cyclohexanone (**10**) and bromofuran-2,5-dione (**69**) followed by the functionalization reactions.

In summary, the bromofuran-2,5-dione (**69**) alkene did not work as hoped under irradiation conditions, and no desired oxetane product was isolated. There is a possibility of the Br radical formation in the reaction mixture due to the presence of the Br on the alkene; it may be possible for the C-Br bond to be broken homolytically, which would lead to formation of Br radical, although the resulting sp<sup>2</sup> radical is not particularly stable. If formed, a Br radical is very reactive and can lead to a mixture of products under those reaction conditions. Due to difficulties with the reaction tracking as well as possible degradation of the bromofuran-2,5-dione (**69**), this alkene was no longer investigated.

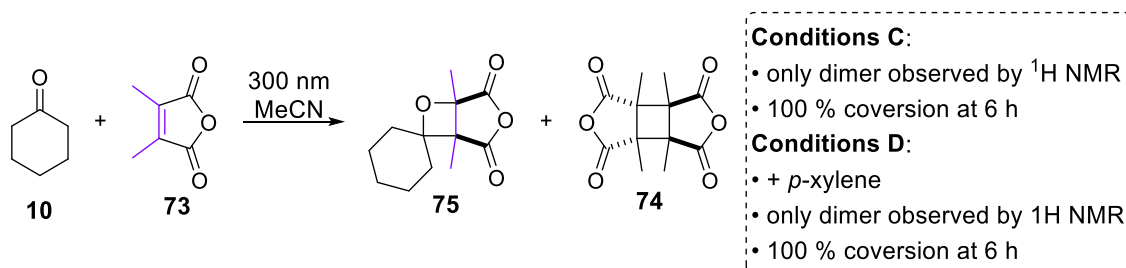
### 5.2.3 Dimethyl maleic anhydride (**73**)

Next, dimethyl maleic anhydride (**73**) was tested and underwent rapid dimerization, with an initial test reaction showing crystallization of the dimer **74** from the reaction mixture, making it impossible to accurately assess the percentage of the compounds present in the reaction mixture, as the solid would crash out of solution. A handful of dimerization reactions was performed under different conditions to try to slow down the rate of dimerization (Scheme 5-7). Reaction conditions A and B showed very fast dimerization rate with 100% and 40% conversion of the alkene after 3 h without and with *p*-xylene respectively. It was theorized that the alkene is absorbing too much energy and reacting rapidly which was confirmed by the UV-vis showing a very high absorption at 300 nm, therefore the wavelength was changed to 350 nm in attempt to slow down the dimerization reaction. Reaction conditions A2 and B2 show the conversion of the alkene into the dimer at 350 nm without and with *p*-xylene respectively. The reactions were shown 61-72% conversion of the alkene **73** into the dimer **74** after 24 hours, with the higher conversion in the presence of the *p*-xylene, which was an unusual result. Nonetheless, the Paternò-Büchi reaction with cyclohexanone was tested.



**Scheme 5-7** Percentage conversion based on  $^1\text{H}$  NMR (solvent suppression, MeCN, 400 MHz).

Due to the nature of the oxetane products formed in this reaction, the expected  $^1\text{H}$  NMR signals of the formed oxetane **75** were likely to overlap with the starting materials: both dimethyl maleic anhydride (**73**) and/or cyclohexanone. Additionally, tracking the reaction by performing solvent suppression  $^1\text{H}$  NMR spectroscopy (in MeCN) caused suppression in the  $^1\text{H}$  NMR region of interest ( $\sim 2.6 - 2.9$  ppm). Annoyingly, no oxetane **75** was observed in the reaction, while dimer **74** formation consumed the alkene **73** within 6 hours.



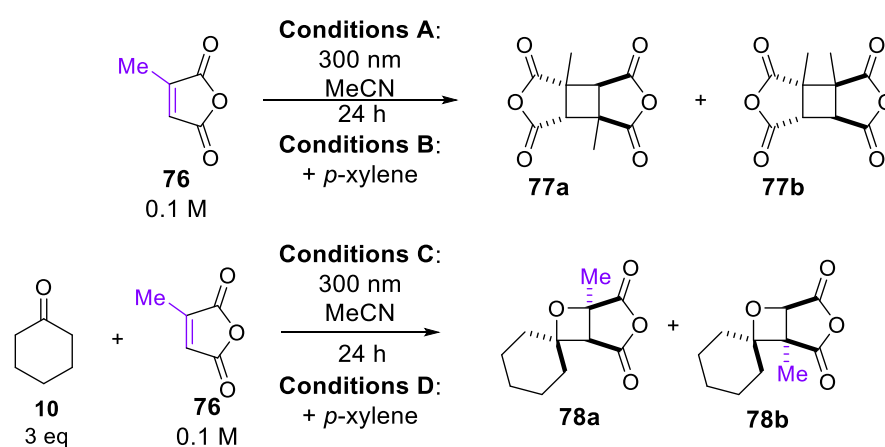
**Scheme 5-8** Summary of the reactions with dimethyl maleic anhydride (**73**).

Additionally, it is important to mention that the most likely reaction pathway for the Paternò-Büchi reaction between the cyclohexanone and electron poor alkene is via the singlet excited state of cyclohexanone and the ground state of the alkene. Therefore, increasing the wavelength as a way of decreasing the rate of dimerization would most likely not result in formation of the oxetane **75** as the cyclohexanone would not be excited. Furthermore, the lack of the effect of the *p*-xylene on the dimerization reaction could be due to the lack of the possible  $\pi$ - $\pi$  stacking, as the two methyl groups make the molecules much less flat.

#### 5.2.4 Methyl maleic anhydride (**76**)

Using methyl maleic anhydride (**76**) can give rise to a mixture of products again, due to the loss of the symmetry of the alkene. Standard reaction conditions were tested to show the rate of dimerization reaction of methyl maleic anhydride (**76**), showing full consumption of alkene after irradiating at 300 nm for 24 h (Table 5-1, entry 1). Addition of the *p*-xylene slowed down the dimerization, showing 47% of dimer **77** is present in the reaction mixture after 24 hours. When performing the Paternò-Büchi reaction (Table 5-1, entry 3-4) 85% of the alkene **76** was converted into dimer in 24 hours while 14% of the

alkene was used in the desired Paternò-Büchi reaction. However, the addition of 1 equivalent of *p*-xylene decreased the dimerization rate, showing only 31% of starting alkene **76** being lost to the dimerization reaction (Table 5-1, entry 4). The percentage of the conversion of the alkene **76** into oxetane **78** increased from 14 to 69% by adding 1 equivalent of *p*-xylene to the reaction. Overall, the test reactions were successful, showing formation of the desired product at good rates, and the dimerization reaction was partially suppressed with 1 equivalent of *p*-xylene, meaning a higher number of equivalents of the *p*-xylene will be used in future reactions to fully suppress the dimerization reaction. It is possible that due to the methyl group being present, the interaction between the *p*-xylene and alkene **76** is weaker compared to maleic anhydride.



Entry	Reaction conditions	reaction mixture at 24 h			Conversion of alkene <b>76</b> into	
		<b>76</b> (%)	<b>78</b> (%)	<b>77</b> (%)	<b>78</b> (%)	<b>77</b> (%)
1	A	0	-	100	-	100
2	B	69	-	31	-	47
3	C	0	25	75	14	85
4	D	34	54	12	69	31

Table 5-1 Results of the test reaction conditions with methyl maleic anhydride (**76**) as alkene. Percentage of components in the reaction mixture based on <sup>1</sup>H NMR (solvent suppression, MeCN, 400 MHz).

The Paternò-Büchi reaction gave rise to a major oxetane product (**78a**). Figure 5-2 compares the <sup>1</sup>H NMR of the Paternò-Büchi reaction and dimerization reaction. The top spectrum shows the Paternò-Büchi reaction, where three product signals at ~4.2 ppm are observed, two of them due to the dimerization reaction of the methyl maleic anhydride, which can be clearly seen based on the spectrum 2, which shows the dimerization reaction. Having only one signal for oxetane implies regioselective formation of the oxetane. Based on the previous NMR assignment, it is more likely that oxetane **78a** is formed, as the proton signal H<sup>A</sup> would be expected in that region, while in **78b**, proton H<sup>A</sup> would be expected to be more downfield (5-6 ppm). There was a very small signal at 5.6 ppm but it was never isolated as pure product, and therefore cannot

be confirmed to be the other oxetane isomer. Formation of one product **78a** is most likely due to steric effects, as the cyclohexane ring and the methyl group are both bulky, and prefer not to be next to each other. This steric argument could also explain why no oxetane **75** was reported during the reaction with dimethyl maleic anhydride (**73**) (Section 5.2.3).

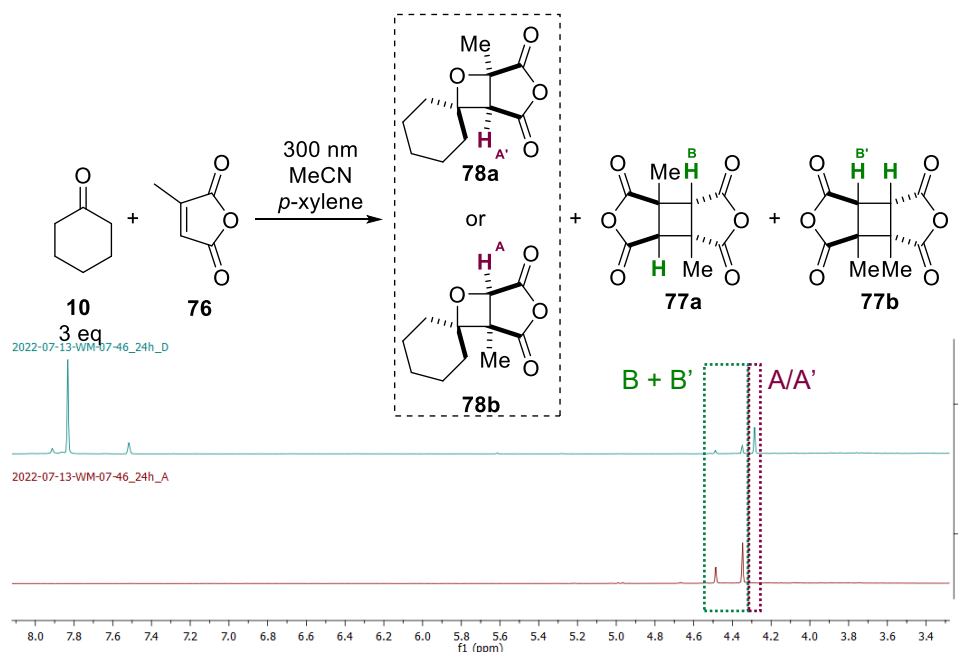
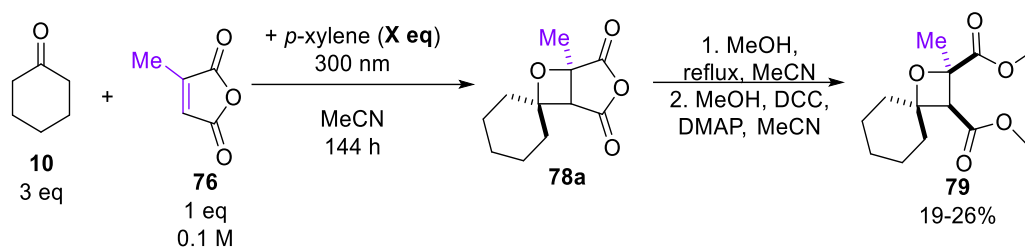


**Figure 5-2**  $^1\text{H}$  NMR spectra (solvent suppression, MeCN, 400 MHz) of the Paternò-Büchi reaction (top) between methyl maleic anhydride (**76**) and cyclohexanone and dimerization reaction (bottom) of the methyl maleic anhydride.

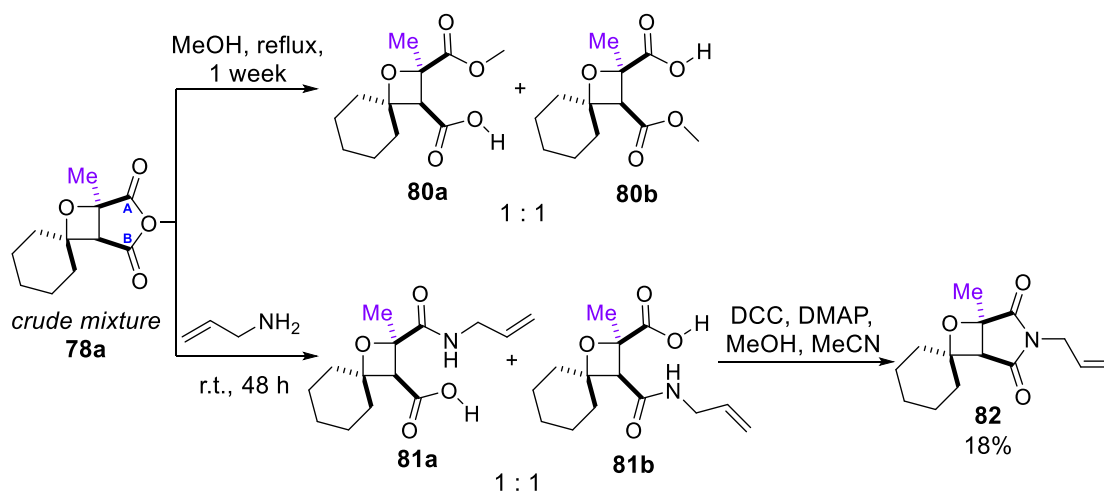
Three parallel reactions were performed to test the effect of the *p*-xylene on the final yield of the isolated oxetane (**79**) (Table 5-2). When 1 equivalent of the *p*-xylene was used in the reaction a significant amount of dimer was present at the end of the Paternò-Büchi reaction, 13%, giving the lowest yield of the isolated oxetane at the end of the telescoped reaction pathway with 19%. Increasing the amount of *p*-xylene to 2 equivalents decreased the amount of dimer to only 6% and therefore improved the final oxetane yield to 32%. Using 3 equivalents of *p*-xylene further decreased the amount of dimer present, however had a slight negative effect on the final oxetane yield, as it decreased to 26%.



Entry	<i>p</i> -xylene (eq)	% of dimer <b>77</b> in the reaction mixture after Paternò-Büchi reaction	<b>79</b> % yield
1	1	13	19
2	2	6	32
3	3	<1	26

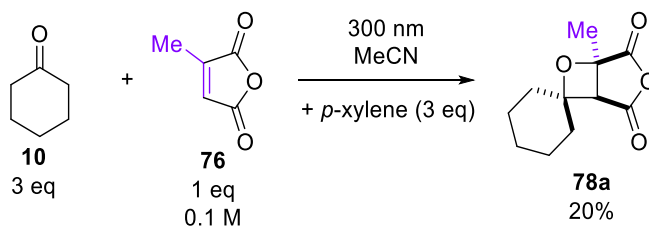
Table 5-2 Results of the effect of the equivalent of the *p*-xylene on the percentage yield of the isolated oxetane **79** (over three reaction steps).

Methyl maleic anhydride (**76**) worked well in the Paternò-Büchi reaction, yielding **78a**. However, ring opening of the anhydride proved frustrating, as loss of regioselectivity was observed and two products **80a** and **80b** were formed in a 1:1 ratio (Scheme 5-9). It is important to note that the reaction took a week, showing an increase in stability of the anhydride ring towards nucleophilic attack. A ring-opening reaction with allyl amine was performed to check if the loss of regioselectivity is observed when an amide functional group is formed, but again two products were formed with 1 : 1 ratio, and the mixture of products: **81a** and **81b** underwent carboxylic acid coupling reaction to form a methyl ester from a carboxylic acid and isolate the final products. However, the oxetane product isolated from the reaction was unexpected - **82** was formed in 18% yield, showing the ring closure onto the amide and formation of an imide ring. The loss of regioselectivity is most likely due to the presence of the methyl group, which now blocks carbonyl A (on oxetane **78a**), while carbonyl B is still being blocked by the presence of the cyclohexane ring. With both carbonyl groups being slightly blocked by the bulky groups, formation of two products is observed.



**Scheme 5-9** Ring opening of oxetane **78a** with MeOH or allyl amine. (yield based on alkene used in the Paternò-Büchi reaction)

The difficulty in the ring opening of the anhydride ring on the oxetane **78a** inspired the next reaction (Scheme 5-10) in which the oxetane **78a** was isolated without further functionalization in 20% yield.



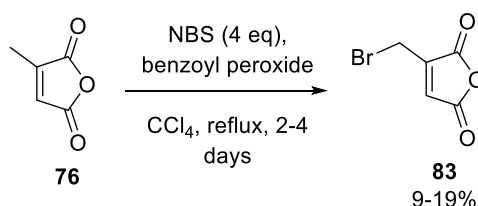
**Scheme 5-10** Paternò-Büchi reaction between cyclohexanone (**10**) and methyl maleic anhydride (**76**).

Overall, addition of the methyl group on the maleic anhydride and using it in the reaction works well, resulting in formation of the oxetane **78a** which can be either isolated in its current state or further functionalized. Disappointingly, the ring opening of the anhydride was no longer regioselective and the ester/amide can be formed on either side of the oxetane ring. Pleasingly, although the methyl maleic anhydride (**76**) is not symmetrical, the Paternò-Büchi reaction with cyclohexanone yields one product **78a**, presumably because the cyclohexane ring and methyl group prefer not to be next to each other. Methyl maleic anhydride (**76**) is the first derivative of the maleic anhydride (**1**) that worked well in the reaction showing the difficulty in finding a good alkene to pair with cyclohexanone in the Paternò-Büchi reaction.

### 5.2.5 3-(Bromomethyl)-2,5-furandione (**83**)

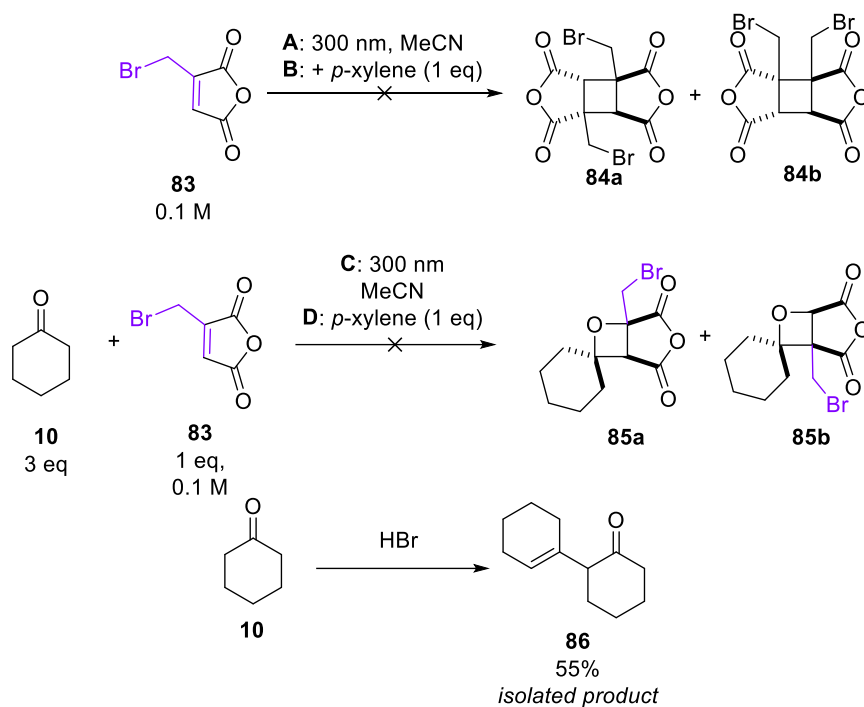
Given the success of methyl maleic anhydride (**76**), investigation of a bromomethyl group was envisaged. This would allow an extra site for further functionalization reactions, and it was hoped that bromomethyl maleic anhydride (**83**) would behave similarly to methyl maleic anhydride (**76**). The reaction of methyl maleic anhydride (**76**) with NBS and

benzoyl peroxide in  $\text{CCl}_4$  yielded the 3-bromomethyl-2,5-furandione (**83**) in 9-19% yield. The reaction was heated at reflux over 4 days, and additional portions of benzoyl peroxide were added as a radical initiator, therefore only a sub-stoichiometric amount was in the reaction, however it did not reach full conversion and starting material (30%) was present in the crude mixture. The procedure called for distillation under vacuum conditions, however the separation was not successful. Column chromatography yielded a cleaner product, however a significant amount of product was not isolated from the column. The yield of the reaction was not as high as the reported yield (50-55%)<sup>101,102</sup> but enough alkene **83** was isolated to test the Paternò-Büchi reaction.



**Scheme 5-11 Formation of 3-bromomethyl-2,5-furandione (83).**

Starting with dimerization reaction, under conditions A and B no consumption of the starting alkene was observed (Scheme 5-12). Next, the alkene was placed under conditions C and D, showing clear consumption of the starting alkene **83**. However, the desired oxetane **85a** or **85b** was not isolated, instead a product of aldol condensation of the cyclohexanone was isolated in 55% yield. Product **86** was most likely due to the formation of HBr in the reaction mixture, which was due to the loss of Br from the alkene, which implies break down of the alkene **83**.

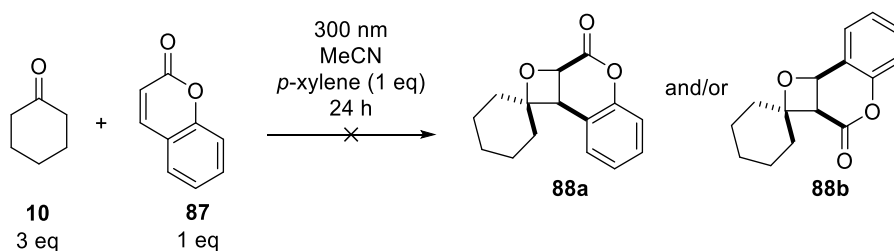


Scheme 5-12 Summary of reactions with 3-bromomethyl-2,5-furandione (**83**).

In summary, the 3-bromomethyl-2,5-furandione (**83**) did not work in the Paternò-Büchi reaction. Additionally, it was suspected that HBr was formed during the reaction leading to a side reaction of the cyclohexanone. Therefore, the alkene **83** was no longer investigated.

### 5.2.6 Coumarin (**87**)

The final alkene tested in the Paternò-Büchi reaction was coumarin (**87**). However, after 24 hours of irradiation no reaction was observed (only starting materials were observed by <sup>1</sup>H NMR spectroscopy) (Scheme 5-13).



Scheme 5-13 Attempted Paternò-Büchi reaction between cyclohexanone (**10**) and coumarin (**87**).

### 5.2.7 Conclusion of the Paternò-Büchi reactions between cyclohexanone and maleic anhydride derivatives

In summary, finding a good partner for the Paternò-Büchi reaction with cyclohexanone is challenging. A series of different maleic anhydride derivatives were tested under the reaction conditions in order to expand on the reaction scope as well to create new functional handles on the formed oxetanes. Methyl maleic anhydride (**76**) was the only



alkene that yielded the desired oxetane product; pleasingly only one product was formed most likely due to the bulky methyl group present on the alkene. Two bromine-containing alkenes (**69** and **83**) were tested under the Paternò-Büchi reaction conditions, but disappointingly, although consumption of the alkene was reported in both cases, the desired oxetane was not isolated. The <sup>1</sup>H NMR spectra showed a mixture of products, likely caused by Br radical or even formation of HBr during the reaction. Overall, changing the alkene has a large effect on the Paternò-Büchi reaction, and although many of the alkenes tested so far did not work well in the reaction, oxetanes formed from maleic anhydride and cyclohexanone can give rise to a series of oxetanes, as the anhydride group can be easily and broadly functionalized as shown in Chapter 3, section 3.3. As discussed in section 4.3, maleimides do form oxetanes when placed under Paternò-Büchi reaction conditions with cyclohexanone, and the isolation of oxetanes formed in those reactions will be discussed next.

### 5.3 Maleimide derivatives

Simultaneously with the reactions reported in section 1.3, an attempt to isolate the oxetanes formed from reactions between cyclohexanone and maleimide was undertaken. Figure 5-3 compares the <sup>1</sup>H NMR spectra of different oxetanes formed, starting with the purified **14c** at the top highlighting the two characteristic <sup>1</sup>H NMR proton signals. The second spectrum shows the solvent suppression <sup>1</sup>H NMR spectrum of the maleic anhydride reaction with cyclohexanone, again highlighting the two protons. Spectra 3 and 4 shows the two reactions mixtures when maleimide was used as the alkene in the Paternò-Büchi reaction with cyclohexanone. These spectra show that the oxetane was clearly formed in the reaction, however the lack of protecting group on *N*-H-maleimide (spectrum 4) leads to possible reactions between the NH and cyclohexanone or its side products (aldehyde) formed in the reaction, resulting in a more complex reaction mixture, and lowering the possible reaction yield.

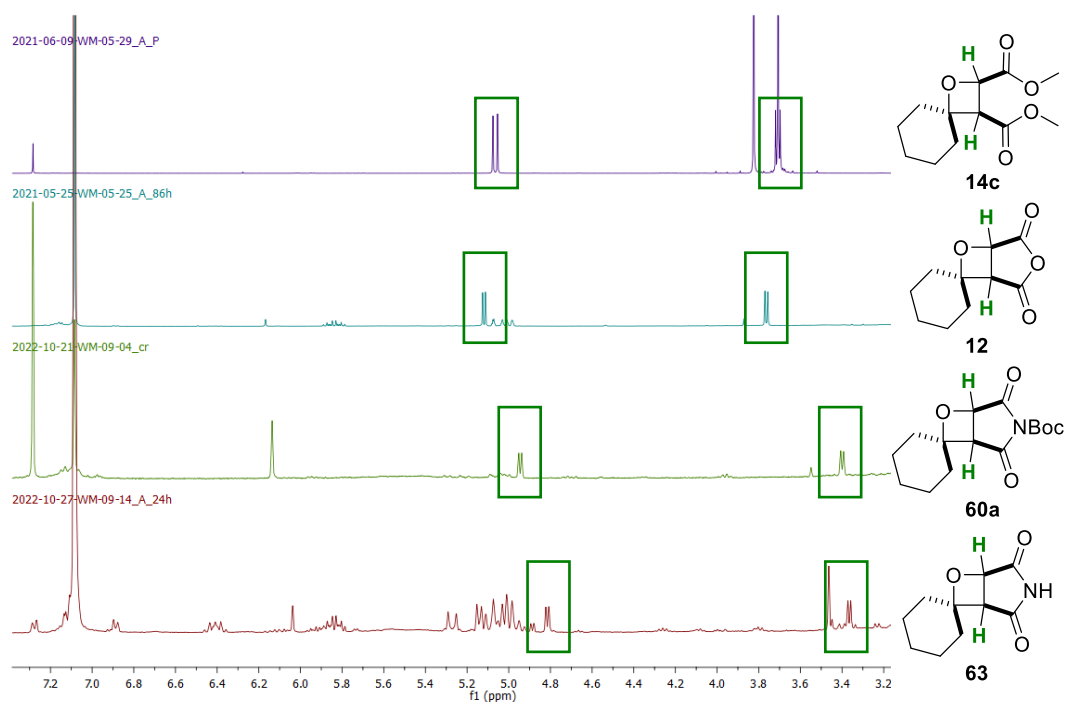
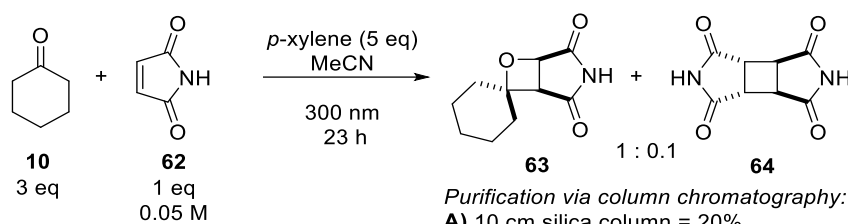


Figure 5-3 Comparison of the  $^1\text{H}$  NMR spectra of different oxetanes.

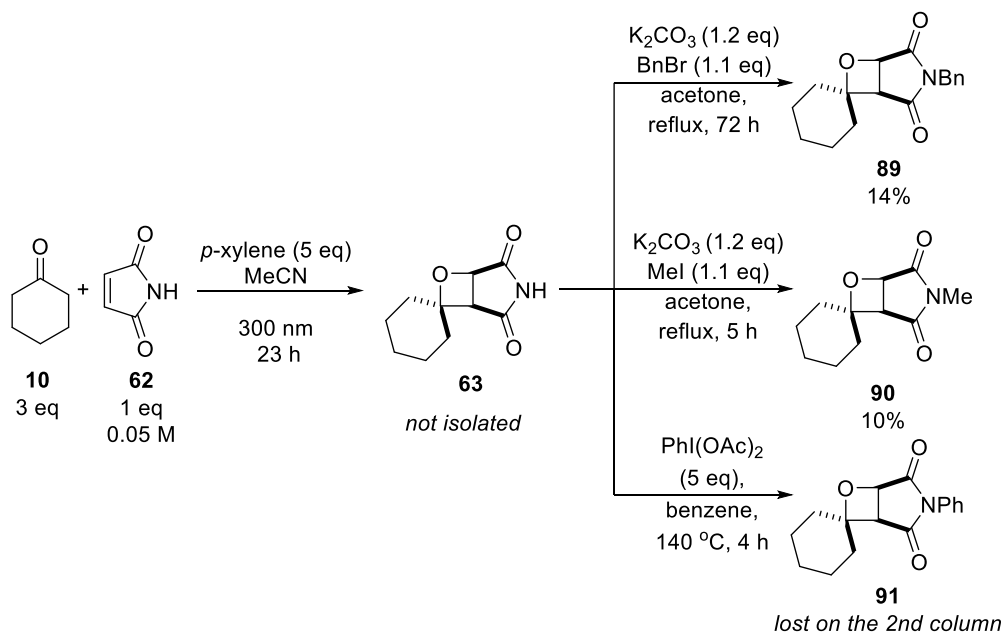
*N*-H-maleimide underwent a series of reactions and several purification attempts were made of the formed oxetanes. These reactions took place before realizing that the precipitate formed during the irradiation of the reaction was the dimer, therefore the ratio of the dimer and oxetane is likely not accurate. Purification of the formed oxetane proved less successful than expected, yielding only 20-26% of the isolated oxetane **63**. A 26% isolated yield was obtained through purification with a shorter column length, and as expected the purification was not as good, showing a much higher percentage of impurities. Different purification conditions were tested with no major improvement in the isolated yield (Scheme 5-14). It was concluded that most likely the low yield of the reactions is due to the unprotected imide group and therefore a series of protecting groups were added to the formed oxetane **63** to improve the isolation of the final oxetane. These reactions were performed simultaneously with the investigation discussed in sections 4.2-4.3, which showed that  $^1\text{H}$  NMR assessments in  $d_6$ -DMSO are needed to truly assess the ratio of the formed oxetane **63** and dimer **64**. This implies that although the isolated yield is low, it might not be due to the difficulties during the purification step, but actually due to the consumption of the *N*-H-maleimide in the dimerization reaction.



Purification via column chromatography:  
**A)** 10 cm silica column = 20%  
**B)** 6 cm silica column = 26% (<80% purity)  
**C)** 10 cm florisil column = 22%

**Scheme 5-14** Paternò-Büchi reaction between NH-maleimide (**62**) and cyclohexanone (**10**) and tested purification methods.

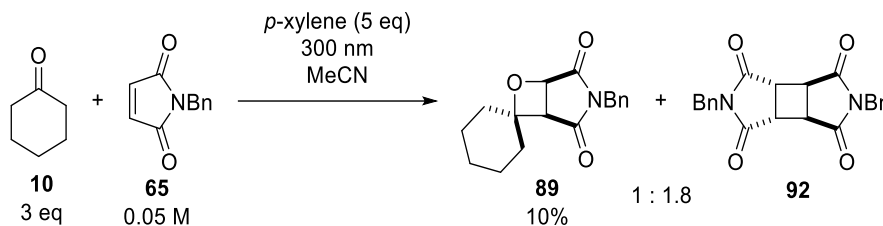
Nonetheless, the protecting groups were added in attempt to aid in the isolation of the formed oxetanes. Three reactions were performed on the crude oxetane **63**, benzyl and methyl group protections worked well, showing full conversion by TLC and  $^1\text{H}$  NMR spectroscopy, and yielding 14% and 10% respectively of the oxetane products, therefore showing a decrease in the isolated yield compared to **63** (Scheme 5-14). Phenyl group protection showed only ~36% conversion based on  $^1\text{H}$  NMR spectroscopy, and the final product was lost during purification. The aim of these reactions was to see if any of the protected imides is easier to isolate by column chromatography compared to NH, but frustratingly this was not the case.



**Scheme 5-15** The Paternò-Büchi reaction between cyclohexanone (**10**) and NH-maleimide (**62**) followed by different protecting groups reactions.

Next, the Paternò-Büchi reaction between cyclohexanone and *N*-Bn-maleimide was performed to directly yield oxetane **89**, but frustratingly the isolated percentage yield was even lower, with only 10% of the final oxetane isolated. This is most likely due to a very high amount of dimer **92** formed during the reaction, with the  $^1\text{H}$  NMR (solvent suppression, MeCN) ratio of oxetane **89** : dimer **92** equal to 1 : 1.8, meaning that over

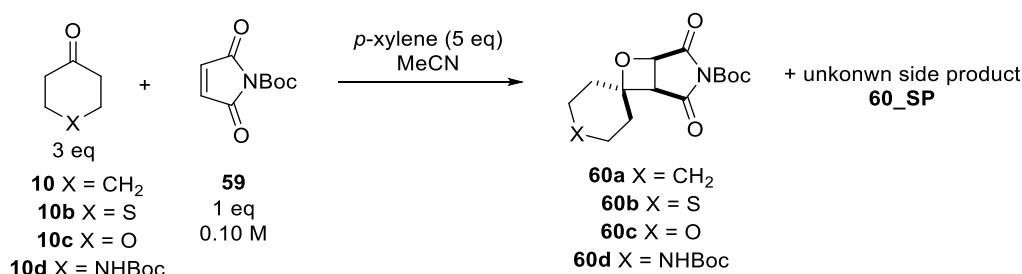
78% of the *N*-Bn-maleimide was used in the dimerization reaction instead of the desired Paternò-Büchi reaction.



**Scheme 5-16** Paternò-Büchi reaction between cyclohexanone (**10**) and *N*-Bn-maleimide (**65**). Ratio based on  $^1\text{H}$  NMR spectroscopy (solvent suppression, MeCN, 400 MHz).

Based on Figure 5-3, the crude mixture of the Paternò-Büchi reaction forming the *N*-Boc-oxetane **60** looks relatively clean, showing a minimal amount of the dimer formation. Therefore, it was hoped it could be a good starting point of creating a new library of oxetanes synthesised from cyclic ketones and *N*-Boc-maleimide (**59**). Only one other product was observed while tracking the reaction, which had a singlet at ~6.8 ppm visible by  $^1\text{H}$  NMR spectroscopy (MeCN, solvent suppression). Previously, a singlet in this region was due to the ring opening of the maleic anhydride before it had a chance to react in the Paternò-Büchi reaction, however a ring opening of the *N*-Boc-maleimide would not yield a symmetrical product and therefore the singlet signal was unusual.

As discussed before, the oxetanes formed in the Paternò-Büchi reaction between cyclohexanone and maleic anhydride required a series of transformations as the anhydride ring is often unstable under purification conditions. It was speculated that when maleimides were used in the reaction, the purification can take place without further functionalization. *N*-Boc-maleimide underwent Paternò-Büchi reaction with a series of different cyclic ketones with the aim of gaining rapid access to oxetane-containing spirocycles **60a-d** (Scheme 5-17).



**Scheme 5-17** The Paternò-Büchi reactions between *N*-Boc-maleimide and different cyclic ketones.

As shown by the spectra in Figure 5-4, the oxetanes **60a-d** were formed, additionally a side product **60\_SP** was formed with a singlet at ~6.8 ppm in the  $^1\text{H}$  NMR spectrum (solvent suppression). Attempts to purify oxetane **60b-d** did not work well, and in general only traces of oxetanes were isolated from the column chromatography. These reactions were tracked by  $^1\text{H}$  NMR spectroscopy and took a long time, therefore it is possible that

water and air entered the reaction mixture, causing unpredictable side reactions, and a long reaction time could lead to unexpected transformations/ leading to the **60\_SP**.

**60\_SP** was not identified, however it was isolated in small amounts and a full NMR analysis was run. Based on the series of NMR spectra, there is clear evidence that the **60\_SP** is likely derived from *N*-Boc-maleimide, as it has a Boc group, an alkene and two carbonyl groups present by NMR spectroscopy.

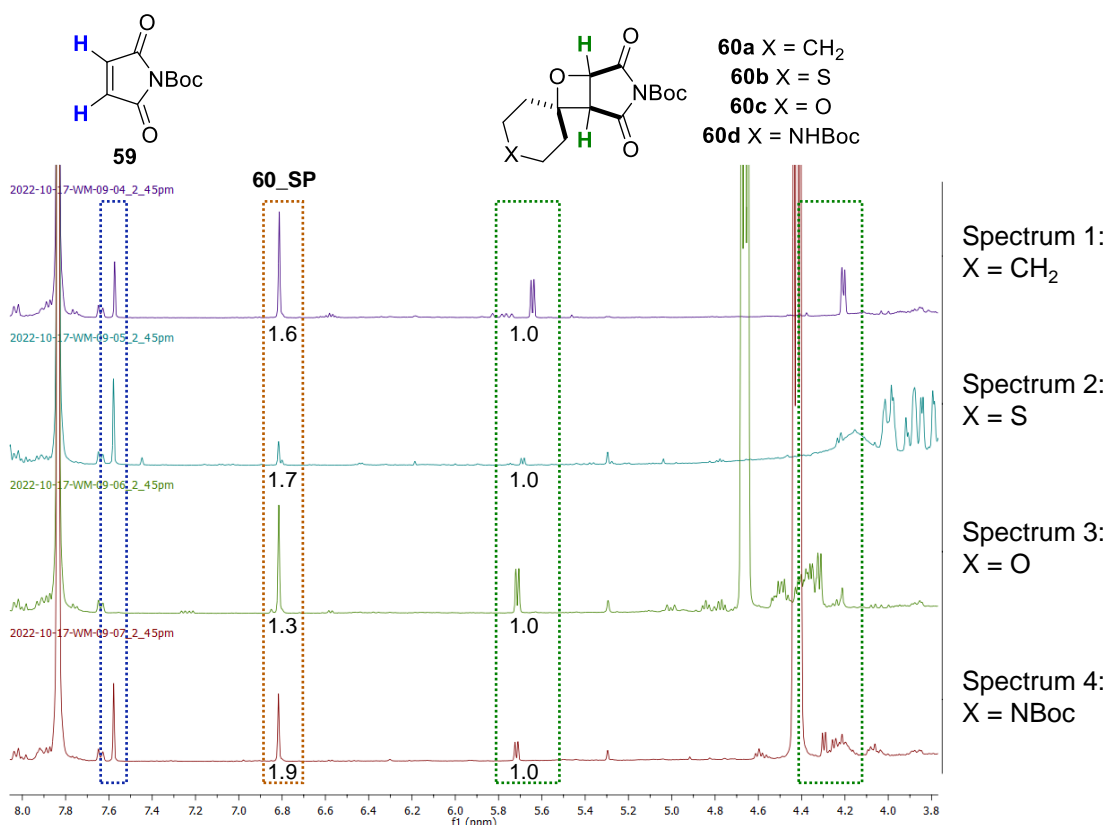
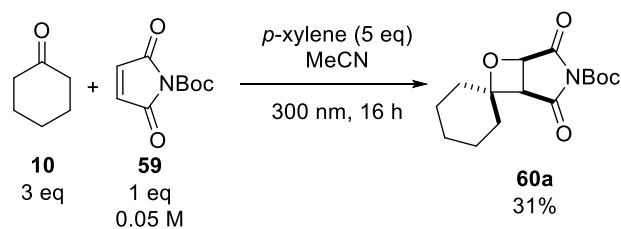


Figure 5-4 <sup>1</sup>H NMR spectra of the Paternò-Büchi reactions between *N*-Boc-maleimide and different cyclic ketones.

Upon repeating the reaction at a lower concentration (0.05 M) and using new lamps (which led to shorter reaction time), >95% conversion of *N*-Boc-maleimide was observed in 16 h, and there was a much smaller amount of the **60\_SP**, with the integration ratio of oxetane to **60\_SP** 1 : 0.3. Due to the now only minor presence of the side product, the focus was on the isolation of the formed oxetane **60a**, which was isolated in 31% yield, by changing the eluent to acetone in heptane. Due to time constraints the additional ketones were not tested again in the reaction.

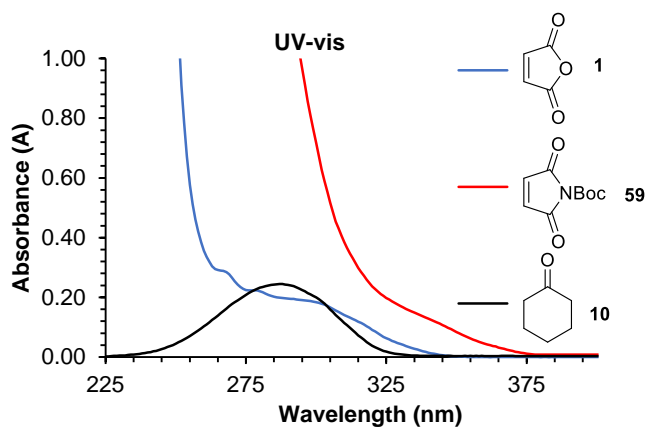


**Scheme 5-18 Paternò-Büchi reaction between the cyclohexanone (10) and *N*-Boc-maleimide (59).**

To summarize, in practice use of maleimides in the Paternò-Büchi reaction with cyclohexanone works well, however it could be more optimized but due to time constraints only initial tests were performed. All of the tested examples of maleimides showed the formation of the oxetanes, however isolation of the formed products proved difficult, a detailed purification optimization is needed. Compared to maleic anhydride, additional *p*-xylene is needed to suppress the dimerization reaction showing that the initial method of suppression of the side reaction works well with other substrates. Only four oxetanes were fully isolated and purified using this method (**60a**, **63**, **89** and **90**) direct from the Paternò-Büchi reaction between maleimide and cyclohexanone, although reactions of maleimides with different cyclic ketones worked based on the crude products, pure oxetane containing spirocycles were not isolated. Overall, the scope of the reaction was further expanded and the maleimides show potential as a very good Paternò-Büchi partner to cyclohexanone, but further studies are necessary.

## 5.4 Conclusions

This chapter showed a small expansion of the scope by using a variety of different electron-poor alkenes in the reaction (Figure 5-5). A series of different electron-poor alkenes were tested in the reaction, the majority of which did not yield the desired oxetane. Maleimides were involved in mechanistic studies as well as expanding the scope of the reaction. Overall, the desired oxetanes were formed however the reaction would benefit from an optimization of the purification steps as column chromatography of these products proved challenging. In total, seven oxetanes were isolated further expanding the scope of the reaction.

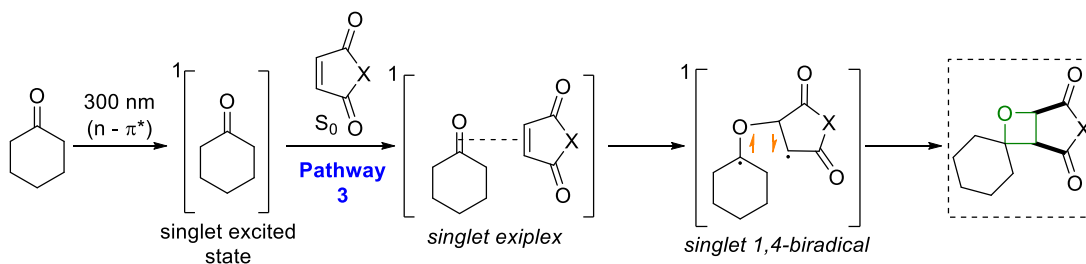


**1. Determining the mechanism of the Paterno-Buchi reaction:**

- A)** O<sub>2</sub> reaction showed no effect on the reaction rates  
→ triplet states not used in the reaction  
**B)** *N*-Boc-maleimide (**59**) reactions at 300 nm vs 350 nm → showed cyclohexanone (**10**) excited state is needed for the reaction

**2. Using UV-vis spectra** to confirm an interaction between maleic anhydride and *p*-xylene which suppressed the dimerization reaction.

Proposed mechanism for the Paterno-Buchi reaction under direct irradiation:



Examples of novel isolated oxetanes

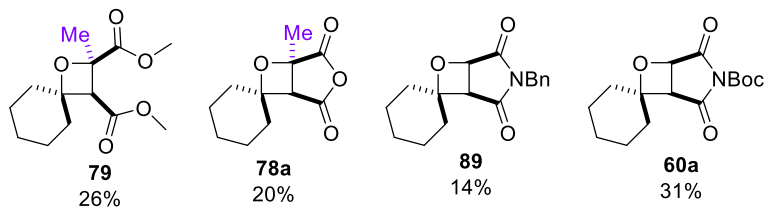
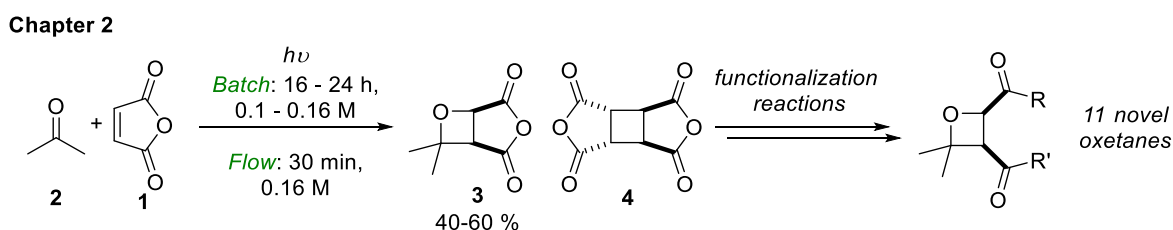


Figure 5-5 Summary of the results from Chapter 5.

## Chapter 6 Conclusions and further work

The Paternò-Büchi reaction between aliphatic ketones and electron-poor alkenes was investigated to expand the scope of the reaction, based on Turro's reaction between maleic anhydride and acetone, originally reported in 1967 Chapter 2 focused on optimization of that reaction, followed by a series of transformations in order to purify a library of oxetanes (Scheme 6-1). The Paternò-Büchi reaction between maleic anhydride and acetone was optimized under both batch and flow reaction conditions, allowing for quick formation of the desired oxetane **3**. Regioselective ring opening of oxetane **3** allowed for isolation of 11 novel oxetanes. Dimer **4** formed from maleic anhydride was removed via a recrystallization method. Overall, the results gathered and reported in Chapter 2 gave the basis for Chapter 3, allowing for expanding of the Paternò-Büchi reaction into cyclic ketones.



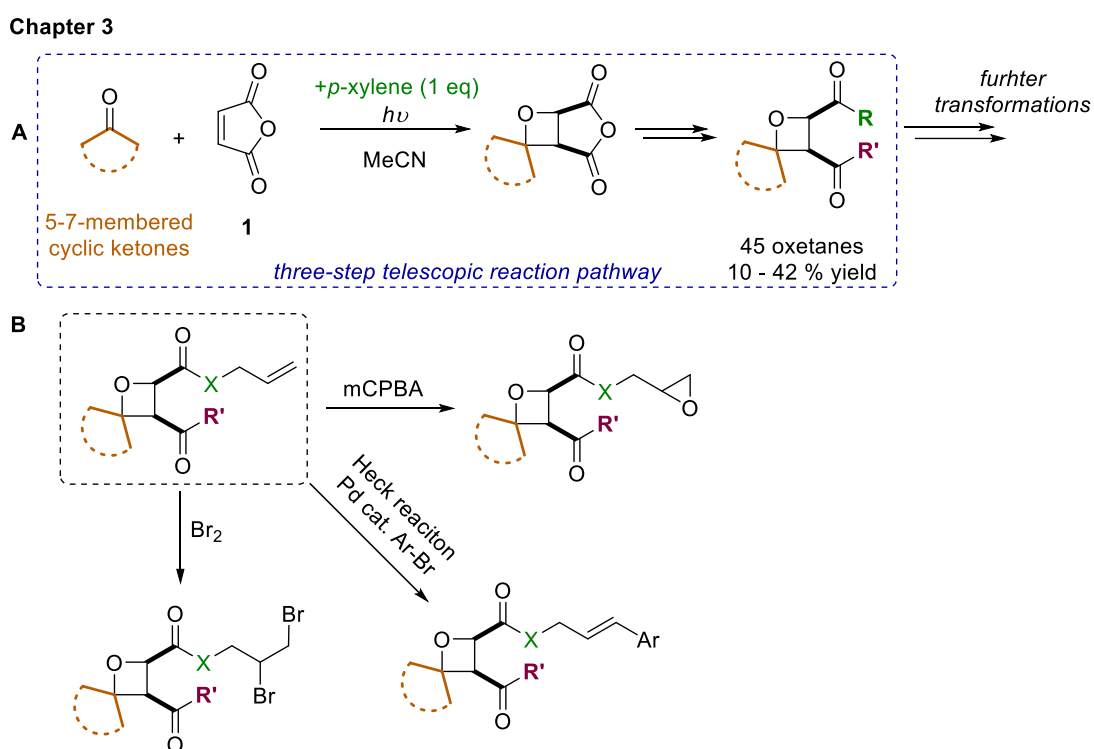
**Scheme 6-1 Summary of results from Chapter 2.**

Chapter 3 focused on a practical approach for the Paternò-Büchi reaction between cyclic ketones and maleic anhydride, starting with initial optimization of the reaction yield (which was increased from 5 to 20%). The competing dimerization reaction proved to be the biggest downside of the system as it consumed ~50% of the starting maleic anhydride. Therefore, a series of additives was tested in order to suppress the dimerization reaction; one of the successful additives was *p*-xylene, which allowed for 95% of maleic anhydride to be used in the Paternò-Büchi reaction, further increasing the isolated yield of the oxetane product (~40%). Disappointingly, the Paternò-Büchi reaction between cyclohexanone and maleic anhydride could not be translated into flow using the flow system available. However, using a different flow system the reaction would likely be successful. Large-scale batch reactions gave satisfactory results on gram scale, additionally the available batch photoreactor allowed for parallel reaction to take place allowing for a quick and efficient formation of oxetanes. Next, Chapter 3 showed the advantage of the three-step telescoped reaction pathway, which was designed in order to efficiently make and functionalize oxetanes **12** (Scheme 6-2, A). Simple changes to the reagents used in each step gave rise to a variety of different products:



- 1) Paternò-Büchi reaction between cyclic ketone and maleic anhydride – use of different cyclic ketones gave rise to a series of different oxetane-containing spirocycles.
- 2) Regioselective ring opening of anhydride – allowed formation of different amide or ester functional groups.
- 3) Carboxylic acid coupling – formation of various of ester groups.

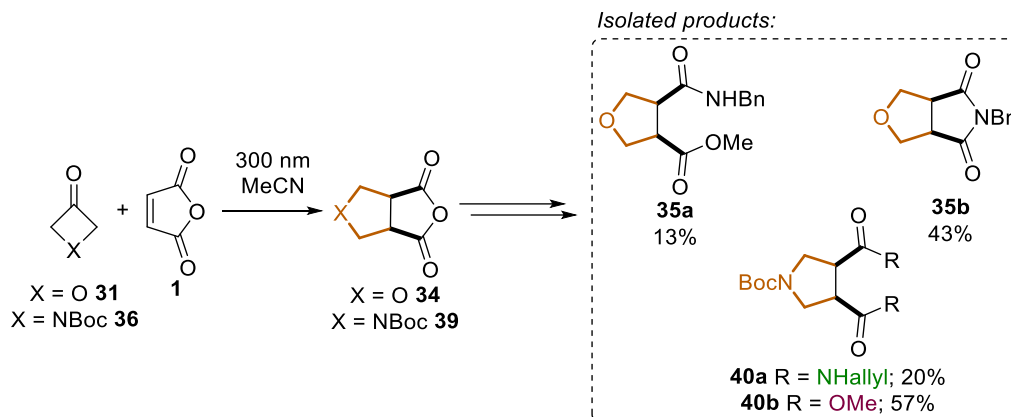
Some of oxetanes formed in the three-step telescoped pathway underwent further transformations on one of the functional handles; with successful reactions including: benzyl ester removal, acetal removal, oxidation of sulfane, Boc group removal. Section 3.3.3 summarized the tested transformations, potential further work could include finding better/correct conditions of the failed reactions such as the reduction of the ester or carboxylic acid group. Additionally, due to the vast variety of functional handles that were added, there are many more different transformations that could take place, and possible transformations arising from one of the oxetane functional handles are summarized in Scheme 6-2, B. Finally, asymmetric ketones could be further explored in the reaction, however, selectivity would likely be an issue, addition of bulky group onto the ketone could potentially improve the selectivity but these ketones would have to be synthesised.



Scheme 6-2 Summary of results from chapter 3 and further work.

Importantly, 4-membered cyclic ketones did not yield the desired oxetane products, instead a 5-membered ring was formed, the structure of the product was confirmed by crystal structures of **35b** and **40a**. The mechanism for the reaction was proposed based

on reported literature, however the reaction requires further investigation and optimization to fully understand and unlock its potential Scheme 6-3. It is important to note that the isolated yields of these products were higher compared to isolated yields of the oxetanes, implying that the oxetane ring lacks stability upon purification on silica.

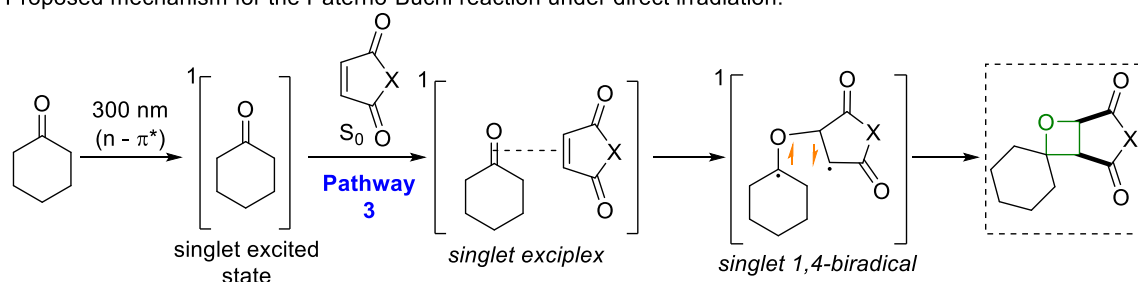


Scheme 6-3 Summary of results from chapter 3.

Chapter 4 showed the investigation into the mechanism of the Paternò-Büchi and dimerization reactions. A series of different experiments were performed including the use of molecular oxygen in order to determine singlet vs triplet excited state reaction pathway, indicating that the Paternò-Büchi reaction between cyclohexanone and maleic anhydride most likely takes place via a singlet excited state. Next, the excited state partner was determined by the use of maleimides in the reaction instead of maleic anhydride. Based on UV-vis measurements, the maleimides can absorb energy at 350 nm, while cyclohexanone and maleic anhydride do not. A series of reactions at 300 and 350 nm took place between *N*-Boc-maleimide and cyclohexanone, showing dimerization reaction taking place at 300 and 350 nm, while Paternò-Büchi reaction took place only at 300 nm, suggesting that the Paternò-Büchi reaction takes place between the excited state of cyclohexanone and ground state *N*-Boc-maleimide. Based on all of the experimental results the mechanism for the Paternò-Büchi reaction between cyclohexanone and electron poor alkene was proposed (Scheme 6-4). Additional analytical methods could be used to finish the mechanistic studies; as discussed in literature review (Chapter 1) triplet lifetimes and triplet energies can be very useful in determining mechanisms of photochemical reactions. Also, computational studies could be performed into the reaction.

#### Chapter 4

Proposed mechanism for the Paternò-Büchi reaction under direct irradiation:



Scheme 6-4 Summary of results from chapter 4.

Using different electron-poor alkenes in Chapter 5 allowed for formation of novel oxetanes. Most of the new alkenes tested in the reaction did not give a desired product, however, a handful did form the desired oxetane ring, giving seven new oxetanes. In the case of maleimides, the reaction worked well, and the dimerization reaction was suppressed with *p*-xylene; additional optimizations are needed in order to maximise the amount of oxetane isolated, however the initial reactions showed promising results.

Overall, a large library of oxetanes have been created using cheap, readily available starting materials. The majority of the isolated oxetanes were spirocycles, adding to the complexity of the products. Crystal structures of the formed oxetane **7b**, **16a** and **21** were reported, confirming the *cis* relationship between the two groups in the C(2) and C(3) positions on the oxetanes, as well as the regioselective ring opening of the anhydride ring. The scope of the Paternò-Büchi reaction was expanded by using aliphatic ketones with electron-poor alkenes; one of the biggest downsides to the reaction was the dimerization of the maleic anhydride (and other alkenes) which was successfully suppressed by addition of *p*-xylene into reaction mixture. Investigations into the mechanism of the reaction showed that the reaction pathway most likely takes place via the singlet excited state of the ketone, meaning direct irradiation is likely necessary as the triplet energy of aliphatic ketones is high and will be difficult to reach with a triplet sensitizer.

## Chapter 7 Experimental

### 7.1 General information

Reagents were purchased in the highest purity available from Acros Organics, Alfa Aesar or Sigma Aldrich. Anhydrous solvents used in reactions were purchased from Acros Organics equipped with AcroSeal™ and all other solvents used were of reagent grade. Reaction vessels were oven dried and cooled under an argon atmosphere prior to use and experiments were performed under argon gas. Reactions were monitored by thin-layer chromatography (TLC) and/or <sup>1</sup>H NMR spectroscopic analysis.

Photochemical reactions were performed in Duran phototubes (20-mL or 50-mL volume) using a Rayonet RPR-100 photochemical batch reactor equipped with 16 lamps (300 nm). When operating, the approximate temperature inside the reactor chamber is 40 °C. Flow reactions were performed using Vapourtec UV-150 photochemical reactor. Steady state emission and excitation spectra were recorded on an Agilent Technologies Cary Eclipse spectrophotometer.

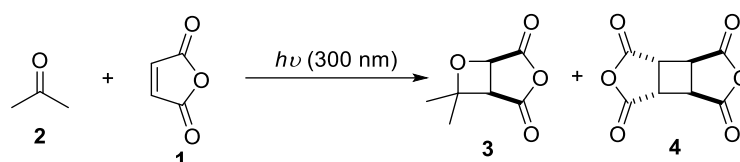
Analytical TLC was carried out using Merck pre-coated aluminium-backed TLC silica gel plates (silica gel 60 F<sub>254</sub>) and the plates were visualised by UV light (254 nm) and by staining with either potassium permanganate or *p*-anisaldehyde stain (a solution of concentrated H<sub>2</sub>SO<sub>4</sub> (5 mL), glacial acetic acid (1.5 mL) and *p*-anisaldehyde (3.7 mL) in absolute ethanol (135 mL); prepared with vigorous stirring). Most oxetanes were visualized using the *p*-anisaldehyde stain, showing as a dark blue spot. Normal phase flash column chromatography on silica gel was carried out using silica gel from VWR (40-63 microns).

<sup>1</sup>H NMR spectroscopic data were obtained on either 300 or 400 MHz instruments and <sup>13</sup>C{<sup>1</sup>H} NMR data were obtained at 101 MHz (Bruker Ultrashield 400 Plus) at 298 K unless otherwise specified. The chemical shifts are reported in parts per million (δ) relative to residual CHCl<sub>3</sub> (δ<sub>H</sub> = 7.26 ppm) and CDCl<sub>3</sub> (δ<sub>C</sub> = 77.2 ppm, central line), residual d<sub>5</sub>-DMSO (δ<sub>H</sub> = 2.50 ppm) and d<sub>6</sub>-DMSO (δ<sub>C</sub> = 39.5 ppm, central line), residual C<sub>6</sub>HD<sub>5</sub> (δ<sub>H</sub> = 7.16 ppm) and C<sub>6</sub>D<sub>6</sub> (δ<sub>C</sub> = 128.1 ppm), residual CHD<sub>2</sub>CN (δ<sub>H</sub> = 1.93 ppm) and CD<sub>3</sub>CN (δ<sub>C</sub> = 1.3 ppm). The assignment of the signals in the <sup>1</sup>H and <sup>13</sup>C NMR spectra was achieved through 2D-NMR techniques: COSY, HSQC and HMBC. Coupling constants (*J*) are quoted in Hertz. Infrared spectra were recorded on an Agilent Technologies Cary 630 FTIR spectrometer. Melting points were performed on a Sanyo Gallenkamp capillary melting point apparatus and are uncorrected. High resolution mass spectrometry data were recorded using electron spray ionization (ESI) or atmospheric

pressure chemical ionization (APCI) on a Shimadzu LCMS-IT-TOF mass spectrometer. UV/Vis spectra were recorded using an Agilent Cary 60 UV-Vis spec spectrophotometer. For X-ray crystallography, a suitable crystal was selected and mounted on a Mitegen loop using Paratone-N oil on a SuperNova, Dual, Cu at zero, AtlasS2 diffractometer. The crystal was kept at 100.2(5) K during data collection. Using Olex2,<sup>103</sup> the structure was solved with the ShelXT<sup>104</sup> structure solution program using direct methods and refined with the ShelXL refinement package using least squares minimisation. Figures and tables were prepared using Olex2 software.

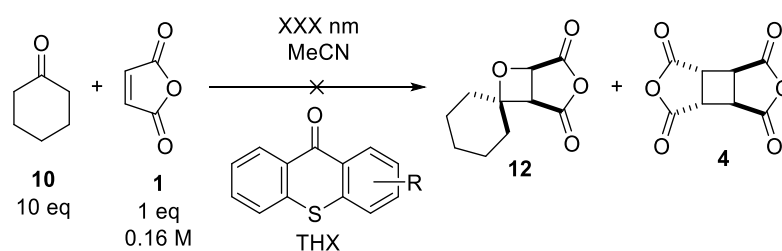
## 7.2 Optimization procedure and reactions tracking tables

### Optimization of concentration of the maleic anhydride in acetone (Chapter 2)



A solution of maleic anhydride (1 eq) in acetone (10mL, anhydrous, 0.04 - 1 M) was prepared in a Duran phototube and the reaction mixture was purged with argon for 15 minutes, then irradiated at approximately 40 °C ( $\lambda = 300$  nm) the reaction was tracked by <sup>1</sup>H NMR spectroscopy (acetone, solvent suppression).

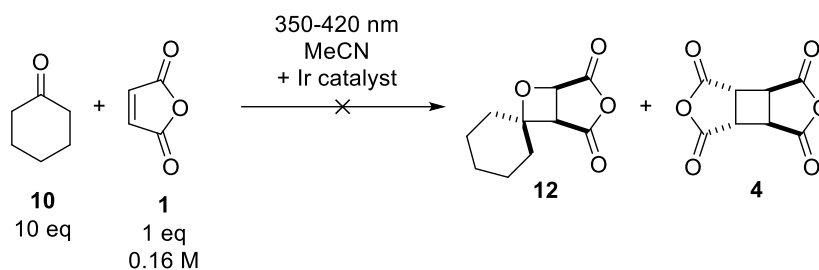
### Results of the Paternò-Büchi reaction in the presence of triplet sensitizers (Chapter 3)



Entry	Compound	Wavelength (nm) (reaction time)	Formation of 12 or 4 (%)	$E_T$ (kcal mol <sup>-1</sup> )
1		385 (24 h) / 350 (3 h)	0	66.2308
2		385 (24 h) / 350 (3 h)	0	65.0693

3		385 (24 h) / 350 (3 h)	0	71.5898
4		365 (24 h)/ 350 (3 h)	0	70.6606
5		385 (24 h) / 350 (3 h)	0	68.8367
6		365 (24 h)/ 350 (3 h)	0	64.2873
7		385 (24 h) / 350 (3 h)	0	67.8454
8		385 (24 h) / 350 (3 h)	0	58.0106

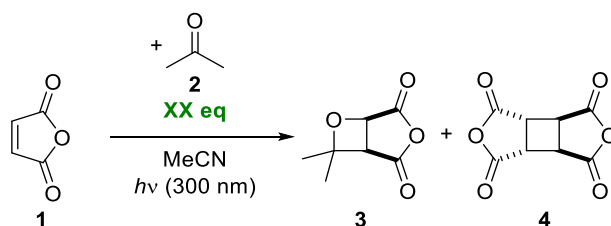
Table 7-1



Entry	Compound	Formation of oxetane 12 or dimer 4 (%)	E <sub>T</sub> (kcalmol <sup>-1</sup> )
1	[Ir{dFCF <sub>3</sub> ppy} <sub>2</sub> (bpy)]PF <sub>6</sub>	0	60.4
2	[Ir(dF(Me)ppy) <sub>2</sub> (dtbbpy)]PF <sub>6</sub>	0	60.2
3	Ir[(dF(CF <sub>3</sub> )ppy) <sub>2</sub> (dtbbpy)]PF <sub>6</sub>	0	60.1
4	Ir(dFppy) <sub>3</sub>	0	60.1
5	Ir(p-F-ppy) <sub>3</sub>	0	58.6
6	Ir(p-CF <sub>3</sub> -ppy) <sub>3</sub>	0	56.4
7	[Ir(dFppy) <sub>2</sub> (dtbbpy)]PF <sub>6</sub>	0	55.4
8	Ir[(dF(CF <sub>3</sub> )ppy) <sub>2</sub> (d(CF <sub>3</sub> )bpy)]PF <sub>6</sub>	0	48.8
9	[Ir(dF(CF <sub>3</sub> )ppy) <sub>2</sub> (5,5'-dCF <sub>3</sub> bpy)]PF <sub>6</sub>	0	47.2

Table 7-2

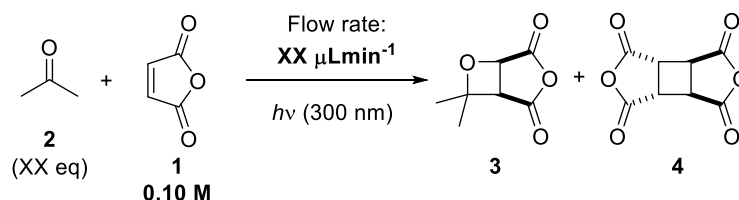
### 7.3 Flow reactions



A solution of maleic anhydride (1.0 eq) and acetone (number of equivalents specified in table) in acetonitrile (0.10 M) was prepared in a Duran phototube and purged with argon for 15 minutes, then irradiated at approximately 40 °C ( $\lambda = 300$  nm). The consumption of the maleic anhydride was judged by  $^1\text{H}$  NMR spectroscopy (with solvent suppression).

Eq. of acetone	2 h			4 h			6 h			24 h		
	3	4	1	3	4	1	3	4	1	3	4	1
1	0	0.25	2.31	0	0.25	1.42	0	0.25	0.30	0	0.25	0.30
5	1	1.13	9.67	1	1.15	5.71	1	1.39	0.33	1	1.31	0.17
10	1	0.93	6.04	1	0.93	3.37	1	0.96	0.01	1	0.95	0
15	1	0.79	5.78	1	0.79	2.83	1	0.80	0.01	1	0.78	0
20	1	0.73	3.58	1	0.79	1.71	1	0.82	0	1	0.76	0

Table 7-3 Ratio of 3 : 4 : 1 during reaction between maleic anhydride (1 eq) and acetone (1, 5, 10, 15 and 20 eq) in acetonitrile at 2, 4, 6 and 24 h (batch reaction).



A solution of maleic anhydride (1.0 eq) and acetone (number of equivalents specified in table) in acetonitrile (10 mL 0.10 M) was prepared and purged with argon for 15 minutes, then irradiated in a flow photoreactor (flow rate and concentration details in table) at approximately 20 - 40 °C ( $\lambda = 300$  nm). The consumption of the maleic anhydride was judged by  $^1\text{H}$  NMR spectroscopy (solvent suppression).

Eq. of acetone	Flow rate ( $\mu\text{m}/\text{min}$ )	Exposure time (min)	3 (%)	4 (%)
1	333	30	12	20
	479	20	12	19
5	625	16	21	15
	479	20	32	26
	333	30	37	32
	250	40	48	52
	225	45	46	54
10	1000	10	20	14
	813	12	23	16
	625	16	30	24
	333	30	51	49
20	333	30	57	43
	479	20	48	41
	625	16	36	25

Table 7-4 % of **3** : **4** during reaction between maleic anhydride (1 eq) and acetone (1, 5, 10, 15 and 20 eq) in acetonitrile at different flow rates (flow reaction).

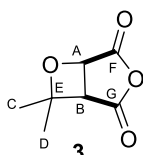
## 7.4 Characterization data of novel compounds

### 7.4.1 Chapter 2: Reactions of maleic anhydride (**1**) and acetone (**2**)

#### *rac*-(1*R*,5*R*)-7,7-Dimethyl-3,6-dioxabicyclo[3.2.0]heptane-2,4-dione (**3**) and (3*aR*,3*bR*,6*aS*,6*bS*)-tetrahydrocyclobuta[1,2-*c*:3,4-*c'*]difuran-1,3,4,6-tetraone (**4a**)

A solution of maleic anhydride (1.0 eq) in acetone (anhydrous, 0.10 M) was prepared in a Duran phototube and the reaction mixture was purged with argon for 15 minutes, then irradiated at approximately 40 °C ( $\lambda = 300 \text{ nm}$ ) until complete consumption of the maleic anhydride, as judged by  $^1\text{H}$  NMR spectroscopy (acetone, solvent suppression). The solvent was partially removed and once the crystals of dimer **4a** formed, the evaporation was stopped and the crystals were filtered off. The filtrate of **3** was reacted further in ring-opening reactions.

#### *rac*-(1*R*,5*R*)-7,7-Dimethyl-3,6-dioxabicyclo[3.2.0]heptane-2,4-dione (**3**)



Chemical Formula:  $\text{C}_7\text{H}_8\text{O}_4$   
Molecular Weight: 156.13

$^1\text{H}$  NMR (400 MHz, Acetone- $\text{H}_6$ , solvent suppression)  $\delta$  5.35 (d,  $J = 5.3 \text{ Hz}$ , 1H,  $\text{H}^{\text{A}}$ ), 4.03 (d,  $J = 5.3 \text{ Hz}$ , 1H,  $\text{H}^{\text{B}}$ ), 1.79 (s, 3H,  $\text{H}^{\text{C/D}}$ ), 1.53 (s, 3H,  $\text{H}^{\text{C/D}}$ ).



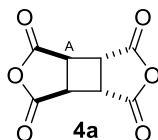
**<sup>1</sup>H NMR** (300 MHz, Acetone-D<sub>6</sub>) δ 5.25 (d, *J* = 5.3 Hz, 1H, H<sup>A</sup>), 3.92 (d, *J* = 5.3 Hz, 1H, H<sup>B</sup>), 1.67 (s, 3H, H<sup>C/D</sup>), 1.41 (s, 3H, H<sup>C/D</sup>).

**<sup>13</sup>C NMR** (75 MHz, Acetone-D<sub>6</sub>) δ 169.4 (C<sup>F</sup>), 169.4 (C<sup>G</sup>), 85.2 (C<sup>E</sup>), 73.1 (C<sup>A</sup>), 50.1 (C<sup>B</sup>), 28.8 (C<sup>C/D</sup>), 25.4 (C<sup>C/D</sup>).

**FTIR** (ATR) ν (cm<sup>-1</sup>): 2980 (C-H), 1869 (C=O), 1781 (C=O).

**Lab-book reference:** WM-03-01\_E\_24h, WM-03-83.

**(3a*R*,3b*R*,6a*S*,6b*S*)-Tetrahydrocyclobuta[1,2-*c*:3,4-*c'*]difuran-1,3,4,6-tetraone (4a)**



Chemical Formula: C<sub>8</sub>H<sub>4</sub>O<sub>6</sub>

Molecular Weight: 196.11

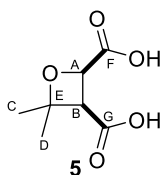
**<sup>1</sup>H NMR** (400 MHz, Acetone-H<sub>6</sub>, solvent suppression) δ 4.23 (s, 4H, H<sup>A</sup>)

**FTIR** (ATR) ν (cm<sup>-1</sup>): 3011, 1846 (C=O), 1774 (C=O).

**Lab-book reference:** WM-03-01\_E\_24h and WM-03-83.

**Characterization matches Ref.** <sup>105</sup>

***rac*-(2*R*,3*R*)-4,4-Dimethyloxetane-2,3-dicarboxylic acid (5)**



Chemical Formula: C<sub>7</sub>H<sub>10</sub>O<sub>5</sub>

Molecular Weight: 174.15

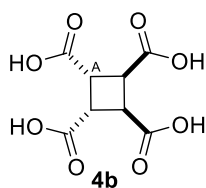
A solution of maleic anhydride (235 mg, 2.40 mmol) in anhydrous acetone (15 mL, 0.16 M) was prepared in a Duran phototube and purged with argon for 15 minutes, then irradiated at approximately 40 °C (λ = 300 nm) until complete consumption of the maleic anhydride, as judged by <sup>1</sup>H NMR spectroscopy (solvent suppression). The reaction mixture was transferred into a round bottom flask and water was added (0.5 mL). The reaction was stirred at 40 °C until completion of the ring opening of the anhydride (24 h), then evaporated under reduced pressure. The crude mixture was dissolved in a minimal amount of solvent (acetone), and placed in the fridge overnight. Crystals of **4b** formed overnight and were removed via filtration giving the crude oxetane **5** (211 mg, 1.21 mmol, 50%, 87% purity with respect to dimer **4a**) was used directly in further reactions.

**<sup>1</sup>H NMR** (300 MHz, acetone-d<sub>6</sub>) δ 5.04 (d, *J* = 8.8 Hz, 1H, H<sup>A</sup>), 3.90 (d, *J* = 8.8 Hz, 1H, H<sup>B</sup>), 3.72 (s, 2H, O-H), 1.57 (s, 3H, H<sup>C/D</sup>), 1.42 (s, 3H, H<sup>C/D</sup>).

**FTIR** (ATR) ν (cm<sup>-1</sup>): 2976 (very broad, O-H), 1705 (C=O).

**Lab-book reference:** WM-03-40\_cr or 96 75\_h2o\_dry.

***rac*-(1*R*,2*R*,3*S*,4*S*)-Cyclobutane-1,2,3,4-tetracarboxylic acid (**4b**)**



Chemical Formula: C<sub>8</sub>H<sub>8</sub>O<sub>8</sub>  
Molecular Weight: 232.14

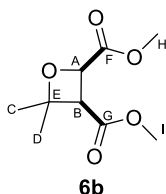
**<sup>1</sup>H NMR** (300 MHz, acetone-d<sub>6</sub>) δ 3.72 (s, 4H, H<sup>A</sup>).

**FTIR** (ATR) ν (cm<sup>-1</sup>): 3442 (broad, O-H), 2963 (C-H), 1733 (C=O), 1712 (C=O).

**Lab-book reference:** WM-03-40

**Characterization matches Ref.** <sup>105</sup>

**Dimethyl *rac*-(2*R*,3*R*)-4,4-dimethyloxetane-2,3-dicarboxylate (**6b**)**



Chemical Formula: C<sub>9</sub>H<sub>14</sub>O<sub>5</sub>  
Molecular Weight: 202.21

The crude oxetane **5** (278 mg, 1.60 mmol, 90% purity with respect to dimer **4**) was added to a suspension of Me<sub>3</sub>O<sup>+</sup>BF<sub>4</sub><sup>-</sup> (353 mg, 2.40 mmol) in dichloromethane (10 mL) under nitrogen. *N,N*-diisopropylethylamine (0.42 mL, 2.40 mmol) was added, and the reaction was stirred at room temperature for 20 h. The reaction mixture was washed with 1 M aqueous HCl (7 mL) and 1 M aqueous potassium bicarbonate (7 mL). Both aqueous phases were extracted with dichloromethane (2 x 10 mL), the combined organic phases were washed with brine (10 mL), dried (MgSO<sub>4</sub>) and evaporated under reduced pressure. Purification by flash chromatography (eluent: 19 : 1 hexane–EtOAc) gave oxetane **6b** (52 mg, 0.26 mmol, 16%) as a colourless oil.

**<sup>1</sup>H NMR** (300 MHz, CDCl<sub>3</sub>) δ 5.06 (d, *J* = 8.9 Hz, 1H, H<sup>A</sup>), 3.82 (s, 3H, H<sup>H/I</sup>), 3.80 (d, *J* = 8.9 Hz, 1H, H<sup>B</sup>), 3.70 (s, 3H, H<sup>H/I</sup>), 1.61 (s, 3H, H<sup>C/D</sup>), 1.44 (s, 3H, H<sup>C/D</sup>).

**<sup>13</sup>C NMR** (101 MHz, CDCl<sub>3</sub>) δ 171.2 (C<sup>F</sup>), 168.8 (C<sup>G</sup>), 84.3 (C<sup>E</sup>), 71.2 (C<sup>A</sup>), 52.2 (C<sup>H/I</sup>), 52.0 (C<sup>H/I</sup>), 51.1 (C<sup>B</sup>), 30.3 (C<sup>C/D</sup>), 24.9 (C<sup>C/D</sup>).

**FTIR** (ATR) ν (cm<sup>-1</sup>): 2954, 1735 (C=O)

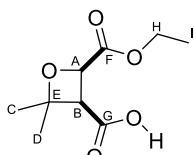
**HRMS (ESI):** *m/z* calculated for C<sub>9</sub>H<sub>14</sub>O<sub>5</sub>Na [M+Na<sup>+</sup>]: 225.0773, found 225.0723.

**R<sub>f</sub>:** 0.50 (1 : 1, hexane - EtOAc)

**Reference:** The Journal of Organic Chemistry **1979** 44 (7), 1149-1154

**Lab-book reference:** WM-03-86 → WM-03-87 → WM-03-88

***rac*-(3*R*,4*R*)-4-(Ethoxycarbonyl)-2,2-dimethyloxetane-3-carboxylic acid (7a)**



**7a**

Chemical Formula: C<sub>9</sub>H<sub>14</sub>O<sub>5</sub>

Molecular Weight: 202.21

A solution of **3** (156 mg, 1.00 mmol, 93% purity with respect to dimer **4**) in ethanol (10 mL) was stirred at room temperature until complete consumption of the starting material (24 h). The solvent was evaporated under reduced pressure to give the crude product. Purification by flash column chromatography on silica gel (eluent: 1 : 1, hexane - EtOAc + 10 % MeOH) gave **7a** (91 mg, 0.55 mmol, 45%) as a colourless oil.

**<sup>1</sup>H NMR** (400 MHz, CDCl<sub>3</sub>) δ 5.05 (d, *J* = 8.8 Hz, 1H, H<sup>A</sup>), 4.32 – 4.20 (m, 2H, H<sup>H</sup>), 3.85 (d, *J* = 8.8 Hz, 1H, H<sup>B</sup>), 1.63 (s, 3H, H<sup>C/D</sup>), 1.52 (s, 3H, H<sup>C/D</sup>), 1.29 (t, *J* = 7.2 Hz, 3H, H<sup>I</sup>).

**<sup>13</sup>C NMR** (101 MHz, CDCl<sub>3</sub>) δ 171.7 (C<sup>F</sup>), 170.5 (C<sup>G</sup>), 84.2 (C<sup>E</sup>), 71.0 (C<sup>A</sup>), 61.3 (C<sup>H</sup>), 50.8 (C<sup>B</sup>), 30.3 (C<sup>C/D</sup>), 24.9 (C<sup>C/D</sup>), 14.1 (C<sup>I</sup>).

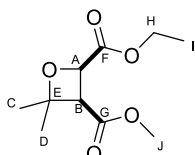
**FTIR** (ATR) ν (cm<sup>-1</sup>): 3455 (broad, O-H), 2924 (C-H), 1735 (C=O).

**HRMS (ESI)**: *m/z* calculated for C<sub>9</sub>H<sub>14</sub>O<sub>5</sub>Na [M<sup>+</sup>Na<sup>+</sup>]: 225.0773, found: 225.0737.

**R<sub>f</sub>**: 0.23 (1 : 4, hexane - EtOAc)

**Lab-book reference**: WM-03-51 → WM-03-52/3 (data under WM-03-50)

**2-Ethyl-3-methyl *rac*-(2*R*,3*R*)-4,4-dimethyloxetane-2,3-dicarboxylate (8a)**



**8a**

Chemical Formula: C<sub>10</sub>H<sub>16</sub>O<sub>5</sub>

Molecular Weight: 216.23

**Method A**: A solution of **3** (165 mg, 1.17 mmol, 93% purity with respect to dimer **4**) in ethanol (10 mL) was stirred at room temperature until complete consumption of the starting material (24 h). The solvent was evaporated under reduced pressure to give the crude product. The crude product was dissolved in methanol (5 mL), then TMSCHN<sub>2</sub> (1.0 mL of a 2 M solution in hexane, 2.00 mmol) was added dropwise at room temperature. The reaction was stirred at room temperature until complete consumption of the starting material (<10 min). The solvent was evaporated under reduced pressure to give the crude product. Purification by flash column chromatography on silica gel (eluent: 4 : 1 to 7 : 3, hexanes – EtOAc) gave **8a** (20 mg, 0.09 mmol, 8%) as a colourless oil.

**Method B:** **7a** (91 mg, 0.55 mmol) was dissolved in methanol (2.5 mL), then TMSCHN<sub>2</sub> (0.6 mL of a 2 M solution in hexane, 2.00 mmol) was added dropwise at room temperature. The reaction was stirred at room temperature until complete consumption of the starting material (<10 min). The solvent was evaporated under reduced pressure to give the crude product. Purification by flash column chromatography on silica gel (eluent: 4 : 1 to 7 : 3, hexanes – EtOAc) gave **8a** (35 mg, 0.16 mmol, 29%) as a colourless oil.

**<sup>1</sup>H NMR** (400 MHz, acetone-d<sub>6</sub>) δ 5.02 (d, *J* = 9.0 Hz, 1H, H<sup>A</sup>), 4.16 (q, *J* = 7.1 Hz, 2H, H<sup>H</sup>), 3.95 (d, *J* = 9.0 Hz, 1H, H<sup>B</sup>), 3.65 (s, 3H, H<sup>J</sup>), 1.55 – 1.52 (m, 3H, H<sup>C/D</sup>), 1.38 – 1.34 (m, 3H, H<sup>C/D</sup>), 1.24 (t, *J* = 7.1 Hz, 3H, H<sup>I</sup>)

**<sup>13</sup>C NMR** (101 MHz, acetone-d<sub>6</sub>) δ 170.2 (C<sup>F</sup>), 168.8 (C<sup>G</sup>), 83.5 (C<sup>E</sup>), 71.0 (C<sup>A</sup>), 60.1 (C<sup>H</sup>), 51.0 (C<sup>B</sup>), 50.4 (C<sup>J</sup>), 40.6 (C<sup>C/D</sup>), 24.3 (C<sup>C/D</sup>), 13.5 (C<sup>I</sup>).

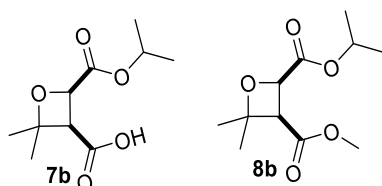
**FTIR** (ATR): ν (cm<sup>-1</sup>): 2978 (C-H), 1735 (C=O).

**HRMS (ESI):** m/z calculated for C<sub>10</sub>H<sub>16</sub>O<sub>5</sub>Na [M<sup>+</sup>Na<sup>+</sup>]: 217.1066, found: 217.1066.

**R<sub>f</sub>:** 0.30 (eluent: 1 : 1, hexane – EtOAc)

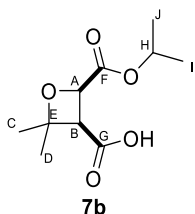
**Lab-book reference:** WM-03-56

***rac*-(3*R*,4*R*)-4-(isopropoxycarbonyl)-2,2-dimethyloxetane-3-carboxylic acid (**7b**) and 2-isopropyl 3-methyl *rac*-(2*R*,3*R*)-4,4-dimethyloxetane-2,3-dicarboxylate (**8b**)**



A solution of **3** (156 mg, 1.00 mmol, 93% purity with respect to dimer **4**) in isopropanol (10 mL) was stirred at room temperature until complete consumption of the starting material (24 h). The solvent was evaporated under reduced pressure to give the crude product. The crude product was dissolved in methanol (5 mL), then TMSCHN<sub>2</sub> (1.0 mL of a 2 M solution in hexane, 2.00 mmol) was added dropwise at room temperature. The reaction was stirred at room temperature for 10 min, then the solvent was evaporated under reduced pressure to give the crude product. Purification by flash column chromatography on silica gel (eluent: 1 : 1, hexane - EtOAc + 10 % MeOH) gave **7b** (137 mg, 0.63 mmol, 63%) as white crystals, and **8b** (60 mg, 0.11 mmol, 11%) as a colourless oil.

***rac*-(3*R*,4*R*)-4-(Isopropoxycarbonyl)-2,2-dimethyloxetane-3-carboxylic acid  
(7b)**



Chemical Formula: C<sub>10</sub>H<sub>16</sub>O<sub>5</sub>  
Molecular Weight: 216.23

**<sup>1</sup>H NMR** (400 MHz, CDCl<sub>3</sub>) δ 5.15 (septet, *J* = 6.3 Hz, 1H, H<sup>H</sup>), 5.01 (d, *J* = 8.8 Hz, 1H, H<sup>A</sup>), 3.83 (d, *J* = 8.8 Hz, 1H, H<sup>B</sup>), 1.63 (s, 3H, H<sup>C/D</sup>), 1.52 (s, 3H, H<sup>C/D</sup>), 1.28 (d, *J* = 6.3 Hz, 2H, H<sup>J/I</sup>), 1.26 (d, *J* = 6.3 Hz, 3H, H<sup>J/I</sup>).

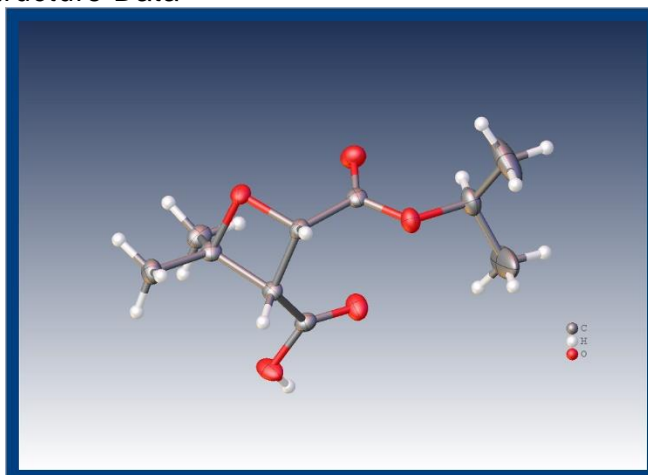
**<sup>13</sup>C NMR** (101 MHz, CDCl<sub>3</sub>) δ 171.9 (C<sup>F</sup>), 169.9 (C<sup>G</sup>), 84.0 (C<sup>E</sup>), 71.1 (C<sup>A</sup>), 69.1 (C<sup>H</sup>), 50.8 (C<sup>B</sup>), 30.3 (C<sup>C/D</sup>), 24.9 (C<sup>C/D</sup>), 21.8 (C<sup>J/I</sup>), 21.6 (C<sup>J/I</sup>).

**FTIR** (ATR) ν (cm<sup>-1</sup>): 3459 (O-H), 2880 (C-H), 1718 (C=O).

**R<sub>f</sub>**: 0.24 (eluent: 4 : 1, hexane - EtOAc + 10 % MeOH)

**Lab-book reference**: WM-03-65 – data (WM-03-61 PB → WM-03-62 ring opening)

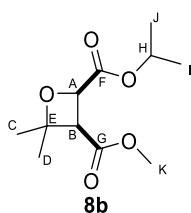
X-Ray Crystal Structure Data



Empirical formula	C <sub>10</sub> H <sub>16</sub> O <sub>5</sub>
Formula weight	216.23
Temperature/K	100.01(10)
Crystal system	monoclinic
Space group	P2 <sub>1</sub> /c
<i>a</i> /Å	11.1043(2)
<i>b</i> /Å	8.53260(10)
<i>c</i> /Å	12.6510(2)
<i>α</i> /°	90
<i>β</i> /°	109.140(2)
<i>γ</i> /°	90
Volume/Å <sup>3</sup>	1132.40(3)
<i>Z</i>	4
ρ <sub>calc</sub> /cm <sup>3</sup>	1.268
μ/mm <sup>-1</sup>	0.858
F(000)	464.0

Crystal size/mm <sup>3</sup>	0.423 × 0.262 × 0.072
Radiation	Cu Kα (λ = 1.54184)
2θ range for data collection/°	8.428 to 152.382
Index ranges	-13 ≤ h ≤ 13, -10 ≤ k ≤ 10, -15 ≤ l ≤ 15
Reflections collected	36457
Independent reflections	2363 [R <sub>int</sub> = 0.0279, R <sub>sigma</sub> = 0.0100]
Data/restraints/parameters	2363/0/141
Goodness-of-fit on F <sup>2</sup>	1.057
Final R indexes [I > 2σ (I)]	R <sub>1</sub> = 0.0390, wR <sub>2</sub> = 0.0999
Final R indexes [all data]	R <sub>1</sub> = 0.0408, wR <sub>2</sub> = 0.1014
Largest diff. peak/hole / e Å <sup>-3</sup>	0.29/-0.32

**2-Isopropyl-3-methyl *rac*-(2*R*,3*R*)-4,4-dimethyloxetane-2,3-dicarboxylate (8b)**



Chemical Formula: C<sub>11</sub>H<sub>18</sub>O<sub>5</sub>  
Molecular Weight: 230.26

**<sup>1</sup>H NMR** (400 MHz, CDCl<sub>3</sub>) δ 5.17 (septet, *J* = 6.3 Hz, 1H, H<sup>H</sup>), 5.00 (d, *J* = 8.9 Hz, 1H, H<sup>A</sup>), 3.78 (d, *J* = 8.9 Hz, 1H, H<sup>B</sup>), 3.69 (s, 3H, H<sup>K</sup>), 1.60 (s, 3H, H<sup>C/D</sup>), 1.45 (s, 3H, H<sup>C/D</sup>), 1.30 (d, *J* = 6.3 Hz, 3H, H<sup>J/I</sup>), 1.27 (d, *J* = 6.3 Hz, 3H, H<sup>J/I</sup>).

**<sup>13</sup>C NMR** (101 MHz, CDCl<sub>3</sub>) δ 170.1 (C<sup>F</sup>), 168.7 (C<sup>G</sup>), 84.1 (C<sup>E</sup>), 71.4 (C<sup>A</sup>), 68.9 (C<sup>H</sup>), 51.8 (C<sup>K</sup>), 51.1 (C<sup>B</sup>), 30.3 (C<sup>C/D</sup>), 24.9 (C<sup>C/D</sup>), 21.9 (C<sup>J/I</sup>), 21.7 (C<sup>J/I</sup>).

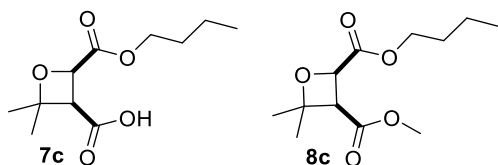
**FTIR** (ATR) ν (cm<sup>-1</sup>): 2978 (C-H), 1741 (C=O).

**HRMS (ESI)**: *m/z* calculated for C<sub>11</sub>H<sub>18</sub>O<sub>5</sub>Na [M+Na<sup>+</sup>]: 253.1046, found: 253.1048

**R<sub>f</sub>**: 0.59 (eluent: 1 : 1, hexane - EtOAc)

**Lab-book ref.** WM-03-65

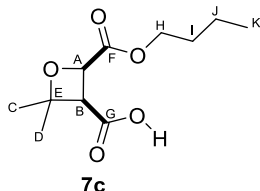
***rac*-(3*R*,4*R*)-4-(Butoxycarbonyl)-2,2-dimethyloxetane-3-carboxylic acid (7c) and 2-butyl 3-methyl *rac*-(2*R*,3*R*)-4,4-dimethyloxetane-2,3-dicarboxylate (8c)**



A solution of **3** (156 mg, 1.00 mmol, 93% purity with respect to dimer **4**) in isopropanol (10 mL) was stirred at room temperature until complete consumption of the starting material (24 h). The solvent was evaporated under reduced pressure to give the crude product. The crude product was dissolved in methanol (5 mL), then TMSCHN<sub>2</sub> (1.0 mL of a 2 M solution in hexane, 2.00 mmol) was added dropwise at room temperature. The

reaction was stirred at room temperature for 10 min, then the solvent was evaporated under reduced pressure to give the crude product. Purification by flash column chromatography on silica gel (eluent: 4 : 1 to 3 : 1, hexane - EtOAc + 10 % MeOH) gave **7c** (70 mg, 23%) as a colourless oil and **8c** (35 mg, 11%) as a colourless oil.

***rac*-(3*R*,4*R*)-4-(Butoxycarbonyl)-2,2-dimethyloxetane-3-carboxylic acid (**7c**)**



Chemical Formula: C<sub>11</sub>H<sub>18</sub>O<sub>5</sub>  
Molecular Weight: 230.26

**<sup>1</sup>H NMR** (400 MHz, CDCl<sub>3</sub>) δ 5.06 (d, *J* = 8.9 Hz, 1H, H<sup>A</sup>), 4.27 – 4.11 (m, 2H, H<sup>H</sup>), 3.85 (d, *J* = 8.9 Hz, 1H, H<sup>B</sup>), 1.68 – 1.57 (m, 2H, H<sup>I/J</sup>) and s, 3H, H<sup>C/D</sup>), 1.52 (s, 3H, H<sup>C/D</sup>), 1.47 – 1.31 (m, 2H, H<sup>I/J</sup>), 0.93 (t, *J* = 5.3 Hz, 3H, H<sup>K</sup>).

**<sup>13</sup>C NMR** (101 MHz, CDCl<sub>3</sub>) δ 170.6 (C<sup>F/G</sup>), 84.1 (C<sup>E</sup>), 71.1 (C<sup>A</sup>), 65.2 (C<sup>H</sup>), 50.8 (C<sup>B</sup>), 30.4 (C<sup>D/C/I</sup>), 30.3 (C<sup>D/C/I</sup>), 24.9(C<sup>D/C</sup>), 19.1 (C<sup>J</sup>), 13.7 (C<sup>K</sup>).

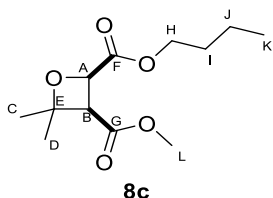
**FTIR** (ATR) ν (cm<sup>-1</sup>): 3478 (O-H), 2961 (C-H), 1735 (C=O).

**HRMS (ESI)**: Not found.

**R<sub>f</sub>**: 0.22 (eluent: 4 : 1, hexane - EtOAc + 10 % MeOH)

**Lab-book reference**: WM-03-66 (PB batch WM-03-61, ring opening WM-03-64).

***rac*-(2*R*,3*R*)-2-Butyl-3-methyl 4,4-dimethyloxetane-2,3-dicarboxylate (**8c**)**



Chemical Formula: C<sub>12</sub>H<sub>20</sub>O<sub>5</sub>  
Molecular Weight: 244.28

**<sup>1</sup>H NMR** (400 MHz, CDCl<sub>3</sub>) δ 5.03 (d, *J* = 8.9 Hz, 1H, H<sup>A</sup>), 4.28 – 4.14 (m, 2H, H<sup>H</sup>), 3.79 (d, *J* = 8.9 Hz, 1H, H<sup>B</sup>), 3.69 (s, 3H, H<sup>L</sup>), 1.68 – 1.63 (m, 2H, H<sup>I</sup>), 1.60 (s, 3H, H<sup>C/D</sup>), 1.44 (s, 3H, H<sup>C/D</sup>), 1.38 (m, 2H, H<sup>J</sup>), 0.93 (t, *J* = 7.4 Hz, 3H, H<sup>K</sup>).

**<sup>13</sup>C NMR** (101 MHz, CDCl<sub>3</sub>) δ 170.8 (C<sup>F</sup>), 168.8 (C<sup>G</sup>), 84.2 (C<sup>E</sup>), 71.3 (C<sup>A</sup>), 65.1 (C<sup>H</sup>), 51.9 (C<sup>L</sup>), 51.1 (C<sup>B</sup>), 30.5 (C<sup>I</sup>), 30.3 (C<sup>C/D</sup>), 24.9 (C<sup>C/D</sup>), 19.1 (C<sup>J</sup>), 13.7 (C<sup>K</sup>).

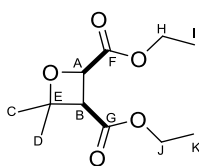
**FTIR** (ATR) ν (cm<sup>-1</sup>): 2958 (C-H), 1735 (C=O).

**HRMS (ESI)**: *m/z* calculated for C<sub>12</sub>H<sub>20</sub>O<sub>5</sub>Na [M+Na<sup>+</sup>]: 267.1194, found: 267.1194.

**R<sub>f</sub>**: 0.65 (eluent: 1 : 1, hexane - EtOAc)

**Lab-book reference**: WM-03-66

***rac*-(2*R*,3*R*)-2,3-Diethyl 4,4-dimethyloxetane-2,3-dicarboxylate (6b)**



**6b**

Chemical Formula: C<sub>11</sub>H<sub>18</sub>O<sub>5</sub>

Molecular Weight: 230.26

*Reaction employing Meerwein salt at room temperature or reflux:* The crude oxetane **3** (225 mg, 1.3 mmol, 93% purity with respect to dimer **4**) added to a suspension of Et<sub>3</sub>O<sup>+</sup>BF<sub>4</sub><sup>-</sup> (740 mg, 3.9 mmol) in dichloromethane (10 mL) under nitrogen. Next, *N,N*-diisopropylethylamine (0.68 mL, 3.9 mmol) was added. The reaction was stirred at room temperature or reflux for 20 h. The reaction mixture was washed with 1 M aqueous HCl (1 x 10 mL) and 1 M aqueous potassium bicarbonate (1 x 10 mL). Both aqueous phases were extracted with EtOAc (2 x 10 mL), the combined organic phases were washed with brine (10 mL), dried (MgSO<sub>4</sub>) and evaporated under reduced pressure. Purification by flash chromatography (eluent: 9 : 1 to 4: 1, hexane–EtOAc) gave oxetane **6b** (*r.t.*: 80 mg, 0.35 mmol, 27%; *reflux*: 64 mg, 0.28 mmol, 21%) as a colourless oil.

**<sup>1</sup>H NMR** (400 MHz, CDCl<sub>3</sub>) δ 5.05 (d, *J* = 8.9 Hz, 1H, H<sup>A</sup>), 4.38 – 4.12 (m, 4H, H<sup>H,J</sup>), 3.79 (d, *J* = 8.9 Hz, 1H, H<sup>B</sup>), 1.63 (s, 3H, H<sup>C/D</sup>), 1.48 (s, 3H, H<sup>C/D</sup>), 1.33 (t, *J* = 7.2 Hz, 3H, H<sup>I/K</sup>), 1.28 (t, *J* = 7.1 Hz, 3H, H<sup>I/K</sup>).

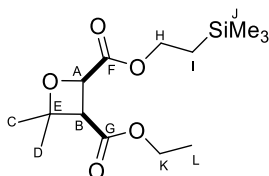
**<sup>13</sup>C NMR** (101 MHz, CDCl<sub>3</sub>) δ 170.8 (C<sup>F</sup>), 168.31 (C<sup>G</sup>), 84.2 (C<sup>E</sup>), 71.4 (C<sup>A</sup>), 61.2 (C<sup>H/J</sup>), 61.0 (C<sup>H/J</sup>), 51.2 (C<sup>B</sup>), 30.3 (C<sup>C/D</sup>), 24.9 (C<sup>C/D</sup>), 14.2 (C<sup>I/K</sup>), 14.1 (C<sup>I/K</sup>).

**FTIR** (ATR)  $\nu$  (cm<sup>-1</sup>): 2980 (C-H), 2937 (C-H), 1731 (C=O).

**HRMS (ESI):** *m/z* calculated for C<sub>11</sub>H<sub>18</sub>O<sub>5</sub>Na [M+Na<sup>+</sup>]: 231.1227, found at 231.1219.

**Lab-book reference:** WM-04-05,06

***rac*-(2*R*,3*R*)-3-Ethyl 2-[2-(trimethylsilyl)ethyl] 4,4-dimethyloxetane-2,3-dicarboxylate (8d)**



**8d**

Chemical Formula: C<sub>14</sub>H<sub>26</sub>O<sub>5</sub>Si

Molecular Weight: 302.44

2-(Trimethylsilyl)ethanol (0.37 mL, 2.60 mmol) was added to a stirred solution of **3** (224 mg, 1.3 mmol, 93% purity with respect to dimer **4**) in acetonitrile (5 mL). The reaction was stirred at room temperature until complete consumption of the starting material (72



h). The crude product was added to a suspension of  $\text{Et}_3\text{O}^+\text{BF}_4^-$  (567 mg, 3.0 mmol) in dichloromethane (10 mL) under nitrogen. Next, *N,N*-diisopropylethylamine (0.52 mL, 3.0 mmol) was added. The reaction was stirred at room temperature for 20 h. The reaction mixture was washed with 1 M aqueous HCl (1 x 10 mL) and 1 M aqueous potassium bicarbonate (1 x 10 mL). Both aqueous phases were extracted with EtOAc (2 x 10 mL), the combined organic phases were washed with brine (10 mL), dried ( $\text{MgSO}_4$ ) and evaporated under reduced pressure. Purification by flash chromatography (eluent: 17 : 3 hexane–EtOAc) gave oxetane **8d** (115 mg, 0.38 mmol, 25%) as a colourless oil.

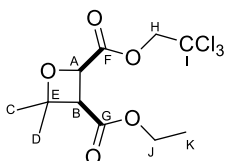
**$^1\text{H}$  NMR** (400 MHz,  $\text{CDCl}_3$ )  $\delta$  5.01 (d,  $J = 8.9$  Hz, 1H,  $\text{H}^{\text{A}}$ ), 4.40 – 4.23 (m, 2H,  $\text{H}^{\text{K}}$ ), 4.16 (m, 2H,  $\text{H}^{\text{H}}$ ), 3.76 (d,  $J = 8.9$  Hz, 1H,  $\text{H}^{\text{B}}$ ), 1.60 (s, 3H,  $\text{H}^{\text{C/D}}$ ), 1.46 (s, 3H,  $\text{H}^{\text{C/D}}$ ), 1.26 (t,  $J = 7.1$  Hz, 3H,  $\text{H}^{\text{L}}$ ), 1.08-1.06 (m, 2H,  $\text{H}^{\text{I}}$ ), 0.04 (s, 9H,  $\text{H}^{\text{J}}$ ).  
 **$^{13}\text{C}$  NMR** (101 MHz,  $\text{CDCl}_3$ )  $\delta$  170.9 ( $\text{C}^{\text{F}}$ ), 168.3 ( $\text{C}^{\text{G}}$ ), 84.1 ( $\text{C}^{\text{E}}$ ), 71.4 ( $\text{C}^{\text{A}}$ ), 63.5 ( $\text{C}^{\text{H}}$ ), 61.0 ( $\text{C}^{\text{K}}$ ), 51.2 ( $\text{C}^{\text{B}}$ ), 30.3 ( $\text{C}^{\text{C/D}}$ ), 24.9 ( $\text{C}^{\text{C/D}}$ ), 17.2 ( $\text{C}^{\text{I}}$ ), 14.2 ( $\text{C}^{\text{L}}$ ), -1.5 ( $\text{C}^{\text{J}}$ ).

**FTIR** (ATR)  $\nu$  ( $\text{cm}^{-1}$ ): 2953 (C-H), 1735 (C=O).

**HRMS (ESI)**:  $m/z$  calculated for  $\text{C}_{14}\text{H}_{26}\text{O}_5\text{SiNa}$ ,  $[\text{M}+\text{Na}^+]$ : 325.1442, found at 325.1434.

**Lab-book reference**: WM-04-07

***rac*-(2*R*,3*R*)-3-Ethyl 2-(2,2,2-trichloroethyl) 4,4-dimethyloxetane-2,3-dicarboxylate(**8e**)**



**8e**

Chemical Formula:  $\text{C}_{11}\text{H}_{15}\text{Cl}_3\text{O}_5$

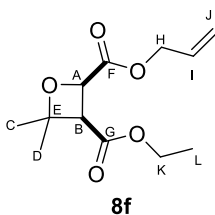
Molecular Weight: 333.59

2,2,2-Trichloroethanol (0.30 mL, 3.14 mmol) was added to a stirred solution of **3** (230 mg, 1.54 mmol, purity 93%) in acetonitrile (5 mL), and the resulting mixture was stirred at room temperature for 72 h, then heated at 50 °C until complete consumption of the starting material (16 h). The crude product was added to a suspension of  $\text{Et}_3\text{O}^+\text{BF}_4^-$  (436 mg, 2.31 mmol) in dichloromethane (5 mL) under nitrogen. Next, *N,N*-diisopropylethylamine (0.40 mL, 2.31 mmol) was added. The reaction was stirred at room temperature for 20 h. The reaction mixture was washed with 1 M aqueous HCl (1 x 10 mL) and 1 M aqueous potassium bicarbonate (1 x 10 mL). Both aqueous phases were extracted with EtOAc (2 x 10 mL), the combined organic phases were washed with brine (10 mL), dried ( $\text{MgSO}_4$ ) and evaporated under reduced pressure. Purification by flash chromatography (eluent: 9 : 1 to 4:1 hexane–EtOAc) gave oxetane **8e** (130 mg, 0.39 mmol, 24%) as colourless oil.

**<sup>1</sup>H NMR** (400 MHz, CDCl<sub>3</sub>) δ 5.18 (d, *J* = 8.9 Hz, 1H, H<sup>A</sup>), 5.00 (d, *J* = 11.9 Hz, 1H, H<sup>H</sup>), 4.63 (d, *J* = 11.9 Hz, 1H, H<sup>H</sup>), 4.21 – 4.13 (m, 2H, H<sup>J</sup>), 3.87 (d, *J* = 8.9 Hz, 1H, H<sup>B</sup>), 1.63 (s, 3H, H<sup>C/D</sup>), 1.47 (s, 3H, H<sup>C/D</sup>), 1.26 (t, *J* = 7.1 Hz, 3H, H<sup>K</sup>).  
**<sup>13</sup>C NMR** (101 MHz, CDCl<sub>3</sub>) δ 169.5 (C<sup>F</sup>), 168.2 (C<sup>G</sup>), 94.5 (C<sup>I</sup>), 84.9 (C<sup>E</sup>), 74.9 (C<sup>H</sup>), 71.0 (C<sup>A</sup>), 61.3 (C<sup>J</sup>), 51.2 (C<sup>B</sup>), 30.4 (C<sup>C/D</sup>), 24.9 (C<sup>C/D</sup>), 14.2 (C<sup>K</sup>).  
**FTIR** (ATR) ν (cm<sup>-1</sup>): 2976 (C-H), 1774 (C=O), 1735 (C=O)

**Lab-book reference:** WM-04-15

***rac*-(2*R*,3*R*)-3-Ethyl 2-prop-2-en-1-yl 4,4-dimethyloxetane-2,3-dicarboxylate(8f)**



Chemical Formula: C<sub>12</sub>H<sub>18</sub>O<sub>5</sub>  
Molecular Weight: 242.27

Allyl alcohol (0.21 mL, 3.00 mmol) was added to a stirred solution of **3** (223 mg, 1.43 mmol, 93% purity with respect to dimer **4**) in acetonitrile (5 mL), and the resulting mixture was stirred at room temperature for 72 h, then heated at 50 °C until complete consumption of the starting material (16 h). The crude was added to a suspension of Et<sub>3</sub>O<sup>+</sup>BF<sub>4</sub><sup>-</sup> (436 mg, 2.31 mmol) in dichloromethane (5 mL) under nitrogen. Next, *N,N*-diisopropylethylamine (0.40 mL, 2.31 mmol) was added. The reaction was stirred at room temperature for 20 h. The reaction mixture was washed with 1 M aqueous HCl (1 x 10 mL) and 1 M aqueous potassium bicarbonate (1 x 10 mL). Both aqueous phases were extracted with EtOAc (2 x 10 mL), the combined organic phases were washed with brine (10 mL), dried (MgSO<sub>4</sub>) and evaporated under reduced pressure. Purification by flash chromatography (eluent: 7 : 3 hexane–EtOAc) gave oxetane **8f** (106 mg, 0.44 mmol, 31%).

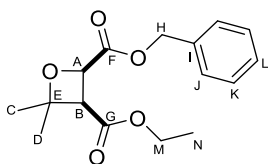
**<sup>1</sup>H NMR** (400 MHz, CDCl<sub>3</sub>) δ 5.92 – 5.91 (m, 1H, H<sup>I</sup>), 5.35 (dq, *J* = 17.2, 1.5 Hz, 1H, H<sup>J</sup>), 5.25 (ddd, *J* = 10.4, 2.5, 1.2 Hz, 1H, H<sup>J</sup>), 5.06 (d, *J* = 8.9 Hz, 1H, H<sup>A</sup>), 4.79 – 4.64 (m, 2H, H<sup>H</sup>), 4.22 – 4.12 (m, 2H, H<sup>K</sup>), 3.79 (d, *J* = 8.9 Hz, 1H, H<sup>B</sup>), 1.61 (s, 3H, H<sup>C/D</sup>), 1.46 (s, 3H, H<sup>C/D</sup>), 1.25 (t, *J* = 7.1 Hz, 3H, H<sup>L</sup>).  
**<sup>13</sup>C NMR** (101 MHz, CDCl<sub>3</sub>) δ 170.5 (C<sup>F</sup>), 168.3 (C<sup>G</sup>), 132.0 (C<sup>I</sup>), 118.7 (C<sup>J</sup>), 84.4 (C<sup>E</sup>), 71.4 (C<sup>A</sup>), 65.9 (C<sup>H</sup>), 61.1 (C<sup>K</sup>), 51.2 (C<sup>B</sup>), 30.3 (C<sup>C/D</sup>), 24.9 (C<sup>C/D</sup>), 14.2 (C<sup>L</sup>).

**FTIR** (ATR) ν (cm<sup>-1</sup>): 2980 (C-H), 1735 (C=O)

**HRMS (ESI):** *m/z* calculated for C<sub>12</sub>H<sub>19</sub>O<sub>5</sub> [M+H]<sup>+</sup>: 243.1227, found at 243.1217.

**Lab-book reference:** WM-04-16

***rac*-(2*R*,3*R*)-2-Benzyl 3-ethyl 4,4-dimethyloxetane-2,3-dicarboxylate (**8g**)**



**8g**

Chemical Formula: C<sub>16</sub>H<sub>20</sub>O<sub>5</sub>

Molecular Weight: 292.33

Benzyl alcohol (0.33 mL, 3.00 mmol) was added to a stirred solution of **3** (231 mg, 1.48 mmol, 93% purity with respect to dimer **4**) in acetonitrile (5 mL), and the resulting mixture was stirred at room temperature for 72 h, then heated at 50 °C until complete consumption of the starting material (16 h). The crude was added to a suspension of Et<sub>3</sub>O<sup>+</sup>BF<sub>4</sub><sup>-</sup> (425 mg, 2.25 mmol) in dichloromethane (5 mL) under nitrogen. Next, *N,N*-diisopropylethylamine (0.40 mL, 2.25 mmol) was added. The reaction was stirred at room temperature for 20 h. The reaction mixture was washed with 1 M aqueous HCl (1 x 10 mL) and 1 M aqueous potassium bicarbonate (1 x 10 mL). Both aqueous phases were extracted with EtOAc (2 x 10 mL), the combined organic phases were washed with brine (10 mL), dried (MgSO<sub>4</sub>) and evaporated under reduced pressure. Purification by flash chromatography (eluent: 18 : 3 hexane–EtOAc) gave oxetane **8g** (161 mg, with BnOH still present; 1 : 0.37 ratio by <sup>1</sup>H NMR spectroscopy).

**<sup>1</sup>H NMR** (400 MHz, CDCl<sub>3</sub>) δ 7.40 – 7.31 (m, 5H, H<sup>J, K, L</sup>), 5.29 (d, *J* = 12.1 Hz, 1H, H<sup>H</sup>), 5.19 (d, *J* = 12.1 Hz, 1H, H<sup>H</sup>), 5.07 (d, *J* = 8.9 Hz, 1H, H<sup>A</sup>), 4.18 – 4.07 (m, 2H, H<sup>M</sup>), 3.78 (d, *J* = 8.9 Hz, 1H, H<sup>B</sup>), 1.60 (s, 3H, H<sup>C/D</sup>), 1.47 (s, 3H, H<sup>C/D</sup>), 1.23 (t, *J* = 7.1 Hz, 3H, H<sup>N</sup>).

**<sup>13</sup>C NMR** (101 MHz, CDCl<sub>3</sub>) δ 170.7 (C<sup>F</sup>), 168.3 (C<sup>G</sup>), 135.5 (C<sup>I</sup>), 128.6 (C<sup>K</sup>), 128.5 (C<sup>J</sup>), 127.0 (C<sup>L</sup>), 84.4 (C<sup>E</sup>), 71.4 (C<sup>A</sup>), 67.0 (C<sup>H</sup>), 61.1 (C<sup>M</sup>), 51.2 (C<sup>B</sup>), 30.4 (C<sup>C/D</sup>), 24.9 (C<sup>C/D</sup>), 14.2 (C<sup>N</sup>).

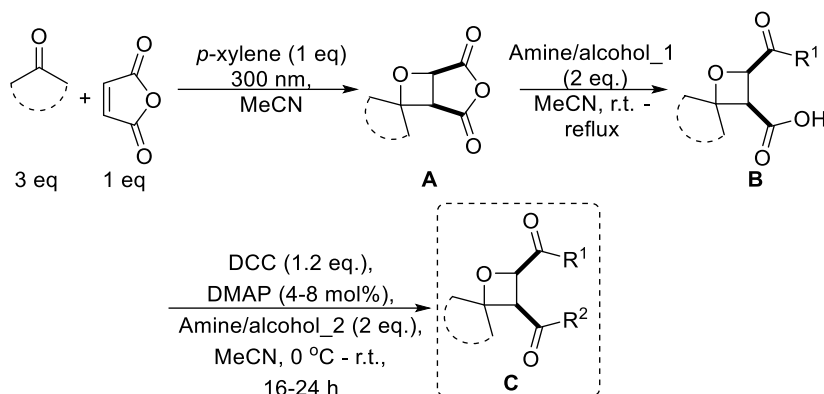
**FTIR** (ATR)  $\nu$  (cm<sup>-1</sup>): 2976 (C-H), 1731 (C=O).

**HRMS (ESI)**: *m/z* calculated for C<sub>16</sub>H<sub>21</sub>O<sub>5</sub> [M+H]<sup>+</sup>: 293.1384, found at 293.1370.

**Lab-book reference**: WM-04-17

## 7.4.2 Chapter 3: Reactions of cyclic ketones and maleic anhydride

### 7.4.2.1 General procedure

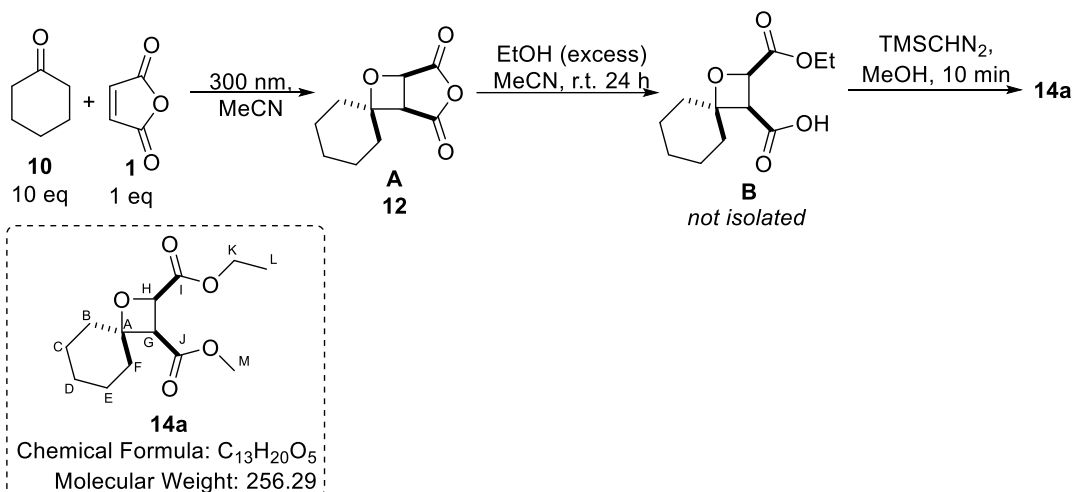


A solution of maleic anhydride (1.0 eq, scale specified for each procedure), ketone (3.0 eq) and *p*-xylene (1.0 eq) in anhydrous MeCN (0.1 M, with respect to maleic anhydride) was prepared in a Duran phototube and purged with argon for 15 minutes, then irradiated at approximately 40 °C ( $\lambda = 300$  nm) until complete consumption of the maleic anhydride, as judged by  $^1\text{H}$  NMR spectroscopy (solvent suppression). Next, the solution was decanted into a round-bottomed flask, and amine/alcohol\_1 (1-2.0 eq) was added. The reaction mixture was stirred at room temperature or reflux for 24-72 h (specified for each procedure) until full consumption of oxetane **A**, as judged by  $^1\text{H}$  NMR spectroscopy (solvent suppression). The solvent was evaporated under reduced pressure to give the crude product **B**. Crude product **B** was dried under high vacuum overnight to fully remove unreacted alcohol/amine\_1, then dissolved in anhydrous MeCN (0.3-0.5 M) under nitrogen. Next, DMAP (5 mol%) was added, followed by amine/alcohol\_2 (2.0 eq). The reaction mixture was cooled to 0 °C and DCC (1.2 eq) was added portion-wise. The reaction was slowly warmed to room temperature and stirred overnight. The precipitated urea was filtered off and the filtrate was concentrated under reduced pressure to give crude product **C**. Purification by flash column chromatography on silica gel gave the purified oxetane product (column details specified for each procedure).

## 7.4.2.2 Cyclohexanone (10) and maleic anhydride (1) reactions

### 7.4.2.2.1 Ring opening of anhydride with various alcohols

#### *rac*-(2*R*,3*R*)-2-Ethyl 3-methyl 1-oxaspiro[3.5]nonane-2,3-dicarboxylate (14a)



A solution of maleic anhydride (147 mg, 1.50 mmol) and ketone (1.47 mL, 15.00 mmol) in anhydrous MeCN (0.1 M, 15 mL) was prepared in a Duran phototube and purged with argon for 15 minutes, then irradiated at approximately 40 °C ( $\lambda = 300$  nm) until complete consumption of the maleic anhydride, as judged by <sup>1</sup>H NMR spectroscopy (solvent suppression). Next, the solution was decanted into a round-bottomed flask, and ethanol (5 mL) was added. The reaction mixture was stirred at room temperature 24 h until full consumption of oxetane **A**, as judged by <sup>1</sup>H NMR spectroscopy (solvent suppression). The solvent was evaporated under reduced pressure to give the crude product **B**. The crude product was dissolved in methanol (5 mL), then TMSCHN<sub>2</sub> (1.0 mL of a 2 M solution in hexane, 2.00 mmol) was added dropwise at room temperature. The reaction was stirred at room temperature for 10 min, then the solvent was evaporated under reduced pressure to give the crude product. Purification by flash chromatography (eluent: 4 : 1 → 3 : 1; hexane–EtOAc) gave oxetane **14a** (20 mg, 5 % yield) as yellow oil.

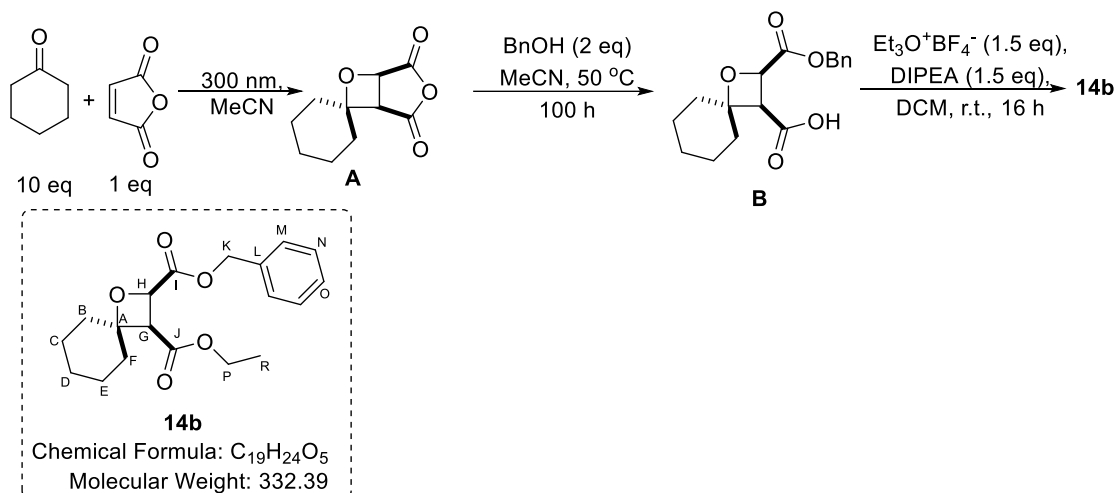
<sup>1</sup>H NMR (400 MHz, CDCl<sub>3</sub>)  $\delta$  5.04 (d,  $J = 8.8$  Hz, 1H, H<sup>H</sup>), 4.36 – 4.22 (m, 2H, H<sup>K</sup>), 3.71 (d,  $J = 8.8$  Hz, 1H, H<sup>G</sup>), 3.71 (s, 3H, H<sup>M</sup>), 1.99 – 1.39 (m, 10H, H<sup>B, C, D, E, F</sup>), 1.32 (t,  $J = 7.2$  Hz, 3H, H<sup>L</sup>).

<sup>13</sup>C NMR (101 MHz, CDCl<sub>3</sub>)  $\delta$  170.8 (C<sup>I</sup>), 168.9 (C<sup>J</sup>), 85.5 (C<sup>A</sup>), 71.6 (C<sup>H</sup>), 61.2 (C<sup>K</sup>), 51.8 (C<sup>M</sup>), 50.9 (C<sup>G</sup>), 39.5 (C<sup>B/C/D/E/F</sup>), 33.5 (C<sup>B/C/D/E/F</sup>), 24.8 (C<sup>B/C/D/E/F</sup>), 22.3 (C<sup>B/C/D/E/F</sup>), 21.6 (C<sup>B/C/D/E/F</sup>), 14.2 (C<sup>L</sup>).

HRMS (ESI):  $m/z$  calculated for C<sub>13</sub>H<sub>20</sub>O<sub>5</sub>Na [M + Na]<sup>+</sup>: 279.1203, found at 279.1190.

Lab-book reference: WM-03-71

***rac*-(2*R*,3*R*)-2-Benzyl 3-ethyl 1-oxaspiro[3.5]nonane-2,3-dicarboxylate  
(14b)**



A solution of maleic anhydride (98 mg, 1.00 mmol) and ketone (1.03 mL, 10.00 mmol) in anhydrous MeCN (0.1 M, 10 mL) was prepared in a Duran phototube and purged with argon for 15 minutes, then irradiated at approximately 40 °C ( $\lambda = 300 \text{ nm}$ ) until complete consumption of the maleic anhydride, as judged by <sup>1</sup>H NMR spectroscopy (solvent suppression). Next, the solution was decanted into a round-bottomed flask, and benzyl alcohol (0.21 mL, 2.00 mmol) was added. The reaction mixture was stirred at 5 °C for 100 h until full consumption of oxetane **A**, as judged by <sup>1</sup>H NMR spectroscopy (solvent suppression). The solvent was evaporated under reduced pressure to give the crude product **B**. The crude **B** was added to a suspension of Et<sub>3</sub>O<sup>+</sup>BF<sub>4</sub><sup>-</sup> (283 mg, 1.50 mmol) in dichloromethane (5 mL) under nitrogen. Next, *N,N*-diisopropylethylamine (0.26 mL, 1.50 mmol) was added. The reaction was stirred at room temperature for 20 h. The reaction mixture was washed with 1 M aqueous HCl (1 x 8 mL) and 1 M aqueous potassium bicarbonate (1 x 8 mL). Both aqueous phases were extracted with EtOAc (2 x 8 mL), the combined organic phases were washed with brine (8 mL), dried (MgSO<sub>4</sub>) and evaporated under reduced pressure. Purification by flash chromatography (eluent: 4 : 1 → 3 : 1; hexane–EtOAc) gave oxetane **14b** (16 mg, 5 % yield) as a colourless oil.

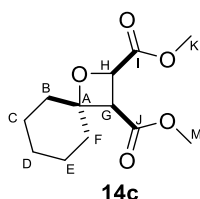
**<sup>1</sup>H NMR** (400 MHz, CDCl<sub>3</sub>)  $\delta$  7.39 – 7.30 (m, 5H, H<sup>M, N, O</sup>), 5.27 (d,  $J = 12.2 \text{ Hz}$ , 1H H<sup>K</sup>), 5.18 (d,  $J = 12.2 \text{ Hz}$ , 1H, H<sup>K</sup>), 5.06 (d,  $J = 8.8 \text{ Hz}$ , 1H, H<sup>H</sup>), 4.15 – 4.04 (m, 2H, H<sup>P</sup>), 3.67 (d,  $J = 8.8 \text{ Hz}$ , 1H, H<sup>G</sup>), 1.93 - 1.30 (m, 10H, H<sup>B, C, D, E, F</sup>), 1.22 (t,  $J = 7.1 \text{ Hz}$ , 3H, H<sup>R</sup>).

**<sup>13</sup>C NMR** (101 MHz, CDCl<sub>3</sub>)  $\delta$  170.7 (C<sup>I</sup>), 168.3 (C<sup>J</sup>), 135.6 (C<sup>L</sup>), 128.6 (C<sup>N</sup>), 128.5 (C<sup>M</sup>), 128.3 (C<sup>O</sup>), 85.7 (C<sup>A</sup>), 71.6 (C<sup>H</sup>), 66.9 (C<sup>K</sup>), 61.0 (C<sup>P</sup>), 51.1 (C<sup>G</sup>), 39.6 (C<sup>B/C/D/E/F</sup>), 33.5 (C<sup>B/C/D/E/F</sup>), 24.8 (C<sup>B/C/D/E/F</sup>), 22.3 (C<sup>B/C/D/E/F</sup>), 21.6 (C<sup>B/C/D/E/F</sup>), 14.2 (C<sup>R</sup>).

**FTIR** (ATR)  $\nu$  (cm<sup>-1</sup>): 2931 (C-H), 1731 (C=O).

**Lab-book reference:** WM-04-20

### *rac*-(2*R*,3*R*)-Dimethyl 1-oxaspiro[3.5]nonane-2,3-dicarboxylate (**14c**)



Chemical Formula: C<sub>12</sub>H<sub>18</sub>O<sub>5</sub>  
Molecular Weight: 242.27

Using the general procedure, maleic anhydride (98 mg, 1.00 mmol) and cyclohexanone (0.32 mL, 3.00 mmol) were used in the Paternò-Büchi reaction (86 h irradiation). Using methanol (0.10 mL, 2.00 mmol) and stirring at reflux for 48 h in the second step, the crude product **B** was obtained, then dissolved in MeCN (3 mL) and used in the final step using methanol (0.10 mL, 2.00 mmol). Purification by flash chromatography (eluent 19:1-9:1 hexane-EtOAc) gave **14c** (98 mg, 0.33 mmol, 42%) as a colourless oil.

**<sup>1</sup>H NMR** (400 MHz, CDCl<sub>3</sub>) δ 5.05 (d, *J* = 8.8 Hz, 1H, H<sup>H</sup>), 3.80 (s, 3H, H<sup>K</sup>), 3.69 (d, *J* = 8.8 Hz, 1H, H<sup>G</sup>), 3.68 (s, 3H, H<sup>M</sup>), 1.87-1.29 (m, 10H, H<sup>B, C, D, E, F</sup>).

**<sup>13</sup>C NMR** (101 MHz, CDCl<sub>3</sub>) δ 171.3 (C<sup>I</sup>), 168.8 (C<sup>J</sup>), 85.6 (C<sup>A</sup>), 71.6 (C<sup>H</sup>), 52.1 (C<sup>K/M</sup>), 51.9 (C<sup>K/M</sup>), 51.0 (C<sup>G</sup>), 39.4 (C<sup>B/F</sup>), 33.6 (C<sup>B/F</sup>), 24.8 (C<sup>C/D/E</sup>), 22.2 (C<sup>C/D/E</sup>), 21.6 (C<sup>C/D/E</sup>).

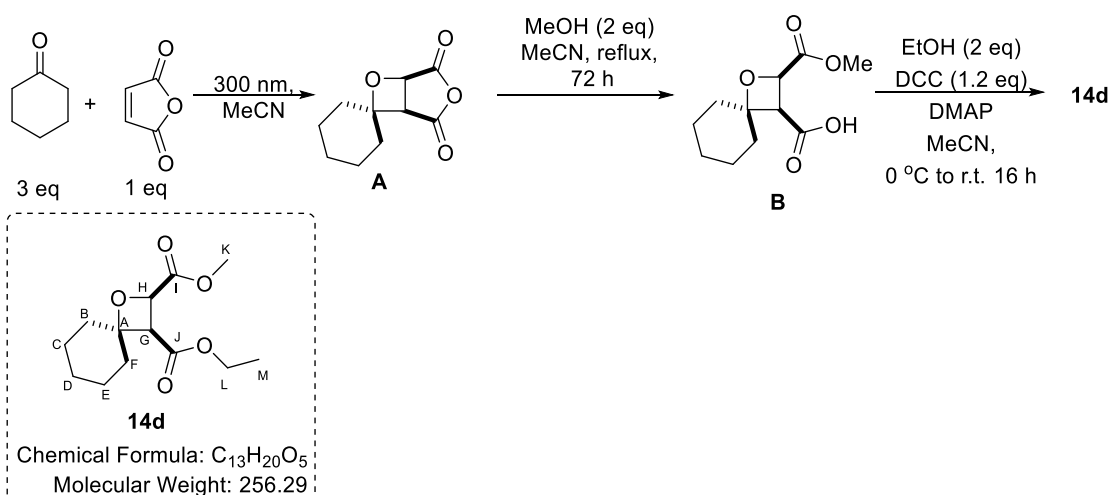
**FTIR** (ATR) ν (cm<sup>-1</sup>): 2931 (C-H), 1761 (C=O), 1735 (C=O).

**HRMS (ESI)**: *m/z* calculated for C<sub>12</sub>H<sub>18</sub>O<sub>5</sub>Na [M + Na]<sup>+</sup>: 265.1046, found at 265.1039.

**R<sub>f</sub>**: (acetone-hexane, 1:4) = 0.41.

**Lab-book reference**: WM-05-29

### *rac*-(2*R*,3*R*)-3-ethyl 2-methyl 1-oxaspiro[3.5]nonane-2,3-dicarboxylate (**14d**)



A solution of maleic anhydride (98 mg, 1.00 mmol) and cyclohexanone (0.32 mL, 3.00 mmol) in anhydrous MeCN (0.16 M, with respect to maleic anhydride) was prepared in a Duran phototube and purged with argon for 15 minutes, then irradiated at approximately 40 °C ( $\lambda = 300$  nm) until complete consumption of the maleic anhydride,

as judged by  $^1\text{H}$  NMR spectroscopy (solvent suppression). Next, the solution was decanted into a round-bottomed flask, and methanol (0.10 mL, 2.00 mmol) was added. The reaction mixture was stirred at room temperature or reflux for 72 h until full consumption of oxetane **A**, as judged by  $^1\text{H}$  NMR spectroscopy (solvent suppression). The solvent was evaporated under reduced pressure to give the crude product **B**. Crude product **B** was dried under high vacuum overnight to fully remove unreacted methanol, then dissolved in anhydrous MeCN (5 mL) under nitrogen. Next, DMAP (10 mg, 5 mol%) was added, followed by ethanol (0.12 mL, 2 mmol). The reaction mixture was cooled to 0 °C and DCC (226 mg, 1.2 mmol) was added portion-wise. The reaction was slowly warmed to room temperature and stirred overnight. The precipitated urea was filtered off and the filtrate was concentrated under reduced pressure to give crude product. Purification by flash chromatography (eluent 19:1-9:1 hexane-acetone) gave **14d** (51 mg, 0.20 mmol, 20%) as a colourless oil.

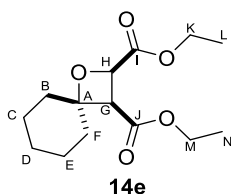
$^1\text{H}$  NMR (400 MHz,  $\text{CDCl}_3$ )  $\delta$  5.08 (d,  $J = 8.8$  Hz, 1H), 4.18 (q,  $J = 7.1$  Hz, 1H), 3.83 (s, 1H), 3.69 (d,  $J = 8.8$  Hz, 1H), 1.92 – 1.35 (m, 1H), 1.29 (t,  $J = 7.1$  Hz, 1H).

FTIR (ATR)  $\nu$  ( $\text{cm}^{-1}$ ): 2931 (C-H), 1731 (C=O).

HRMS (ESI):  $m/z$  calculated for  $\text{C}_{13}\text{H}_{20}\text{O}_5\text{Na}$  [ $\text{M} + \text{Na}$ ] $^+$ : 279.1203, found at 279.1190.

Lab-book reference: WM-04-89-91, 89 form MS and IR, 91 for NMR.

#### ***rac*-(2*R*,3*R*)-Diethyl 1-oxaspiro[3.5]nonane-2,3-dicarboxylate (**14e**)**



Chemical Formula:  $\text{C}_{14}\text{H}_{22}\text{O}_5$

Molecular Weight: 270.33

Using the general procedure, maleic anhydride (98 mg, 1.00 mmol) and cyclohexanone (0.32 mL, 3.00 mmol) were used in the Paternò-Büchi reaction (86 h irradiation). Using ethanol (0.12 mL, 2.00 mmol) and stirring at reflux for 48 h in the second step, the crude product **B** was obtained, then dissolved in MeCN (3 mL) and used in the final step (using ethanol (0.12 mL, 2.00 mmol)). Purification by flash chromatography (eluent 19:1-9:1 hexane-acetone) gave **14e** (92 mg, 0.34 mmol, 34%) as a colourless oil.



**<sup>1</sup>H NMR** (400 MHz, CDCl<sub>3</sub>) δ 5.02 (d, *J* = 8.8 Hz, 1H, H<sup>H</sup>), 4.26-4.22 (m, 2H, H<sup>K/M</sup>), 4.22-4.10 (m, 2H, H<sup>K/M</sup>), 3.67 (d, *J* = 8.8 Hz, 1H, H<sup>G</sup>), 1.93-1.61 (m, 10H, H<sup>B, C, D, E, F</sup>), 1.32-1.22 (m, 6H, H<sup>L,N</sup>).

**<sup>13</sup>C NMR** (101 MHz, CDCl<sub>3</sub>) δ 170.9 (C<sup>I</sup>), 168.3 (C<sup>J</sup>), 85.5 (C<sup>A</sup>), 71.7 (C<sup>H</sup>), 61.3 (C<sup>K/M</sup>), 61.0 (C<sup>K/M</sup>), 51.1 (C<sup>G</sup>), 40.9 (C<sup>B/F</sup>), 39.5 (C<sup>B/F</sup>), 33.5 (C<sup>C/D/E</sup>), 24.9 (C<sup>C/D/E</sup>), 22.3 (C<sup>C/D/E</sup>), 14.2 (C<sup>L/N</sup>), 14.1 (C<sup>L/N</sup>).

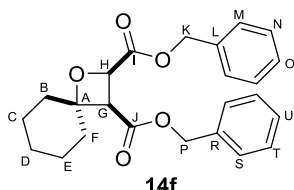
**FTIR** (ATR)  $\nu$  (cm<sup>-1</sup>): 2933 (C-H), 1731 (C=O).

**HRMS (ESI)**: *m/z* calculated for C<sub>14</sub>H<sub>22</sub>O<sub>5</sub>Na [M + Na]<sup>+</sup>: 293.1359, found at 293.1346.

*R<sub>f</sub>* (acetone-hexane, 1:9) = 0.32.

**Lab-book reference**: WM-04-74,87

### ***rac*-(2*R*,3*R*)-Dibenzyl 1-oxaspiro[3.5]nonane-2,3-dicarboxylate (14f)**



**14f**

Chemical Formula: C<sub>24</sub>H<sub>26</sub>O<sub>5</sub>

Molecular Weight: 394.47

Using the general procedure, maleic anhydride (98 mg, 1.00 mmol) and cyclohexanone (0.32 mL, 3.00 mmol) were used in the Paternò-Büchi reaction (86 h irradiation). Using benzyl alcohol (0.20 mL, 2.00 mmol) and stirring at reflux for 72 h in the second step, the crude product **B** was obtained, then dissolved in MeCN (5 mL) and used in the final step using benzyl alcohol (0.20 mL, 2.00 mmol). Purification by flash chromatography (eluent 7:3 hexane-EtOAc) gave **14f** (100 mg, 0.29 mmol, 29%) as a colourless oil.

**<sup>1</sup>H NMR** (400 MHz, CDCl<sub>3</sub>) δ 7.38-7.30 (m, 10H, H<sup>M, N, O, S, T, U</sup>), 5.21 (d, *J* = 12.2 Hz, 1H, H<sup>K/P</sup>), 5.08-5.05 (m, 3H, H<sup>K, P</sup>), 5.07 (d, *J* = 8.9 Hz, 1H, H<sup>H</sup>), 3.73 (d, *J* = 8.9 Hz, 1H, H<sup>G</sup>), 1.80-1.26 (m, 10H, H<sup>B, C, D, E, F</sup>).

**<sup>13</sup>C NMR** (101 MHz, CDCl<sub>3</sub>) δ 170.6 (C<sup>I</sup>), 168.1 (C<sup>J</sup>), 135.5 (C<sup>L/R</sup>), 135.2 (C<sup>L/R</sup>), 128.7 (C<sup>N/T</sup>), 128.6 (2 peaks, (C<sup>N/T</sup> and C<sup>M/S</sup>), 128.5 (C<sup>M/S</sup>), 128.5 (C<sup>O/U</sup>), 127.7 (C<sup>O/U</sup>), 85.9 (C<sup>A</sup>), 71.6 (C<sup>H</sup>), 66.9 (C<sup>K/P</sup>), 66.8 (C<sup>K/P</sup>), 51.0 (C<sup>G</sup>), 39.6 (C<sup>B/F</sup>), 33.5 (C<sup>B/F</sup>), 24.8 (C<sup>C/D/E</sup>), 22.3 (C<sup>C/D/E</sup>), 21.6 (C<sup>C/D/E</sup>).

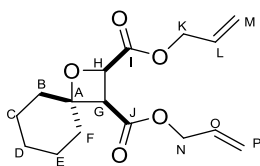
**FTIR** (ATR)  $\nu$  (cm<sup>-1</sup>): 2933 (C-H), 1735 (C=O).

**HRMS (ESI)**: *m/z* calculated for C<sub>24</sub>H<sub>26</sub>O<sub>5</sub>Na [M + Na]<sup>+</sup>: 417.1672, found at 417.1663.

*R<sub>f</sub>* (EtOAc-hexane, 2:3) = 0.47

**Lab-book reference**: WM-04-71,80

### ***rac*-(2*R*,3*R*)-Diallyl 1-oxaspiro[3.5]nonane-2,3-dicarboxylate (14g)**



**14g**

Chemical Formula: C<sub>16</sub>H<sub>22</sub>O<sub>5</sub>

Molecular Weight: 294.35

Using the general procedure, maleic anhydride (490 mg, 5.00 mmol) and cyclohexanone (1.60 mL, 15.00 mmol) were used in the Paternò-Büchi reaction (86 h irradiation). Using allyl alcohol (0.70 mL, 7.50 mmol) and stirring at reflux for 48 h in the second step, the crude product **B** was obtained, then dissolved in MeCN (25 mL) and used in the final step using allyl alcohol (0.70 mL, 7.50 mmol). Purification by flash chromatography (eluent 4:1-3:2 hexane-EtOAc) gave **14g** (361 mg, 1.23 mmol, 26%) as a colourless oil.

**<sup>1</sup>H NMR** (400 MHz, CDCl<sub>3</sub>) δ 6.00 – 5.83 (m, 2H, H<sup>L/O</sup>), 5.37 – 5.28 (m, 2H, H<sup>P/M</sup>), 5.28-5.21 (m, 2H, H<sup>P/M</sup>), 5.06 (d, *J* = 8.8 Hz, 1H, H<sup>H</sup>), 4.76-4.62 (m, 2H, H<sup>N/K</sup>), 4.62-4.52 (m, 2H, H<sup>N/K</sup>), 3.72 (d, *J* = 8.8 Hz, 1H, H<sup>G</sup>), 1.99-1.31 (m, 10H, H<sup>B, C, D, E, F</sup>).

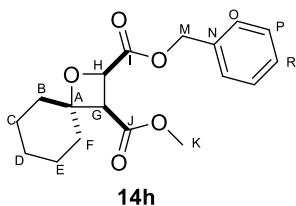
**<sup>13</sup>C NMR** (101 MHz, CDCl<sub>3</sub>) δ 170.5 (C<sup>I</sup>), 168.0 (C<sup>J</sup>), 132.0 (C<sup>L/O</sup>), 131.6 (C<sup>L/O</sup>), 119.1 (C<sup>M/P</sup>), 118.6 (C<sup>M/P</sup>), 85.7 (C<sup>A</sup>), 71.6 (C<sup>H</sup>), 65.8 (C<sup>K/N</sup>), 65.7 (C<sup>K/N</sup>), 51.1 (C<sup>G</sup>), 39.6 (C<sup>B/F</sup>), 33.5 (C<sup>B/F</sup>), 24.8 (C<sup>C/D/E</sup>), 22.3 (C<sup>C/D/E</sup>), 21.6 (C<sup>C/D/E</sup>).

**FTIR** (ATR) ν (cm<sup>-1</sup>): 2933 (C-H), 1735 (C=O).

**HRMS (ESI)**: *m/z* calculated for C<sub>16</sub>H<sub>22</sub>O<sub>5</sub>Na [M + Na]<sup>+</sup>: 317.1353, found at 317.1353

**Lab-book reference**: WM-06-28

### ***rac*-(2*R*,3*R*)-2-Benzyl 3-methyl 1-oxaspiro[3.5]nonane-2,3-dicarboxylate (14h)**



Chemical Formula: C<sub>18</sub>H<sub>22</sub>O<sub>5</sub>  
Molecular Weight: 318.37

**1 mmol scale** - Using the general procedure, maleic anhydride (98 mg, 1 mmol) and cyclohexanone (0.32 mL, 3.00 mmol) were used in the Paternò-Büchi reaction (86 h irradiation). Using benzyl alcohol (0.10 mL, 1 mmol) and stirring at reflux for 72 h in the second step, the crude product **B** was obtained, then dissolved in MeCN (5 mL) and used in the final step methanol (0.10 mL, 2 mmol). Purification by flash chromatography (eluent 9:1-3:2 hexane-EtOAc) gave **14h** (70 mg, 0.22 mmol, 22%) as a colourless oil.

**30 mmol scale** Using the general procedure, maleic anhydride (2.94 g, 30 mmol) and cyclohexanone (9.60 mL, 90.0 mmol) were used in the Paternò-Büchi reaction (86 h irradiation). Using benzyl alcohol (3.12 mL, 30 mmol) and stirring at reflux for 72 h in the second step, the crude product **B** was obtained, then dissolved in MeCN (60 mL) and used in the final step methanol (2.42 mL, 60 mmol). Purification by flash chromatography (eluent 9:1-3:2 hexane-EtOAc) gave **14h** (2.26 mg, 6.1 mmol, 20%) as a colourless oil.

**<sup>1</sup>H NMR** (400 MHz, CDCl<sub>3</sub>) δ 7.38-7.31 (m, 5H, H<sup>O,P,R</sup>), 5.27 (d, *J* = 12.2 Hz, 1H, H<sup>M</sup>), 5.21 (d, *J* = 12.2 Hz, 1H, H<sup>M</sup>), 5.07 (d, *J* = 8.9 Hz, 1H, H<sup>H</sup>), 3.70 (d, *J* = 8.9 Hz, 1H, H<sup>G</sup>), 3.59 (s, 3H, H<sup>K</sup>), 1.92-1.30 (m, 10H, H<sup>B,C,D,E,F</sup>).

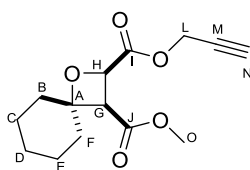
**<sup>13</sup>C NMR** (101 MHz, CDCl<sub>3</sub>) δ 170.6 (C<sup>I</sup>), 168.7 (C<sup>J</sup>), 135.5 (C<sup>N</sup>), 128.7 (C<sup>P</sup>), 128.5 (C<sup>O</sup>), 128.3 (C<sup>R</sup>), 85.7 (C<sup>A</sup>), 71.6 (C<sup>H</sup>), 66.9 (C<sup>M</sup>), 51.8 (C<sup>K</sup>), 50.9 (C<sup>G</sup>), 39.5 (C<sup>B/F</sup>), 33.5 (C<sup>B/F</sup>), 24.8 (C<sup>C/D/E</sup>), 22.2 (C<sup>C/D/E</sup>), 21.6 (C<sup>C/D/E</sup>).

**FTIR** (ATR)  $\nu$  (cm<sup>-1</sup>): 2931 (C-H), 1735 (C=O).

**HRMS (APCI)**: *m/z* calculated for C<sub>18</sub>H<sub>23</sub>O<sub>5</sub> [M + H]<sup>+</sup>: 319.1540, found at 319.1531.

**Lab-book reference**: WM-06-90

### ***rac*-(2*R*,3*R*)-3-Methyl 2-prop-2-yn-1-yl 1-oxaspiro[3.5]nonane-2,3-dicarboxylate (14i)**



**14i**

Chemical Formula: C<sub>14</sub>H<sub>18</sub>O<sub>5</sub>

Molecular Weight: 266.29

Using the general procedure, maleic anhydride (98 mg, 1.00 mmol) and cyclohexanone (0.32 mL, 3.00 mmol) were used in the Paternò-Büchi reaction (86 h irradiation). Using propargyl alcohol (0.12 mL, 2.00 mmol) and stirring at reflux for 48 h in the second step, the crude product **B** was obtained, then dissolved in MeCN (4 mL) and used in the final step using methanol (0.10 mL, 2.00 mmol). Purification by flash chromatography (eluent 9:1-4:1 hexane-EtOAc) gave **14i** (40 mg, 0.17 mmol, 17%) as a colourless oil.

**<sup>1</sup>H NMR** (400 MHz, CDCl<sub>3</sub>) δ 5.07 (d, *J* = 8.8 Hz, 1H, H<sup>H</sup>), 4.86 (dd, *J* = 15.6, 2.5 Hz, 1H, H<sup>L</sup>), 4.82 (dd, *J* = 15.6, 2.5 Hz, 1H, H<sup>L</sup>), 3.71 (d, *J* = 8.8 Hz, 1H, H<sup>G</sup>), 3.68 (s, 3H, H<sup>O</sup>), 2.48 (t, *J* = 2.5 Hz, 1H, H<sup>N</sup>), 1.90-1.29 (m, 10H, H<sup>B,C,D,E,F</sup>).

**<sup>13</sup>C NMR** (101 MHz, CDCl<sub>3</sub>) δ 170.1 (C<sup>I</sup>), 168.6 (C<sup>J</sup>), 86.0 (C<sup>A</sup>), 77.3 (C<sup>N</sup>), 75.2 (C<sup>H</sup>), 71.4 (C<sup>M</sup>), 52.5 (C<sup>L</sup>), 52.0 (C<sup>O</sup>), 51.0 (C<sup>G</sup>), 39.5 (C<sup>B/F</sup>), 33.5 (C<sup>B/F</sup>), 24.8 (C<sup>C/D/E</sup>), 22.2 (C<sup>C/D/E</sup>), 21.5 (C<sup>C/D/E</sup>).

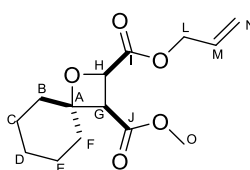
**FTIR** (ATR)  $\nu$  (cm<sup>-1</sup>): 2933 (C-H), 2120 (weak, C≡C), 1764 (C=O), 1735 (C=O).

**HRMS (ESI)**: *m/z* calculated for C<sub>14</sub>H<sub>19</sub>O<sub>5</sub> [M + H]<sup>+</sup>: 267.1227, found: 267.1240.

**R<sub>f</sub>**: (EtOAc-hexane, 1:4) = 0.16.

**Lab-book reference**: WM-05-67

### ***rac*-(2*R*,3*R*)-2-Allyl 3-methyl 1-oxaspiro[3.5]nonane-2,3-dicarboxylate (14j)**



**14j**

Chemical Formula: C<sub>14</sub>H<sub>20</sub>O<sub>5</sub>

Molecular Weight: 268.30

Using the general procedure, maleic anhydride (98 mg, 1.00 mmol) and cyclohexanone (0.32 mL, 3.00 mmol) were used in the Paternò-Büchi reaction (86 h irradiation). Using allyl alcohol (0.14 mL, 2.00 mmol) and stirring at reflux for 48 h in the second step, the crude product **B** was obtained, then dissolved in MeCN (3 mL) and used in the final step using methanol (0.10 mL, 2.00 mmol). Purification by flash chromatography (eluent 1:4 EtOAc-hexane) gave **14j** (81 mg, 0.31 mmol, 31%) as a yellow oil.

**<sup>1</sup>H NMR** (400 MHz, CDCl<sub>3</sub>) δ 5.95 (ddt, *J* = 17.2, 10.4, 5.9 Hz, 1H, H<sup>M</sup>), 5.34 (dq, *J* = 17.2, 1.5 Hz, 1H, H<sup>N</sup>), 5.24 (ddd, *J* = 10.4, 2.5, 1.2 Hz, 1H, H<sup>N</sup>), 5.05 (d, *J* = 8.8 Hz, 1H, HH), 4.74 (ddt, *J* = 13.0, 5.9, 1.3 Hz, 1H, H<sup>L</sup>), 4.67 (ddt, *J* = 13.0, 5.9, 1.3 Hz, 1H, H<sup>L</sup>), 3.70 (d, *J* = 8.8 Hz, 1H, H<sup>G</sup>), 3.68 (s, 3H, H<sup>O</sup>), 1.87-1.31 (m, 10H, H<sup>B/C/D/E/F</sup>).

**<sup>13</sup>C NMR** (101 MHz, CDCl<sub>3</sub>) δ 170.5 (C<sup>I</sup>), 168.7 (C<sup>J</sup>), 132.0 (C<sup>M</sup>), 118.7 (C<sup>N</sup>), 85.7 (C<sup>A</sup>), 71.6 (C<sup>H</sup>), 65.8 (C<sup>L</sup>), 51.9 (C<sup>O</sup>), 51.0 (C<sup>G</sup>), 39.5 (C<sup>B/F</sup>), 33.5 (C<sup>B/F</sup>), 24.8 (C<sup>C/D/E</sup>), 22.2 (C<sup>C/D/E</sup>), 21.6 (C<sup>C/D/E</sup>).

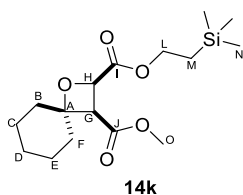
**FTIR** (ATR) ν (cm<sup>-1</sup>): 2933 (C-H), 1735 (C=O).

**HRMS (ESI)**: *m/z* calculated for C<sub>14</sub>H<sub>20</sub>NO<sub>5</sub>Na [M + Na]<sup>+</sup>: 291.1203, found: 219.1202.

**R<sub>f</sub>**: (EtOAc-hexane, 1:4) = 0.31.

**Lab-book reference**: WM-05-46

**(2*R*,3*R*)-3-Methyl 2-(2-(trimethylsilyl)ethyl) 1-oxaspiro[3.5]nonane-2,3-dicarboxylate (14k)**



**14k**

Chemical Formula: C<sub>16</sub>H<sub>28</sub>O<sub>5</sub>Si  
Molecular Weight: 328.48

Using the general procedure, maleic anhydride (98 mg, 1.00 mmol) and cyclohexanone (0.32 mL, 3.00 mmol) were used in the Paternò-Büchi reaction (86 h irradiation). Using 2-(trimethylsilyl)ethanol (0.29 mL, 2.00 mmol) and stirring at reflux for 48 h in the second step, the crude product **B** was obtained, then dissolved in MeCN (3 mL) and used in the final step, using methanol (0.10 mL, 2.00 mmol). Purification by flash chromatography (eluent 19:1-9:1 hexane-EtOAc) gave **14k** (60 mg, 0.19 mmol, 19%) as a colourless oil.

**<sup>1</sup>H NMR** (400 MHz, CDCl<sub>3</sub>) δ 5.01 (d, *J* = 8.8 Hz, 1H, H<sup>H</sup>), 4.45 – 4.21 (m, 4H, H<sup>L, M</sup>), 3.69 (d, *J* = 8.8 Hz, 1H, H<sup>G</sup>), 3.69 (s, 3H, H<sup>O</sup>), 1.92-1.62 (m, 10H, H<sup>B, C, D, E, F</sup>), 0.04 (s, 9H, H<sup>N</sup>).

**<sup>13</sup>C NMR** (101 MHz, CDCl<sub>3</sub>) δ 170.9 (C<sup>I</sup>), 168.8 (C<sup>J</sup>), 85.5 (C<sup>A</sup>), 71.6 (C<sup>H</sup>), 63.5 (C<sup>L</sup>), 51.8 (C<sup>G</sup>), 50.9 (C<sup>O</sup>), 39.5 (C<sup>B/F</sup>), 33.6 (C<sup>B/F</sup>), 24.8 (C<sup>C/D/E</sup>), 22.3 (C<sup>C/D/E</sup>), 21.6 (C<sup>C/D/E</sup>), 17.3 (C<sup>M</sup>), -1.5 (C<sup>N</sup>).

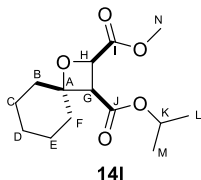
**FTIR** (ATR) ν (cm<sup>-1</sup>): 2935 (C-H), 1740 (C=O).

**HRMS (ESI)**: *m/z* calculated for C<sub>16</sub>H<sub>28</sub>O<sub>5</sub>SiNa [M + Na]<sup>+</sup>: 351.1603, found at 351.1603.

**R<sub>f</sub>**: (EtOAc-hexane, 2:3) = 0.52

Lab-book reference: WM-05-69

***rac*-(2*R*,3*R*)-3-Isopropyl 2-methyl 1-oxaspiro[3.5]nonane-2,3-dicarboxylate (14l)**



Chemical Formula: C<sub>14</sub>H<sub>22</sub>O<sub>5</sub>  
Molecular Weight: 270.33

Using the general procedure, maleic anhydride (98 mg, 1.00 mmol) and cyclohexanone (0.32 mL, 3.00 mmol) were used in the Paternò-Büchi reaction (86 h irradiation). Using methanol (0.10 mL, 2.00 mmol) and stirring at reflux for 48 h in the second step, the crude product B was obtained, then dissolved in MeCN (3 mL) and used in the final step using isopropanol (0.15 mL, 2.00 mmol). Purification by flash chromatography (eluent 4:1-3:2 hexane-EtOAc) gave **14l** (61 mg, 0.23 mmol, 23%) as a yellow oil.

<sup>1</sup>H NMR (400 MHz, CDCl<sub>3</sub>) δ 5.06 (d, *J* = 8.8 Hz, 1H, H<sup>H</sup>), 5.02 (sept, *J* = 6.2 Hz, 1H, H<sup>K</sup>), 3.80 (s, 1H, H<sup>M</sup>), 3.62 (d, *J* = 8.8 Hz, 1H, H<sup>G</sup>), 1.91-1.63 (m, 10H, H<sup>B, C, D, E, F</sup>), 1.24 (d, *J* = 6.3 Hz, 3H, H<sup>L/M</sup>), 1.23 (d, *J* = 6.3 Hz, 3H, H<sup>L/M</sup>).

<sup>13</sup>C NMR (101 MHz, CDCl<sub>3</sub>) δ 171.4 (C<sup>I</sup>), 167.9 (C<sup>J</sup>), 85.6 (C<sup>A</sup>), 71.8 (C<sup>H</sup>), 68.8 (C<sup>K</sup>), 52.0 (C<sup>N</sup>), 51.4 (C<sup>G</sup>), 39.4 (C<sup>B/F</sup>), 33.5 (C<sup>B/F</sup>), 24.9 (C<sup>C/D/E</sup>), 22.3 (C<sup>C/D/E</sup>), 21.8 (C<sup>C/D/E</sup>), 21.8 (C<sup>M/L</sup>), 21.6 (C<sup>M/L</sup>).

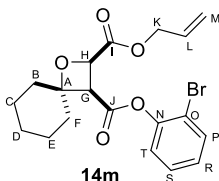
FTIR (ATR) ν (cm<sup>-1</sup>): 2933 (C-H), 1763 (C=O), 1729 (C=O).

HRMS (ESI): *m/z* calculated for C<sub>14</sub>H<sub>22</sub>O<sub>5</sub>Na [M + Na]<sup>+</sup>: 293.1359, found: 293.1351.

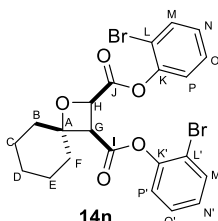
*R*<sub>f</sub> (EtOAc – hexane, 2:3) = 0.20

Lab-book reference: WM-06-04

***rac*-(2*R*,3*R*)-3-(2-Bromophenyl) 2-prop-2-en-1-yl 1-oxaspiro[3.5]nonane-2,3-dicarboxylate (14m) and *rac*-(2*R*,3*R*)-2,3-bis(2-bromophenyl) 1-oxaspiro[3.5]nonane-2,3-dicarboxylate (14n)**



Chemical Formula: C<sub>19</sub>H<sub>21</sub>BrO<sub>5</sub>  
Molecular Weight: 409.28



Chemical Formula: C<sub>22</sub>H<sub>20</sub>Br<sub>2</sub>O<sub>5</sub>  
Molecular Weight: 524.21

Using the general procedure, maleic anhydride (490 mg, 5.00 mmol) and cyclohexanone (1.60 mL, 15.00 mmol) were used in the Paternò-Büchi reaction. The reaction was irradiated for 86 h. Using allyl alcohol (0.70 mL, 7.50 mmol) and the reaction mixture

was heated at reflux for 72 h in the second step, the crude product B was obtained. Crude product B was directly used in final step (1-bromophenol (0.7 mL, 5.50 mmol). Purification by flash chromatography (eluent 4:1-3:2 hexane-EtOAc) gave **14m** (329 mg, 0.78 mmol, 16 %) as a colourless oil and **14n** (40 mg, 0.08 mmol, 2 %).

**14m:**

**<sup>1</sup>H NMR** (400 MHz, CDCl<sub>3</sub>) δ 7.63 – 7.58 (m, 1H, H<sup>P</sup>), 7.36 – 7.28 (m, 1H, H<sup>S</sup>), 7.17 – 7.11 (m, 2H, H<sup>R, T</sup>), 5.99 – 5.87 (m, 1H, H<sup>L</sup>), 5.32 (dd, *J* = 17.2, 1.5 Hz, 1H, H<sup>M</sup>), 5.21 (dd, *J* = 10.4, 1.5 Hz, 1H, H<sup>M</sup>), 5.18 (d, *J* = 8.9 Hz, 1H, H<sup>H</sup>), 4.73 (ddd, *J* = 7.2, 5.9, 3.6 Hz, 1H, H<sup>K</sup>), 4.63 (ddd, *J* = 13.0, 7.2, 3.6 Hz, 1H, H<sup>K</sup>), 4.04 (d, *J* = 8.9 Hz, 1H, H<sup>G</sup>), 2.09 – 1.24 (m, 10H, H<sup>B, C, D, E, F</sup>).

**<sup>13</sup>C NMR** (101 MHz, CDCl<sub>3</sub>) δ 170.1 (C<sup>I</sup>), 166.0 (C<sup>J</sup>), 147.7 (C<sup>N</sup>), 133.5 (C<sup>P</sup>), 131.9 (C<sup>L</sup>), 128.5 (C<sup>S</sup>), 127.6 (C<sup>R</sup>), 123.61 (C<sup>T</sup>), 118.8 (C<sup>M</sup>), 115.7 (C<sup>O</sup>), 86.0 (C<sup>A</sup>), 71.5 (C<sup>H</sup>), 66.01 (C<sup>K</sup>), 50.6 (C<sup>G</sup>), 39.7 (C<sup>B/F</sup>), 33.6 (C<sup>B/F</sup>), 24.8 (C<sup>C/D/E</sup>), 22.2 (C<sup>C/D/E</sup>), 21.7 (C<sup>C/D/E</sup>).

**FTIR** (ATR)  $\nu$  (cm<sup>-1</sup>): 2933 (C-H), 1734 (C=O).

**HRMS (APCI):** *m/z* calculated for C<sub>19</sub>H<sub>21</sub>O<sub>5</sub>BrNa [M + Na]<sup>+</sup>: 431.0465, found at 431.0444 (<sup>79</sup>Br); 433.0447 (<sup>81</sup>Br).

**R<sub>f</sub>:** (EtOAc-hexane, 1:4) = 0.23

**Lab-book reference:** WM-06-30

**14n:**

**<sup>1</sup>H NMR** (400 MHz, CDCl<sub>3</sub>) δ 7.65-7.58 (m, 2H, H<sup>M, M'</sup>), 7.36 – 7.24 (m, 3H, H<sup>N/N'/O/O'</sup>), 7.17 – 7.07 (m, 3H, H<sup>N/N'/P/P'</sup>), 5.48 (d, *J* = 8.8 Hz, 1H, H<sup>H</sup>), 4.20 (d, *J* = 8.8 Hz, 1H, H<sup>G</sup>), 2.19 – 1.35 (m, 10H, H<sup>B, C, D, E, F</sup>).

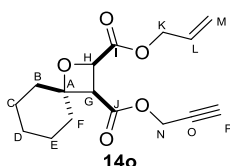
**<sup>13</sup>C NMR** (101 MHz, CDCl<sub>3</sub>) δ 168.0 (C<sup>J</sup>), 166.2 (C<sup>I</sup>), 147.8 (C<sup>K/K'</sup>), 147.7 (C<sup>K/K'</sup>), 133.6 (C<sup>M/M'</sup>), 133.1 (C<sup>M/M'</sup>), 128.5 (C<sup>O/O'</sup>), 128.5 (C<sup>O/O'</sup>), 127.7 (C<sup>N/N'</sup>), 127.4 (C<sup>N/N'</sup>), 124.0 (C<sup>P/P'</sup>), 123.6 (C<sup>P/P'</sup>), 115.8 (C<sup>L/L'</sup>), 115.7 (C<sup>L/L'</sup>), 86.4 (C<sup>A</sup>), 71.3 (C<sup>H</sup>), 50.9 (C<sup>G</sup>), 39.6 (C<sup>B/F</sup>), 33.6 (C<sup>B/F</sup>), 24.8 (C<sup>C/D/E</sup>), 22.2 (C<sup>C/D/E</sup>), 21.6 (C<sup>C/D/E</sup>).

**FTIR** (ATR)  $\nu$  (cm<sup>-1</sup>): 2935 (C-H), 1778 (C=O), 1763 (C=O)

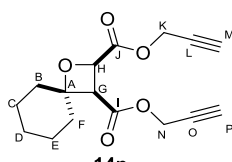
**R<sub>f</sub>:** (EtOAc-hexane, 1:4) = 0.34

**Lab-book reference:** WM-06-30\_SP

***rac*-(2*R*,3*R*)-2-Prop-2-en-1-yl 3-prop-2-yn-1-yl 1-oxaspiro[3.5]nonane-2,3-dicarboxylate (14o) and *rac*-(2*R*,3*R*)-2,3-bis(prop-2-yn-1-yl) 1-oxaspiro[3.5]nonane-2,3-dicarboxylate (14p)**



**14o**  
Chemical Formula: C<sub>16</sub>H<sub>20</sub>O<sub>5</sub>  
Molecular Weight: 292.33



**14p**  
Chemical Formula: C<sub>16</sub>H<sub>18</sub>O<sub>5</sub>  
Molecular Weight: 290.32

Using the general procedure, maleic anhydride (490 mg, 5.00 mmol) and cyclohexanone (1.60 mL, 15.00 mmol) were used in the Paternò-Büchi reaction. The reaction was irradiated for 86 h. Using allyl alcohol (0.70 mL, 7.50 mmol) and the reaction mixture

was heated at reflux for 72 h in the second step, the crude product B was obtained. Crude product B was directly used in final step propargyl alcohol (0.57 mL, 5.50 mmol). Purification by flash chromatography (eluent 4:1-3:2 hexane-EtOAc) gave **14o** (143 mg, 0.49 mmol, 10 %) as a colourless oil and **14p** (43 mg, 0.15 mmol, 3 %).

**14o:**

**<sup>1</sup>H NMR** (400 MHz, CDCl<sub>3</sub>) δ 5.95 (dq, *J* = 10.4, 5.9 Hz, 1H, H<sup>L</sup>), 5.34 (dd, *J* = 17.2, 1.4 Hz, 1H, H<sup>M</sup>), 5.24 (d, *J* = 10.4 Hz, 1H, H<sup>M</sup>), 5.07 (d, *J* = 8.8 Hz, 1H, H<sup>H</sup>), 4.78 – 4.60 (m, 4H, H<sup>N, K</sup>), 3.74 (d, *J* = 8.8 Hz, 1H, H<sup>G</sup>), 2.47 (t, *J* = 2.5 Hz, 1H, H<sup>P</sup>), 1.98 – 1.30 (m, 10H, H<sup>B, C, D, E, F</sup>).

**<sup>13</sup>C NMR** (101 MHz, CDCl<sub>3</sub>) δ 170.3 (C<sup>I</sup>), 167.5 (C<sup>J</sup>), 131.9 (C<sup>L</sup>), 118.7 (C<sup>M</sup>), 85.8 (C<sup>A</sup>), 75.4 (C<sup>O</sup>), 71.4 (C<sup>H</sup>), 65.9 (C<sup>K</sup>), 52.3 (C<sup>N</sup>), 50.7 (C<sup>G</sup>), 39.5 (C<sup>B/F</sup>), 33.5 (C<sup>B/F</sup>), 24.8 (C<sup>C/D/E</sup>), 22.2 (C<sup>C/D/E</sup>), 21.6 (C<sup>C/D/E</sup>).

C<sup>P</sup> likely under chloroform peak at 77.3

**FTIR** (ATR) ν (cm<sup>-1</sup>): 2933 (C-H), 1735 (C=O).

**MS (ESI):** *m/z* calculated for C<sub>16</sub>H<sub>20</sub>O<sub>5</sub>Na [M+Na]<sup>+</sup>: 315.1203, found at 315.1191.

*R<sub>f</sub>*: (EtOAc-hexane, 2:3) = 0.45

Lab-book reference: WM-06-29

**14p:**

**<sup>1</sup>H NMR** (400 MHz, CDCl<sub>3</sub>) δ 5.09 (d, *J* = 8.8 Hz, 1H, H<sup>H</sup>), 4.87 (dd, *J* = 15.6, 2.5 Hz, 1H, H<sup>N/K</sup>), 4.76 (dd, *J* = 15.6, 2.5 Hz, 1H, H<sup>N/K</sup>), 4.74 (dd, *J* = 15.6, 2.5 Hz, 1H, H<sup>N/K</sup>), 4.66 (dd, *J* = 15.6, 2.5 Hz, 1H, H<sup>N/K</sup>), 3.75 (d, *J* = 8.8 Hz, 1H, H<sup>G</sup>), 2.49 (t, *J* = 2.5 Hz, 2H, H<sup>M, P</sup>), 1.97 – 1.28 (m, 10H, H<sup>B, C, D, E, F</sup>).

**<sup>13</sup>C NMR** (101 MHz, CDCl<sub>3</sub>) δ 169.8 (C<sup>J</sup>), 167.5 (C<sup>I</sup>), 86.1 (C<sup>A</sup>), 77.3 (C<sup>P, M</sup> two peaks) 75.5 (C<sup>O/L</sup>), 75.3 (C<sup>O/L</sup>), 71.3 (C<sup>H</sup>), 52.7 (C<sup>N/K</sup>), 52.4 (C<sup>N/K</sup>), 50.8 (C<sup>G</sup>), 39.5 (C<sup>B/F</sup>), 33.5 (C<sup>B/F</sup>), 24.7 (C<sup>C/D/E</sup>), 22.2 (C<sup>C/D/E</sup>), 21.6 (C<sup>C/D/E</sup>).

C<sup>M</sup> and C<sup>P</sup> peaks likely under chloroform peak ~77.3

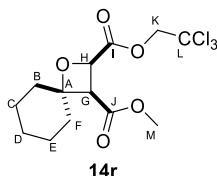
**FTIR** (ATR) ν (cm<sup>-1</sup>): 2935 (C-H), 1742 (C=O).

**MS (ESI):** *m/z* calculated for C<sub>16</sub>H<sub>18</sub>O<sub>5</sub>Na [M+Na]<sup>+</sup>: 313.1049, found at 313.1049

*R<sub>f</sub>*: (EtOAc-hexane, 2:3) = 0.32

Lab-book reference: WM-06-29\_SP

***rac*-(2*R*,3*R*)-3-Methyl 2-(2,2,2-trichloroethyl) 1-oxaspiro[3.5]nonane-2,3-dicarboxylate (**14r**)**



Chemical Formula: C<sub>13</sub>H<sub>17</sub>Cl<sub>3</sub>O<sub>5</sub>  
Molecular Weight: 359.62

Using the general procedure, maleic anhydride (98 mg, 1.00 mmol) and cyclohexanone (0.32 mL, 3.00 mmol) were used in the Paternò-Büchi reaction (86 h irradiation). Using

2,2,2-trichloroethanol (0.29 mL, 2.00 mmol) and stirring at reflux for 30 h in the second step, the crude product B was obtained, then dissolved in MeCN (3 mL) and used in the final step using methanol (0.10 mL, 2.00 mmol). Purification by flash chromatography (eluent 19:1-9:1 hexane-EtOAc) gave **14r** (35 mg, 0.10 mmol, 10%) as a yellow oil.

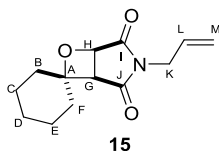
**<sup>1</sup>H NMR** (400 MHz, CDCl<sub>3</sub>) δ 5.19 (d, *J* = 8.9 Hz, 1H, H<sup>H</sup>), 5.01 (d, *J* = 11.9 Hz, 1H, H<sup>K</sup>), 4.64 (d, *J* = 11.9 Hz, 1H, H<sup>K</sup>), 3.81 (d, *J* = 8.9 Hz, 1H, H<sup>G</sup>), 3.72 (s, 3H, H<sup>M</sup>), 2.04 – 1.31 (m, 10H, H<sup>B, C, D, E, F</sup>).

**<sup>13</sup>C NMR** (101 MHz, CDCl<sub>3</sub>) δ 169.4 (C<sup>I</sup>), 168.6 (C<sup>J</sup>), 94.5 (C<sup>L</sup>), 86.3 (C<sup>A</sup>), 74.9 (C<sup>H</sup>), 71.3 (C<sup>K</sup>), 52.1 (C<sup>M</sup>), 50.9 (C<sup>G</sup>), 39.6 (C<sup>B/C/D/E/F</sup>), 33.5 (C<sup>B/C/D/E/F</sup>), 24.8 (C<sup>B/C/D/E/F</sup>), 22.2 (C<sup>B/C/D/E/F</sup>), 21.5 (C<sup>B/C/D/E/F</sup>).

**FTIR** (ATR)  $\nu$  (cm<sup>-1</sup>): 2931 (C-H), 1735 (C=O).

**Lab-book reference:** WM-06-70 (2021-12-01-WM-06-72\_all-but nmr run under wrong name) (WM-06-08, WM-6-70)

### 3-(Prop-2-en-1-yl)-7-oxa-3-azaspiro[bicyclo[3.2.0]heptane-6,1'-cyclohexane]-2,4-dione (**15**)



Chemical Formula: C<sub>13</sub>H<sub>17</sub>NO<sub>3</sub>  
Molecular Weight: 235.2830

Using the general procedure, maleic anhydride (98 mg, 1.00 mmol) and cyclohexanone (0.32 mL, 3.00 mmol) were used in the Paternò-Büchi reaction (86 h irradiation). Using methanol (0.10 mL, 2.00 mmol) and stirring at reflux for 30 h in the second step, the crude product B was obtained, then dissolved in MeCN (3 mL) and used in the final step using allyl amine (0.13 mL, 2.00 mmol). Purification by flash chromatography (eluent 19:1-9:1 hexane-EtOAc) gave **15** (40 mg, 0.15 mmol, 15%) as a yellow oil.

**<sup>1</sup>H NMR** (400 MHz, CDCl<sub>3</sub>) δ 5.93 – 5.79 (m, 1H, H<sup>L</sup>), 5.35 (dq, *J* = 17.1, 1.2 Hz, 1H, H<sup>M</sup>), 5.26 (dq, *J* = 10.2, 1.2 Hz, 1H, H<sup>M</sup>), 4.95 (d, *J* = 5.6 Hz, 1H, H<sup>H</sup>), 4.27 – 4.21 (m, 1H, H<sup>K</sup>), 4.21 – 4.16 (m, 1H, H<sup>K</sup>), 3.37 (d, *J* = 5.6 Hz, 1H, H<sup>G</sup>), 1.99 – 1.32 (m, 10H, H<sup>B, C, D, E, F</sup>).

**<sup>13</sup>C NMR** (101 MHz, CDCl<sub>3</sub>) δ 174.4 (C<sup>I</sup>), 173.8 (C<sup>J</sup>), 130.2 (C<sup>L</sup>), 119.4 (C<sup>M</sup>), 87.8 (C<sup>A</sup>), 72.1 (C<sup>H</sup>), 47.8 (C<sup>G</sup>), 41.1 (C<sup>K</sup>), 39.0 (C<sup>B/C/D/E/F</sup>), 35.3 (C<sup>B/C/D/E/F</sup>), 24.6 (C<sup>B/C/D/E/F</sup>), 22.1 (C<sup>B/C/D/E/F</sup>), 21.8 (C<sup>B/C/D/E/F</sup>).

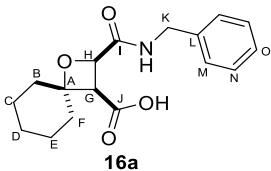
**FTIR** (ATR)  $\nu$  (cm<sup>-1</sup>): 2933 (C-H), 1703 (C=O, broad/could be two peaks)

**Lab-book reference:** WM-06-03



#### 7.4.2.2.2 Ring opening of anhydride with various amines

### ***rac*-(2*R*,3*R*)-2-(Benzylcarbamoyl)-1-oxaspiro[3.5]nonane-3-carboxylic acid (16a)**



Chemical Formula: C<sub>17</sub>H<sub>21</sub>NO<sub>4</sub>  
Molecular Weight: 303.3580

Using the general procedure, maleic anhydride (98 mg, 1 mmol) and cyclohexanone (0.32 mL, 3.00 mmol) were used in the Paternò-Büchi reaction. The reaction was irradiated for 86 h. Next, the benzyl amine (0.20 mL 2.00 mmol) was added, and the reaction mixture was stirred at room temperature for 24 h, until full consumption of oxetane A, as judged by <sup>1</sup>H NMR spectroscopy (solvent suppression). The solvent was evaporated under reduced pressure to give the crude product **16a**. Solid formed upon drying the crude mixture, the solid was separated by filtration and dried by vacuum filtration. Recrystallization from MeOH gave **16a** (10 mg, 0.03 mmol, 3%) as a white solid.

**<sup>1</sup>H NMR** (400 MHz, CDCl<sub>3</sub>) δ 7.41 – 7.15 (m, 5H, H<sup>M, N, O</sup>), 5.15 (s, 1H, *N*-H), 4.82 (d, *J* = 8.8 Hz, 1H, H<sup>H</sup>), δ 4.46 (dd, *J* = 15.1, 6.4 Hz, 1H, H<sup>K</sup>), 4.31 (dd, *J* = 15.1, 6.4 Hz, 1H, H<sup>K</sup>). 3.43 (d, *J* = 8.8 Hz, 1H, H<sup>G</sup>), 1.94 – 1.21 (m, 10H, H<sup>B, C, D, E, F</sup>).

**<sup>13</sup>C NMR** (101 MHz, CDCl<sub>3</sub>) δ 174.0 (C<sup>I</sup>), 173.3 (C<sup>J</sup>), 138.0 (C<sup>L</sup>), 128.7 (C<sup>N</sup>), 128.6 (C<sup>M</sup>), 128.1 (C<sup>O</sup>), 85.8 (C<sup>A</sup>), 74.1 (C<sup>H</sup>), 53.3 (C<sup>G</sup>), 44.0 (C<sup>K</sup>), 39.8 (C<sup>B/F</sup>), 34.0 (C<sup>B/F</sup>), 25.0 (C<sup>C/D/E</sup>), 22.4 (C<sup>C/D/E</sup>), 21.9 (C<sup>C/D/E</sup>).

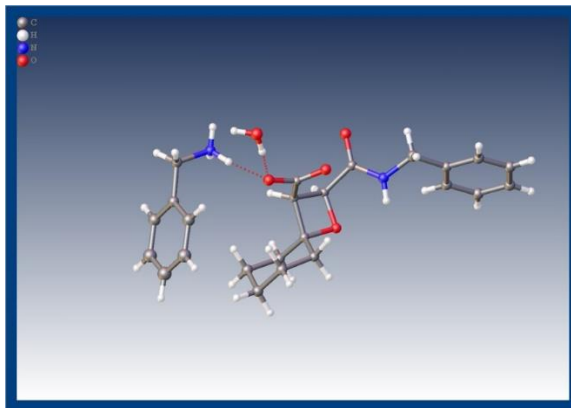
**MS (ESI):** *m/z* calculated for C<sub>17</sub>H<sub>22</sub>NO<sub>4</sub> [M+H]<sup>+</sup>: 302.1398, found: 302.1385.

**FTIR** (ATR) *v* (cm<sup>-1</sup>): 3390 (*N*-H), 2931-2853 (very broad, O-H + *N*-H), 1647 (C=O, amide).

**Melting point:** 130-135 °C

**Lab-book reference:** WM-05-44\_B

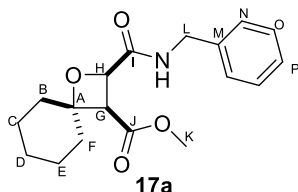
**Crystal structure:**



Empirical formula	C <sub>24</sub> H <sub>32</sub> N <sub>2</sub> O <sub>5</sub>
Formula weight	428.51

Temperature/K	99.95(13)
Crystal system	triclinic
Space group	P-1
a/Å	6.2334(2)
b/Å	12.7173(4)
c/Å	14.4459(4)
$\alpha$ /°	75.632(3)
$\beta$ /°	84.642(2)
$\gamma$ /°	84.812(2)
Volume/Å <sup>3</sup>	1101.80(6)
Z	2
$\rho_{\text{calc}}/\text{cm}^3$	1.292
$\mu/\text{mm}^{-1}$	0.734
F(000)	460.0
Crystal size/mm <sup>3</sup>	0.101 × 0.063 × 0.039
Radiation	Cu K $\alpha$ ( $\lambda$ = 1.54184)
2 $\theta$ range for data collection/°	7.194 to 152.79
Index ranges	-7 ≤ h ≤ 7, -15 ≤ k ≤ 15, -18 ≤ l ≤ 17
Reflections collected	16698
Independent reflections	4467 [R <sub>int</sub> = 0.0167, R <sub>sigma</sub> = 0.0140]
Data/restraints/parameters	4467/0/284
Goodness-of-fit on F <sup>2</sup>	1.041
Final R indexes [ $I \geq 2\sigma(I)$ ]	R <sub>1</sub> = 0.0323, wR <sub>2</sub> = 0.0801
Final R indexes [all data]	R <sub>1</sub> = 0.0344, wR <sub>2</sub> = 0.0816
Largest diff. peak/hole / e Å <sup>-3</sup>	0.26/-0.33

***rac*-(2*R*,3*R*)-Methyl 2-(benzylcarbamoyl)-1-oxaspiro[3.5]nonane-3-carboxylate (**17a**)**



Chemical Formula: C<sub>18</sub>H<sub>23</sub>NO<sub>4</sub>  
Molecular Weight: 317.38

Using the general procedure, maleic anhydride (98 mg, 1 mmol) and cyclohexanone (0.32 mL, 3.00 mmol) were used in the Paternò-Büchi reaction (86 h irradiation). Using benzylamine (0.22 mL, 2.00 mmol) and stirring at room temperature for 16 h in the second step, the crude product **B** was obtained, then dissolved in MeCN (4 mL) and directly used in the final step, using methanol (0.10 mL, 2.00 mmol). Purification by flash chromatography (eluent 7:3 to 1:4 hexane-EtOAc) gave **17a** (60 mg, 0.19 mmol, 19%) as a yellow oil.

**<sup>1</sup>H NMR** (400 MHz, CDCl<sub>3</sub>) δ 7.39-7.28 (m, 5H, H<sup>N, O, P</sup>), 7.07 (s, 1H, N-H), 5.00 (d, *J* = 8.8 Hz, 1H, H<sup>H</sup>), 4.57 (s - broad, 1H, H<sup>L</sup>), 4.55 (br s, 1H, H<sup>L</sup>), 3.68 (s, 3H, H<sup>K</sup>), 3.66 (d, *J* = 8.8 Hz, 1H, H<sup>G</sup>), 1.93-1.21 (m, 10H, H<sup>B, C, D, E, F</sup>).

**<sup>13</sup>C NMR** (101 MHz, CDCl<sub>3</sub>) δ 170.4 (C<sup>I</sup>), 168.8 (C<sup>J</sup>), 138.0 (C<sup>M</sup>), 128.7 (C<sup>O</sup>), 127.9 (C<sup>N</sup>), 127.5 (C<sup>P</sup>), 85.1 (C<sup>A</sup>), 72.7 (C<sup>H</sup>), 51.9 (C<sup>K</sup>), 50.2 (C<sup>G</sup>), 43.1 (C<sup>L</sup>), 39.6 (C<sup>B/F</sup>), 33.8 (C<sup>B/F</sup>), 24.7 (C<sup>C/D/E</sup>), 22.4 (C<sup>C/D/E</sup>), 21.8 (C<sup>C/D/E</sup>).

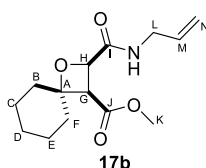
**FTIR** (ATR)  $\nu$  (cm<sup>-1</sup>): 3412 (broad, N-H), 2931 (C-H), 1735 (C=O, ester), 1669 (C=O, amide).

**HRMS (ESI)**: *m/z* calculated for C<sub>18</sub>H<sub>23</sub>NO<sub>4</sub>Na [M + Na]<sup>+</sup>: 340.1519, found at 340.1514.

**R<sub>f</sub>**: (EtOAc-hexane, 2:3) = 0.13.

**Lab-book reference**: WM-05-48

### ***rac*-(2*R*,3*R*)-Methyl 2-(allylcarbamoyl)-1-oxaspiro[3.5]nonane-3-carboxylate (**17b**)**



Chemical Formula: C<sub>14</sub>H<sub>21</sub>NO<sub>4</sub>

Molecular Weight: 267.3250

Using the general procedure, maleic anhydride (98 mg, 1 mmol) and cyclohexanone (0.32 mL, 3.00 mmol) were used in the Paternò-Büchi reaction (86 h irradiation). Using allyl amine (0.22 mL, 2.00 mmol) and stirring at room temperature for 16 h in the second step, the crude product **B** was obtained, then dissolved in MeCN (5 mL) and used in the final step using methanol (0.10 mL, 2.00 mmol). Purification by flash chromatography (eluent 3:2 hexane-EtOAc) gave **17b** (68 mg, 0.25 mmol, 25%) as a yellow oil.

**<sup>1</sup>H NMR** (400 MHz, CDCl<sub>3</sub>) δ 6.86 (s, 1H, N-H), 5.90 (ddt, *J* = 15.9, 10.3, 5.6 Hz, 1H, H<sup>M</sup>), 5.33-5.24 (m, 1H, H<sup>N</sup>), 5.16 (ddd, *J* = 10.3, 1.7, 1.1 Hz, 1H, H<sup>N</sup>), 4.94 (d, *J* = 8.8 Hz, 1H, H<sup>H</sup>), 4.07-3.89 (m, 2H, H<sup>L</sup>), 3.66 (s, 3H, H<sup>K</sup>), 3.62 (d, *J* = 8.8 Hz, 1H, H<sup>G</sup>), 1.96-1.15 (m, 10H, H<sup>B, C, D, E, F</sup>).

**<sup>13</sup>C NMR** (101 MHz, CDCl<sub>3</sub>) δ 170.3 (C<sup>I</sup>), 168.8 (C<sup>J</sup>), 134.1 (C<sup>M</sup>), 116.5 (C<sup>N</sup>), 85.1 (C<sup>A</sup>), 72.6 (C<sup>H</sup>), 51.8 (C<sup>K</sup>), 50.2 (C<sup>G</sup>), 41.3 (C<sup>L</sup>), 39.5 (C<sup>B/F</sup>), 33.8 (C<sup>B/F</sup>), 24.7 (C<sup>C/D/E</sup>), 22.4 (C<sup>C/D/E</sup>), 21.8 (C<sup>C/D/E</sup>).

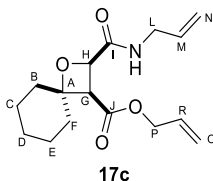
**FTIR** (ATR)  $\nu$  (cm<sup>-1</sup>): 3298 (N-H), 2931 (C-H), 1748 (C=O, ester), 1654 (C=O, amide).

**HRMS (ESI)**: *m/z* calculated for C<sub>14</sub>H<sub>22</sub>NO<sub>4</sub> [M + H]<sup>+</sup>: 268.1543, found: 268.1554.

**R<sub>f</sub>**: (EtOAc-hexane, 2:3) = 0.16.

**Lab-book reference**: WM-05-50

***rac*-(2*R*,3*R*)-Allyl 2-(allylcarbamoyl)-1-oxaspiro[3.5]nonane-3-carboxylate (17c)**



Chemical Formula: C<sub>16</sub>H<sub>23</sub>NO<sub>4</sub>  
Molecular Weight: 293.36

Using the general procedure, maleic anhydride (98 mg, 1 mmol) and cyclohexanone (0.32 mL, 3.00 mmol) were used in the Paternò-Büchi reaction (86 h irradiation). Using allyl amine (0.14 mL, 2.00 mmol) and stirring at room temperature for 16 h in the second step, the crude product **B** was obtained, then dissolved in MeCN (5 mL) and directly used in the final step using allyl alcohol (0.14 mL, 2.00 mmol). Purification by flash chromatography (eluent 9:1-4:1 hexane-EtOAc) gave **17c** (45 mg, 0.15 mmol, 15%) as a colourless oil.

**<sup>1</sup>H NMR** (400 MHz, CDCl<sub>3</sub>) δ 6.86 (s, 1H, *N*-H), 5.96-5.83 (m, 2H, H<sup>M, R</sup>), 5.36-5.13 (m, 4H, H<sup>N, O</sup>), 4.96 (d, *J* = 8.8 Hz, 1H, H<sup>H</sup>), 4.58 (s - broad, 1H, H<sup>P</sup>), 4.57 (s - broad, 1H, H<sup>P</sup>), 4.01-3.95 (m, 2H, H<sup>L</sup>), 3.65 (d, *J* = 8.8 Hz, 1H, H<sup>G</sup>), 1.96-1.20 (m, 10H, H<sup>B, C, D, E, F</sup>).

**<sup>13</sup>C NMR** (101 MHz, CDCl<sub>3</sub>) δ 170.2 (C<sup>I</sup>), 168.0 (C<sup>J</sup>), 134.1 (C<sup>R</sup>), 131.8 (C<sup>M</sup>), 118.9 (C<sup>O</sup>), 116.5 (C<sup>N</sup>), 85.1 (C<sup>A</sup>), 72.7 (C<sup>H</sup>), 65.6 (C<sup>P</sup>), 50.3 (C<sup>G</sup>), 41.3 (C<sup>L</sup>), 39.6 (C<sup>B/F</sup>), 33.8 (C<sup>B/F</sup>), 24.8 (C<sup>C/D/E</sup>), 22.4 (C<sup>C/D/E</sup>), 21.8 (C<sup>C/D/E</sup>).

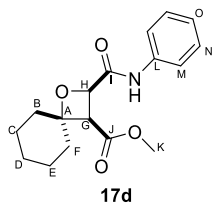
**FTIR** (ATR)  $\nu$  (cm<sup>-1</sup>): 3324 (broad, *N*-H), 2931 (C-H), 1738 (C=O, ester), 1671 (C=O, amide).

**HRMS (APCI)**: *m/z* calculated for C<sub>16</sub>H<sub>23</sub>O<sub>5</sub>Na [M + Na]<sup>+</sup>: 316.1519, found at 316.1515.

**R<sub>f</sub>**: (EtOAc-hexane, 2:3) = 0.16.

**Lab-book reference**: WM-06-09

***rac*-(2*R*,3*R*)-Methyl 2-(phenylcarbamoyl)-1-oxaspiro[3.5]nonane-3-carboxylate (17d)**



Chemical Formula: C<sub>17</sub>H<sub>21</sub>NO<sub>4</sub>  
Molecular Weight: 303.3580

Using the general procedure, maleic anhydride (98 mg, 1 mmol) and cyclohexanone (0.32 mL, 3.00 mmol) were used in the Paternò-Büchi reaction (86 h irradiation). Using aniline (0.10 mL, 1.10 mmol) and stirring at room temperature for 16 h in the second step, the crude product **B** was obtained, then dissolved in MeCN (5 mL) and used in the

final step, using methanol (0.10 mL, 2.00 mmol). Purification by flash chromatography (eluent 3:2 hexane-EtOAc) gave **17d** (63 mg, 0.22 mmol, 23%) as a yellow oil.

**<sup>1</sup>H NMR** (400 MHz, CDCl<sub>3</sub>) δ 8.52 (s, 1H, N-H) 7.61-7.57 (m, 2H, H<sup>N</sup>), 7.38-7.31 (m, 2H, H<sup>M</sup>), 7.20-7.16 (m, 1H, H<sup>O</sup>), 5.04 (d, *J* = 8.7 Hz, 1H, H<sup>H</sup>), 3.71 (d, *J* = 8.7 Hz, 1H, H<sup>G</sup>), 3.67 (s, 3H, H<sup>K</sup>), 1.91-1.23 (m, 10H, H<sup>B, C, D, E, F</sup>).

**<sup>13</sup>C NMR** (101 MHz, CDCl<sub>3</sub>) δ 168.7 (C<sup>O</sup>), 168.6 (C<sup>J</sup>), 137.0 (C<sup>L</sup>), 129.1 (C<sup>N</sup>), 124.6 (C<sup>O</sup>), 120.1 (C<sup>M</sup>), 85.5 (C<sup>A</sup>), 72.7 (C<sup>H</sup>), 52.0 (C<sup>K</sup>), 50.6 (C<sup>G</sup>), 39.6 (C<sup>B/F</sup>), 33.8 (C<sup>B/F</sup>), 24.7 (C<sup>C/D/E</sup>), 22.4 (C<sup>C/D/E</sup>), 21.8 (C<sup>C/D/E</sup>).

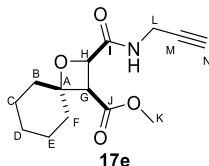
**FTIR** (ATR) ν (cm<sup>-1</sup>): 3375 (broad, N-H), 2931 (C-H), 1735 (C=O, ester), 1686 (C=O, amide).

**HRMS (ESI)**: *m/z* calculated for C<sub>24</sub>H<sub>26</sub>O<sub>5</sub>Na [M + Na]<sup>+</sup>: 304.1543, found at 304.1543.

**R<sub>f</sub>**: (EtOAc-hexane, 2:3) = 0.21.

**Lab-book reference**: WM-05-56

### ***rac*-(2*R*,3*R*)-Methyl 2-(prop-2-yn-1-ylcarbamoyl)-1-oxaspiro[3.5]nonane-3-carboxylate (**17e**)**



Chemical Formula: C<sub>14</sub>H<sub>19</sub>NO<sub>4</sub>  
Molecular Weight: 265.3090

Using the general procedure, maleic anhydride (98 mg, 1 mmol) and cyclohexanone (0.32 mL, 3.00 mmol) were used in the Paternò-Büchi reaction (86 h irradiation). Using propargylamine (0.13 mL, 2.00 mmol) and stirring at room temperature for 16 h in the second step, the crude product **B** was obtained, then dissolved in MeCN (3 mL) and used in the final step using methanol (0.10 mL, 2.00 mmol). Purification by flash chromatography (eluent 3:2 hexane-EtOAc) gave **17e** (78 mg, 0.33 mmol, 33%) as a colourless oil.

**<sup>1</sup>H NMR** (400 MHz, CDCl<sub>3</sub>) δ 6.95 (s, 1H, N-H), 4.95 (d, *J* = 8.7 Hz, 1H, H<sup>H</sup>), 4.22 (ddd, *J* = 17.6, 6.1, 2.6 Hz, 1H, H<sup>L</sup>), 4.10 (ddd, *J* = 17.6, 4.9, 2.6 Hz, 1H, H<sup>L</sup>), 3.68 (s, 3H, H<sup>K</sup>), 3.63 (d, *J* = 8.7 Hz, 1H, H<sup>G</sup>), 2.26 (t, *J* = 2.6 Hz, 1H, H<sup>N</sup>), 1.93-1.20 (m, 10H, H<sup>B, C, D, E, F</sup>).

**<sup>13</sup>C NMR** (101 MHz, CDCl<sub>3</sub>) δ 170.2 (C<sup>I</sup>), 168.7 (C<sup>J</sup>), 85.3 (C<sup>A</sup>), 79.2 (C<sup>M</sup>), 72.6 (C<sup>H</sup>), 71.7 (C<sup>N</sup>), 51.9 (C<sup>K</sup>), 50.4 (C<sup>G</sup>), 39.5 (C<sup>B/F</sup>), 33.8 (C<sup>B/F</sup>), 28.7 (C<sup>L</sup>), 24.7 (C<sup>C/D/E</sup>), 22.4 (C<sup>C/D/E</sup>), 21.8 (C<sup>C/D/E</sup>).

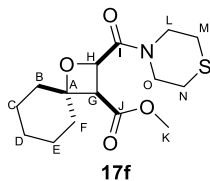
**FTIR** (ATR) ν (cm<sup>-1</sup>): 3280 (broad, N-H), 2931 (C-H), 1735 (C=O, ester), 1671 (C=O, amide).

**HRMS (ESI)**: *m/z* calculated for C<sub>14</sub>H<sub>20</sub>NO<sub>4</sub> [M + H]<sup>+</sup>: 266.1387, found: 266.1374.

**R<sub>f</sub>**: (EtOAc-hexane, 2:3) = 0.27.

**Lab-book reference**: WM-05-54

***rac*-(2*R*,3*R*)-Methyl 2-(thiomorpholine-4-carbonyl)-1-oxaspiro[3.5]nonane-3-carboxylate (17f)**



**17f**

Chemical Formula: C<sub>15</sub>H<sub>23</sub>NO<sub>4</sub>S  
Molecular Weight: 313.4120

Using the general procedure, maleic anhydride (98 mg, 1 mmol) and cyclohexanone (0.32 mL, 3.00 mmol) were used in the Paternò-Büchi reaction (86 h irradiation). Using thiomorpholine (0.11 mL, 1.10 mmol) and stirring at room temperature for 16 h in the second step, the crude product **B** was obtained, then dissolved in MeCN (5 mL) and used in the final step using methanol (0.10 mL, 2.00 mmol). Purification by flash chromatography (eluent 3:2 hexane-EtOAc) gave **17f** (99 mg, 0.32 mmol, 32%) as a yellow oil.

**<sup>1</sup>H NMR** (400 MHz, CDCl<sub>3</sub>) δ 5.23 (d, *J* = 8.3 Hz, 1H, H<sup>H</sup>), 4.20 (ddd, *J* = 13.5, 6.1, 2.8 Hz, 1H, H<sup>L/O</sup>), 4.07 (ddd, *J* = 13.5, 6.1, 2.8 Hz, 1H, H<sup>L/O</sup>), 3.71 (s, 3H, H<sup>K</sup>), 3.63 (d, *J* = 8.3 Hz, 1H, H<sup>G</sup>), 3.62 – 3.51 (m, 2H, H<sup>L/O</sup>), 2.89-2.74 (m, 2H, H<sup>M/N</sup>), 2.61-2.53 (m, 1H, H<sup>M/N</sup>), 2.48 (dd, *J* = 12.8, 5.5 Hz, 1H, H<sup>M/N</sup>), 1.90-1.60 (m, 5H, H<sup>B, C, D, E, F</sup>), 1.56-1.26 (m, 5H, H<sup>B, C, D, E, F</sup>).

**<sup>13</sup>C NMR** (101 MHz, CDCl<sub>3</sub>) δ 169.5 (C<sup>I</sup>), 168.5 (C<sup>J</sup>), 84.0 (C<sup>A</sup>), 73.4 (C<sup>H</sup>), 52.0 (C<sup>K</sup>), 51.8 (C<sup>L/O</sup>), 47.4 (C<sup>L/O</sup>), 45.1 (C<sup>G</sup>), 38.7 (C<sup>B/F</sup>), 33.6 (C<sup>B/F</sup>), 27.6 (C<sup>M/N</sup>), 27.3 (C<sup>M/N</sup>), 24.9 (C<sup>C/D/E</sup>), 22.5 (C<sup>C/D/E</sup>), 21.8 (C<sup>C/D/E</sup>).

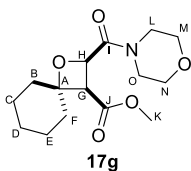
**FTIR** (ATR)  $\nu$  (cm<sup>-1</sup>): 2927 (C-H), 1735 (C=O, ester), 1656 (C=O, amide).

**HRMS (ESI)**: *m/z* calculated for C<sub>15</sub>H<sub>24</sub>NO<sub>4</sub>S [M + H]<sup>+</sup>: 314.1421, found: 314.1408.

**R<sub>f</sub>**: (EtOAc-hexane, 2:3) = 0.10.

**Lab-book reference**: WM-05-52

***rac*-(2*R*,3*R*)-Methyl 2-(morpholine-4-carbonyl)-1-oxaspiro[3.5]nonane-3-carboxylate (17g)**



**17g**

Chemical Formula: C<sub>15</sub>H<sub>23</sub>NO<sub>5</sub>  
Molecular Weight: 297.35

Using the general procedure, maleic anhydride (98 mg, 1 mmol) and cyclohexanone (0.32 mL, 3.00 mmol) were used in the Paternò-Büchi reaction (86 h irradiation). Using morpholine (0.10 mL, 1.10 mmol) and stirring at room temperature for 16 h in the second step, the crude product **B** was obtained, then dissolved in MeCN (5 mL) and used in final step using methanol (0.10 mL, 2.00 mmol). Purification by flash

chromatography (eluent 4:1 hexane-EtOAc) gave **17g** (92 mg, 0.31 mmol, 31%) as a colourless oil.

**<sup>1</sup>H NMR** (400 MHz, CDCl<sub>3</sub>) δ 5.26 (d, *J* = 8.4 Hz, 1H, H<sup>H</sup>), 3.71 (s, 3H, H<sup>K</sup>), 3.64 (d, *J* = 8.4 Hz, 1H, H<sup>G</sup>), 3.76-3.48 (m, 8H, H<sup>L, M, N, O</sup>), 1.91-1.28 (m, 10H, H<sup>B, C, D, E, F</sup>).

**<sup>13</sup>C NMR** (101 MHz, CDCl<sub>3</sub>) δ 169.4 (C<sup>I</sup>), 168.4 (C<sup>J</sup>), 84.4 (C<sup>A</sup>), 73.3 (C<sup>H</sup>), 66.9 (C<sup>M/N</sup>), 66.5 (C<sup>M/N</sup>), 51.8 (C<sup>K</sup> and C<sup>G</sup>), 45.1 (C<sup>L/O</sup>), 42.6 (C<sup>L/O</sup>), 38.9 (C<sup>B/F</sup>), 33.6 (C<sup>B/F</sup>), 24.9 (C<sup>C/D/E</sup>), 22.5 (C<sup>C/D/E</sup>), 21.7 (C<sup>C/D/E</sup>).

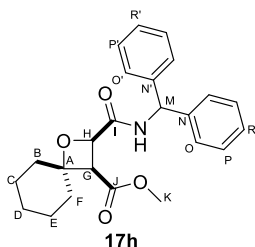
**FTIR** (ATR) ν (cm<sup>-1</sup>): 2926 (C-H), 1735 (C=O, ester), 1653 (C=O, amide).

**HRMS (ESI)**: *m/z* calculated for C<sub>15</sub>H<sub>24</sub>ONO<sub>5</sub> [M + H]<sup>+</sup>: 298.1639, found: 298.1649.

**R<sub>f</sub>**: (EtOAc-hexane, 1:4) = 0.19.

**Lab-book reference**: WM-05-58

### ***rac*-(2*R*,3*R*)-Methyl 2-(benzhydrylcarbamoyl)-1-oxaspiro[3.5]nonane-3-carboxylate (**17h**) and **17i****



Chemical Formula: C<sub>24</sub>H<sub>27</sub>NO<sub>4</sub>  
Molecular Weight: 393.4830

Using the general procedure, maleic anhydride (98 mg, 1 mmol) and cyclohexanone (0.32 mL, 3.00 mmol) were used in the Paternò-Büchi reaction (86 h irradiation). Using benzhydrylamine (0.19 mL, 1.10 mmol) and stirring at room temperature for 16 h in the second step, the crude product **B** was obtained, then dissolved in MeCN (5 mL) and used in the final step using methanol (0.10 mL, 2.00 mmol). Purification by flash chromatography (eluent 3:2 hexane-EtOAc) gave **17h** (80 mg, 0.20 mmol, 20%) as a yellow oil and **17i** (2 mg, <1 % yield) as a yellow oil.

**<sup>1</sup>H NMR** (400 MHz, CDCl<sub>3</sub>) δ 7.38-7.24 (m, 10H, H<sup>N, O, P, R, N', O', P', R'</sup>), 6.33 (d, *J* = 8.4 Hz, 1H, H<sup>M</sup>), 5.00 (d, *J* = 8.9 Hz, 1H, H<sup>H</sup>), 3.66 (d, *J* = 8.9 Hz, 1H, H<sup>G</sup>), 3.59 (s, 3H, H<sup>K</sup>), 1.98-1.14 (m, 10H, H<sup>B/C/D/E/F</sup>).

**<sup>13</sup>C NMR** (101 MHz, CDCl<sub>3</sub>) δ 169.5 (C<sup>I</sup>), 168.6 (C<sup>J</sup>), 141.5 (C<sup>N/N'</sup>), 141.4 (C<sup>N/N'</sup>), 128.6 (C<sup>O/O'</sup>), 128.5 (C<sup>O/O'</sup>), 127.8 (C<sup>P/P'</sup>), 127.6 (C<sup>P/P'</sup>), 127.4 (C<sup>R/R'</sup>), 127.4 (C<sup>R/R'</sup>), 85.3 (C<sup>A</sup>), 72.7 (C<sup>H</sup>), 56.3 (C<sup>K</sup>), 51.8 (C<sup>G</sup>), 50.3 (C<sup>M</sup>), 39.7 (C<sup>B/F</sup>), 33.8 (C<sup>B/F</sup>), 24.7 (C<sup>C/D/E</sup>), 22.4 (C<sup>C/D/E</sup>), 21.9 (C<sup>C/D/E</sup>).

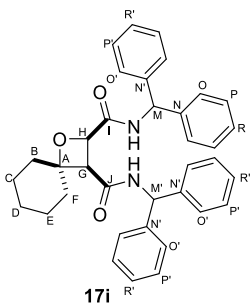
**FTIR** (ATR) ν (cm<sup>-1</sup>): 3315 (broad, N-H), 2931 (C-H), 1735 (C=O, ester), 1675 (C=O, amide).

**HRMS (ESI)**: *m/z* calculated for C<sub>24</sub>H<sub>28</sub>NO<sub>4</sub> [M + H]<sup>+</sup>: 394.2013, found: 394.1997.

**R<sub>f</sub>**: (EtOAc-hexane, 2:3) = 0.20.

**Lab-book reference**: WM-05-51

**17i**:



17i

Chemical Formula:  $C_{36}H_{36}N_2O_3$   
Molecular Weight: 544.69

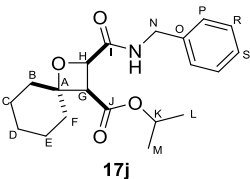
$^1H$  NMR (400 MHz,  $CDCl_3$ )  $\delta$  7.39 – 7.14 (m, 20H,  $H^{N-R}$ ), 6.31 (d,  $J = 8.9$  Hz, 1H,  $H^M$ ), 6.21 (d,  $J = 8.1$  Hz, 1H,  $H^{M'}$ ), 5.08 (d,  $J = 9.9$  Hz, 1H,  $H^H$ ), 3.85 (d,  $J = 9.9$  Hz, 1H,  $H^G$ ), 2.02 – 1.30 (m, 10H,  $H^{B, C, D, E, F}$ ).

$^{13}C$  NMR insufficient material obtained for  $^{13}C$  NMR analysis

FTIR (ATR)  $\nu$  ( $cm^{-1}$ ): 3287 (broad,  $N-H$ ), 1654 ( $C=O$ )

HRMS (ESI):  $m/z$  calculated for  $C_{36}H_{36}N_2O_3Na$  [ $M + Na$ ] $^+$ : 567.2618, found: 567.2624.

***rac*-(2*R*,3*R*)-Isopropyl 2-(benzylcarbamoyl)-1-oxaspiro[3.5]nonane-3-carboxylate (17j)**



17j

Chemical Formula:  $C_{20}H_{27}NO_4$   
Molecular Weight: 345.44

Using the general procedure, maleic anhydride (98 mg, 1 mmol) and cyclohexanone (0.32 mL, 3.00 mmol) were used in the Paternò-Büchi reaction (86 h irradiation). Using benzylamine (0.11 mL, 2.00 mmol) and stirring at room temperature for 16 h in the second step, the crude product **B** was obtained, then dissolved in MeCN (5 mL) and used in final step using isopropanol (0.15 mL, 2.00 mmol). Purification by flash chromatography (eluent 19:1-9:1 hexane-EtOAc) gave **17j** (114 mg, 0.33 mmol, 35%) as a colourless oil.



**<sup>1</sup>H NMR** (400 MHz, CDCl<sub>3</sub>) δ 7.39-7.27 (m, 5H, H<sup>P,R,S</sup>), 7.05 (s, 1H, N-H), 5.10-5.03 (m, 1H, H<sup>K</sup>), 5.00 (d, *J* = 8.7 Hz, 1H, H<sup>H</sup>), 4.65 (dd, *J* = 14.9, 6.5 Hz, 1H, H<sup>N</sup>), 4.47 (dd, *J* = 14.9, 5.2 Hz, 1H, H<sup>N</sup>), 3.59 (d, *J* = 8.7 Hz, 1H, H<sup>G</sup>), 1.96-1.27 (m, 10H, H<sup>B, C, D, E, F</sup>), 1.25 (d, *J* = 6.3 Hz, 3H, H<sup>L/M</sup>), 1.23 (d, *J* = 6.3 Hz, 3H, H<sup>L/M</sup>).

**<sup>13</sup>C NMR** (101 MHz, CDCl<sub>3</sub>) δ 170.4 (C<sup>I</sup>), 167.8 (C<sup>J</sup>), 138.0 (C<sup>O</sup>), 128.7 (C<sup>R</sup>), 127.9 (C<sup>P</sup>), 127.4 (C<sup>S</sup>), 85.1 (C<sup>A</sup>), 72.9 (C<sup>H</sup>), 68.6 (C<sup>K</sup>), 50.7 (C<sup>G</sup>), 43.0 (C<sup>N</sup>), 39.5 (C<sup>B/F</sup>), 33.7 (C<sup>B/F</sup>), 24.8 (C<sup>C/D/E</sup>), 22.4 (C<sup>C/D/E</sup>), 21.9 (C<sup>C/D/E</sup>), 21.9 (C<sup>L/M</sup>), 21.8 (C<sup>L/M</sup>).

**FTIR** (ATR) ν (cm<sup>-1</sup>): 3461 (broad, N-H), 2931 (C-H), 1731 (C=O, ester), 1765 (C=O, amide).

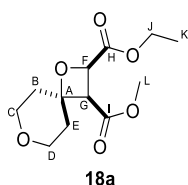
**HRMS (ESI)**: *m/z* calculated for C<sub>20</sub>H<sub>27</sub>NO<sub>4</sub>Na [M + Na]<sup>+</sup>: 368.1829, found: 368.1832.

**R<sub>f</sub>**: (EtOAc-hexane, 2:3) = 0.26.

**Lab-book reference**: WM-05-91

### 7.4.2.3 Reactions of other 6-membered cyclic ketones with maleic anhydride (1)

#### *rac*-(2*R*,3*R*)-2-Ethyl 3-methyl 1,7-dioxaspiro[3.5]nonane-2,3-dicarboxylate (18a)



18a

Chemical Formula: C<sub>12</sub>H<sub>18</sub>O<sub>6</sub>

Molecular Weight: 258.27

Using the general procedure, maleic anhydride (98 mg, 1.00 mmol) and tetrahydro-4H-pyran-4-one (0.30 mL, 3.00 mmol) were used in the Paternò-Büchi reaction (96 h irradiation). Using ethanol (0.12 mL, 2.00 mmol) and stirring at reflux for 48 h in the second step, the crude product **B** was obtained, then dissolved in MeCN (5 mL) and used in the final step (using methanol 0.10 mL, 2.00 mmol). Purification by flash chromatography (eluent 4:1-3:2 hexane-EtOAc) gave **18a** (79 mg, 0.31 mmol, 31%) as a colourless oil.

**<sup>1</sup>H NMR** (400 MHz, CDCl<sub>3</sub>) δ 5.06 (d, *J* = 8.9 Hz, 1H, H<sup>F</sup>), 4.33-4.23 (m, 2H, H<sup>J</sup>), 3.81-3.73 (m, 3H, H<sup>C,D</sup>), 3.75 (d, *J* = 8.9 Hz, 1H, H<sup>G</sup>), 3.70 (s, 3H, H<sup>L</sup>), 3.68-3.62 (m, 1H, H<sup>C/D</sup>), 2.09 (dt, *J* = 13.5, 3.7 Hz, 1H, H<sup>B/E</sup>), 2.01 (m, 2H, H<sup>B/E</sup>), 1.87-1.77 (m, 1H, H<sup>B/E</sup>), 1.30 (t, *J* = 7.2 Hz, 3H, H<sup>K</sup>).

**<sup>13</sup>C NMR** (101 MHz, CDCl<sub>3</sub>) δ 170.4 (C<sup>H</sup>), 168.1 (C<sup>I</sup>), 82.5 (C<sup>A</sup>), 71.9 (C<sup>F</sup>), 63.6 (C<sup>C/D</sup>), 63.3 (C<sup>C/D</sup>), 61.4 (C<sup>J</sup>), 52.0 (C<sup>L</sup>), 50.7 (C<sup>G</sup>), 39.3 (C<sup>B/E</sup>), 34.1 (C<sup>B/E</sup>), 14.1 (C<sup>K</sup>).

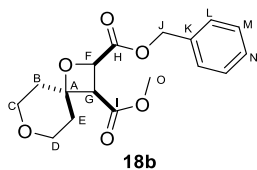
**FTIR** (ATR) ν (cm<sup>-1</sup>): 2957 (C-H), 1735 (C=O).

**HRMS (APCI)**: *m/z* calculated for C<sub>12</sub>H<sub>19</sub>O<sub>6</sub> [M + H]<sup>+</sup>: 259.1176, found at 259.1168.

**R<sub>f</sub>**: (EtOAc-hexane, 2:3) = 0.14.

**Lab-book reference**: WM-06-49

***rac*-(2*R*,3*R*)-2-Benzyl 3-methyl 1,7-dioxaspiro[3.5]nonane-2,3-dicarboxylate (**18b**)**



Chemical Formula: C<sub>17</sub>H<sub>20</sub>O<sub>6</sub>  
Molecular Weight: 320.34

Using the general procedure, maleic anhydride (98 mg, 1.00 mmol) and tetrahydro-4H-pyran-4-one (0.30 mL, 3.00 mmol) were used in the Paternò-Büchi reaction (96 h irradiation). Using benzyl alcohol (0.21 mL, 2.00 mmol) and stirring at reflux for 48 h in the second step, the crude product **B** was obtained, then dissolved in MeCN (5 mL) and used in the final step using methanol (0.10 mL, 2.00 mmol). Purification by flash chromatography (eluent 4:1-3:2 hexane-EtOAc) gave **18b** (86 mg, 0.27 mmol, 27%) as a colourless oil.

<sup>1</sup>H NMR (400 MHz, CDCl<sub>3</sub>) δ 7.38-7.32 (m, 5H, H<sup>L, M, N</sup>), 5.27 (d, *J* = 12.1 Hz, 1H, H<sup>J</sup>), 5.20 (d, *J* = 12.1 Hz, 1H, H<sup>J</sup>), 5.10 (d, *J* = 8.9 Hz, 1H, H<sup>F</sup>), 3.76 (d, *J* = 8.9 Hz, 1H, H<sup>G</sup>), 3.80-3.63 (m, 4H, H<sup>C, D</sup>), 3.61 (s, 1H, H<sup>O</sup>), 2.10 (dt, *J* = 13.5, 3.7 Hz, 1H, H<sup>B/E</sup>), 2.03-1.98 (m, 2H, H<sup>B/E</sup>), 1.87-1.78 (m, 1H, H<sup>B/E</sup>).

<sup>13</sup>C NMR (101 MHz, CDCl<sub>3</sub>) δ 170.3 (C<sup>H</sup>), 168.1 (C<sup>I</sup>), 135.3 (C<sup>K</sup>), 128.7 (C<sup>M</sup>), 128.6 (C<sup>L</sup>), 128.4 (C<sup>N</sup>), 82.7 (C<sup>A</sup>), 71.9 (C<sup>F</sup>), 67.1 (C<sup>J</sup>), 63.5 (C<sup>C/D</sup>), 63.3 (C<sup>C/D</sup>), 52.0 (C<sup>O</sup>), 50.7 (C<sup>G</sup>), 39.4 (C<sup>B/E</sup>), 34.1 (C<sup>B/E</sup>).

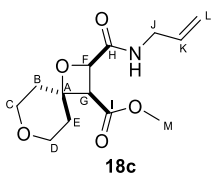
FTIR (ATR) ν (cm<sup>-1</sup>): 2953 (C-H), 1735 (C=O)

HRMS (APCI): *m/z* calculated for C<sub>17</sub>H<sub>20</sub>O<sub>6</sub>Na [M + Na]<sup>+</sup>: 343.1152, found at 343.1142.

R<sub>f</sub>: (EtOAc-hexane, 3:7) = 0.13.

Lab-book reference: WM-06-50

***rac*-(2*R*,3*R*)-Methyl 2-(allylcarbamoyl)-1,7-dioxaspiro[3.5]nonane-3-carboxylate (**18c**)**



Chemical Formula: C<sub>13</sub>H<sub>19</sub>NO<sub>5</sub>  
Molecular Weight: 269.30

Using the general procedure, maleic anhydride (98 mg, 1.00 mmol) and tetrahydro-4H-pyran-4-one (0.30 mL, 3.00 mmol) were used in the Paternò-Büchi reaction (96 h irradiation). Using allyl amine (0.14 mL, 2.00 mmol) and stirring at room temperature for 24 h in the second step, the crude product **B** was obtained, then dissolved in MeCN (3 mL) and used in the final step using methanol (0.10 mL, 2.00 mmol). Purification by flash

chromatography (eluent 4:1-3:2 hexane-EtOAc) gave **18c** (42 mg, 0.16 mmol, 16%) as colourless oil.

**<sup>1</sup>H NMR** (400 MHz, CDCl<sub>3</sub>) δ 6.81 (s, 1H, N-H), 5.91 (ddd, *J* = 16.0, 10.8, 5.6 Hz, 1H, H<sup>K</sup>), 5.32-5.26 (m, 1H, H<sup>L</sup>), 5.21-5.15 (m, 1H, H<sup>L</sup>), 5.01 (d, *J* = 8.8 Hz, 1H, H<sup>F</sup>), 4.01 (m, 2H, H<sup>J</sup>), 3.82-3.74 (m, 2H, H<sup>C/D</sup>), 3.70 (d, *J* = 8.8 Hz, 1H, H<sup>G</sup>), 3.69 (s, 1H, H<sup>M</sup>), 3.54 (dt, *J* = 16.9, 5.1 Hz, 1H, H<sup>C/D</sup>), 2.05-1.84 (m, 5H, H<sup>B, E, C/D</sup>).

**<sup>13</sup>C NMR** (101 MHz, CDCl<sub>3</sub>) δ 169.7 (C<sup>H</sup>), 168.3 (C<sup>I</sup>), 133.9 (C<sup>K</sup>), 116.7 (C<sup>L</sup>), 81.8 (C<sup>A</sup>), 72.8 (C<sup>F</sup>), 63.8 (C<sup>C/D</sup>), 63.3 (C<sup>C/D</sup>), 52.1 (C<sup>M</sup>), 50.2 (C<sup>G</sup>), 41.3 (C<sup>J</sup>), 39.4 (C<sup>B/E</sup>), 34.5 (C<sup>B/E</sup>).

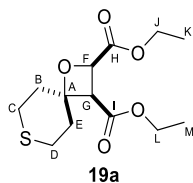
**FTIR** (ATR)  $\nu$  (cm<sup>-1</sup>): 3404 (N-H), 2857 (C-H), 1736 (C=O, ester), 1664 (C=O, amide).

**HRMS (APCI)**: *m/z* calculated for C<sub>13</sub>H<sub>20</sub>NO<sub>5</sub> [M + H]<sup>+</sup>: 270.1336, found at: 270.1325.

**R<sub>f</sub>**: (EtOAc-hexane, 1:4) = 0.10.

**Lab-book reference**: WM-06-46

### ***rac*-(2*R*,3*R*)-Diethyl 1-oxa-7-thiaspiro[3.5]nonane-2,3-dicarboxylate (**19a**)**



**19a**

Chemical Formula: C<sub>13</sub>H<sub>20</sub>O<sub>5</sub>S

Molecular Weight: 288.36

Using the general procedure, maleic anhydride (98 mg, 1.00 mmol) and tetrahydro-4H-thiopyran-4-one (350 mg, 3.00 mmol) used in the Paternò-Büchi reaction. The reaction was irradiated for 2 weeks. Using ethanol (0.12 mL, 2.00 mmol) and stirring at reflux for 72 h in the second step, the crude product **B** was obtained, then dissolved in MeCN (5 mL) and used in the final step using ethanol (0.10 mL, 2.00 mmol). Purification by flash chromatography (eluent: 9:1 to 3:1 hexane-EtOAc) gave **19a** (62 mg, 0.22 mmol, 22%) as a yellow oil.

**<sup>1</sup>H NMR** (400 MHz, CDCl<sub>3</sub>) δ 5.02 (d, *J* = 9.0 Hz, 1H, H<sup>F</sup>), 4.28-4.23 (m, 1H, H<sup>J</sup>), 4.23-4.14 (m, 1H, H<sup>J</sup>), 4.16 (q, *J* = 7.2 Hz, 2H, H<sup>L</sup>), 3.65 (d, *J* = 9.0 Hz, 1H, H<sup>G</sup>), 2.98-2.90 (m, 2H, H<sup>C/D</sup>), 2.55-2.43 (m, 2H, H<sup>C/D</sup>), 2.39-2.29 (m, 2H, H<sup>B/E</sup>), 2.17-2.09 (m, 1H, H<sup>B/E</sup>), 1.97-1.89 (m, 1H, H<sup>B/E</sup>), 1.30 (t, *J* = 7.1 Hz, 3H, H<sup>K</sup>), 1.26 (t, *J* = 6.8 Hz, 3H, H<sup>M</sup>).

**<sup>13</sup>C NMR** (101 MHz, CDCl<sub>3</sub>) δ 170.5 (C<sup>H</sup>), 167.6 (C<sup>I</sup>), 83.8 (C<sup>A</sup>), 72.0 (C<sup>F</sup>), 61.3 (C<sup>J/L</sup>), 61.2 (C<sup>J/L</sup>), 51.2 (C<sup>G</sup>), 40.3 (C<sup>B/E</sup>), 34.7 (C<sup>B/E</sup>), 24.5 (C<sup>C/D</sup>), 23.9 (C<sup>C/D</sup>), 14.2 (C<sup>K/M</sup>), 14.1 (C<sup>K/M</sup>).

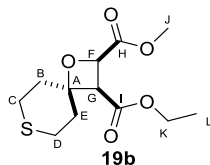
**FTIR** (ATR)  $\nu$  (cm<sup>-1</sup>): 2980 (C-H), 1731 (C=O).

**HRMS (APCI)**: *m/z* calculated for C<sub>13</sub>H<sub>20</sub>O<sub>5</sub>Na [M + Na]<sup>+</sup>: 311.0924, found at 311.0931.

**R<sub>f</sub>**: (EtOAc-hexane, 1:4) = 0.41.

**Lab-book reference**: WM-06-59

***rac*-(2*R*,3*R*)-3-Ethyl 2-methyl 1-oxa-7-thiaspiro[3.5]nonane-2,3-dicarboxylate (**19b**)**



Chemical Formula: C<sub>12</sub>H<sub>18</sub>O<sub>5</sub>S  
Molecular Weight: 274.33

Using the general procedure, maleic anhydride (490 mg, 5.00 mmol) and tetrahydro-4*H*-thiopyran-4-one (1.75 mg, 15.00 mmol) were used in the Paternò-Büchi reaction. The reaction was irradiated for 2 weeks. Using methanol (0.50 mL, 10.00 mmol) and stirring at reflux for 48 h in the second step, the crude product **B** was obtained, then dissolved in MeCN (25 mL) and used in the final step using ethanol (0.60 mL, 10.00 mmol). Purification by flash chromatography (eluent: 9:1 to 3:1 hexane-EtOAc) gave **19b** (275 mg, 1.00 mmol, 20%) as a yellow oil.

**<sup>1</sup>H NMR** (400 MHz, CDCl<sub>3</sub>) δ 5.05 (d, *J* = 8.9 Hz, 1H, H<sup>F</sup>), 4.16 (q, *J* = 7.1 Hz, 2H, H<sup>K</sup>), 3.81 (s, *J* = 1.8 Hz, 3H, H<sup>J</sup>), 3.66 (d, *J* = 8.9 Hz, 1H, H<sup>G</sup>), 2.98-2.89 (m, 2H, H<sup>C/D</sup>), 2.55-2.29 (m, 4H, H<sup>B/C/D/E</sup>), 2.17-2.08 (m, 1H, H<sup>B/E</sup>), 1.97-1.87 (m, 1H, H<sup>B/E</sup>), 1.27 (t, *J* = 7.1 Hz, 3H, H<sup>L</sup>).

**<sup>13</sup>C NMR** (101 MHz, CDCl<sub>3</sub>) δ 171.0 (C<sup>H</sup>), 167.6 (C<sup>I</sup>), 83.9 (C<sup>A</sup>), 72.0 (C<sup>F</sup>), 61.3 (C<sup>K</sup>), 52.2 (C<sup>J</sup>), 51.3 (C<sup>G</sup>), 40.3 (C<sup>B/E</sup>), 34.7 (C<sup>B/E</sup>), 24.5 (C<sup>C/D</sup>), 23.8 (C<sup>C/D</sup>), 14.2 (C<sup>L</sup>).

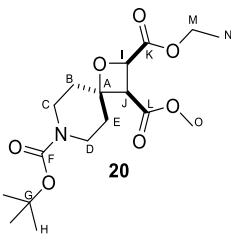
**FTIR** (ATR) ν (cm<sup>-1</sup>): 2931 (C-H), 1731 (C=O).

**HRMS (APCI)**: *m/z* calculated for C<sub>12</sub>H<sub>19</sub>O<sub>5</sub>S [M + H]<sup>+</sup>: 275.0948, found at 275.0948.

**R<sub>f</sub>**: (EtOAc-hexane, 3:7) = 0.29.

**Lab-book reference**: WM-07-03

***rac*-(2*R*,3*R*)-7-*tert*-Butyl 2-ethyl 3-methyl 1-oxa-7-azaspiro[3.5]nonane-2,3,7-tricarboxylate (**20**)**



Chemical Formula: C<sub>17</sub>H<sub>27</sub>NO<sub>7</sub>  
Molecular Weight: 357.40

**1 mmol scale** - Using the general procedure, maleic anhydride (98 mg, 1.00 mmol) and 1-Boc-4-piperidone (597 mg, 3.00 mmol) were used in the Paternò-Büchi reaction (86 h irradiation). Using ethanol (0.12 mL, 2.00 mmol) and stirring at reflux for 86 h in the second step, the crude product **B** was obtained, then dissolved in MeCN (5 mL) and used in the final step using methanol (0.10 mL, 2.00 mmol). Purification by flash

chromatography (eluent 7:3 hexane-EtOAc) gave **20** (49 mg, 0.14 mmol, 14%) as a yellow oil.

**5 mmol scale** - Using the general procedure, maleic anhydride (490 mg, 5.00 mmol) and 1-Boc-4-piperidone (2.98 g, 15.00 mmol) were used in the Paternò-Büchi reaction (86 h irradiation). Using ethanol (0.60 mL, 10.00 mmol) and stirring at reflux for 86 h in the second step, the crude product **B** was obtained, then dissolved in MeCN (25 mL) and used in the final step using methanol (0.50 mL, 10.00 mmol). Purification by flash chromatography (eluent 7:3 hexane-EtOAc) gave **20** (246 mg, 0.69 mmol, 14%) as a yellow oil.

**<sup>1</sup>H NMR** (400 MHz, CDCl<sub>3</sub>) δ 5.05 (d, *J* = 8.9 Hz, 1H, H<sup>I</sup>), 4.34-4.21 (m, 2H, H<sup>M</sup>), 3.74 (d, *J* = 8.9 Hz, 1H, H<sup>J</sup>), 3.69 (s, 3H, H<sup>O</sup>), 3.31-3.22 (m, 2H, H<sup>B/C/D/E</sup>), 2.13-1.97 (m, 2H, H<sup>B/C/D/E</sup>), 1.93-1.82 (m, 2H, H<sup>B/C/D/E</sup>), 1.71-1.63 (m, 2H, H<sup>B/C/D/E</sup>), 1.44 (s, 9H, H<sup>H</sup>), 1.30 (t, *J* = 7.2 Hz, 3H, H<sup>N</sup>).

**<sup>13</sup>C NMR** (101 MHz, CDCl<sub>3</sub>) δ 170.3 (C<sup>K</sup>), 168.1 (C<sup>L</sup>), 154.6 (C<sup>F</sup>), 83.4 (C<sup>A</sup>), 79.8 (C<sup>G</sup>), 72.0 (C<sup>I</sup>), 61.4 (C<sup>M</sup>), 52.0 (C<sup>O</sup>), 50.4 (C<sup>J</sup>), 38.4 (C<sup>C, D</sup>), 33.1 (C<sup>B, E</sup>), 28.3 (C<sup>H</sup>), 14.1 (C<sup>N</sup>).

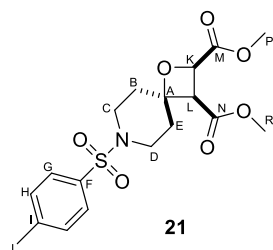
**FTIR** (ATR)  $\nu$  (cm<sup>-1</sup>): 2976 (C-H), 1735 (C=O, ester), 1686 (C=O, carbamate).

**HRMS (APCI)**: *m/z* calculated for C<sub>17</sub>H<sub>27</sub>NO<sub>7</sub>Na [M + Na]<sup>+</sup>: 380.1680, found at 380.1667.

**R<sub>f</sub>**: (EtOAc-hexane, 2:3) = 0.23.

**Lab-book reference**: WM-06-77/WM-06-92

### ***rac*-(2*R*,3*R*)-Dimethyl 7-tosyl-1-oxa-7-azaspiro[3.5]nonane-2,3-dicarboxylate (**21**)**



Chemical Formula: C<sub>18</sub>H<sub>23</sub>NO<sub>7</sub>S  
Molecular Weight: 397.44

Using the general procedure, maleic anhydride (147 mg, 1.50 mmol) and 1-tosyl-4-piperidinone (570 mg, 4.50 mmol) used in the Paternò-Büchi reaction (168 h irradiation; 80 % conversion). Using methanol (0.15 mL, 3.00 mmol) and stirring at reflux for 72 h in the second step, the crude product **B** was obtained, then dissolved in MeCN (7 mL) and used in the final step using methanol (0.15 mL, 3.00 mmol). Purification by flash chromatography (eluent: 7:3 hexane-EtOAc) gave **21** (91 mg, 0.22 mmol, 21%) as a colourless solid.

**<sup>1</sup>H NMR** (400 MHz, CDCl<sub>3</sub>) δ 7.63-7.59 (m, 2H, H<sup>G</sup>), 7.30 (dd, *J* = 8.5, 0.6 Hz, 2H, H<sup>H</sup>), 4.99 (d, *J* = 8.9 Hz, 1H, H<sup>K</sup>), 3.78 (s, 3H, H<sup>P/R</sup>), 3.73 (d, *J* = 8.9 Hz, 1H, H<sup>L</sup>), 3.67 (s, 3H, H<sup>P/R</sup>), 3.63-3.52 (m, 2H, H<sup>C/D</sup>), 2.67-2.59 (m, 2H, H<sup>C/D</sup>), 2.42 (s, 3H, H<sup>J</sup>), 2.24-2.03 (m, 4H, H<sup>B/E</sup>), 1.79-1.71 (m, 1H, H<sup>B/E</sup>).

**<sup>13</sup>C NMR** (101 MHz, CDCl<sub>3</sub>) δ 170.6 (C<sup>M</sup>), 167.9 (C<sup>N</sup>), 143.8 (C<sup>I</sup>), 132.7 (C<sup>G</sup>), 129.8 (C<sup>H</sup>), 127.7 (C<sup>F</sup>), 82.2 (C<sup>A</sup>), 72.0 (C<sup>K</sup>), 52.3 (C<sup>P/R</sup>), 52.2 (C<sup>P/R</sup>), 49.9 (C<sup>L</sup>), 42.0 (C<sup>C/D</sup>), 41.5 (C<sup>C/D</sup>), 37.7 (C<sup>B/F</sup>), 32.6 (C<sup>B/F</sup>), 21.5 (C<sup>J</sup>).

**FTIR** (ATR)  $\nu$  (cm<sup>-1</sup>): 2926 (C-H), 1742 (C=O).

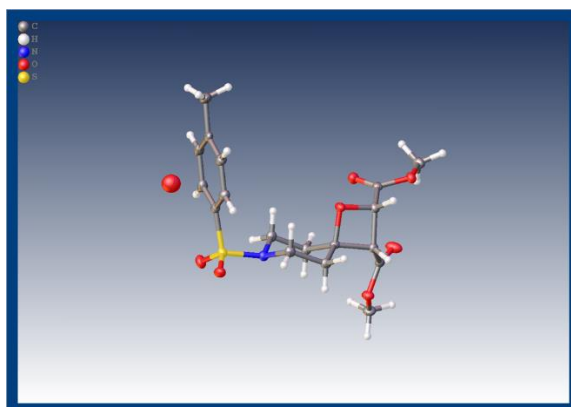
**HRMS (APCI)**: *m/z* calculated for C<sub>18</sub>H<sub>24</sub>NO<sub>7</sub>S [M + H]<sup>+</sup>: 398.1268, found at: 398.1269.

**R<sub>f</sub>**: (EtOAc-hexane, 2:3) = 0.11

**Melting point**: 130 - 136 °C.

**Lab-book reference**: WM-06-55

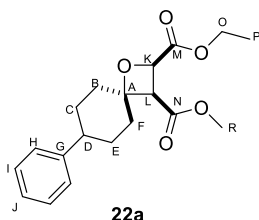
**Crystal structure**:



Identification code	SC139_autored
Empirical formula	C <sub>18</sub> H <sub>23</sub> NO <sub>7.06</sub> S
Formula weight	398.43
Temperature/K	100.00(16)
Crystal system	monoclinic
Space group	I2/a
<i>a</i> /Å	19.2318(2)
<i>b</i> /Å	8.22860(10)
<i>c</i> /Å	24.0575(2)
$\alpha$ /°	90
$\beta$ /°	94.6890(10)
$\gamma$ /°	90
Volume/Å <sup>3</sup>	3794.38(7)
<i>Z</i>	8
$\rho_{\text{calc}}$ /cm <sup>3</sup>	1.395
$\mu$ /mm <sup>-1</sup>	1.881
<i>F</i> (000)	1684.0
Crystal size/mm <sup>3</sup>	0.17 × 0.14 × 0.12
Radiation	Cu K $\alpha$ ( $\lambda$ = 1.54184)
2 $\theta$ range for data collection/°	7.374 to 152.528
Index ranges	-19 ≤ <i>h</i> ≤ 24, -10 ≤ <i>k</i> ≤ 7, -30 ≤ <i>l</i> ≤ 27
Reflections collected	15168
Independent reflections	3947 [R <sub>int</sub> = 0.0185, R <sub>sigma</sub> = 0.0127]
Data/restraints/parameters	3947/0/252

Goodness-of-fit on $F^2$	1.066
Final R indexes [ $I > 2\sigma(I)$ ]	$R_1 = 0.0332$ , $wR_2 = 0.0890$
Final R indexes [all data]	$R_1 = 0.0338$ , $wR_2 = 0.0895$
Largest diff. peak/hole / $e \text{ \AA}^{-3}$	0.31/-0.49
Deposition number	2180492

***rac*-(2*R*,3*R*)-2-Ethyl 3-methyl 7-phenyl-1-oxaspiro[3.5]nonane-2,3-dicarboxylate (**22a**)**



**22a**

Chemical Formula:  $C_{19}H_{24}O_5$   
Molecular Weight: 332.40

Using the general procedure, maleic anhydride (98 mg, 1.00 mmol) and 4-phenylcyclohexanone (520 mg, 3.00 mmol) were used in the Paternò-Büchi reaction (86 h irradiation). Using ethanol (0.12 mL, 2.00 mmol) and stirring at reflux for 48 h in the second step, the crude product **B** was obtained, then dissolved in MeCN (5 mL) and used in the final step using methanol (0.10 mL, 2.00 mmol). Purification by flash chromatography (eluent 9:1 hexane-EtOAc) gave **22a** (101 mg, 0.30 mmol, 30%) as yellow oil.

**$^1H$  NMR** (400 MHz,  $CDCl_3$ )  $\delta$  7.35 – 7.29 (m, 2H, H<sup>I</sup>), 7.23-7.13 (m, 3H, H<sup>H</sup>, J), 5.08 (d,  $J = 8.8$  Hz, 1H, H<sup>K</sup>), 4.30 (m, 2H, H<sup>O</sup>), 3.85 (d,  $J = 8.8$  Hz, 1H, H<sup>L</sup>), 3.74 (s, 3H, H<sup>R</sup>), 2.55-2.49 (m, 2H, H<sup>D</sup>, B/C/E/F), 2.34-2.27 (m, 1H, H<sup>B/C/E/F</sup>), 1.89 (m, 4H, H<sup>B/C/F/E</sup>), 1.72-1.63 (m, 2H, H<sup>B/C/E/F</sup>), 1.32 (t,  $J = 7.1$  Hz, 3H, H<sup>P</sup>), 1.25-1.20 (m, 1H, H<sup>B/C/E/F</sup>).

**$^{13}C$  NMR** (101 MHz,  $CDCl_3$ )  $\delta$  170.6 (C<sup>M</sup>), 169.0 (C<sup>N</sup>), 145.8 (C<sup>G</sup>), 128.5 (C<sup>I</sup>), 126.6 (C<sup>H</sup>), 126.3 (C<sup>J</sup>), 85.5 (C<sup>A</sup>), 71.3 (C<sup>K</sup>), 61.3 (C<sup>O</sup>), 52.0 (C<sup>R</sup>), 50.4 (C<sup>L</sup>), 42.6 (C<sup>D</sup>), 40.0 (C<sup>B/C/E/F</sup>), 33.9 (C<sup>B/C/E/F</sup>), 30.4 (C<sup>B/C/E/F</sup>), 29.9 (C<sup>B/C/E/F</sup>), 14.2 (C<sup>P</sup>).

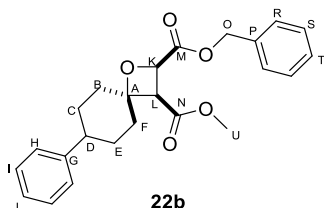
**FTIR** (ATR)  $\nu$  ( $cm^{-1}$ ): 2931 (C-H), 1757 and 1731 (C=O).

**HRMS (APCI)**:  $m/z$  calculated for  $C_{19}H_{25}O_5$  [ $M + H$ ]<sup>+</sup>: 333.1697, found at 333.1695.

**R<sub>f</sub>**: (EtOAc-hexane, 1:4) = 0.09.

**Lab-book reference**: WM-06-71

***rac*-(2*R*,3*R*)-2-Benzyl 3-methyl 7-phenyl-1-oxaspiro[3.5]nonane-2,3-dicarboxylate (**22b**)**



Chemical Formula: C<sub>24</sub>H<sub>26</sub>O<sub>5</sub>  
Molecular Weight: 394.47

Using the general procedure, maleic anhydride (98 mg, 1.00 mmol) and 4-phenylcyclohexanone (520 mg, 3.00 mmol) were used in the Paternò-Büchi reaction (86 h irradiation). Using benzyl alcohol (0.20 mL, 2.00 mmol) and stirring at reflux for 72 h in the second step, the crude product **B** was obtained, then dissolved in MeCN (5 mL) and used in the final step using methanol (0.10 mL, 2.00 mmol). Purification by flash chromatography (eluent 9:1 hexane-EtOAc) gave **22b** (65 mg, 0.16 mmol, 16%) as yellow oil.

<sup>1</sup>H NMR (400 MHz, CDCl<sub>3</sub>) δ 7.39-7.12 (m, 10H, H<sup>H, I, J, R, S, T</sup>), 5.25 (s, 2H, H<sup>O</sup>), 5.11 (d, *J* = 8.9 Hz, 1H, H<sup>K</sup>), 3.85 (d, *J* = 8.9 Hz, 1H, H<sup>L</sup>), 3.65 (s, 3H, H<sup>U</sup>), 2.59-2.49 (m, 2H, H<sup>D, B/C/F/E</sup>), 2.33-2.25 (m, 1H, H<sup>B/C/F/E</sup>), 2.00-1.78 (m, 3H, H<sup>B/C/F/E</sup>), 1.72-1.60 (m, 2H, H<sup>B/C/F/E</sup>), 1.28-1.18 (m, 1H, H<sup>B/C/F/E</sup>).

<sup>13</sup>C NMR (101 MHz, CDCl<sub>3</sub>) δ 170.5 (C<sup>M</sup>), 168.9 (C<sup>N</sup>), 145.7 (C<sup>G</sup>), 135.4 (C<sup>P</sup>), 128.7 (C<sup>I/S/R</sup>), 128.5 (C<sup>I/S/R</sup>), 128.5 (C<sup>I/S/R</sup>), 128.4 (C<sup>T/J</sup>), 126.6 (C<sup>H</sup>), 126.3 (C<sup>T/J</sup>), 85.7 (C<sup>A</sup>), 71.3 (C<sup>K</sup>), 67.0 (C<sup>O</sup>), 51.9 (C<sup>U</sup>), 50.4 (C<sup>L</sup>), 42.6 (C<sup>D</sup>), 40.0 (C<sup>B/C/E/F</sup>), 33.9 (C<sup>B/C/E/F</sup>), 30.4 (C<sup>B/C/E/F</sup>), 29.9 (C<sup>B/C/E/F</sup>).

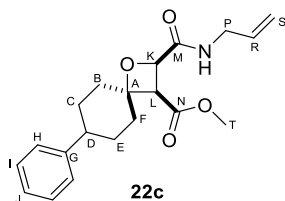
FTIR (ATR) ν (cm<sup>-1</sup>): 2929 (C-H), 1759 and 1733 (C=O).

HRMS (APCI): *m/z* calculated for C<sub>24</sub>H<sub>27</sub>O<sub>5</sub> [M + H]<sup>+</sup>: 395.1853, found at 395.1853.

*R<sub>f</sub>*: (EtOAc-hexane, 1:4) = 0.12.

Lab-book reference: WM-06-72

***rac*-(2*R*,3*R*)-Methyl 2-(allylcarbamoyl)-7-phenyl-1-oxaspiro[3.5]nonane-3-carboxylate (**22c**)**



Chemical Formula: C<sub>20</sub>H<sub>25</sub>NO<sub>4</sub>  
Molecular Weight: 343.42

Using the general procedure, maleic anhydride (98 mg, 1.00 mmol) and 4-phenylcyclohexanone (520 mg, 3.00 mmol) were used in the Paternò-Büchi reaction (86 h irradiation). Using allyl amine (0.14 mL, 2.00 mmol) and stirring at room temperature



for 24 h in the second step, the crude product **B** was obtained, then dissolved in MeCN (4 mL) and used in the final step using methanol (0.10 mL, 2.00 mmol). Purification by flash chromatography (eluent 1:1 hexane-EtOAc) gave **22c** (81 mg, 0.24 mmol, 24%) as a colourless oil.

**<sup>1</sup>H NMR** (400 MHz, CDCl<sub>3</sub>) δ 7.34-7.27 (m, 2H, H<sup>I</sup>), 7.24-7.17 (m, 1H, H<sup>J</sup>), 7.14 (dd, *J* = 5.2, 3.3 Hz, 2H, H<sup>H</sup>), 6.90 (s, 1H, *N*-H), 5.93 (ddt, *J* = 17.2, 10.3, 5.6 Hz, 1H, H<sup>R</sup>), 5.31 (ddd, *J* = 17.2, 3.1, 1.7 Hz, 1H, H<sup>S</sup>), 5.19 (dq, *J* = 10.3, 1.4 Hz, 1H, H<sup>S</sup>), 5.01 (d, *J* = 8.8 Hz, 1H, H<sup>K</sup>), 4.09-3.91 (m, 2H, H<sup>P</sup>), 3.79 (d, *J* = 8.8 Hz, 1H, H<sup>L</sup>), 3.73 (s, 3H, H<sup>T</sup>), 2.58-2.47 (m, 2H, H<sup>B/C/D/F/E</sup>), 2.36-2.29 (m, 1H, H<sup>B/C/F/E</sup>), 1.97 (dd, *J* = 9.8, 6.8 Hz, 1H, H<sup>B/C/F/E</sup>), 1.92-1.78 (m, 2H, H<sup>B/C/F/E</sup>), 1.69-1.54 (m, 2H, H<sup>B/C/F/E</sup>), 1.18 (dd, *J* = 12.2, 3.5 Hz, 1H, H<sup>B/C/F/E</sup>).

**<sup>13</sup>C NMR** (101 MHz, CDCl<sub>3</sub>) δ 170.1 (C<sup>M</sup>), 169.0 (C<sup>N</sup>), 145.5 (C<sup>G</sup>), 134.0 (C<sup>R</sup>), 128.5 (C<sup>I</sup>), 126.6 (C<sup>H</sup>), 126.4 (C<sup>S</sup>), 116.6 (C<sup>J</sup>), 85.1 (C<sup>A</sup>), 72.5 (C<sup>K</sup>), 52.0 (C<sup>T</sup>), 49.5 (C<sup>L</sup>), 42.6 (C<sup>D</sup>), 41.3 (C<sup>P</sup>), 40.0 (C<sup>B/C/E/F</sup>), 34.0 (C<sup>B/C/E/F</sup>), 30.4 (C<sup>B/C/E/F</sup>), 30.0 (C<sup>B/C/E/F</sup>).

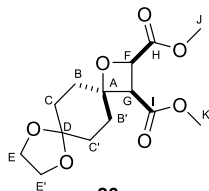
**FTIR** (ATR) ν (cm<sup>-1</sup>): 3412 (broad, *N*-H), 2931 (C-H), 1735 (C=O, ester), 1671 (C=O, amide)

**HRMS (APCI)**: *m/z* calculated for C<sub>20</sub>H<sub>26</sub>NO<sub>4</sub> [M + H]<sup>+</sup>: 344.1856, found at 344.1839.

**R<sub>f</sub>**: (EtOAc-hexane, 4:1) = 0.26.

**Lab-book reference**: WM-06-73

## 2-Benzyl 3-methyl *rac*-(2*R*,3*R*)-1,8,11-trioxadispiro[3.2.47.24]tridecane-2,3-dicarboxylate (**23a**)



**23a**

Chemical Formula: C<sub>14</sub>H<sub>20</sub>O<sub>7</sub>

Molecular Weight: 300.30

Using the general procedure, maleic anhydride (98 mg, 1.00 mmol) and 1,4-cyclohexanedione monoethylene acetal (460 mg, 3.00 mmol) were used in the Paternò-Büchi reaction (86 h irradiation). Using benzyl alcohol (0.21 mL, 2.00 mmol) and stirring at reflux for 72 h in the second step, the crude product **B** was obtained, then dissolved in MeCN (3 mL) and used in the final step using methanol (0.10 mL, 2.00 mmol). Purification by flash chromatography (eluent 4:1-3:2 hexane-EtOAc) gave **23a** (80 mg, 0.21 mmol, 21%) as a colourless oil.

**<sup>1</sup>H NMR** (400 MHz, CDCl<sub>3</sub>) δ 7.42-7.31 (m, 5H, H<sup>L, M, N</sup>), 5.29 (d, *J* = 12.2 Hz, 1H, H<sup>J</sup>), 5.22 (d, *J* = 12.2 Hz, 1H, H<sup>J</sup>), 5.10 (d, *J* = 8.9 Hz, 1H, H<sup>F</sup>), 4.00-3.91 (m, 4H, H<sup>E, E'</sup>), 3.78 (d, *J* = 8.9 Hz, 1H, H<sup>G</sup>), 3.63 (s, *J* = 2.7 Hz, 3H, H<sup>O</sup>), 2.25-1.53 (m, 8H, H<sup>B, B', C, C'</sup>).

**<sup>13</sup>C NMR** (101 MHz, CDCl<sub>3</sub>) δ 170.5 (C<sup>H</sup>), 168.5 (C<sup>I</sup>), 135.5 (C<sup>K</sup>), 128.6 (C<sup>M</sup>), 128.5 (C<sup>L</sup>), 128.4 (C<sup>N</sup>), 107.6 (C<sup>D</sup>), 84.4 (C<sup>A</sup>), 71.8 (C<sup>F</sup>), 67.0 (C<sup>J</sup>), 64.4 (C<sup>E/E'</sup>), 64.3 (C<sup>E/E'</sup>), 51.9 (C<sup>O</sup>), 50.1 (C<sup>G</sup>), 36.6 (C<sup>B, B', C, C'</sup>), 30.7 (C<sup>B, B', C, C'</sup>), 30.5 (C<sup>B, B', C, C'</sup>), 29.7 (C<sup>B, B', C, C'</sup>).

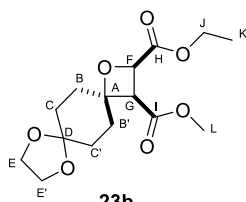
**FTIR** (ATR)  $\nu$  (cm<sup>-1</sup>): 2952 (C-H), 1735 (C=O).

**HRMS (ESI)**: *m/z* calculated for C<sub>20</sub>H<sub>24</sub>O<sub>7</sub>Na [M + Na]<sup>+</sup>: 399.1397, found at 399.1397.

**R<sub>f</sub>**: (EtOAc-hexane, 1:1) = 0.30.

**Lab-book reference**: WM-06-34

### 2-Ethyl 3-methyl *rac*-(2*R*,3*R*)-1,8,11-trioxadispiro[3.2.47.24]tridecane-2,3-dicarboxylate (**23b**)



**23b**

Chemical Formula: C<sub>15</sub>H<sub>22</sub>O<sub>7</sub>

Molecular Weight: 314.33

Using the general procedure, maleic anhydride (98 mg, 1.00 mmol) and 1,4-cyclohexanedione monoethylene acetal (460 mg, 3.00 mmol) were used in the Paternò-Büchi reaction (86 h irradiation). Using ethanol (0.11 mL, 2.00 mmol) and stirring at reflux for 72 h in the second step, the crude product **B** was obtained, then dissolved in MeCN (3 mL) and used in the final step using methanol (0.10 mL, 2.00 mmol). Purification by flash chromatography (eluent 4:1-3:2 hexane-EtOAc) gave **23b** (77 mg, 0.26 mmol, 26%) as colourless oil.

**<sup>1</sup>H NMR** (400 MHz, CDCl<sub>3</sub>) δ 5.04 (d, *J* = 8.9 Hz, 1H, H<sup>F</sup>), 4.33-4.23 (m, 2H, H<sup>J</sup>), 3.98-3.89 (m, 4H, H<sup>E</sup>), 3.75 (d, *J* = 8.9 Hz, 1H, H<sup>G</sup>), 3.68 (s, *J* = 2.0 Hz, 3H, H<sup>L</sup>), 2.20-1.50 (m, 8H, H<sup>B, B', C, C'</sup>), 1.30 (t, *J* = 7.2 Hz, 3H, H<sup>K</sup>).

**<sup>13</sup>C NMR** (101 MHz, CDCl<sub>3</sub>) δ 170.6 (C<sup>H</sup>), 168.6 (C<sup>I</sup>), 107.6 (C<sup>D</sup>), 84.2 (C<sup>A</sup>), 71.8 (C<sup>F</sup>), 64.4 (C<sup>E/E'</sup>), 64.3 (C<sup>E/E'</sup>), 61.3 (C<sup>J</sup>), 51.9 (C<sup>L</sup>), 50.1 (C<sup>G</sup>), 36.5 (C<sup>B, B', C, C'</sup>), 30.7 (C<sup>B, B', C, C'</sup>), 30.5 (C<sup>B, B', C, C'</sup>), 29.7 (C<sup>B, B', C, C'</sup>), 14.1 (C<sup>K</sup>).

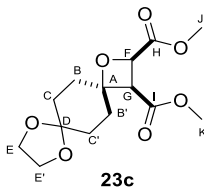
**FTIR** (ATR)  $\nu$  (cm<sup>-1</sup>): 2952 (C-H), 1735 (C=O).

**HRMS (ESI)**: *m/z* calculated for C<sub>15</sub>H<sub>22</sub>O<sub>7</sub>Na [M + Na]<sup>+</sup>: 337.1258, found at 337.1245.

**R<sub>f</sub>**: (EtOAc-hexane, 1:1) = 0.20.

**Lab-book reference**: WM-06-33

### 2,3-Dimethyl *rac*-(2*R*,3*R*)-1,8,11-trioxadispiro[3.2.47.24]tridecane-2,3-dicarboxylate (**23c**)



Chemical Formula: C<sub>14</sub>H<sub>20</sub>O<sub>7</sub>  
Molecular Weight: 300.30

Using the general procedure, maleic anhydride (3.85 g, 39.30 mmol) and 1,4-cyclohexanedione monoethylene acetal (18.35 g, 18.00 mmol) were used in the Paternò-Büchi reaction (86 h irradiation). Using methanol (4.00 mL, 80.00 mmol) and stirring at reflux for 72 h in the second step, the crude product **B** was obtained, then dissolved in MeCN (50 mL) and used in the final step using methanol (4.00 mL, 80.00 mmol). Purification by flash chromatography (eluent 4:1-3:2 hexane-EtOAc) gave **23c** (2.0 g, 6.00 mmol, 15%) as colourless oil.

<sup>1</sup>H NMR (400 MHz, CDCl<sub>3</sub>) δ 5.09 (d, *J* = 8.8 Hz, 1H, H<sup>F</sup>), 4.00 – 3.91 (m, 4H, H<sup>E,E'</sup>), 3.84 (s, 3H, H<sup>J</sup>), 3.78 (d, *J* = 8.8 Hz, 1H, H<sup>G</sup>), 3.71 (s, 3H, H<sup>K</sup>), 2.19 – 1.89 (m, 8H, H<sup>B, B', C, C'</sup>).

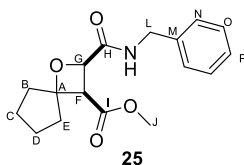
<sup>13</sup>C NMR (101 MHz, CDCl<sub>3</sub>) δ 171.1 (C<sup>H</sup>), 168.7 (C<sup>I</sup>), 107.5 (C<sup>D</sup>), 84.3 (C<sup>A</sup>), 71.8 (C<sup>F</sup>), 64.5 (C<sup>E/E'</sup>), 64.3 (C<sup>E/E'</sup>), 52.2 (C<sup>J</sup>), 52.0 (C<sup>K</sup>), 50.13 (C<sup>G</sup>), 36.5 (C<sup>B/B'/C/C'</sup>), 30.8 (C<sup>B/B'/C/C'</sup>), 30.5 (C<sup>B/B'/C/C'</sup>), 29.7 (C<sup>B/B'/C/C'</sup>).

HRMS (APCI): *m/z* calculated for C<sub>14</sub>H<sub>20</sub>O<sub>7</sub> [M + H]<sup>+</sup>: 301.1282, found at 301.1267.

Lab-book reference: WM-09-28SM/P (acetal and ketone under the same number, from the same column)

#### 7.4.2.4 Reactions of 5- and 7-membered cyclic ketones with maleic anhydride (1)

### *rac*-(2*R*,3*R*)-Methyl 2-(benzylcarbamoyl)-1-oxaspiro[3.4]octane-3-carboxylate (**25**)



Chemical Formula: C<sub>17</sub>H<sub>21</sub>NO<sub>4</sub>  
Exact Mass: 303.15

Using the general procedure, maleic anhydride (98 mg, 1 mmol) and cyclopentanone (0.26 mL, 3.00 mmol) were used in the Paternò-Büchi reaction (86 h irradiation). Using benzyl amine (0.11 mL, 2.00 mmol) and stirring at room temperature for 48 h in the second step, the crude product **B** was obtained, then dissolved in MeCN (5 mL) and used in the final step using methanol (0.10 mL, 2.00 mmol). Purification by flash

chromatography (eluent 4:1-3:2 hexane-EtOAc) gave **25** (30 mg, 0.10 mmol, 10%) as a colourless oil.

**<sup>1</sup>H NMR** (400 MHz, CDCl<sub>3</sub>) δ 7.40-7.27 (m, 5H, H<sup>N, O, P</sup>), 7.01 (broad-s, 1H, N-H), 5.02 (d, *J* = 8.6 Hz, 1H, H<sup>G</sup>), 4.55 (d, *J* = 5.9 Hz, 2H, H<sup>L</sup>), 3.91 (d, *J* = 8.6 Hz, 1H, H<sup>F</sup>), 3.68 (s, 3H, H<sup>J</sup>), 2.26-1.02 (m, 10H, H<sup>B, C, D, E</sup>).

**<sup>13</sup>C NMR** (101 MHz, CDCl<sub>3</sub>) δ 170.1 (C<sup>H</sup>), 169.4 (C<sup>I</sup>), 138.0 (C<sup>M</sup>), 128.7 (C<sup>O</sup>), 127.9 (C<sup>P</sup>), 127.5 (C<sup>N</sup>), 92.9 (C<sup>A</sup>), 72.8 (C<sup>G</sup>), 51.9 (C<sup>J</sup>), 49.5 (C<sup>F</sup>), 43.0 (C<sup>L</sup>), 40.5 (C<sup>B, E</sup>), 36.1 (C<sup>B, E</sup>), 22.7 (C<sup>C, D</sup>), 22.5 (C<sup>C, D</sup>).

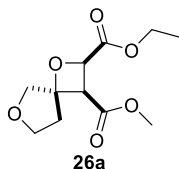
**FTIR** (ATR) ν (cm<sup>-1</sup>): 3404 (broad, N-H), 2950 (C-H), 1735 (C=O, ester), 1669 (C=O, amide).

**HRMS (ESI)**: *m/z* calculated for C<sub>17</sub>H<sub>22</sub>NO<sub>4</sub> [M + H]<sup>+</sup>: 304.1543, found at 304.1537.

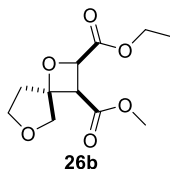
**R<sub>f</sub>**: (EtOAc-hexane, 1:1) = 0.20.

**Lab-book reference**: WM-05-72

### ***rac*-(2*R*,3*R*)-2-Ethyl 3-methyl 1,6-dioxaspiro[3.4]octane-2,3-dicarboxylate (26)**



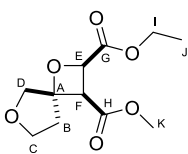
Chemical Formula: C<sub>11</sub>H<sub>16</sub>O<sub>6</sub>  
Molecular Weight: 244.2430



Chemical Formula: C<sub>11</sub>H<sub>16</sub>O<sub>6</sub>  
Molecular Weight: 244.2430

**1 mmol scale** - Using the general procedure, maleic anhydride (98 mg, 1.00 mmol) and tetrahydrofuran-3-one (0.23 mL, 3.00 mmol) were used in the Paternò-Büchi reaction (144 h irradiation). Using ethanol (0.12 mL, 2.00 mmol) and stirring at reflux for 48 h in the second step, the crude product **B** was obtained, then dissolved in MeCN (3 mL) and used in the final step using methanol (0.10 mL, 2.00 mmol). Purification by flash chromatography (eluent 4:1 – 1:1 hexane-EtOAc) gave **26** (**a** : **b** - 1 : 1) (28 mg, 0.11 mmol, 11 %) as a colourless oil.

**5 mmol scale** - Using the general procedure, maleic anhydride (490 mg, 5.00 mmol) and tetrahydrofuran-3-one (1.15 mL, 15.0 mmol) were used in the Paternò-Büchi reaction (144 h irradiation). Using ethanol (0.60 mL, 10.0 mmol) and stirring at reflux for 48 h in the second step, the crude product **B** was obtained, then dissolved in MeCN (3 mL) and used in the final step using methanol (0.50 mL, 10.0 mmol). Purification by flash chromatography (eluent 4:1 – 1:1 hexane-EtOAc) gave **26a** (21 mg, 0.09 mmol, 2 %) as a colourless oil and **26b** (59 mg, 0.24 mmol, 5 %) as a colourless oil.

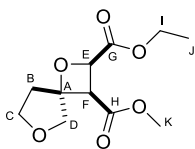
**26a**

Chemical Formula: C<sub>11</sub>H<sub>16</sub>O<sub>6</sub>  
Molecular Weight: 244.2430

**<sup>1</sup>H NMR** (400 MHz, CDCl<sub>3</sub>) δ 5.06 (d, *J* = 8.8 Hz, 1H, H<sup>E</sup>), 4.32 – 4.23 (m, 2H, H<sup>I</sup>), 4.17 (d, *J* = 8.8 Hz, 1H, H<sup>F</sup>), 4.16 (d, *J* = 11.1 Hz, 1H, H<sup>D</sup>), 3.93 – 3.84 (m, 2H, H<sup>C</sup>), 3.88 (d, *J* = 11.1 Hz, 1H, H<sup>D</sup>), 3.72 (s, 3H, H<sup>K</sup>), 2.48 (dddd, *J* = 13.4, 6.2, 3.7, 0.7 Hz, 1H, H<sup>B</sup>), 2.24 – 2.16 (m, 1H, H<sup>B</sup>), 1.31 (t, *J* = 7.2 Hz, 3H, H<sup>J</sup>).  
**<sup>13</sup>C NMR** (101 MHz, CDCl<sub>3</sub>) δ 169.8 (C<sup>G</sup>), 168.5 (C<sup>H</sup>), 91.0 (C<sup>A</sup>), 74.9 (C<sup>D</sup>), 72.7 (C<sup>E</sup>), 66.6 (C<sup>C</sup>), 61.5 (C<sup>I</sup>), 52.2 (C<sup>K</sup>), 48.8 (C<sup>F</sup>), 40.8 (C<sup>B</sup>), 14.1 (C<sup>J</sup>).  
**FTIR** (ATR) ν (cm<sup>-1</sup>): 2953 (C-H), 1735 (C=O).

**HRMS (APCI):** m/z calculated for C<sub>11</sub>H<sub>17</sub>O<sub>5</sub> [M+H]<sup>+</sup>: 245.1020 found at: 245.1012.

**Lab-book reference:** WM-07-64\_e7-9\_all

**26b**

Chemical Formula: C<sub>11</sub>H<sub>16</sub>O<sub>6</sub>  
Molecular Weight: 244.2430

**<sup>1</sup>H NMR** (400 MHz, CDCl<sub>3</sub>) δ 5.03 (d, *J* = 8.9 Hz, 1H, H<sup>E</sup>), 4.35-4.40 (m, 2H, H<sup>I</sup>), 4.17 (dd, *J* = 10.4, 0.6 Hz, 1H, H<sup>D</sup>), 4.11 (d, *J* = 8.9 Hz, 1H, H<sup>F</sup>), 4.01 – 3.90 (m, 2H, H<sup>C</sup>), 3.89 (d, *J* = 10.5 Hz, 1H, H<sup>D</sup>), 3.75 (s, 3H, H<sup>K</sup>), 2.54 (dddd, *J* = 13.8, 6.5, 4.1, 0.8 Hz, 1H, H<sup>B</sup>), 2.11 (dt, *J* = 13.9, 8.7 Hz, 1H, H<sup>B</sup>), 1.34 (t, *J* = 7.2 Hz, 3H, H<sup>J</sup>).  
**<sup>13</sup>C NMR** (101 MHz, CDCl<sub>3</sub>) δ 169.9 (C<sup>G</sup>), 168.4 (C<sup>H</sup>), 91.4 (C<sup>A</sup>), 78.1 (C<sup>D</sup>), 72.7 (C<sup>E</sup>), 67.3 (C<sup>C</sup>), 61.5 (C<sup>I</sup>), 52.2 (C<sup>K</sup>), 46.8 (C<sup>F</sup>), 36.3 (C<sup>B</sup>), 14.1 (C<sup>J</sup>).  
**FTIR** (ATR) ν (cm<sup>-1</sup>): 2953 (C-H), 1735 (C=O).

**HRMS (APCI):** m/z calculated for C<sub>11</sub>H<sub>17</sub>O<sub>5</sub> [M+H]<sup>+</sup>: 245.1020 found at: 245.1012.

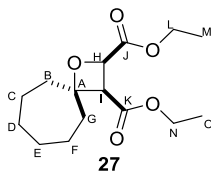
**Lab-book reference:** WM-07-64\_i1\_all

**NOSEY 2D <sup>1</sup>H-<sup>1</sup>H NMR**

 <b>26b</b>	 <b>26a</b>
4.11 (d, <i>J</i> = 8.9 Hz, 1H, H <sup>F</sup> ) and 3.89 (d, <i>J</i> = 10.5 Hz, 1H, H <sup>D</sup> )	5.06 (d, <i>J</i> = 8.8 Hz, 1H, H <sup>E</sup> ) + 2.24 – 2.16 (m, 1H, H <sup>B</sup> ) and 2.48 (dddd, <i>J</i> = 13.4, 6.2, 3.7, 0.7 Hz, 1H, H <sup>B</sup> )

	4.17 (d, $J = 8.8$ Hz, 1H, H <sup>F</sup> ) + 2.24 – 2.16 (m, 1H, H <sup>B</sup> ) and 2.48 (dddd, $J = 13.4, 6.2, 3.7, 0.7$ Hz, 1H, H <sup>B</sup> )
--	---

***rac*-(2*R*,3*R*)-2,3-Diethyl 1-oxaspiro[3.6]decane-2,3-dicarboxylate (27)**



Chemical Formula: C<sub>15</sub>H<sub>24</sub>O<sub>5</sub>  
Molecular Weight: 284.3520

Using the general procedure, maleic anhydride (98 mg, 1.00 mmol) and cycloheptanone (0.35 mL, 3.00 mmol) were used in the Paternò-Büchi reaction (144 h irradiation). Using ethanol (0.12 mL, 2.00 mmol) and stirring at reflux for 48 h in the second step, the crude product **B** was obtained, then dissolved in MeCN (3 mL) and used in the final step using ethanol (0.12 mL, 2.00 mmol). Purification by flash chromatography (eluent: 4:1 hexane-EtOAc) gave **27** (41 mg, 0.14 mmol, 14 %) as a colourless oil.

**<sup>1</sup>H NMR** (400 MHz, CDCl<sub>3</sub>) δ 5.00 (d,  $J = 8.8$  Hz, 1H, H<sup>H</sup>), 4.29 (dq,  $J = 10.8, 7.2$  Hz, 2H, H<sup>L</sup>), 4.21 – 4.13 (m, 2H, H<sup>N</sup>), 3.73 (d,  $J = 8.8$  Hz, 1H, H<sup>I</sup>), 2.27 – 2.20 (m, 1H, H<sup>B/C/D/E/F/G</sup>), 2.08 – 1.98 (m, 3H, H<sup>B/C/D/E/F/G</sup>), 1.61 – 1.47 (m, 6H, H<sup>B/C/D/E/F/G</sup>), 1.32 (t,  $J = 7.2$  Hz, 3H, H<sup>M</sup>), 1.28 (t,  $J = 7.2$  Hz, 3H, H<sup>O</sup>).

**<sup>13</sup>C NMR** (101 MHz, CDCl<sub>3</sub>) δ 170.9 (C<sup>J</sup>), 168.4 (C<sup>K</sup>), 88.8 (C<sup>A</sup>), 71.3 (C<sup>H</sup>), 61.1 (C<sup>L</sup>), 61.0 (C<sup>N</sup>), 52.1 (C<sup>I</sup>), 42.6 (C<sup>B/C/D/E/F/G</sup>), 37.0 (C<sup>B/C/D/E/F/G</sup>), 28.8 (C<sup>B/C/D/E/F/G</sup>), 28.4 (C<sup>B/C/D/E/F/G</sup>), 21.1 (C<sup>B/C/D/E/F/G</sup>), 20.9 (C<sup>B/C/D/E/F/G</sup>), 14.2 (C<sup>M</sup>), 14.1 (C<sup>O</sup>).

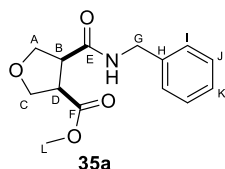
**FTIR** (ATR)  $\nu$  (cm<sup>-1</sup>): 2926 (C-H), 1735 (C=O).

**HRMS (APCI)**:  $m/z$  calculated for C<sub>15</sub>H<sub>25</sub>O<sub>5</sub> [M+H]<sup>+</sup>: 285.1697, found: 285.1693.

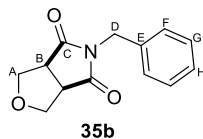
**Lab-book reference**: WM-07-43

**7.4.2.5 Reactions of 4-membered ketones**

**methyl *rac*-(3*R*,4*S*)-4-(benzylcarbamoyl)tetrahydrofuran-3-carboxylate (35a) and 5-Benzylidihydro-1*H*-furo[3,4-*c*]pyrrole-4,6(5*H*,6*aH*)-dione (35b)**



Chemical Formula: C<sub>14</sub>H<sub>17</sub>NO<sub>4</sub>  
Molecular Weight: 263.29



Chemical Formula: C<sub>13</sub>H<sub>13</sub>NO<sub>3</sub>  
Molecular Weight: 231.25

Using the general procedure, maleic anhydride (98 mg, 1.00 mmol) and 3-oxetanone (0.19 mL, 3.00 mmol) were used in the Paternò-Büchi reaction (86 h irradiation). Using benzylamine (0.11 mL, 2.00 mmol) and stirring at room temperature for 16 h in the second step, the crude product **B** was obtained, then dissolved in MeCN (5 mL) and

used in the final step using methanol (0.10 mL, 2.00 mmol). Purification by flash chromatography (eluent 4:1-3:2 hexane-EtOAc) gave **35a** (33 mg, 0.13 mmol, 13%) as a colourless oil and **35b** as white crystals (100 mg, 0.43 mmol, 43%).

**35a:**

**<sup>1</sup>H NMR** (400 MHz, CDCl<sub>3</sub>) δ 7.38 – 7.27 (m, 5H, H<sup>I, J, K</sup>), 6.04 (s, 1H, N-H), 4.49 (m, 1H, H<sup>G</sup>), 4.40-4.35 (m, 1H, H<sup>G</sup>), 4.26-4.20 (m, 1H, H<sup>A/C</sup>), 4.11 – 4.00 (m, 3H, H<sup>A/C</sup>), 3.61 (s, 3H, H<sup>L</sup>), 3.36 – 3.28 (m, 1H, H<sup>B/D</sup>), 3.21 (ddd, *J* = 8.8, 6.8, 4.9 Hz, 1H, H<sup>B/D</sup>).

**<sup>13</sup>C NMR** (101 MHz, CDCl<sub>3</sub>) δ 171.4 (C<sup>E</sup>), 171.0 (C<sup>F</sup>), 138.0 (C<sup>H</sup>), 128.7 (C<sup>I</sup>), 127.9 (C<sup>K</sup>), 127.6 (C<sup>J</sup>), 71.3 (C<sup>A/C</sup>), 69.3 (C<sup>A/C</sup>), 52.1 (C<sup>L</sup>), 48.3 (C<sup>B/D</sup>), 47.4 (C<sup>B/D</sup>), 43.7 (C<sup>G</sup>).

**FTIR** (ATR)  $\nu$  (cm<sup>-1</sup>): 3300 (broad, N-H), 2950 (C-H), 1735 (C=O, ester), 1653 (C=O, amide).

**HRMS (ESI):** *m/z* calculated for C<sub>14</sub>H<sub>17</sub>NO<sub>4</sub>Na [M+Na]<sup>+</sup>: 286.1055, found at: 286.1040

**R<sub>f</sub>:** (EtOAc-hexane, 4:1) = 0.26.

**Lab-book reference:** WM-05-81/82

**35b:**

**<sup>1</sup>H NMR** (400 MHz, CDCl<sub>3</sub>) δ 7.34 – 7.27 (m, 5H, H<sup>F, G, D</sup>), 4.65 (s, 2H, H<sup>D</sup>), 4.35 (d, *J* = 9.5 Hz, 2H, H<sup>A</sup>), 3.77 – 3.69 (m, 2H, H<sup>A</sup>), 3.39 – 3.33 (m, 2H, H<sup>B</sup>).

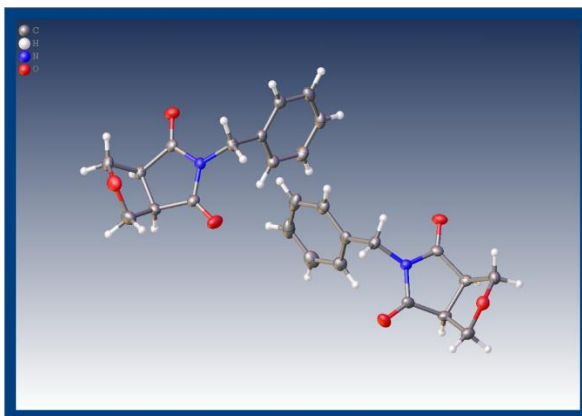
**<sup>13</sup>C NMR** (101 MHz, CDCl<sub>3</sub>) δ 177.8 (C<sup>C</sup>), 135.4 (C<sup>E</sup>), 128.7 (C<sup>F</sup>), 128.4 (C<sup>G</sup>), 128.0 (C<sup>H</sup>), 71.0 (C<sup>A</sup>), 46.0 (C<sup>B</sup>), 42.8 (C<sup>D</sup>).

**FTIR** (ATR)  $\nu$  (cm<sup>-1</sup>): 2927 (C-H), 1694 (C=O).

**R<sub>f</sub>:** (EtOAc-hexane, 4:1) = 0.49.

**Melting point** = 108 – 112 °C

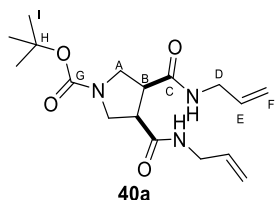
**Crystal structure:**



Identification code	SC130_autored
Empirical formula	C <sub>13</sub> H <sub>13</sub> NO <sub>3</sub>
Formula weight	231.24
Temperature/K	120.01(10)
Crystal system	monoclinic
Space group	P2 <sub>1</sub> /c
a/Å	20.80612(17)
b/Å	6.30721(4)
c/Å	17.98812(14)

$\alpha/^\circ$	90
$\beta/^\circ$	108.5384(9)
$\gamma/^\circ$	90
Volume/ $\text{\AA}^3$	2238.07(3)
Z	8
$\rho_{\text{calc}}/\text{cm}^3$	1.373
$\mu/\text{mm}^{-1}$	0.809
F(000)	976.0
Crystal size/ $\text{mm}^3$	0.2 x 0.12 x 0.1
Radiation	Cu K $\alpha$ ( $\lambda = 1.54184$ )
2 $\theta$ range for data collection/ $^\circ$	8.966 to 152.498
Index ranges	$-25 \leq h \leq 26$ , $-7 \leq k \leq 5$ , $-22 \leq l \leq 20$
Reflections collected	16999
Independent reflections	4595 [ $R_{\text{int}} = 0.0280$ , $R_{\text{sigma}} = 0.0187$ ]
Data/restraints/parameters	4595/0/308
Goodness-of-fit on $F^2$	1.051
Final R indexes [ $I \geq 2\sigma(I)$ ]	$R_1 = 0.0395$ , $wR_2 = 0.1025$
Final R indexes [all data]	$R_1 = 0.0406$ , $wR_2 = 0.1035$
Largest diff. peak/hole / e $\text{\AA}^{-3}$	0.32/-0.20

***tert*-Butyl *rac*-(3*R*,4*S*)-3,4-bis(allylcarbamoyl)pyrrolidine-1-carboxylate (40a)**



Chemical Formula:  $\text{C}_{17}\text{H}_{27}\text{N}_3\text{O}_4$   
Molecular Weight: 337.42

Using the general procedure, maleic anhydride (98 mg, 1.00 mmol) and 1-Boc-3-azetidinone (513 mg, 3.00 mmol) used in the Paternò-Büchi reaction (86 h irradiation). Using allyl amine (0.10 mL, 2.00 mmol) and stirring at room temperature for 16 h in the second step, the crude product **B** was obtained, then dissolved in MeCN (3 mL) and used in final step using methanol (0.10 mL, 2.00 mmol). Purification by flash chromatography (eluent 9:1 – 3:2 hexane-EtOAc) gave **40a** (68 mg, 0.20 mmol, 20%) as white solid.



**<sup>1</sup>H NMR** (400 MHz, CD<sub>3</sub>CN) δ 6.49 (s, 2H, *N*-H), 5.88-5.77 (m, 2H, H<sup>E</sup>), 5.22-5.19 (m, 1H, H<sup>F</sup>), 5.18-5.14 (m, 1H, H<sup>F</sup>), 5.10 (dd, *J* = 3.1, 1.5 Hz, 1H, H<sup>F</sup>), 5.07 (dd, *J* = 3.1, 1.5 Hz, 1H, H<sup>F</sup>), 3.80-3.71 (m, 4H, H<sup>D</sup>), 3.61 (td, *J* = 10.9, 5.3 Hz, 2H, H<sup>A</sup>), 3.54 – 3.47 (m, 2H, H<sup>A</sup>), 3.17-3.14 (m, 2H, H<sup>B</sup>), 1.46 (s, 9H, H<sup>I</sup>).

**<sup>13</sup>C NMR** (101 MHz, CD<sub>3</sub>CN) δ 170.6 (C<sup>C</sup>), 170.5 (C<sup>C</sup>), 154.0 (C<sup>G</sup>), 135.0 (C<sup>E</sup>), 114.9 (C<sup>F</sup>), 78.7 (C<sup>H</sup>), 48.0 (C<sup>A</sup>), 46.5 (C<sup>B</sup>), 45.6 (C<sup>B</sup>), 41.2 (C<sup>D</sup>), 27.7 (C<sup>I</sup>).

Peaks in <sup>1</sup>H NMR and <sup>13</sup>C NMR spectra broad and split due to the presence of *N*-Boc rotamers.

**FTIR** (ATR)  $\nu$  (cm<sup>-1</sup>): 3278 (*N*-H), 1697 (C=O)

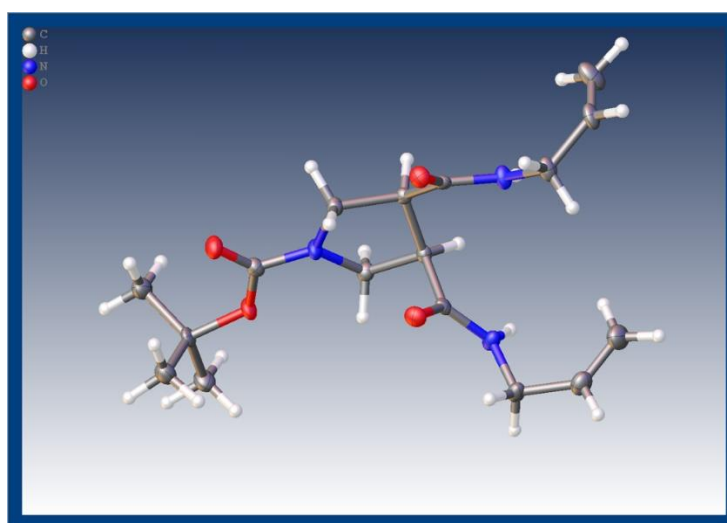
**HRMS (APCI)**: *m/z* calculated for C<sub>17</sub>H<sub>26</sub>N<sub>3</sub>O<sub>4</sub> [M-H]<sup>-</sup>: 336.1926, found at: 336.1875.

**R<sub>f</sub>**: (EtOAc-hexane, 4:1) = 0.20.

**Melting point**: 205-207 °C (decomposition)

**Lab-book reference** WM-07-25

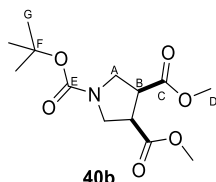
**Crystal structure**:



Identification code	SC140_auto
Empirical formula	C <sub>17</sub> H <sub>27</sub> N <sub>3</sub> O <sub>4</sub>
Formula weight	337.41
Temperature/K	100.5(10)
Crystal system	monoclinic
Space group	P2 <sub>1</sub> /c
<i>a</i> /Å	11.2326(5)
<i>b</i> /Å	17.5473(10)
<i>c</i> /Å	9.3007(3)
$\alpha$ /°	90
$\beta$ /°	91.748(3)
$\gamma$ /°	90
Volume/Å <sup>3</sup>	1832.33(15)
<i>Z</i>	4
$\rho_{\text{calc}}$ /cm <sup>3</sup>	1.223
$\mu$ /mm <sup>-1</sup>	0.716
<i>F</i> (000)	728.0
Crystal size/mm <sup>3</sup>	0.08 × 0.03 × 0.02
Radiation	Cu K $\alpha$ ( $\lambda$ = 1.54184)
2 $\theta$ range for data collection/°	7.874 to 152.42
Index ranges	-12 ≤ <i>h</i> ≤ 13, -15 ≤ <i>k</i> ≤ 10, -11 ≤ <i>l</i> ≤ 7
Reflections collected	3525

Independent reflections	2163 [ $R_{\text{int}} = 0.0121$ , $R_{\text{sigma}} = 0.0189$ ]
Data/restraints/parameters	2163/0/228
Goodness-of-fit on $F^2$	1.097
Final R indexes [ $I \geq 2\sigma(I)$ ]	$R_1 = 0.0341$ , $wR_2 = 0.0818$
Final R indexes [all data]	$R_1 = 0.0392$ , $wR_2 = 0.0848$
Largest diff. peak/hole / $e \text{ \AA}^{-3}$	0.15/-0.16

**1-(*tert*-Butyl) 3,4-dimethyl *rac*-(3*R*,4*S*)-pyrrolidine-1,3,4-tricarboxylate (40b)**



Chemical Formula:  $C_{13}H_{21}NO_6$   
Molecular Weight: 287.31

Using the general procedure, maleic anhydride (98 mg, 1.00 mmol) and 1-Boc-3-azetidinone (513 mg, 3.00 mmol) used in the Paternò-Büchi reaction (86 h irradiation). Using methanol (0.10 mL, 2.00 mmol) and stirring at reflux for 86 h in the second step, the crude product **B** was obtained, then dissolved in MeCN (3 mL) and used in the final step using methanol (0.10 mL, 2.00 mmol). Purification by flash chromatography (eluent 9:1 – 3:2 hexane-EtOAc) gave **40b** (164 mg, 0.57 mmol, 57%) as colourless oil.

**$^1\text{H NMR}$**  (400 MHz,  $C_6D_6$ )  $\delta$  4.01-3.94 (m, 1H,  $H^A$ ), 3.93-3.86 (m, 1H,  $H^A$ ), 3.47-3.39 (m, 2H,  $H^A$ ), 3.26 (s, 3H,  $H^D$ ), 3.20 (s, 3H,  $H^D$ ), 2.78-2.71 (m, 1H,  $H^B$ ), 2.70-2.62 (m, 1H,  $H^B$ ), 1.43 (s, 9H,  $H^G$ ).

**$^{13}\text{C NMR}$**  (101 MHz,  $C_6D_6$ )  $\delta$  171.6 ( $C^C$ ), 171.0 ( $C^C$ ), 153.8 ( $C^E$ ), 79.0 ( $C^F$ ), 51.3 ( $C^D$ ), 48.1 ( $C^A$ ), 47.2 ( $C^A$ ), 45.2 ( $C^B$ ), 44.2 ( $C^B$ ), 28.2 ( $C^G$ ).

Peaks in  $^1\text{H NMR}$  and  $^{13}\text{C NMR}$  spectra broad and split due to the presence of N-Boc rotamers.

**FTIR** (ATR)  $\nu$  ( $\text{cm}^{-1}$ ): 2976 (C-H), 1735 (C=O, ester), 1690 (C=O, Boc)

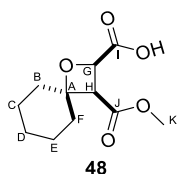
**HRMS (APCI)**:  $m/z$  calculated for (fragment)  $C_8H_{14}NO_4$  [ $M + H$ ] $^+$ : 188.0923, found at: 188.0914

**R<sub>f</sub>**: (EtOAc-hexane, 4:1) = 0.27.

**Lab-book reference**: WM-07-20

**7.4.2.6 Further transformations**

***rac*-(2*R*,3*R*)-3-(Methoxycarbonyl)-1-oxaspiro[3.5]nonane-2-carboxylic acid (48)**



Chemical Formula:  $C_{11}H_{16}O_5$   
Molecular Weight: 228.2440

**Flow procedure:** A solution of **14h** (365 mg, 1.15 mmol) in EtOAc : EtOH (HPLC grade solvents; 1:1; 12 mL) was prepared. The reaction mixture was passed through the H-cube Mini+ flow system at a flow rate of 1 mL min<sup>-1</sup>, equipped with a 10% Pd/C catalyst at 60 °C with H<sub>2(g)</sub>. The mixture was run through again under the same conditions due to incomplete conversion. The collected reaction mixture evaporated under reduced pressure to yield product **48** (204 mg, 0.89 mmol, 78%) as colourless oil.

**Batch procedure:**<sup>106</sup> 10% Pd/C (200 mg) was added to a solution of **14h** (2.123 g, 6.70 mmol) in anhydrous methanol (15 mL) in an oven-dried flask under nitrogen (an additional empty balloon was used for capturing H<sub>2</sub>). Next, triethylsilane (10.67 mL, 67.00 mmol) was added dropwise at 0 °C (over ~2 h). The reaction was allowed to warm to room temperature and stirred at room temperature for 20 minutes (completion by TLC). The reaction mixture was passed through a Celite plug, and the filtrate was evaporated under reduced pressure to give the crude product. Purification by flash chromatography (eluent 3:2 hexane-EtOAc) gave **48** (839 mg, 3.69 mmol, 55%) as colourless oil.

**<sup>1</sup>H NMR** (400 MHz, CDCl<sub>3</sub>) δ 5.08 (d, *J* = 8.7 Hz, 1H, H<sup>G</sup>), 4.82 (s, 1H, OH), 3.74 (s, 3H, H<sup>K</sup>), 3.73 (d (overlapped with singlet, *J* = 8.7 Hz, 1H, H<sup>H</sup>), 1.98 – 1.32 (m, 10H, H<sup>B/C/D/E/F</sup>).

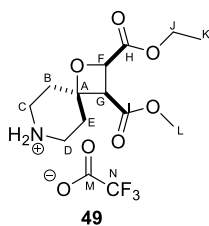
**<sup>13</sup>C NMR** (101 MHz, CDCl<sub>3</sub>) δ 173.4 (C<sup>I</sup>), 168.5 (C<sup>J</sup>), 86.1 (C<sup>A</sup>), 71.3 (C<sup>G</sup>), 52.1 (C<sup>K</sup>), 51.1 (C<sup>H</sup>), 39.3 (C<sup>B/C/D/E/F</sup>), 33.7 (C<sup>B/C/D/E/F</sup>), 24.7 (C<sup>B/C/D/E/F</sup>), 22.2 (C<sup>B/C/D/E/F</sup>), 21.6 (C<sup>B/C/D/E/F</sup>).

**FTIR (ATR) ν (cm<sup>-1</sup>):** 3472 (broad, O-H), 2931 (C-H), 1729 (C=O).

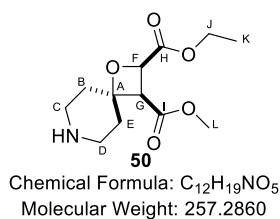
**HRMS (APCI):** *m/z* calculated for C<sub>11</sub>H<sub>17</sub>O<sub>5</sub> [M + H]<sup>+</sup>: 229.1071, found at: 229.1066.

**Lab-book reference:** WM-07-73 (batch), WM-07-53 (flow).

### ***rac*-(2*R*,3*R*)-2-Ethyl 3-methyl 1-oxa-7-azaspiro[3.5]nonane-2,3-dicarboxylate (**49** and **50**)**



Chemical Formula: C<sub>14</sub>H<sub>20</sub>NO<sub>7</sub>F<sub>3</sub>  
Molecular Weight: 371.31



Chemical Formula: C<sub>12</sub>H<sub>19</sub>NO<sub>5</sub>  
Molecular Weight: 257.2860

TFA (0.38 mL, 5.00 mmol) was added dropwise to a solution of **20** (68 mg, 0.19 mmol) in dichloromethane (2 mL). The reaction was stirred at room temperature for 1 h, then evaporated under reduced pressure and **49** was isolated (72 mg, 0.19 mmol, 99 %) as a yellow oil.

**49**

**<sup>1</sup>H NMR** (400 MHz, CDCl<sub>3</sub>) δ 9.06 (s, 2H, N-H), 5.06 (d, *J* = 9.1 Hz, 1H, H<sup>F</sup>), 4.32-4.23 (m, 2H, H<sup>J</sup>), 3.84 (d, *J* = 9.1 Hz, 1H, H<sup>G</sup>), 3.71 (s, 3H, H<sup>L</sup>), 3.40-3.19 (m, 4H, H<sup>B/C/D/E</sup>), 2.49 (d, *J* = 14.4 Hz, 1H, H<sup>B/C/D/E</sup>), 2.26 (dd, *J* = 11.1, 4.0 Hz, 2H, H<sup>B/C/D/E</sup>), 1.97 (ddd, *J* = 14.4, 11.6, 6.1 Hz, 1H, H<sup>B/C/D/E</sup>), 1.30 (t, *J* = 7.2 Hz, 3H, H<sup>K</sup>).

**<sup>13</sup>C NMR** (101 MHz, CDCl<sub>3</sub>) δ 170.0 (C<sup>J</sup>), 167.5 (C<sup>I</sup>), 80.6 (C<sup>A</sup>), 72.5 (C<sup>F</sup>), 61.7 (C<sup>J</sup>), 52.3 (C<sup>L</sup>), 49.4 (C<sup>G</sup>), 40.0 (C<sup>B/C/D/E</sup>), 39.7 (C<sup>B/C/D/E</sup>), 34.8 (C<sup>B/C/D/E</sup>), 29.9 (C<sup>B/C/D/E</sup>), 14.1 (C<sup>K</sup>).

**<sup>19</sup>F NMR** (376 MHz, CDCl<sub>3</sub>) δ -75.9.

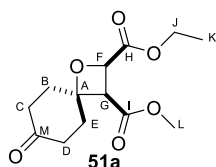
**FTIR (ATR) ν (cm<sup>-1</sup>):** 3375 (broad N-H), 1735 (C=O, ester), 1669 (C=O, amide)

**50:**

**HRMS (APCI):** *m/z* calculated for C<sub>12</sub>H<sub>20</sub>NO<sub>5</sub> [M + H]<sup>+</sup>: 258.1336, found at: 258.1327.

**Lab-book reference:** WM-07-16

***rac*-(2*R*,3*R*)-2-Ethyl 3-methyl 7-oxo-1-oxaspiro[3.5]nonane-2,3-dicarboxylate (51a)**



Chemical Formula: C<sub>13</sub>H<sub>18</sub>O<sub>6</sub>  
Molecular Weight: 270.28

Pyridinium *p*-toluenesulfonate (45 mg, 0.19 mmol) was added to a solution of **23b** (60 mg, 0.19 mmol) in acetone (5 mL). The reaction was stirred at room temperature for 10 days. The solvent was removed under reduced pressure and the residue was dissolved in EtOAc (5 mL). The organic layer was washed with sat. NaHCO<sub>3</sub> (2 x 5 mL) and brine (5 mL). The organic layer was dried over with MgSO<sub>4</sub>, filtered and concentrated to give the desired product **51a** (32 mg, 0.12 mmol, 62 %) as a yellow oil.

**<sup>1</sup>H NMR** (400 MHz, CDCl<sub>3</sub>) δ 5.13 (d, *J* = 9.0 Hz, 1H, H<sup>F</sup>), 4.35-4.25 (m, 2H, H<sup>J</sup>), 3.88 (d, *J* = 9.0 Hz, 1H, H<sup>G</sup>), 3.70 (s, 3H, H<sup>L</sup>), 2.75-2.66 (m, 2H, H<sup>B/C/D/E</sup>), 2.54 (dd, *J* = 9.0, 4.7 Hz, 1H, H<sup>B/C/D/E</sup>), 2.48-2.42 (m, 1H, H<sup>B/C/D/E</sup>), 2.38-2.23 (m, 2H, H<sup>B/C/D/E</sup>), 2.17 (dd, *J* = 13.2, 8.3 Hz, 1H, H<sup>B/C/D/E</sup>), 1.94-1.88 (m, 1H, H<sup>B/C/D/E</sup>), 1.32 (t, *J* = 7.2 Hz, 3H, H<sup>K</sup>).

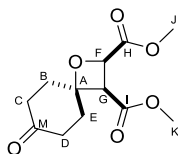
**<sup>13</sup>C NMR** (101 MHz, CDCl<sub>3</sub>) δ 209.3 (C<sup>M</sup>), 170.2 (C<sup>H</sup>), 168.2 (C<sup>I</sup>), 83.4 (C<sup>A</sup>), 72.3 (C<sup>F</sup>), 61.5 (C<sup>J</sup>), 52.1 (C<sup>L</sup>), 49.5 (C<sup>G</sup>), 38.4 (C<sup>B/C/D/E</sup>), 36.5 (C<sup>B/C/D/E</sup>), 35.8 (C<sup>B/C/D/E</sup>), 32.8 (C<sup>B/C/D/E</sup>), 14.1 (C<sup>K</sup>).

**FTIR (ATR) ν (cm<sup>-1</sup>):** 2955 (C-H), 1735 (C=O, ester), 1715 (C=O, ketone).

**HRMS (APCI):** *m/z* calculated for C<sub>13</sub>H<sub>19</sub>O<sub>6</sub> [M + H]<sup>+</sup>: 271.1176, found at 271.1175.

**Lab-book reference:** WM-07-08

***rac*-(2*R*,3*R*)-2,3-Dimethyl 7-oxo-1-oxaspiro[3.5]nonane-2,3-dicarboxylate (51b)**



**51b**

Chemical Formula: C<sub>12</sub>H<sub>16</sub>O<sub>6</sub>  
Molecular Weight: 256.2540

Pyridinium *p*-toluenesulfonate (828 mg, 3.3 mmol) was added to a solution of **23c** (2.00 g, 6.60 mmol) in acetone (50 mL). The reaction was stirred at reflux for 7 days. The solvent was removed under reduced pressure and the residue was dissolved in EtOAc (20 mL). The organic layer was washed with sat. NaHCO<sub>3</sub> (2 x 20 mL) and brine (20 mL). The organic layer was dried over with MgSO<sub>4</sub>, filtered and concentrated to give the desired product **51b** (580 mg, 2.27 mmol, 34%) as a yellow oil (starting material: 142 mg, 0.47 mmol, 7%).

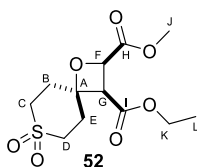
**<sup>1</sup>H NMR** (400 MHz, CDCl<sub>3</sub>) δ 5.18 (d, *J* = 8.9 Hz, 1H, H<sup>F</sup>), 3.91 (d, *J* = 8.9 Hz, 1H, H<sup>G</sup>), 3.86 (s, *J* = 1.5 Hz, 3H, H<sup>J</sup>), 3.73 (s, *J* = 1.0 Hz, 3H, H<sup>K</sup>), 2.80 - 1.93 (m, 8H, H<sup>B,C,D,E</sup>).

**<sup>13</sup>C NMR** (101 MHz, CDCl<sub>3</sub>) δ 209.1 (C<sup>M</sup>), 170.7 (C<sup>H</sup>), 168.2 (C<sup>I</sup>), 83.5 (C<sup>A</sup>), 72.2 (C<sup>F</sup>), 52.4 (C<sup>J</sup>), 52.2 (C<sup>K</sup>), 49.5 (C<sup>G</sup>), 38.4 (C<sup>B/C/D/E</sup>), 36.5 (C<sup>B/C/D/E</sup>), 35.8 (C<sup>B/C/D/E</sup>), 32.8 (C<sup>B/C/D/E</sup>).

**FTIR** (ATR)  $\nu$  (cm<sup>-1</sup>): 2953 (C-H), 1738 (C=O, ester), 1718 (C=O, ketone).

**Lab-book reference:** WM-09-28SM/P (acetal and ketone under the same number, from the same column)

***rac*-(2*R*,3*R*)-3-Ethyl 2-methyl 1-oxa-7-thiaspiro[3.5]nonane-2,3-dicarboxylate 7,7-dioxide (52)**



Chemical Formula: C<sub>12</sub>H<sub>18</sub>O<sub>7</sub>S  
Molecular Weight: 306.33

Sodium perborate monohydrate (69 mg, 0.67 mmol) was added in one portion to a solution of **19b** (63 mg, 0.22 mmol) in THF-water (1:1; 6 mL). The resulting mixture was heated at reflux for 1 h, then allowed to cool to room temperature, and a second portion of sodium perborate monohydrate (69 mg, 0.67 mmol) was added. The resulting mixture was heated at reflux for 1 h, then allowed to cool to room temperature. The mixture was evaporated under reduced pressure, then extracted with EtOAc (3 x 5 mL). The

combined organic phases were dried (MgSO<sub>4</sub>) and evaporated under reduced pressure to give the desired product **52** (53 mg, 0.17 mmol, 79%) as a colourless oil.

**<sup>1</sup>H NMR** (400 MHz, CDCl<sub>3</sub>) δ 5.13 (d, *J* = 9.1 Hz, 1H, H<sup>F</sup>), 4.20 (q, *J* = 7.0 Hz, 2H, H<sup>K</sup>), 3.86 (d, *J* = 9.1 Hz, 1H, H<sup>G</sup>), 3.84 (s, 3H, H<sup>J</sup>), 3.03 – 2.93 (m, 2H, H<sup>C/D</sup>), 3.04-2.92 (m, 3H, H<sup>B/C/D/E</sup>), 2.78-2.72 (m, 1H, H<sup>B/E</sup>), 2.56 (ddd, *J* = 11.1, 9.9, 3.8 Hz, 1H, H<sup>B/E</sup>), 2.27 (td, *J* = 13.7, 3.6 Hz, 1H, H<sup>B/E</sup>), 1.29 (t, *J* = 7.1 Hz, 3H, H<sup>L</sup>).

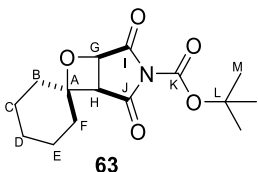
**<sup>13</sup>C NMR** (101 MHz, CDCl<sub>3</sub>) δ 170.5 (C<sup>H</sup>), 167.1 (C<sup>I</sup>), 81.5 (C<sup>A</sup>), 72.6 (C<sup>F</sup>), 61.8 (C<sup>K</sup>), 52.5 (C<sup>J</sup>), 49.3 (C<sup>G</sup>), 46.8 (C<sup>C/D</sup>), 46.2 (C<sup>C/D</sup>), 36.8 (C<sup>B/E</sup>), 31.2 (C<sup>B/E</sup>), 14.2 (C<sup>L</sup>).

**FTIR** (ATR)  $\nu$  (cm<sup>-1</sup>): 3388 (O-H?), 2933 (C-H), 1733 (C=O).

**HRMS (APCI)**: *m/z* calculated for C<sub>12</sub>H<sub>19</sub>O<sub>7</sub>S [M+H]<sup>+</sup>: 307.0846, found at 307.0857.

### 7.4.3 Chapter 4 and 5: Reactions of cyclohexanone (10) with different electron-poor alkenes

#### *rac*-(2*R*,3*R*)-*tert*-Butyl 2,4-dioxo-7-oxa-3-azaspiro[bicyclo[3.2.0]heptane-6,1'-cyclohexane]-3-carboxylate (**63**)



Chemical Formula: C<sub>15</sub>H<sub>21</sub>NO<sub>5</sub>

Molecular Weight: 295.33

A solution of *N*-Boc-maleimide (200 mg, 1.00 mmol), cyclohexanone (0.30 mL, 3.00 mmol) and *p*-xylene (0.60 mL, 6.00 mmol) in anhydrous MeCN (0.05 M, 20 mL) was prepared in a Duran phototube and purged with argon for 15 minutes, then irradiated at approximately 40 °C ( $\lambda$  = 300 nm) until complete consumption of the *N*-Boc-maleimide (20 h), as judged by <sup>1</sup>H NMR spectroscopy (solvent suppression). The solvent was removed under reduced pressure to give the crude product. Purification by flash chromatography (eluent: 1:9 acetone-heptane) gave **63** (90 mg, 0.31 mmol, 31 %) as a colourless oil.

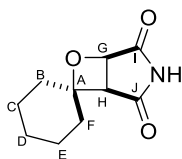
**<sup>1</sup>H NMR** (400 MHz, CDCl<sub>3</sub>) δ 4.95 (d, *J* = 5.7 Hz, 1H, H<sup>G</sup>), 3.40 (d, *J* = 5.7 Hz, 1H, H<sup>H</sup>), 1.62 (s, 9H, H<sup>M</sup>), 1.98 – 1.27 (m, 10H, H<sup>B, C, D, E, F</sup>).

**<sup>13</sup>C NMR** (101 MHz, CDCl<sub>3</sub>) δ 170.4 (C<sup>I</sup>), 170.4 (C<sup>J</sup>), 88.3 (C<sup>A</sup>), 86.8 (C<sup>L</sup>), 72.1 (C<sup>G</sup>), 48.1 (C<sup>H</sup>), 39.1 (C<sup>B/C/D/E/F</sup>), 35.3 (C<sup>B/C/D/E/F</sup>), 27.7 (C<sup>M</sup>), 24.5 (C<sup>B/C/D/E/F</sup>), 22.0 (C<sup>B/C/D/E/F</sup>), 21.7 (C<sup>B/C/D/E/F</sup>). – cannot observe C<sup>K</sup> signal at ~146 ppm

**FTIR** (ATR)  $\nu$  (cm<sup>-1</sup>): 2935 (C-H), 1763 and 1725 (C=O).

**Lab-book reference**: WM-09-24

***rac*-(2*R*,3*R*)-7-Oxa-3-azaspiro[bicyclo[3.2.0]heptane-6,1'-cyclohexane]-2,4-dione (63)**



**63**

Chemical Formula: C<sub>10</sub>H<sub>13</sub>NO<sub>3</sub>

Molecular Weight: 195.21

A solution of maleimide (50 mg, 0.50 mmol), cyclohexanone (0.15 mL, 1.50 mmol) and *p*-xylene (0.30 mL, 3.00 mmol) in anhydrous MeCN (0.05 M, 10 mL) was prepared in a Duran phototube and purged with argon for 15 minutes, then irradiated at approximately 40 °C ( $\lambda = 300$  nm) until complete consumption of the maleimide (23 h), as judged by <sup>1</sup>H NMR spectroscopy (solvent suppression). The solvent was removed under reduced pressure to give the crude product. Purification by flash chromatography (eluent: 1:4 to 2:3 EtOAc-heptane) gave **63** (20 mg, 0.10 mmol, 20 %) as a white solid.

**<sup>1</sup>H NMR** (400 MHz, CDCl<sub>3</sub>)  $\delta$  4.95 (d, *J* = 5.6 Hz, 1H, H<sup>G</sup>), 3.41 (d, *J* = 5.6 Hz, 1H, H<sup>H</sup>), 2.01 – 1.35 (m, 10H, H<sup>B, C, D, E, F</sup>).

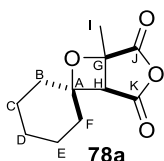
**<sup>13</sup>C NMR** (101 MHz, CDCl<sub>3</sub>)  $\delta$  174.6 (C<sup>I</sup>), 174.0 (C<sup>J</sup>), 87.9 (C<sup>G</sup>), 73.4 (C<sup>A</sup>), 49.3 (C<sup>H</sup>), 39.0 (C<sup>B/C/D/E/F</sup>), 35.2 (C<sup>B/C/D/E/F</sup>), 24.5 (C<sup>B/C/D/E/F</sup>), 22.0 (C<sup>B/C/D/E/F</sup>), 21.8 (C<sup>B/C/D/E/F</sup>).

**FTIR** (ATR)  $\nu$  (cm<sup>-1</sup>): 3218 (broad, N-H), 2935 (C-H), 1718 (C=O).

**HRMS (APCI)**: *m/z* calculated for C<sub>10</sub>H<sub>12</sub>NO<sub>3</sub> [M-H]<sup>-</sup>: 194.0823; found at 194.0827.

**Lab-book reference**: WM-09-09

***rac*-(2*R*,3*R*)-1-Methyl-3,7-dioxaspiro[bicyclo[3.2.0]heptane-6,1'-cyclohexane]-2,4-dione (78a)**



**78a**

Chemical Formula: C<sub>11</sub>H<sub>14</sub>O<sub>4</sub>

Molecular Weight: 210.22

A solution of 2-methylmaleic anhydride (0.24 mL, 1.50 mmol), cyclohexanone (0.48 mL, 4.50 mmol) and *p*-xylene (0.32 mL, 3.00 mmol) in anhydrous MeCN (0.1 M, 15 mL) was prepared in a Duran phototube and purged with argon for 15 minutes, then irradiated at approximately 40 °C ( $\lambda = 300$  nm) until complete consumption of 2-methylmaleic anhydride (168 h), as judged by <sup>1</sup>H NMR spectroscopy (solvent suppression). Purification by flash chromatography (eluent: 4:1 hexane-EtOAc) gave **78a** (33 mg, 0.16 mmol, 10%) as a yellow oil.

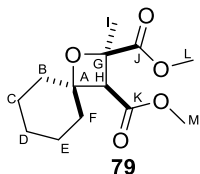
**<sup>1</sup>H NMR** (400 MHz, CDCl<sub>3</sub>) δ 3.35 (s, 1H, H<sup>H</sup>), 1.74 (s, *J* = 7.4 Hz, 3H, H<sup>I</sup>), 1.98 – 1.31 (m, 10H, H<sup>B,C,D,E,F</sup>).

**<sup>13</sup>C NMR** (101 MHz, CDCl<sub>3</sub>) δ 170.7 (C<sup>J</sup>), 167.6 (C<sup>K</sup>), 83.9 (C<sup>A</sup>), 78.9 (C<sup>G</sup>), 52.1 (C<sup>H</sup>), 39.4 (C<sup>B/C/D/E/F</sup>), 35.2 (C<sup>B/C/D/E/F</sup>), 24.3 (C<sup>B/C/D/E/F</sup>), 21.8 (C<sup>B/C/D/E/F</sup>), 21.6 (C<sup>B/C/D/E/F</sup>), 19.6 (C<sup>I</sup>).

**FTIR** (ATR)  $\nu$  (cm<sup>-1</sup>): 2937 (C-H), 1785 and 1712 (C=O, anhydride ring).

**Lab-book reference:** WM-09-38

***rac*-(2*R*,3*R*)-2,3-Dimethyl 2-methyl-1-oxaspiro[3.5]nonane-2,3-dicarboxylate (**79**)**



Chemical Formula: C<sub>13</sub>H<sub>20</sub>O<sub>5</sub>  
Molecular Weight: 256.2980

A solution of 2-methylmaleic anhydride (112 mg, 1.00 mmol), cyclohexanone (0.32 mL, 3.00 mmol) and *p*-xylene (0.12 mL, 1.00 mmol) in anhydrous MeCN (0.1 M, 10 mL) was prepared in a Duran phototube and purged with argon for 15 minutes, then irradiated at approximately 40 °C ( $\lambda$  = 300 nm) until complete consumption of the 2-methylmaleic anhydride (168 h), as judged by <sup>1</sup>H NMR spectroscopy (solvent suppression). Next, the solution was decanted into a round-bottomed flask, and methanol (0.10 mL, 2 mmol) was added. The reaction mixture was stirred at reflux for 48 h until full consumption of oxetane **A**, as judged by <sup>1</sup>H NMR spectroscopy (solvent suppression). The solvent was evaporated under reduced pressure to give the crude product **B**. Crude **B** was then dissolved in anhydrous MeCN (3 mL) under nitrogen. Next, DMAP (10 mg, 5 mol%) was added, followed by methanol (0.10 mL, 2.0 mmol). The reaction mixture was cooled to 0 °C and DCC (226 mg, 1.2 mmol) was added portion-wise. The reaction was slowly warmed to room temperature and stirred overnight. The precipitated urea was filtered off and the filtrate was concentrated under reduced pressure to give crude product **C**. Purification by flash chromatography (eluent: 9:1 hexane-EtOAc) gave **79** (82 mg, 0.32 mmol, 32 %) as a colourless oil.

**<sup>1</sup>H NMR** (400 MHz, CDCl<sub>3</sub>) δ 3.81 (s, 3H, H<sup>L</sup>), 3.69 (s, 3H, H<sup>M</sup>), 3.37 (s, 1H, H<sup>H</sup>), 1.92 – 1.77 (m, 4H, H<sup>B,C,D,E,F</sup>), 1.73 – 1.68 (m, 3H, H<sup>I</sup>), 1.54 – 1.27 (m, 4H, H<sup>B,C,D,E,F</sup>).

**<sup>13</sup>C NMR** (101 MHz, CDCl<sub>3</sub>) δ 173.2 (C<sup>J</sup>), 168.9 (C<sup>K</sup>), 81.5 (C<sup>A</sup>), 78.3 (C<sup>G</sup>), 57.1 (C<sup>H</sup>), 52.4 (C<sup>L</sup>), 51.8 (C<sup>M</sup>), 41.2 (C<sup>I</sup>), 33.1 (C<sup>B/C/D/E/F</sup>), 27.7 (C<sup>B/C/D/E/F</sup>), 24.8 (C<sup>B/C/D/E/F</sup>), 22.1 (C<sup>B/C/D/E/F</sup>), 21.9 (C<sup>B/C/D/E/F</sup>).

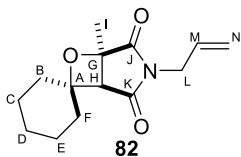
**FTIR** (ATR)  $\nu$  (cm<sup>-1</sup>): 2931 (C-H), 1736 (C=O).

**HRMS (APCI):** *m/z* calculated for C<sub>13</sub>H<sub>21</sub>O<sub>5</sub> [M+H]<sup>+</sup>: 257.1384, found: 257.1378.

**Lab-book reference:** WM-07-62



***rac*-(2*R*,3*R*)-1-Methyl-3-(prop-2-en-1-yl)-7-oxa-3-azaspiro[bicyclo[3.2.0]heptane-6,1'-cyclohexane]-2,4-dione (**82**)**



Chemical Formula: C<sub>14</sub>H<sub>19</sub>NO<sub>3</sub>  
Molecular Weight: 249.31

A solution of 2-methylmaleic anhydride (112 mg, 1.00 mmol), cyclohexanone (0.32 mL, 3.00 mmol) and *p*-xylene (0.12 mL, 1.00 mmol) in anhydrous MeCN (0.1 M, 10 mL) was prepared in a Duran phototube and purged with argon for 15 minutes, then irradiated at approximately 40 °C ( $\lambda = 300$  nm) until complete consumption of the 2-methylmaleic anhydride (168 h), as judged by <sup>1</sup>H NMR spectroscopy (solvent suppression). Next, the solution was decanted into a round-bottomed flask, and allyl amine (0.14 mL, 2 mmol) was added. The reaction mixture was stirred at room temperature for 24 h until full consumption of oxetane **A**, as judged by <sup>1</sup>H NMR spectroscopy (solvent suppression). The solvent was evaporated under reduced pressure to give the crude product **B**. Crude **B** was then dissolved in anhydrous MeCN (3 mL) under nitrogen. Next, DMAP (10 mg, 5 mol%) was added, followed by methanol (0.10 mL, 2.0 mmol). The reaction mixture was cooled to 0 °C and DCC (226 mg, 1.2 mmol) was added portion-wise. The reaction was slowly warmed to room temperature and stirred overnight. The precipitated urea was filtered off and the filtrate was concentrated under reduced pressure to give crude product **C**. Purification by flash chromatography (eluent: 9:1-4:1 hexane-EtOAc) gave **82** (44 mg, 0.18 mmol, 18%) as a yellow oil.

<sup>1</sup>H NMR (400 MHz, CDCl<sub>3</sub>)  $\delta$  5.86 (ddt,  $J = 16.4, 10.2, 6.2$  Hz, 1H, H<sup>M</sup>), 5.34 (dd,  $J = 17.1, 1.1$  Hz, 1H, H<sup>N</sup>), 5.26 (dd,  $J = 10.2, 1.1$  Hz, 1H, H<sup>N</sup>), 4.26 – 4.15 (m, 2H, H<sup>L</sup>), 3.09 (s, 1H, H<sup>H</sup>), 1.66 (s, 3H, H<sup>I</sup>), 1.61 – 1.36 (m, 10H, H<sup>B, C, D, E, F</sup>).

<sup>13</sup>C NMR (101 MHz, CDCl<sub>3</sub>)  $\delta$  176.4 (C<sup>J</sup>), 173.5 (C<sup>K</sup>), 130.3 (C<sup>M</sup>), 119.4 (C<sup>N</sup>), 83.5 (C<sup>A</sup>), 51.6 (C<sup>H</sup>), 41.1 (C<sup>L</sup>), 39.7 (C<sup>B/C/D/E/F</sup>), 34.8 (C<sup>B/C/D/E/F</sup>), 24.5 (C<sup>B/C/D/E/F</sup>), 22.0 (C<sup>B/C/D/E/F</sup>), 21.8 (C<sup>B/C/D/E/F</sup>), 19.5 (C<sup>I</sup>).

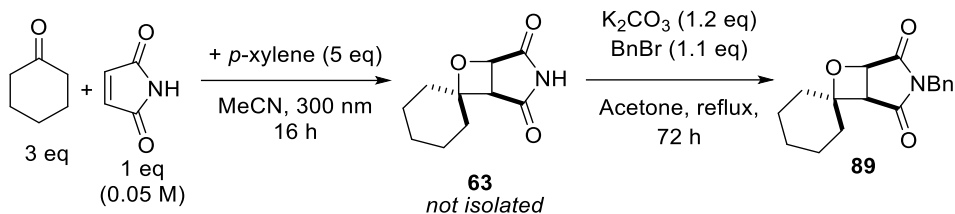
FTIR (ATR)  $\nu$  (cm<sup>-1</sup>): 2933 (C-H), 1709 (C=O)

HRMS (APCI):  $m/z$  calculated for C<sub>14</sub>H<sub>20</sub>NO<sub>3</sub> [M+H]<sup>+</sup>: 250.1438, found at: 250.1426.

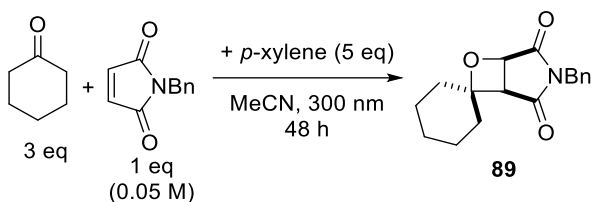
Lab-book reference: WM-07-69

***rac*-(2*R*,3*R*)-3-Benzyl-7-oxa-3-azaspiro[bicyclo[3.2.0]heptane-6,1'-cyclohexane]-2,4-dione (**89**)**

**Method A:**



**Method B:**



**Method A:**

A solution of maleimide (50 mg, 0.50 mmol), cyclohexanone (0.16 mL, 1.50 mmol) and *p*-xylene (0.30 mL, 2.50 mmol) in anhydrous MeCN (0.05 M, 10 mL) was prepared in a Duran phototube and purged with argon for 15 minutes, then irradiated at approximately 40 °C ( $\lambda = 300$  nm) until complete consumption of maleimide (16 h), as judged by <sup>1</sup>H NMR spectroscopy (solvent suppression). The solvent was evaporated under reduced pressure to give the crude product **63**. Crude product **63** was dissolved in acetone (5 mL) and K<sub>2</sub>CO<sub>3</sub> (83 mg, 0.60 mmol) was added. Next, benzyl bromide (0.07 mL, 0.55 mmol) was added and the reaction was heated at reflux for 72 h. Upon completion (based on TLC) the reaction mixture was cooled and filtrated. The solvent was evaporated under reduced pressure to give the crude product. Purification by flash chromatography (eluent: 9:1-2:1 hexane-EtOAc) gave **89** (20 mg, 0.07 mmol, 14%) as a yellow oil.

**Method B:**

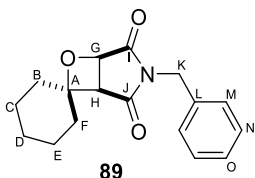
A solution of *N*-benzyl-maleimide (120 mg, 0.64 mmol), cyclohexanone (0.20 mL, 1.92 mmol) and *p*-xylene (0.07 mL, 0.64 mmol) in anhydrous MeCN (0.05 M, 6.4 mL) was prepared in a Duran phototube and purged with argon for 15 minutes, then irradiated at approximately 40 °C ( $\lambda = 300$  nm) until complete consumption of the *N*-benzyl-maleimide (24 h), as judged by <sup>1</sup>H NMR spectroscopy (solvent suppression). The solvent was removed under reduced pressure to give the crude product. Purification by flash chromatography (eluent: 19:1 heptane-acetone) gave **89** (18 mg, 0.06 mmol, 10%) as a yellow oil.

*Comments*

Oxetane : dimer ratio based on

- suppression nmr : 1 : 1.80  $\rightarrow$  3.5 eq of alkene formed dimer. 1 eq formed oxetane  $\rightarrow$  max yield of oxetane = 0.14 mmol. Isolated 18 mg  $\rightarrow$  0.06 mmol (45%)
- cdcl3 nmr : 1 : 1.32

89



Chemical Formula: C<sub>17</sub>H<sub>19</sub>NO<sub>3</sub>

Molecular Weight: 285.34

**<sup>1</sup>H NMR** (400 MHz, CDCl<sub>3</sub>)  $\delta$  7.50-4.36 (m, 2H, H<sup>M/N/O</sup>), 7.33 – 7.28 (m, 3H, H<sup>M/N/O</sup>), 4.92 (d, *J* = 5.6 Hz, 1H, H<sup>G</sup>), 4.77 (d, *J* = 13.9 Hz, 1H, H<sup>K</sup>), 4.72 (d, *J* = 13.9 Hz, 1H, H<sup>K</sup>), 3.33 (d, *J* = 5.6 Hz, 1H, H<sup>H</sup>), 1.89 (t, *J* = 6.0 Hz, 2H, H<sup>B/C/D/E/F</sup>), 1.75 – 1.66 (m, 1H, H<sup>B/C/D/E/F</sup>), 1.53 – 1.29 (m, 5H, H<sup>B/C/D/E/F</sup>).

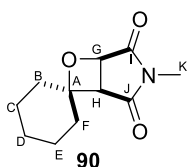
**<sup>13</sup>C NMR** (101 MHz, CDCl<sub>3</sub>)  $\delta$  174.5 (C<sup>I</sup>), 174.0 (C<sup>J</sup>), 135.4 (C<sup>L</sup>), 129.1 (C<sup>N</sup>), 128.7 (C<sup>M</sup>), 128.2 (C<sup>O</sup>), 87.9 (C<sup>A</sup>), 72.1 (C<sup>G</sup>), 47.7 (C<sup>H</sup>), 42.6 (C<sup>K</sup>), 39.1 (C<sup>B/C/D/E/F</sup>), 35.1 (C<sup>B/C/D/E/F</sup>), 24.5 (C<sup>B/C/D/E/F</sup>), 22.1 (C<sup>B/C/D/E/F</sup>), 21.7 (C<sup>B/C/D/E/F</sup>).

**FTIR** (ATR)  $\nu$  (cm<sup>-1</sup>): 2935 (C-H), 1709 (C=O).

**HRMS (APCI)**: *m/z* calculated for C<sub>17</sub>H<sub>18</sub>NO<sub>3</sub> [M-H]<sup>-</sup>: 284.1292, found at: 284.1302.

**Lab-book reference**: WM-09-15-data (2 step method), WM-09-31 for PB reaction

### ***rac*-(2*R*,3*R*)-3-Methyl-7-oxa-3-azaspiro[bicyclo[3.2.0]heptane-6,1'-cyclohexane]-2,4-dione (90)**



Chemical Formula: C<sub>11</sub>H<sub>15</sub>NO<sub>3</sub>

Molecular Weight: 209.24

A solution of maleimide (50 mg, 0.50 mmol), cyclohexanone (0.16mL, 1.50 mmol) and *p*-xylene (0.30 mL, 2.50 mmol) in anhydrous MeCN (0.05 M, 10 mL) was prepared in a Duran phototube and purged with argon for 15 minutes, then irradiated at approximately 40 °C ( $\lambda$  = 300 nm) until complete consumption of the maleimide (16 h), as judged by <sup>1</sup>H NMR spectroscopy (solvent suppression). The solvent was evaporated under reduced pressure to give the crude product **63**. Crude product **63** was dissolved in acetone (5 mL) and K<sub>2</sub>CO<sub>3</sub> (83 mg, 0.60 mmol) was added. Next, methyl iodide (0.03 mL, 0.55 mmol) was added and the reaction was heated at reflux for 5 h. Upon completion (based on TLC) the reaction mixture was cooled and filtrated. The solvent was evaporated under reduced pressure, the residue was dissolved in DCM (5 mL) and washed with water (5 mL) and brine (5 mL). The organic layer was dried (MgSO<sub>4</sub>) and concentrated under

reduced pressure to give the crude product. Purification by flash chromatography (eluent: 9:1-4:1 hexane-EtOAc) gave **89** (10 mg, 0.05 mmol, 10%) as a yellow oil.

**<sup>1</sup>H NMR** (400 MHz, CDCl<sub>3</sub>) δ 4.95 (d, *J* = 5.6 Hz, 1H, H<sup>G</sup>), 3.39 (d, *J* = 5.6 Hz, 1H, H<sup>H</sup>), 3.12 (s, 3H, H<sup>K</sup>), 1.98 – 1.25 (m, 10H, H<sup>B,C,D,E,F</sup>).

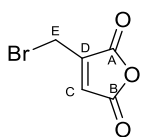
**<sup>13</sup>C NMR** (101 MHz, CDCl<sub>3</sub>) δ 175.0 (C<sup>I</sup>), 174.4 (C<sup>J</sup>), 87.7 (C<sup>A</sup>), 72.1 (C<sup>G</sup>), 47.94 (C<sup>H</sup>), 38.9 (C<sup>B/C/D/E/F</sup>), 35.4 (C<sup>B/C/D/E/F</sup>), 24.9 (C<sup>K</sup>), 24.5 (C<sup>B/C/D/E/F</sup>), 22.0 (C<sup>B/C/D/E/F</sup>), 21.8 (C<sup>B/C/D/E/F</sup>).

**FTIR** (ATR)  $\nu$  (cm<sup>-1</sup>): 2933 (C-H), 1705 (C=O).

**HRMS (APCI)**: *m/z* calculated for C<sub>11</sub>H<sub>16</sub>NO<sub>3</sub> [M+H]<sup>+</sup>: 210.1125, found at: 210.1131.

**Lab-book reference**: WM-09-16

### 3-(Bromomethyl)-2,5-furandione (**83**)



Chemical Formula: C<sub>5</sub>H<sub>3</sub>BrO<sub>3</sub>

Molecular Weight: 190.9800

A mixture of methyl maleic anhydride (2.00g, 17.9 mmol), *N*-bromosuccinimide (14.4 g, 81.4 mmol), and benzoyl peroxide (100 mg, 0.41 mmol) in 100 mL CCl<sub>4</sub> was refluxed for 16 h. Next, the reaction mixture was cooled to room temperature and another portion of benzoyl peroxide (100 mg, 0.41 mmol) was added. The reaction was refluxed for additional 24 h. The reaction mixture was cooled to room temperature and the solid was filtered off and washed with CCl<sub>4</sub> (2 x 20 mL). The organic phase was washed with water (2 x 40 mL) and brine (40 mL). The organic phase was dried (MgSO<sub>4</sub>) and concentrated under reduced pressure to give crude product. Purification by flash chromatography (eluent: 9:1-4:1 hexane-EtOAc) gave **83** (646 mg, 3.40 mmol, 19%) as a yellow oil.

**Procedure based on Ref.** <sup>101,102</sup>

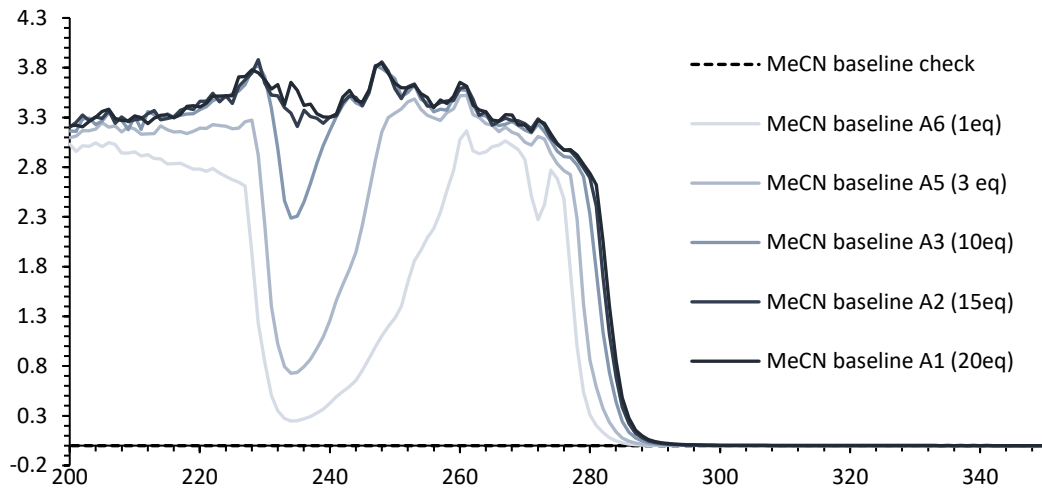
**Assignment matches Ref.** <sup>102</sup>

**<sup>1</sup>H NMR** (400 MHz, CDCl<sub>3</sub>) δ 6.97 (t, *J* = 1.6 Hz, 1H, H<sup>C</sup>), 4.27 (s, 1H, H<sup>E</sup>), 4.26 (s, 1H, H<sup>F</sup>).

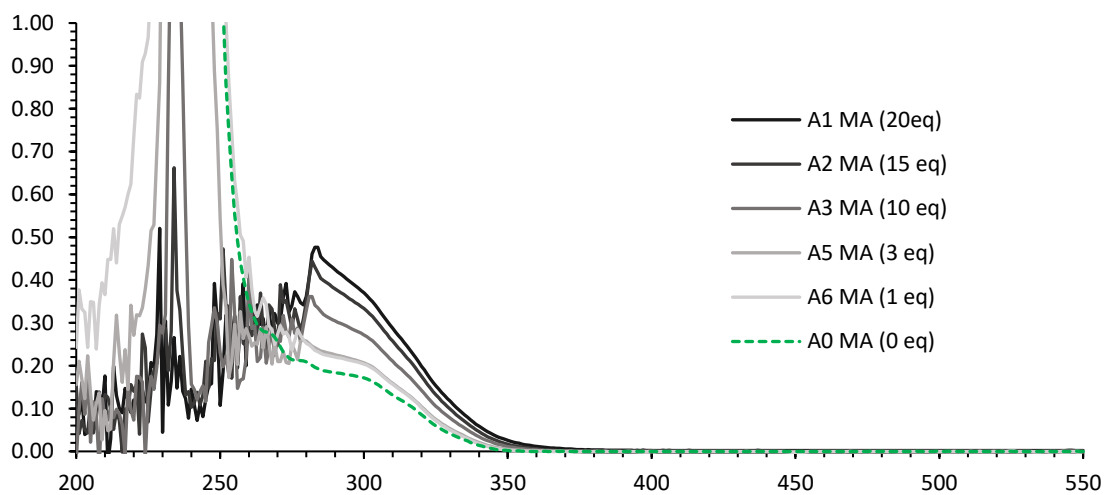
**<sup>13</sup>C NMR** (101 MHz, CDCl<sub>3</sub>) δ 163.3 (C<sup>B</sup>), 162.4 (C<sup>A</sup>), 148.2 (C<sup>D</sup>), 131.9 (C<sup>C</sup>), 18.6 (C<sup>E</sup>).

## 7.5 UV-vis spectra

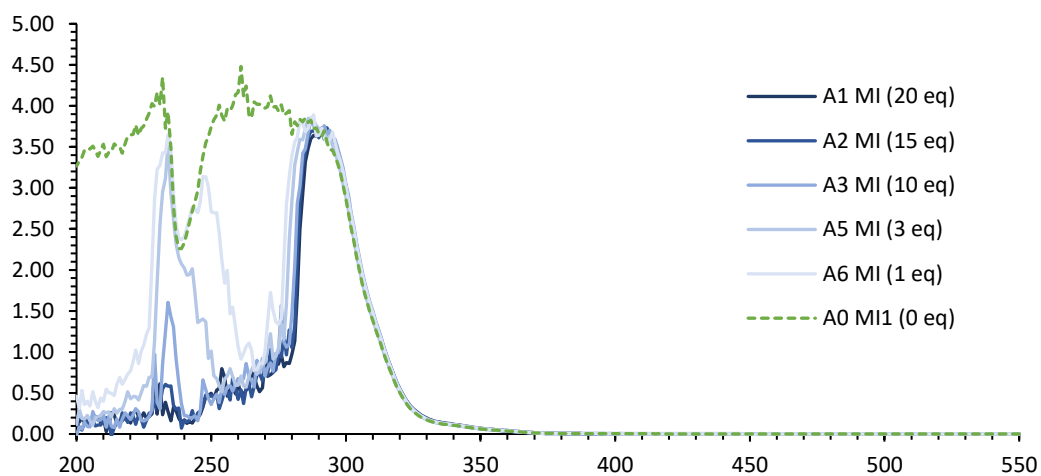
UV-vis - Baseline check – UV-vis of *p*-xylene (eq) in MeCN.



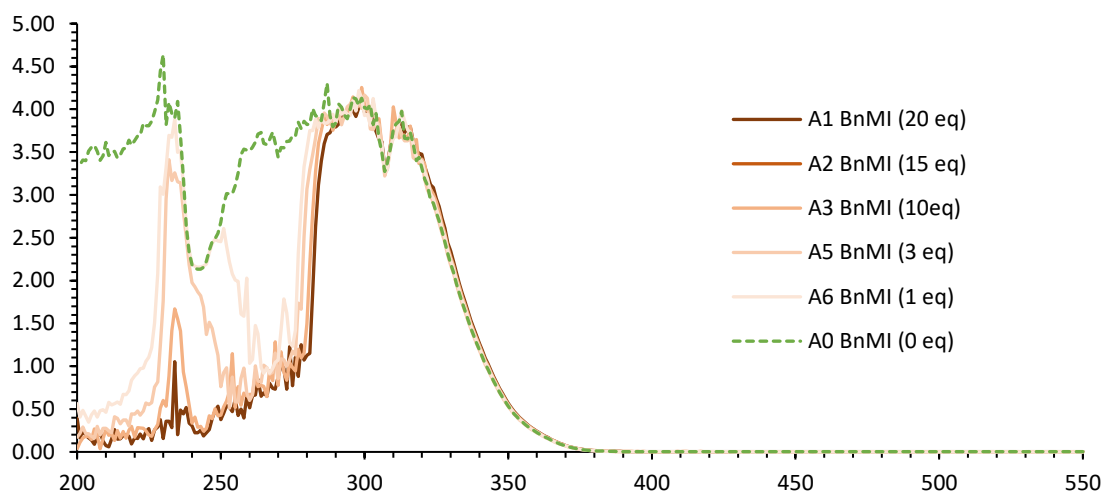
UV-vis spectra of maleic anhydride with different equivalence of *p*-xylene



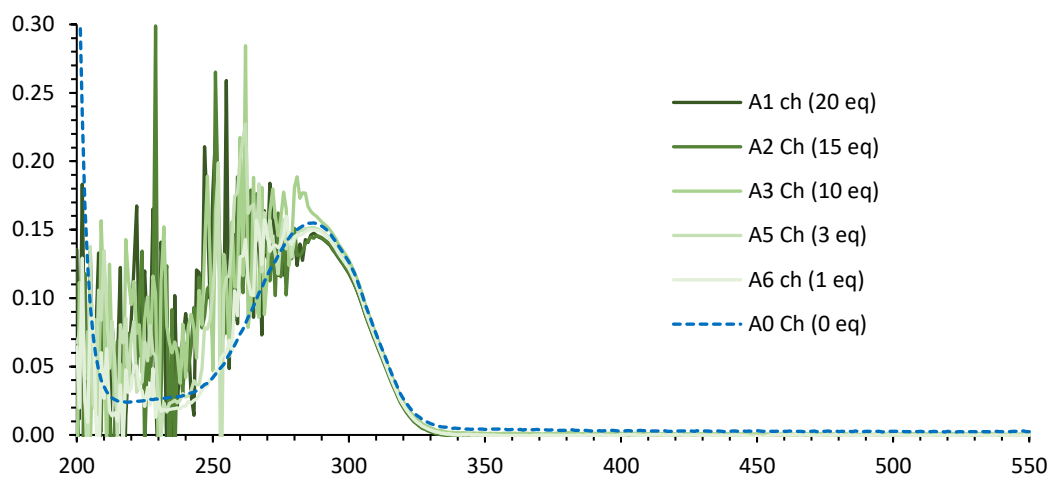
UV-vis spectra of NH-maleimide with different equivalence of *p*-xylene



UV-vis spectra of N-Bn-maleimide with different equivalence of *p*-xylene



UV-vis spectra of cyclohexanone with different equivalence of *p*-xylene



## References

- 1 N. Shimada, S. Hasegawa, T. Harada, T. Tomisawa, A. Fujii and T. Takita, *J. Antibiot. (Tokyo)*, 1986, **39**, 1623–1625.
- 2 C. Li, D. Lee, T. N. Graf, S. S. Phifer, Y. Nakanishi, P. Jason, S. Riswan, F. M. Setyowati, A. M. Saribi, D. Djaja, N. R. Farnsworth, J. O. F. Iii, D. J. Kroll, A. Douglas, M. C. Wani and N. H. Oberlies, *Org. Lett.*, 2005, **7**, 5709–5712.
- 3 Q. Han, J. Zhang, Y. Lu, Y. Wu, Q. Zheng and H. Sun, *Planta Med.*, 2004, **70**, 581–584.
- 4 M. C. Wani, H. L. Taylor, M. E. Wall, P. Coggon and A. T. Mcphail, *J. Am. Chem. Soc.*, 1971, **93**, 2325–2327.
- 5 M. Wang, B. Cornett, J. Nettles, D. C. Liotta and J. P. Snyder, *J. Org. Chem.*, 2000, **65**, 1059–1068.
- 6 M. Serhan, M. Sprowls, D. Jackemeyer, M. Long, I. D. Perez, W. Maret, N. Tao and E. Forzani, *Org. Chem. Front.*, 2022, **9**, 517–571.
- 7 P. Luger and J. Buschmann, *J. Am. Chem. Soc.*, 1984, **106**, 7118–7121.
- 8 C. Jaonathan, G. Nick and W. Stuart, *Organic Chemistry*, 2nd edn., 2012.
- 9 J. A. Bull, R. A. Croft, O. A. Davis, R. Doran and K. F. Morgan, *Chem. Rev.*, 2016, **116**, 12150–12233.
- 10 M. Berthelot, F. Besseau and C. Laurence, *Eur. J. Org. Chem.*, 1998, **5**, 925–931.
- 11 R. Talukdar, *RSC Adv.*, 2020, **10**, 31363–31376.
- 12 J. Shearer, J. L. Castro, A. D. G. Lawson, M. MacCoss and R. D. Taylor, *J. Med. Chem.*, 2022, **65**, 8699–8712.
- 13 M. R. Bauer, P. Di Fruscia, S. C. C. Lucas, I. N. Michaelides, J. E. Nelson, R. I. Storer and B. C. Whitehurst, *RSC Med. Chem.*, 2021, **12**, 448–471.
- 14 C. M. Marson, *Chem. Soc. Rev.*, 2011, **40**, 5514–5533.
- 15 P. D. Leeson, S. A. St-Gallay and M. C. Wenlock, *Medchemcomm*, 2011, **2**, 91–105.
- 16 F. Lovering, *Medchemcomm*, 2013, **4**, 515–519.
- 17 S. M. Nicolle, A. Nortcliffe, H. E. Bartrum, W. Lewis, C. J. Hayes and C. J. Moody, *Chem. - A Eur. J.*, 2017, **23**, 13623–13627.



- 18 K. Oizumi, H. Nishino, H. Koike, T. Sada, M. Miyanoto and T. Kimura, *Jpn. J. Pharmacol.*, 1989, **51**, 57–64.
- 19 J. W. Ellis, *J. Chem. Educ.*, 1995, **72**, 671.
- 20 K. P. Malarney, S. KC and V. A. Schmidt, *Org. Biomol. Chem.*, 2021, **19**, 8425–8441.
- 21 D. A. Smith and L. Cucurull-Sanchez, in *Comprehensive Medicinal Chemistry II*, Elsevier, 2007, pp. 957–969.
- 22 T. N. Thompson, *Med. Res. Rev.*, 2001, **21**, 412–449.
- 23 D. G. I. Kingston, *Pharmacol. Ther.*, 1991, **52**, 1–34.
- 24 M. A. J. Dubois, R. A. Croft, Y. Ding, C. Choi, D. R. Owen, J. A. Bull and J. J. Mousseau, *RSC Med. Chem.*, 2021, **12**, 2045–2052.
- 25 G. Wuitschik, E. M. Carreira, B. Wagner, H. Fischer, I. Parrilla, F. Schuler, M. Rogers-Evans and K. Müller, *J. Med. Chem.*, 2010, **53**, 3227–3246.
- 26 G. Wuitschik, M. Rogers-Evans, K. Müller, H. Fischer, B. Wagner, F. Schuler, L. Polonchuk and E. M. Carreira, *Angew. Chemie Int. Ed.*, 2006, **45**, 7736–7739.
- 27 G. Wuitschik, M. Rogers-Evans, A. Buckl, M. Bernasconi, M. Märki, T. Godel, H. Fischer, B. Wagner, I. Parrilla, F. Schuler, J. Schneider, A. Alker, W. B. Schweizer, K. Müller and E. M. Carreira, *Angew. Chemie - Int. Ed.*, 2008, **47**, 4512–4515.
- 28 E. M. Carreira and T. C. Fessard, *Chem. Rev.*, 2014, **114**, 8257–8322.
- 29 S. Searles, R. G. Nickerson and W. K. Witsiepe, *J. Org. Chem.*, 1959, **24**, 1839–1844.
- 30 S. Hirai, M. Utsugi, M. Iwamoto and M. Nakada, *Chem. A Eur. J.*, 2015, **21**, 355–359.
- 31 K. Yutaka, T. Suguru, I. Nobuo, M. Murata and S. Omura, *Chem. Pharm. Bull.*, 1986, **34**, 3102–3110.
- 32 S. Niitsuma, Y. Ichikawa and T. Takita, *Stud. Nat. Prod. Chem.*, 1992, **10**, 585–627.
- 33 A. O. Fitton, J. Hill, D. E. Jane and R. Millar, *Synthesis (Stuttg.)*, 1987, **12**, 1140–1142.
- 34 D. . Witty, G. W. . Fleet, K. Vogt, F. . Wilson, Y. Wang, R. Storer, P. . Myers and

- C. . Wallis, *Tetrahedron Lett.*, 1990, **31**, 4787–4790.
- 35 S. F. Jenkinson and G. W. J. Fleet, *Chimia (Aarau)*., 2011, **65**, 71–75.
- 36 S. Ahmad, M. Yousaf, A. Mansha, N. Rasool, A. F. Zahoor, F. Hafeez and S. M. A. Rizvi, *Synth. Commun.*, 2016, **46**, 1397–1416.
- 37 P. H. Dussault, T. K. Trullinger and F. Noor-e-Ain, *Org. Lett.*, 2002, **4**, 4591–4593.
- 38 H. Xianming and R. M. Kellogg, *Tetrahedron: Asymmetry*, 1995, **6**, 1399–1408.
- 39 F. Sartillo-Piscil, L. Quintero, C. Villegas, E. Santacruz-Juárez and C. Anaya de Parrodi, *Tetrahedron Lett.*, 2002, **43**, 15–17.
- 40 B. J. Yeh and W. A. Lim, *Nat. Chem. Biol.*, 2007, **3**, 521–525.
- 41 H. Trommsdorff, *Ann. der Pharm.*, 1834, **11**, 190–207.
- 42 A. Natarajan, C. K. Tsai, S. I. Khan, P. McCarren, K. N. Houk and M. A. Garcia-Garibay, *J. Am. Chem. Soc.*, 2007, **129**, 9846–9847.
- 43 P. Klan and J. Wirz, *Photochemistry of Organic Compounds: From Concepts to Practice*, Wiley, 2009.
- 44 M. D'Auria, *Photochem. Photobiol. Sci.*, 2019, **18**, 2297–2362.
- 45 D. L. Dexter, *J. Chem. Phys.*, 1953, **21**, 836–850.
- 46 H.-C. Chen, C.-Y. Hung, K.-H. Wang, H.-L. Chen, W. S. Fann, F.-C. Chien, P. Chen, T. J. Chow, C.-P. Hsu and S.-S. Sun, *Chem. Commun.*, 2009, 4064.
- 47 J. Zhao, W. Wu, J. Sun and S. Guo, *Chem. Soc. Rev.*, 2013, **42**, 5323.
- 48 I. G. Gut, P. D. Wood and R. W. Redmond, *J. Am. Chem. Soc.*, 1996, **118**, 2366–2373.
- 49 P. J. Wagner, *J. Am. Chem. Soc.*, 1966, **3361**, 5672–5673.
- 50 A. Gorman, J. Killoran, C. O'Shea, T. Kenna, W. M. Gallagher and D. F. O'Shea, *J. Am. Chem. Soc.*, 2004, **126**, 10619–10631.
- 51 S. O. McDonnell, M. J. Hall, L. T. Allen, A. Byrne, W. M. Gallagher and D. F. O'Shea, *J. Am. Chem. Soc.*, 2005, **127**, 16360–16361.
- 52 N. J. Turro, V. Ramaurthy and J. C. Scaiano, *Principles of molecular photochemistry: an introduction*, 2009.
- 53 J. He, Z.-Q. Bai, P.-F. Yuan, L.-Z. Wu and Q. Liu, *ACS Catal.*, 2021, **11**, 446–455.

- 54 W. Wu, H. Guo, W. Wu, S. Ji and J. Zhao, *J. Org. Chem.*, 2011, **76**, 7056–7064.
- 55 L. D. Elliott, S. Kayal, M. W. George and K. Booker-Milburn, *J. Am. Chem. Soc.*, 2020, **142**, 14947–14956.
- 56 M. Kira, S. Ishida, T. Iwamoto, A. de Meijere, M. Fujitsuka and O. Ito, *Angew. Chemie Int. Ed.*, 2004, **43**, 4510–4512.
- 57 A. Peter and P. de Julio, *Atkins' Physical Chemistry*, 10th edn., 2014.
- 58 F. F.W. and K. D., *Principles and practice of analytical chemistry*, 4th edn., 1995.
- 59 E. Paternò and G. Chieffi, *Gazz. Chim. Ital*, 1909, **39**, 341–361.
- 60 G. Büchi, C. G. Inman and E. S. Lipinsky, *J. Am. Chem. Soc.*, 1954, **76**, 4327–4331.
- 61 A. G. Griesbeck, M. Abe and S. Bondock, *Acc. Chem. Res.*, 2004, **37**, 919–928.
- 62 N. Hoffmann, *Chem. Rev.*, 2008, **108**, 1052–1103.
- 63 A. G. Griesbeck, *Synlett*, 2003, 0451–0472.
- 64 S. A. Fleming and J. J. Gao, *Tetrahedron Lett.*, 1997, **38**, 5407–5410.
- 65 L. E. Friedrich and J. D. Bower, *J. Am. Chem. Soc.*, 1973, **95**, 6869–6870.
- 66 S. R. Thopate, M. G. Kulkarni and V. G. Puranik, *Angew. Chemie - Int. Ed.*, 1998, **37**, 1110–1112.
- 67 A. G. Griesbeck and S. Stadtmüller, *J. Am. Chem. Soc.*, 1990, **112**, 1281–1283.
- 68 M. D'Auria, F. Pellegrino and L. Viggiani, *J. Photochem. Photobiol. A Chem.*, 2016, **326**, 69–75.
- 69 A. G. Griesbeck, S. Buhr, M. Fiege, H. Schmickler and J. Lex, *J. Org. Chem.*, 1998, **63**, 3847–3854.
- 70 M. Abe, T. Kawakami, S. Ohata, K. Nozaki and M. Nojima, *J. Am. Chem. Soc.*, 2004, **126**, 2838–2846.
- 71 J. Mateos, A. Vega-Peñaloza, P. Franceschi, F. Rigodanza, P. Andreetta, X. Companyó, G. Pelosi, M. Bonchio and L. Dell'Amico, *Chem. Sci.*, 2020, **11**, 6532–6538.
- 72 P. Franceschi, J. Mateos, A. Vega-Peñaloza and L. Dell'Amico, *European J. Org. Chem.*, 2020, **2020**, 6718–6722.

- 73 A. D. Richardson, M. R. Becker and C. S. Schindler, *Chem. Sci.*, 2020, **11**, 7553–7561.
- 74 E. R. Wearing, D. E. Blackmun, M. R. Becker and C. S. Schindler, *J. Am. Chem. Soc.*, 2021, **143**, 16235–16242.
- 75 M. R. Becker, E. R. Wearing and C. S. Schindler, *Nat. Chem.*, 2020, **12**, 898–905.
- 76 D. E. Blackmun, S. A. Chamness and C. S. Schindler, *Org. Lett.*, 2022, **24**, 3053–3057.
- 77 E. Kumarasamy, R. Raghunathan, S. K. Kandappa, A. Sreenithya, S. Jockusch, R. B. Sunoj and J. Sivaguru, *J. Am. Chem. Soc.*, 2017, **139**, 655–662.
- 78 N. J. Turro, P. A. Wriede, J. C. Dalton, D. R. Arnold and A. H. Glick, *J. Am. Chem. Soc.*, 1967, **89**, 3950–3952.
- 79 N. J. Turro and P. A. Wriede, *J. Org. Chem.*, 1969, **34**, 3562–3565.
- 80 R. B. Gagosian, J. C. Dalton and N. J. Turro, *J. Am. Chem. Soc.*, 1970, **92**, 4752–4754.
- 81 D. M. Flores and V. A. Schmidt, *J. Am. Chem. Soc.*, 2019, **141**, 8741–8745.
- 82 P. Klán and J. Wirz, *Photochemistry of Organic Compounds*, Wiley, 2009.
- 83 M. Fréneau and N. Hoffmann, *J. Photochem. Photobiol. C Photochem. Rev.*, 2017, **33**, 83–108.
- 84 P. Franceschi, S. Cuadros, G. Goti and L. Dell’Amico, *Angew. Chemie Int. Ed.*, , DOI:10.1002/anie.202217210.
- 85 D. J. Raber, P. Gariano, A. O. Brod, A. Gariano, W. C. Guida, A. R. Guida and M. D. Herbst, *J. Org. Chem.*, 1979, **44**, 1149–1154.
- 86 B. Neises and W. Steglich, *Angew. Chemie Int. Ed. English*, 1978, **17**, 522–524.
- 87 M. Hardham and C. Laboratories, 1967, **3406**, 3200–3205.
- 88 S. L. Murov, *Handbook of Photochemistry*, 1973.
- 89 F. Strieth-Kalthoff and F. Glorius, *Org. Chem. Front.*, 2020, **6**, 1888–1903.
- 90 B. Wu, W. A. Arnold and L. Ma, *Water Res.*, 2021, **190**, 116659.
- 91 P. Dowd, *J. Am. Chem. Soc.*, 1966, **88**, 2587–2589.
- 92 M. Singh, P. Dhote, D. R. Johnson, S. Figueroa-Lazú, C. G. Elles and Z. Boskovic,

*Angew. Chemie - Int. Ed.*, , DOI:10.1002/anie.202215856.

- 93 J. Zhu, A. J. . Klunder and B. Zwanenburg, *Tetrahedron*, 1995, **51**, 5099–5116.
- 94 E. J. Ko, G. P. Savage, C. M. Williams and J. Tsanaktsidis, *Org. Lett.*, 2011, **13**, 1944–1947.
- 95 C. Grewer and H.-D. Brauer, *J. Phys. Chem.*, 1994, **98**, 4230–4235.
- 96 H. Görner, *Chem. Phys. Lett.*, 1998, **282**, 381–390.
- 97 C. G. Hübner, A. Renn, I. Renge and U. P. Wild, *J. Chem. Phys.*, 2001, **115**, 9619–9622.
- 98 I. Triandafillidi, N. F. Nikitas, P. L. Gkizis, N. Spiliopoulou and C. G. Kokotos, *ChemSusChem*.
- 99 C. R. Martinez and B. L. Iverson, *Chem. Sci.*, 2012, **3**, 2191.
- 100 X. Fang, X. Yang, D. Li, B. Lu and D. Yan, *Cryst. Growth Des.*, 2018, **18**, 6470–6476.
- 101 J. Wang, D. J. Hogenkamp, M. Tran, W.-Y. Li, R. F. Yoshimura, T. B. C. Johnstone, W.-C. Shen and K. W. Gee, *J. Drug Target.*, 2006, **14**, 127–136.
- 102 A. Kar and N. P. Argade, *J. Org. Chem.*, 2002, **67**, 7131–7134.
- 103 O. V. Dolomanov, L. J. Bourhis, R. J. Gildea, J. A. K. Howard and H. Puschmann, *J. Appl. Crystallogr.*, 2009, **42**, 339–341.
- 104 G. M. Sheldrick, *Acta Crystallogr. Sect. A Found. Crystallogr.*, 2008, **64**, 112–122.
- 105 D. N. Nkemngong, PhD thesis, University of North Dakota, 2022.
- 106 P. K. Mandal and J. S. McMurray, *J. Org. Chem.*, 2007, **72**, 6599–6601.